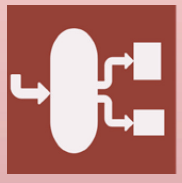

processes

Advances in Microbial Fermentation Processes

Edited by
Maria Tufariello and Francesco Grieco

Printed Edition of the Special Issue Published in *Processes*

www.mdpi.com/journal/processes

Advances in Microbial Fermentation Processes

Advances in Microbial Fermentation Processes

Editors

Maria Tufariello
Francesco Grieco

MDPI • Basel • Beijing • Wuhan • Barcelona • Belgrade • Manchester • Tokyo • Cluj • Tianjin

Editors
Maria Tufariello
CNR-ISPA
Italy

Francesco Grieco
CNR-ISPA
Italy

Editorial Office
MDPI
St. Alban-Anlage 66
4052 Basel, Switzerland

This is a reprint of articles from the Special Issue published online in the open access journal *Processes* (ISSN 2227-9717) (available at: https://www.mdpi.com/journal/processes/special_issues/Processes_Fermentation).

For citation purposes, cite each article independently as indicated on the article page online and as indicated below:

LastName, A.A.; LastName, B.B.; LastName, C.C. Article Title. *Journal Name* **Year**, *Volume Number*, Page Range.

ISBN 978-3-0365-4009-2 (Hbk)
ISBN 978-3-0365-4010-8 (PDF)

Contents

About the Editors . . . . . **vii**

Preface to "Advances in Microbial Fermentation Processes" . . . . . **ix**

Maria Tufariello and Francesco Grieco
Advances in Microbial Fermentation Processes
Reprinted from: *Processes* **2021**, *9*, 1371, doi:10.3390/pr9081371 . . . . . **1**

Xinxin Wang, Jiachen Zhao, Jianye Xia, Guan Wang, Ju Chu and Yingping Zhuang
Impact of Altered Trehalose Metabolism on Physiological Response of *Penicillium chrysogenum* Chemostat Cultures during Industrially Relevant Rapid Feast/Famine Conditions
Reprinted from: *Processes* **2021**, *9*, 118, doi:10.3390/pr9010118 . . . . . **5**

Siti Helmyati, Karina Muthia Shanti, Fahmi Tiara Sari, Martha Puspita Sari, Dominikus Raditya Atmaka, Rio Aditya Pratama, Maria Wigati, Setyo Utami Wisnusanti, Fatma Zuhrotun Nisa' and Endang Sutriswati Rahayu
Synbiotic Fermented Milk with Double Fortification (Fe-Zn) as a Strategy to Address Stunting: A Randomized Controlled Trial among Children under Five in Yogyakarta, Indonesia
Reprinted from: *Processes* **2021**, *9*, 543, doi:10.3390/pr9030543 . . . . . **21**

Ida Bagus Agung Yogeswara, Suwapat Kittibunchakul, Endang Sutriswati Rahayu, Konrad J. Domig, Dietmar Haltrich and Thu Ha Nguyen
Microbial Production and Enzymatic Biosynthesis of γ-Aminobutyric Acid (GABA) Using *Lactobacillus plantarum* FNCC 260 Isolated from Indonesian Fermented Foods
Reprinted from: *Processes* **2021**, *9*, 22, doi:10.3390/pr9010022 . . . . . **33**

Xinxin Li, Xiuhong Wang, Xiangyuan Shi, Baoping Wang, Meiping Li, Qi Wang and Shengwan Zhang
Antifungal Effect of Volatile Organic Compounds from *Bacillus velezensis* CT32 against *Verticillium dahliae* and *Fusarium oxysporum*
Reprinted from: *Processes* **2020**, *8*, 1674, doi:10.3390/pr8121674 . . . . . **51**

Kwanruthai Malairuang, Morakot Krajang, Jatuporn Sukna, Krongchan Rattanapradit and Saethawat Chamsart
High Cell Density Cultivation of *Saccharomyces cerevisiae* with Intensive Multiple Sequential Batches Together with a Novel Technique of Fed-Batch at Cell Level (FBC)
Reprinted from: *Processes* **2020**, *8*, 1321, doi:10.3390/pr8101321 . . . . . **65**

Jeferyd Yepes-García, Carlos Caicedo-Montoya, Laura Pinilla, León F. Toro and Rigoberto Ríos-Estepa
Morphological Differentiation of *Streptomyces clavuligerus* Exposed to Diverse Environmental Conditions and Its Relationship with Clavulanic Acid Biosynthesis
Reprinted from: *Processes* **2020**, *8*, 1038, doi:10.3390/pr8091038 . . . . . **91**

Krešimir Mastanjević, Brankica Kartalović, Leona Puljić, Dragan Kovačević and Kristina Habschied
Influence of Different Smoking Procedures on Polycyclic Aromatic Hydrocarbons Formation in Traditional Dry Sausage *Hercegovačka kobasica*
Reprinted from: *Processes* **2020**, *8*, 918, doi:10.3390/pr8080918 . . . . . **109**

Kwanruthai Malairuang, Morakot Krajang, Rapeepong Rotsattarat and Saethawat Chamsart
Intensive Multiple Sequential Batch Simultaneous Saccharification and Cultivation of *Kluyveromyces marxianus* SS106 Thermotolerant Yeast Strain for Single-Step Ethanol Fermentation from Raw Cassava Starch
Reprinted from: *Processes* **2020**, *8*, 898, doi:10.3390/pr8080898 . . . . . **117**

Chao Wang, Lin Sun, Haiwen Xu, Na Na, Guomei Yin, Sibo Liu, Yun Jiang and Yanlin Xue
Microbial Communities, Metabolites, Fermentation Quality and Aerobic Stability of Whole-Plant Corn Silage Collected from Family Farms in Desert Steppe of North China
Reprinted from: *Processes* **2021**, *9*, 784, doi:10.3390/pr9050784 . . . . . **133**

Chao Wang, Hongyan Han, Lin Sun, Na Na, Haiwen Xu, Shujuan Chang, Yun Jiang and Yanlin Xue
Bacterial Succession Pattern during the Fermentation Process in Whole-Plant Corn Silage Processed in Different Geographical Areas of Northern China
Reprinted from: *Processes* **2021**, *9*, 900, doi:10.3390/pr9050900 . . . . . **149**

Panagiota Stamatopoulou, Juliet Malkowski, Leandro Conrado, Kennedy Brown and Matthew Scarborough
Fermentation of Organic Residues to Beneficial Chemicals: A Review of Medium-Chain Fatty Acid Production
Reprinted from: *Processes* **2020**, *8*, 1571, doi:10.3390/pr8121571 . . . . . **169**

Sandra Pati, Maria Tufariello, Pasquale Crupi, Antonio Coletta, Francesco Grieco and Ilario Losito
Quantification of Volatile Compounds in Wines by HS-SPME-GC/MS: Critical Issues and Use of Multivariate Statistics in Method Optimization
Reprinted from: *Processes* **2021**, *9*, 662, doi:10.3390/pr9040662 . . . . . **195**

About the Editors

Maria Tufariello Researcher at the Institute of Sciences of Food Production of the National Research Council, is involved in:
- 'Omic' approaches (GC-MS, HPLC-DAD, HPLC-FL, HPLC-HRMS) in understanding phenomena related to the biology of lactic bacteria, yeasts and moulds of agri-food interest;
- Extraction, identification and quantification of volatile organic compounds associated with fermentation processes;
- Evaluation of food sensory profile through quantitative–descriptive analytical methods;
- Study and characterization of phenolic profiles of some fermented food and beverages;
- Evaluation of the development of biogenic amines in food and development of extraction techniques;
- Application of multivariate statistical analysis techniques for data processing.

Francesco Grieco, Senior Researcher at the Institute of Sciences of Food Production of the National Research Council, is involved in: i) the study of membrane transport proteins of Saccharomyces cerevisiae; ii) the study of microbial populations present in grape must; iii) the selection of autochthonous Saccharomyces isolates of high oenological value to be used as starters for industrial fermentation; iv) the selection of indigenous yeast isolates to be used for biological control of ochratoxigenous fungi on wine and table grapes; and v) the heterologous expression of fungal proteins of agro-industrial interest in S. cerevisiae. He qualified as a professor of the first and second ranks in the Competitive Sector 07/I1 and he is member of the Italian Society of Agrarian, Food and Environmental Microbiology. He is the author of 247 publications in national and international journals with referees, communications to national and international conferences, and two patents.

Preface to "Advances in Microbial Fermentation Processes"

Fermentation processes are under the spotlight of scientific research in order to improve the quantitative and qualitative properties of the final products. In the food industry, microbial-based fermentation has traditionally been used to obtain edible foods and beverages denoted by extended shelf life and relevant nutritional properties. Furthermore, numerous helpful microorganisms are able to prevent pathogens/spoilers growing and to inactivate undesirable compounds, such as biogenic amines and mycotoxins. Fermented foods can enhance human health by interactions with live microbes (probiotic effect) or indirectly, thanks to the ingestion of microbial metabolites of fermentative origin (biogenic effect).

An incessant investigation concerning microbial diversity is underway, in order to describe and exploit innovative microbial-based biotechnological approaches for the utilization of novel foodstuff to address the current worldwide food crisis. Moreover, numerous micro-organisms have been suggested as cell factories for the synthesis of different desired compounds such as antimicrobial, antioxidants, vitamins and other bioactive molecules, and for use as initial substrate different agro-industrial wastes.

This book, "Advances in Microbial Fermentation Processes", collects the accounts of different investigations concerning the study and the application of new fermentation approaches mediated by microorganisms of industrial interest. In particular, the chapters include innovative studies about the microbial production of valuable compounds: penicillin production by Penicillium chrysogenum under different physiological conditions; the synthesis of GABA using purified recombinant GAD from L. plantarum; the antibiotic biosynthesis in S. clavuligerus strains; and medium-chain fatty acids by using both pure cultures and mixed microbial communities.

Different studies are also reported that investigate the roles of volatile compounds associated with ascomycete/bacteria interaction in fighting plant pathogens, and improving bread and wine quality. Novelties in the microbial-mediated production of a fermented milk-derived food to promote growth in stunted children and of traditional meat-derived foods are also described here. Two interesting chapters show innovative results obtained by the assessment of novel protocols for the production of Saccharomyces cerevisiae and Kluyveromyces marxianus biomasses. The assessment of biodiversity of microbial communities in whole-plant corn silages is included in two different chapters.

This volume contributes to the development of knowledge regarding microbial fermentation processes, by describing the newest applications for the exploitation of microorganism biodiversity in different biotechnological fields.

Maria Tufariello and Francesco Grieco
Editors

processes

MDPI

Editorial

Advances in Microbial Fermentation Processes

Maria Tufariello * and Francesco Grieco *

National Research Council—Institute of Sciences of Food Production (ISPA), Via Prov.le, Lecce-Monteroni, 73100 Lecce, Italy

* Correspondence: maria.tufariello@ispa.cnr.it (M.T.); francesco.grieco@ispa.cnr.it (F.G.); Tel.: +39-083-2422612 (M.T.)

In the food sector, fermentation processes have been the object of great interest in regard to enhancing the yield, the quality, and the safety of the final product. Microbial fermentation has been traditionally used to produce foods denoted by a prolonged shelf life and digestibility. The benefits extended to human health by fermented foods are expressed either directly through the interactions of ingested live microorganisms with the host (probiotic effect) or indirectly as the result of the ingestion of microbial metabolites synthesized during fermentation (biogenic effect). Moreover, several beneficial microbes can inhibit pathogens/spoilers growth and degrade toxins. Several novel microbial-based biotechnological solutions have been recorded and continuous explorations of microbial diversity are being carried out worldwide. In addition, most recently, fermentation has been considered a sustainable approach for maximizing the utilization of bio-resources to address the recent global food crisis. For example, several microbial-based bioconversions have been proposed for the production of enzymes, vitamins, antioxidants, biofuels, feeds, antimicrobial molecules, and other bioactive chemicals, also exploiting agro-industrial wastes [1–6].

The Special Issue "*Advances in Microbial Fermentation Processes*" covers eleven contributes: eleven original research papers and two reviews. As guest editors, we briefly report an overview of these contributions.

Wang et al. [7] investigated, through quantitative metabolomics and a stoichiometric analysis, the role of the trehalose metabolism in the *Penicillium chrysogenum* strain. The authors showed the key role of the intact trehalose metabolism in ensuring penicillin production in the *P. chrysogenum* strain under both steady state and dynamic conditions.

Helmyati and collaborators [8] described an innovation food-based approach to address the stunting problem. They evaluated the ability of a symbiotic milk enriched with iron and zinc and fermented with *Lactobacillus plantarum* to promote growth in stunted children, obtaining excellent results. The investigation of Yogeswara et al. [9] demonstrated a significant increase in the enzymatic synthesis of GABA using purified recombinant GAD from *L. plantarum* FNCC 260. In their original paper, Li and coworkers [10] focused on the activity of volatile compounds produced by Bacillus velezensis CT32 on *Verticillium dahlia* and *Fusarium oxysporum* responsible for strawberry vascular wilt. This study highlighted the key role of some volatile compounds as a biofumigant for the management of vascular wilt pathogens.

The novel cell-level Fed-Batch (FBC) technology for the high-cell-density cultivation of *Saccharomyces cerevisiae* was proposed by Malairuang et al. [11] with a clear illustration of the principle of operation, the potential dextrin substrate, and the mechanism of substrate utilization to regulate FBC, FBC kinetics and material balances through a bioreactor design and scale-up. Yepes-García and coworkers [12] provided an important contribution to the knowledge of antibiotic biosynthesis in the *Streptomyces* genus by studying the relationship between *S. clavuligerus* ATCC 27064 morphology and CA biosynthesis. An interesting contribution of the influence of different smoking techniques on the development of polycyclic aromatic hydrocarbons (PAH) in traditional dry sausage was presented by

Citation: Tufariello, M.; Grieco, F. Advances in Microbial Fermentation Processes. *Processes* **2021**, *9*, 1371. https://doi.org/10.3390/pr9081371

Received: 3 August 2021
Accepted: 4 August 2021
Published: 5 August 2021

Mastanjević et al. [13]. These authors showed the crucial role of the smoking method in the formation of PAHs revealing that collagen samples presented significantly lower values than samples created with traditional gut. Malairuang et al. [14] selected a *Kluyveromyces marxianus* strain for single-step ethanol fermentation, also to establish a practical approach to produce a high-cell-density yeast biomass by an intensive multiple sequential batch simultaneous saccharification and cultivation.

An interesting evaluation of the differences in microbial communities, metabolites, and the aerobic stability between whole-plant corn silages from different areas of Inner Mongolia in North China has been assessed by Wang et al. [15]. Moreover, the same authors investigated the variation of bacterial dynamics during the fermentation process in whole-plant corn silages processed in Heilongjiang, Inner Mongolia and Shanxi of North China [16].

Concerning the review papers, both contributors focused on two interesting topics.

Stamatopoulou et al. summarized the state-of-the-art-concerning Medium-Chain Fatty Acids (MCFA) by using both pure cultures and mixed microbial communities, highlighting future perspectives to improve MCFA production from complex feedstocks [17]. Pati and collaborators [18] reviewed the aspects related to the quantitative analysis of volatile compounds in wines application by HS-SPME-GC/MS, in particular discussing the optimization approaches in the method development stage and the critical aspects related to quantification methods.

This collection contributed to improve the knowledge on the microbial-based fermentation approaches and on the latest innovative application for promoting and monitoring bacterial action in different biotechnological fields.

Author Contributions: Writing—original draft preparation, review and editing, M.T. and F.G. Both authors have read and agreed to the published version of the manuscript.

Funding: This research received no external funding.

Institutional Review Board Statement: Not applicable.

Informed Consent Statement: Not applicable.

Data Availability Statement: None.

Acknowledgments: This work was partially supported by the Apulia Region projects: "Innovazione nella tradizione: tecnologie innovative per esaltare le qualità dei vini autoctoni spumante della murgia barese—INVISPUBA" (P.S.R. Puglia 2014/2020 -Misura 16.2); "Birra: dal campo al boccale—BE^2R" (P.S.R. Puglia 2014/2020—↑Misura 16.2). We would like to thank Giovanni Colella, Domenico Genchi, and Vittorio Falco of the Institute of Sciences of Food Production—CNR—for their skilled technical support provided during the realization of this work.

Conflicts of Interest: The authors declare no conflict of interest.

References

1. Sharma, R.; Garg, P.; Kumar, P.; Bhatia, S.K.; Kulshrestha, S. Microbial Fermentation and Its Role in Quality Improvement of Fermented Foods. *Fermentation* **2020**, *6*, 106. [CrossRef]
2. Hill, D.; Sugrue, I.; Arendt, E.; Hill, C.; Stanton, C.; Ross, R.P. Recent advances in microbial fermentation for dairy and health. *F1000Research* **2017**, *6*, 251. [CrossRef] [PubMed]
3. Pham, J.V.; Yilma, M.A.; Feliz, A.; Majid, M.T.; Maffetone, N.; Walker, J.R. A review of the microbial production of bioactive natural products and biologics. *Front. Microbiol.* **2019**, *10*, 1404. [CrossRef] [PubMed]
4. Parekh, S.; Vinci, V.A.; Strobel, R.J. Improvement of microbial strains and fermentation processes. *Appl. Microbiol. Biotechnol.* **2000**, *54*, 287–301. [CrossRef] [PubMed]
5. Tufariello, M.; Durante, M.; Ramires, F.A.; Grieco, F.; Tommasi, L.; Perbellini, E. New process for production of fermented black table olives using selected autochthonous microbial resources. *Front. Microbiol.* **2015**, *6*, 1007. [CrossRef] [PubMed]
6. De Bellis, P.; Tristezza, M.; Haidukowski, M.; Fanelli, F.; Sisto, A.; Mulè, G.; Grieco, F. Biodegradation of ochratoxin A by bacterial strains isolated from vineyard soils. *Toxins* **2015**, *7*, 5079–5093. [CrossRef] [PubMed]
7. Wang, X.; Zhao, J.; Xia, J.; Wang, G.; Chu, J.; Zhuang, Y. Impact of Altered Trehalose Metabolism on Physiological Response of Penicillium chrysogenum Chemostat Cultures during Industrially Relevant Rapid Feast/Famine Conditions. *Processes* **2021**, *9*, 118. [CrossRef]

8. Helmyati, S.; Shanti, K.M.; Sari, F.T.; Sari, M.P.; Atmaka, D.R.; Pratama, R.A.; Wigati, M.; Wisnusanti, S.U.; Nisa', F.Z.; Rahayu, E.S. Synbiotic Fermented Milk with Double Fortification (Fe-Zn) as a Strategy to Address Stunting: A Randomized Controlled Trial among Children under Five in Yogyakarta, Indonesia. *Processes* **2021**, *9*, 543. [CrossRef]
9. Yogeswara, I.B.A.; Kittibunchakul, S.; Rahayu, E.S.; Domig, K.J.; Haltrich, D.; Nguyen, T.H. Microbial Production and Enzymatic Biosynthesis of γ-Aminobutyric Acid (GABA) Using *Lactobacillus plantarum* FNCC 260 Isolated from Indonesian Fermented Foods. *Processes* **2021**, *9*, 22. [CrossRef]
10. Li, X.; Wang, X.; Shi, X.; Wang, B.; Li, M.; Wang, Q.; Zhang, S. Antifungal Effect of Volatile Organic Compounds from *Bacillus velezensis* CT32 against *Verticillium dahliae* and *Fusarium oxysporum*. *Processes* **2020**, *8*, 1674. [CrossRef]
11. Malairuang, K.; Krajang, M.; Sukna, J.; Rattanapradit, K.; Chamsart, S. High Cell Density Cultivation of *Saccharomyces cerevisiae* with Intensive Multiple Sequential Batches Together with a Novel Technique of Fed-Batch at Cell Level (FBC). *Processes* **2020**, *8*, 1321. [CrossRef]
12. Yepes-García, J.; Caicedo-Montoya, C.; Pinilla, L.; Toro, L.F.; Ríos-Estepa, R. Morphological Differentiation of *Streptomyces clavuligerus* Exposed to Diverse Environmental Conditions and Its Relationship with Clavulanic Acid Biosynthesis. *Processes* **2020**, *8*, 1038. [CrossRef]
13. Mastanjević, K.; Kartalović, B.; Puljić, L.; Kovačević, D.; Habschied, K. Influence of Different Smoking Procedures on Polycyclic Aromatic Hydrocarbons Formation in Traditional Dry Sausage *Hercegovačka kobasica*. *Processes* **2020**, *8*, 918. [CrossRef]
14. Malairuang, K.; Krajang, M.; Rotsattarat, R.; Chamsart, S. Intensive Multiple Sequential Batch Simultaneous Saccharification and Cultivation of *Kluyveromyces marxianus* SS106 Thermotolerant Yeast Strain for Single-Step Ethanol Fermentation from Raw Cassava Starch. *Processes* **2020**, *8*, 898. [CrossRef]
15. Wang, C.; Sun, L.; Xu, H.; Na, N.; Yin, G.; Liu, S.; Jiang, Y.; Xue, Y. Microbial Communities, Metabolites, Fermentation Quality and Aerobic Stability of Whole-Plant Corn Silage Collected from Family Farms in Desert Steppe of North China. *Processes* **2021**, *9*, 784. [CrossRef]
16. Wang, C.; Han, H.; Sun, L.; Na, N.; Xu, H.; Chang, S.; Jiang, Y.; Xue, Y. Bacterial Succession Pattern during the Fermentation Process in Whole-Plant Corn Silage Processed in Different Geographical Areas of Northern China. *Processes* **2021**, *9*, 900. [CrossRef]
17. Stamatopoulou, P.; Malkowski, J.; Conrado, L.; Brown, K.; Scarborough, M. Fermentation of Organic Residues to Beneficial Chemicals: A Review of Medium-Chain Fatty Acid Production. *Processes* **2020**, *8*, 1571. [CrossRef]
18. Pati, S.; Tufariello, M.; Crupi, P.; Coletta, A.; Grieco, F.; Losito, I. Quantification of Volatile Compounds in Wines by HS-SPME-GC/MS: Critical Issues and Use of Multivariate Statistics in Method Optimization. *Processes* **2021**, *9*, 662. [CrossRef]

processes

MDPI

Article

Impact of Altered Trehalose Metabolism on Physiological Response of *Penicillium chrysogenum* Chemostat Cultures during Industrially Relevant Rapid Feast/Famine Conditions

Xinxin Wang, Jiachen Zhao, Jianye Xia *, Guan Wang *, Ju Chu and Yingping Zhuang

State Key Laboratory of Bioreactor Engineering, East China University of Science and Technology (ECUST), Shanghai 200237, China; m18217787017@163.com (X.W.); jczhao@mail.ecust.edu.cn (J.Z.); juchu@ecust.edu.cn (J.C.); ypzhuang@ecust.edu.cn (Y.Z.)

* Correspondence: jyxia@ecust.edu.cn (J.X.); guanwang@ecust.edu.cn (G.W.); Tel.: +86-021-64250719 (G.W.)

Abstract: Due to insufficient mass transfer and mixing issues, cells in the industrial-scale bioreactor are often forced to experience glucose feast/famine cycles, mostly resulting in reduced commercial metrics (titer, yield and productivity). Trehalose cycling has been confirmed as a double-edged sword in the *Penicillium chrysogenum* strain, which facilitates the maintenance of a metabolically balanced state, but it consumes extra amounts of the ATP responsible for the repeated breakdown and formation of trehalose molecules in response to extracellular glucose perturbations. This loss of ATP would be in competition with the high ATP-demanding penicillin biosynthesis. In this work, the role of trehalose metabolism was further explored under industrially relevant conditions by cultivating a high-yielding *Penicillium chrysogenum* strain, and the derived trehalose-null strains in the glucose-limited chemostat system where the glucose feast/famine condition was imposed. This dynamic feast/famine regime with a block-wise feed/no feed regime (36 s on, 324 s off) allows one to generate repetitive cycles of moderate changes in glucose availability. The results obtained using quantitative metabolomics and stoichiometric analysis revealed that the intact trehalose metabolism is vitally important for maintaining penicillin production capacity in the *Penicillium chrysogenum* strain under both steady state and dynamic conditions. Additionally, cells lacking such a key metabolic regulator would become more sensitive to industrially relevant conditions, and are more able to sustain metabolic rearrangements, which manifests in the shrinkage of the central metabolite pool size and the formation of ATP-consuming futile cycles.

Keywords: feast/famine conditions; industrial-scale bioreactor; metabolomics; metabolic response; penicillin; *Penicillium chrysogenum*; scale-down

Citation: Wang, X.; Zhao, J.; Xia, J.; Wang, G.; Chu, J.; Zhuang, Y. Impact of Altered Trehalose Metabolism on Physiological Response of *Penicillium chrysogenum* Chemostat Cultures during Industrially Relevant Rapid Feast/Famine Conditions. *Processes* **2021**, *9*, 118. https://doi.org/10.3390/pr9010118

Received: 17 December 2020
Accepted: 5 January 2021
Published: 7 January 2021

1. Introduction

The filamentous fungus *Penicillium chrysogenum* has long been explored for its production of β-lactam antibiotics (e.g., penicillin G, cephalosporin C), and the potential of the biosynthetic gene clusters in *Penicillium* species has recently been revisited, revealing that it would be a promising cell factory for the production of a series of secondary metabolites and natural products [1,2]. Bioprocess scale-up is the critical step for the commercialization of biotech innovations. Nonetheless, a loss of production capacity in terms of either titer, yield or productivity, or combinations thereof, has often been observed during the process scale-up. Although the interplay between cell systems and their production conditions can be measured, the underlying mechanism is partially unknown, which is, however, seldom accounted for during lab-scale research and development [3,4]. Representatively, the non-ideal mixing and mass transfer limitations at the large scale in most cases are not rigorously considered in lab-scale designs, and thus the outcome of the environmental impacts cannot match the reality at the large scale [5,6]. In industrial settings, the environmental gradients, such as those of substrate, dissolved oxygen and pH, caused by insufficient mixing and

mass transfer restrictions, and of the shear force caused by the impellers, often exert a negative impact on the resulting commercial indicators (i.e., titer, yield and productivity) and thus the economic benefits [7–9].

Although there are many metabolic models being developed to characterize, predict, and evaluate the growth and production dynamics of cell factories in the biological system, a huge gap between laboratory-scale research and industrial applications still exists because of the limited knowledge about the intracellular dynamics under large-scale production limitations [4]. Increasing evidence has shown that steady-state data at the laboratory scale do not suffice to extract transient dynamics and potential regulators in response to a change in conditions, which are, however, very likely actionable at the production scale [10]. To address this, scale-down studies that take into account the environmental conditions experienced by the cells at the large scale have been carried out to evaluate the process performance and elucidate the mechanisms regulating the cellular metabolic flux [8,9,11–15]. As an example, in large-scale penicillin production by *Penicillium chrysogenum*, the cells are often repeatedly forced to experience high/low substrate concentrations (feast-famine cycles), which may partly account for the productivity loss. In an attempt to explain the mechanism behind this, de Jonge et al. (2011) [16] and Wang et al. (2018) [8] have adopted block-wise feeding schemes to simulate the substrate heterogeneity experienced by a high-yielding *Penicillium chrysogenum* strain in glucose-limited chemostat cultures. The results revealed that under feast–famine cycles, the penicillin production capacity was halved, and the intracellular metabolite pools displayed fast dynamics. This efficient and robust control of intracellular metabolite concentration very likely indicated a potential key for the cell homeostasis. For instance, the turnover of intracellular carbohydrates, especially reduced sugars such as mannitol, arabitol, erythritol, as well as trehalose and glycogen, was drastically enhanced during rapid feast/famine conditions in *Penicillium chrysogenum*, which, according to metabolic flux analysis, accounts for about 52% of the gap in the ATP balance, and might partly explain the productivity loss in this scenario [17,18].

Among these ATP-consuming cycles, there has been a focus on the physiological role of transient trehalose futile cycling in the cellular phenotype because trehalose has been proven to harbor a multitude of functions, such as energy and carbon reserves, structural components, and dynamic regulators [19,20]. It has long been known that a functional trehalose pathway is vitally important for *Saccharomyces cerevisiae* grown on rapidly fermentable sugars [21], e.g., glucose, and a sudden shift from glucose-limiting to glucose-excess conditions would lead to growth arrest, which has been linked to the autocatalytic design of the pathway. Additionally, either the unregulated influx of glucose or insufficient phosphate availability have accounted for the appearance of this state [22]. Very recently, van Heerden et al. (2014) reported that trehalose metabolism constitutes a futile cycling that would facilitate metabolic balance via maintaining a proper inorganic phosphate level inside the model eukaryote *Saccharomyces cerevisiae* cell, in order to cope with a sudden glucose availability [23]. In our previous study, as shown in Figure 1, the trehalose synthetic pathway was (partly) blocked by knocking out either the gene *tps1* (encoding trehalose-6-phosphate synthase) or the gene *tps2* (encoding trehalose-6-phosphate phosphatase), and we have concluded that in steady-state glucose-limited chemostat cultures, the intact trehalose pathway plays an important role in metabolic regulation and is instrumental in maintaining a higher penicillin production capacity [24]. Nonetheless, as noted above, it is much more pertinent to evaluate the effect of an altered trehalose metabolism on process performance under industrially relevant conditions, e.g., feast/famine conditions in representative scale-down simulators.

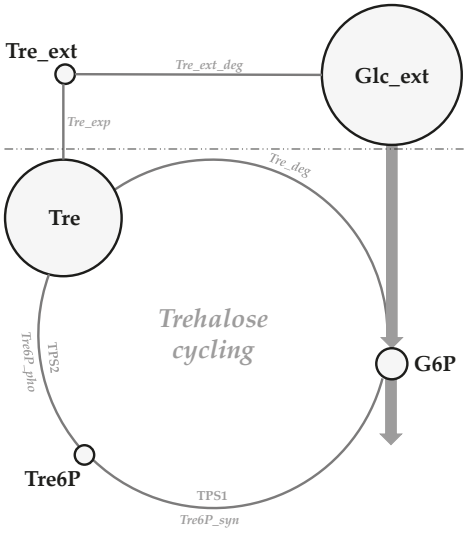

Figure 1. An overview of trehalose cycling in *Penicillium chrysogenum*. Tre6P is formed through the transfer of a glucosyl residue from uridine-diphospho-glucose (UDP-glucose) to G6P, which is catalyzed by Tre6P synthase (encoded by *tps1*). Trehalose is then produced through the dephosphorylation of Tre6P, which is catalyzed by Tre6P phosphatase (encoded by *tps2*). Trehalose can be exported outside the cell, and it can be degraded into glucose via extracellular trehalase. Tre: trehalose; Glc_ext: extracellular glucose; Tre_ext: extracellular trehalose; G6P: glucose-6-phosphate; Tre6P: trehalose-6-phosphate.

In this study, a high-producing industrial strain of *P. chrysogenum* Wisconsin 54-1255, and the derived strains, *P. chrysogenum* Δ*tps1* (lacking trehalose-6-phosphate synthase) and *P. chrysogenum* Δ*tps2* (lacking trehalose-6-phosphate phosphatase), grown in glucose-limited chemostats at the average dilution rate of 0.05 hr^{-1}, were assessed under two substrate availability conditions by performing either a continuous or a block-wise feeding scheme. A systems approach using fluxomics (stoichiometry) and metabolomics for both conditions was for the first time carried out. Overall, we aim at the systematic metabolic characterization and the identification of the potential metabolic role of the trehalose metabolism under industrially relevant conditions.

2. Materials and Methods

2.1. Strains

The *Penicillium chrysogenum* Wisconsin 54-1255 was purchased from ATCC, while the *P. chrysogenum*-Δ*tps1* and *P. chrysogenum*-Δ*tps2* were constructed using the *Agrobacterium* transformation method in our laboratory. For construction details, please refer to Wang et al. (2019) [24]. Fungal spores were prepared on potato dextrose agar (PDA) medium and a concentrated spore suspension was aliquoted and conserved in physiological salt solution (0.9% (*w*/*v*) NaCl in demineralized water) at −80 °C. A spore suspension inoculation method was used for all experiments and the spore suspension was prepared to ensure the final spore concentration in the bioreactor at about 1×10^6/mL after the inoculation, as described previously [24].

2.2. Media

The medium for the batch phase and chemostat cultivation contained the same components (per kg of medium): 16.5 g $C_6H_{12}O_6 \cdot H_2O$, 5 g $(NH_4)_2SO_4$, 1 g KH_2PO_4, 0.5 g $MgSO_4 \cdot 7H_2O$, 2 mL trace elements, 1ml antifoaming agent. The trace element composition (per kg of deionized water) was 75 g $Na_2EDTA \cdot 2H_2O$, 10 g $ZnSO_4 \cdot 7H_2O$,10 g $MnSO_4 \cdot 1H_2O$,

20 g $FeSO_4 \cdot 7H_2O$, 2.5 g $CaCl_2 \cdot 2H_2O$, 2.5 g $CuSO_4 \cdot 5H_2O$. The phenylacetic acid (PAA) concentrations in the batch and the chemostat media were supplied at 0.4085 g/kg and 0.68 g/kg, respectively, which were neither limiting nor toxic for cell growth throughout the cultivation process [25]. The preparation and sterilization of the cultivation medium have been described previously [26]. Briefly, the glucose solution and the PAA-containing salt solution were prepared separately and autoclaved at 110 °C and 121 °C for 40 min and 30 min, respectively. The PAA was dissolved in a KOH solution, with a PAA:KOH molar ratio of 1:1.2.

2.3. Chemostat Cultivation

The chemostat cultivation was performed the same as described previously [24]. Briefly, the chemostat system was based on a 5 L bioreactor (Shanghai Guoqiang Bioengineering Equipment Co., Ltd., Shanghai, China) with a 3 L working volume, followed by the depletion of the initial glucose in the batch phase. As shown in Figure 2, steady state conditions were ensured as the standard reference condition where the medium was continuously fed to the cultivation system; fast feast/famine cycles were initiated via an intermittent feeding regime, which was imposed on the culture through the cultivation. An on/off feeding was applied with a cycle time of 360 s, and the feed pump was precisely controlled by a timer with an algorithm, switching it on every first 36 s of the cycle. During the feeding interval, the pump speed was set 10 times higher than that under reference conditions to keep the average glucose feeding rate of the intermittently fed cultures the same as that of the control chemostats.

All aerobic chemostat cultivations were controlled at the average dilution rate of 0.05 h^{-1}, 2 L/min, and 0.5 bar overpressure. Effluent was removed discontinuously into an effluent vessel if the broth weight exceeded 3 kg by means of a weight-controlled sensor controlling (on/off) a peristaltic pump. Dissolved oxygen tension (DOT) was monitored in situ with an oxygen probe (Mettler-Toledo, Greifensee, Switzerland). The pH of the culture system was monitored using a sterilizable pH probe (Mettler-Toledo, Greifensee, Switzerland) mounted in the bioreactor and was automatically maintained at 6.5 by adding 4M NaOH. The offgas oxygen and carbon dioxide levels were real-time monitored by offgas mass spectrometry (MAX300-LG, Extrel, Pittsburgh, PA, USA). Each experiment was carried out at least in duplicate for biological relevance.

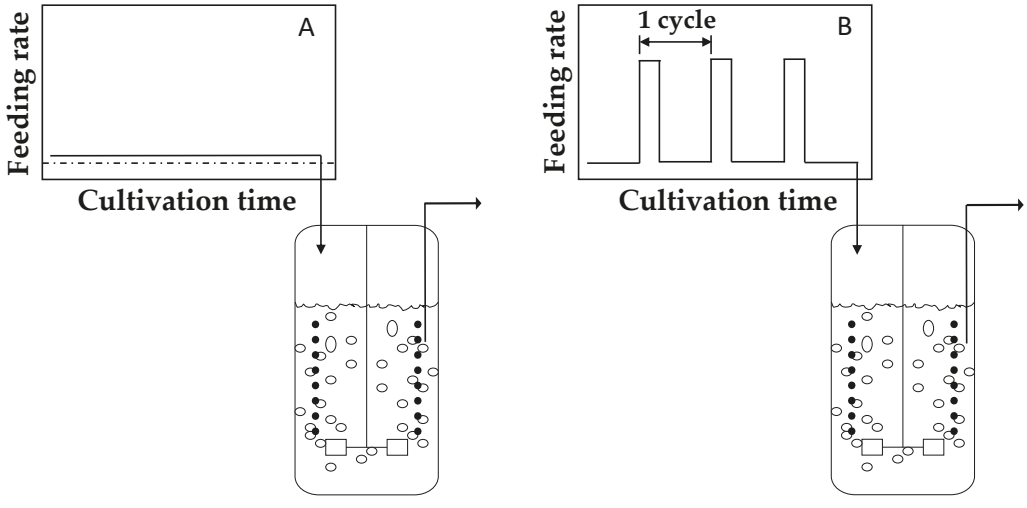

Figure 2. Scheme of the experimental setup. (**A**) Control chemostat cultures, where the culture is continuously fed and (**B**) Experimental chemostat culture, where an intermittent feeding regime (36 s feed, 324 s no feed) is applied.

2.4. Cell Dry Weight

The cell dry weight (CDW) was measured through the weight difference between empty and dried glass fiber filters (47 mm in diameter, 1 µm pore size, type A/E; Pall Corporation, East Hills, NY, USA) with biomass. An amount of 15 mL of broth was withdrawn and divided into three portions for the measurement of the CDW. For each CDW sample, 5 mL of the broth was filtered, and the cell cake was washed twice with 10 mL of demineralized water and dried at 70 °C for 24 h. The biomass-containing filters were cooled to room temperature in a desiccator before weighing.

2.5. Rapid Sampling, Quenching and Metabolite Extraction

Under the reference steady state conditions, samples were taken at each residence time. Under fast feast/famine conditions, the continuous rapid sampling of the broth for the measurement of intracellular metabolites was carried out after 100 h of intermittent feeding at 0, 8, 16, 26, 36, 50, 70, 90, 110, 145, 180, 200, 220, 240, 260, 280, 320 and 350 s within a complete 360 s feeding cycle.

For extracellular sampling, the cold steel-bead method combined with liquid nitrogen was used for the fast filtration and quenching of extracellular enzyme activities, as described previously [27]. For intracellular sampling, about 1 mL of broth was taken from the bioreactor into a tube containing the quenching solution (−27.5 °C, 40% V/V aqueous methanol). To ensure fast sampling and rapid quenching within a second to circumvent as much as possible the change of intracellular metabolites, a customized fast sampling device was developed. The sampling device consists of three normally closed electric pinch valves controlled by a programmed single-chip microcomputer (SCM). The sequential opening and closing of each valve and the combinations thereof can allow sampling with 1 mL of broth within half a second. For detailed sampling procedures, please refer to Li et al. (2018) [28]. Fast filtration and a modified cold washing method were used for the rapid and effective removal of all compounds present outside the cells. In this study, a previously well-established rapid sampling, quenching as well as the follow-up metabolite extraction protocol was followed, as described previously [10].

2.6. Analytical Procedures

Samples for intracellular amino acids, sugar phosphates, organic acids and sugar alcohols quantifications were analyzed using gas chromatography–mass spectrometry (GC–MS) (7890A GC coupled to 5975C MSD; Agilent Technologies, Santa Clara, CA, USA). The analytical procedure undertaken as per de Jonge et al. [16] with some minor modifications in the column and temperature gradients. For more specific settings, please refer to Liu et al. [29].

Concentrations of PAA, Penicillin G and other byproducts in the penicillin biosynthetic pathway were measured with an isocratic reversed-phase high performance liquid chromatography (HPLC) method, which was equipped with an Agilent Zorbax SB-C18 reversed-phase column (150 mm × 4.6 mm ID, 5 µm). The mobile phase consisted of 0.44 g KH_2PO_4 per liter in the acetonitrile/water solution (65/35, V/V). The sample injection volume, the detection wave length, the flow rate and the column temperature were 5 µL, 214 nm, 1.5 mL/min and 25 °C, respectively [27].

2.7. Calculation Methods and Data Reconciliation

The specific rates, such as q_s, q_{CO_2}, q_{O_2} and µ, were calculated using respective mass balances [9], and then were reconciled using the approach of Verheijen based on elemental, charge and degree of reduction balances [30]. The elemental biomass composition and molar weight of 28.05 gDW·Cmol^{-1} were taken from de Jonge et al. [16]. They were assumed to be constant for all conditions.

3. Results and Discussion

3.1. General Observations

To investigate the effect of the altered trehalose metabolism on the physiological response of *Penicillium chrysogenum* under industrially relevant conditions, i.e., dynamic substrate availability in this study, the strains were cultivated in the glucose-limited chemostat mode where rapid feast/famine conditions were imposed via a block-wise feeding strategy. All chemostat cultivations were preceded by a batch phase wherein the strains grew exponentially until all glucose was depleted. The end of batch was determined when the online oxygen uptake rate (OUR) and carbon evolution rate (CER) went down while the dissolved oxygen (DO) level and pH went up. Due to the carbon catabolite repression, no penicillin was produced in the batch phase. After about five residence times (~100 h), all chemostat cultures reached a dynamic steady state (Figure 3). Additionally, the measured time series of the concentrations of biomass, PAA, penicillin-G (PenG) (Figure 3), the main byproducts (Figure 4) associated with penicillin biosynthesis, and the biomass specific rates (Figure 5) show that the chemostat cultivations were well reproducible.

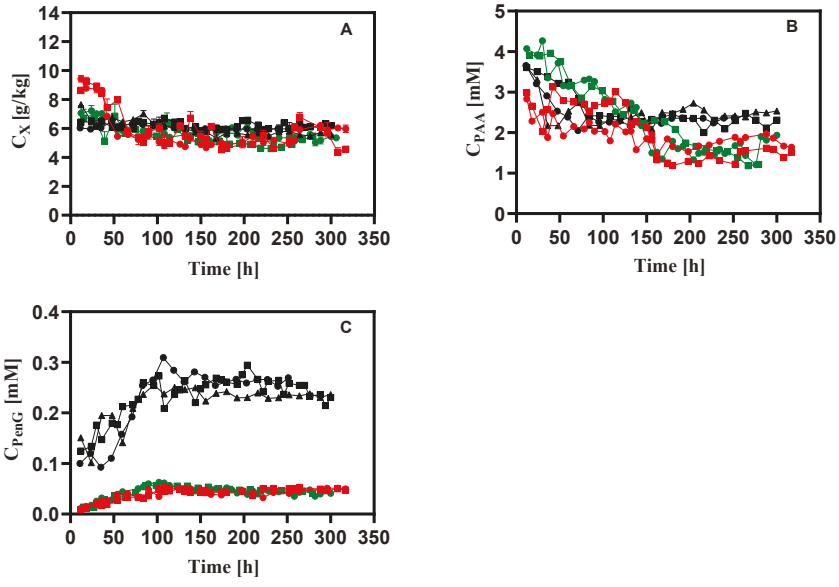

Figure 3. Measured concentrations of (**A**) biomass, (**B**) PAA and (**C**) PenG during rapid feast/famine conditions throughout the chemostat phase. The symbols in black, red and green denote the results obtained from *Penicillium chrysogenum* Wisconsin 54-1255, *Penicillium chrysogenum* Δ*tps1* and *Penicillium chrysogenum* Δ*tps2*, respectively. Time 0 represents the start-up of chemostat cultivation. Abbreviation: PAA, phenylacetic acid; PenG, penicillin-G.

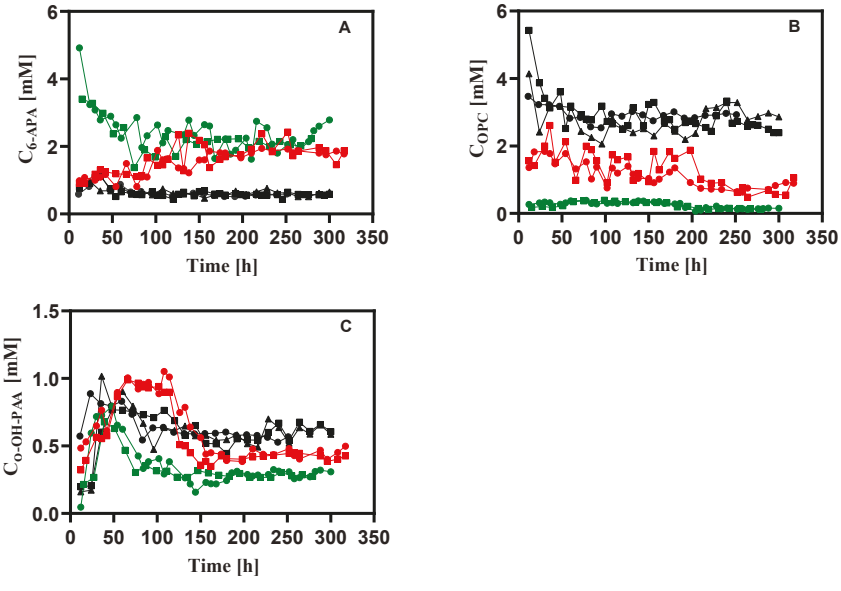

Figure 4. Measured concentrations of (**A**) 6-APA, (**B**) OPC and (**C**) o-OH-PAA during rapid feast/famine conditions throughout the chemostat phase. *Penicillium chrysogenum* Δ*tps1* and *Penicillium chrysogenum* Δ*tps2*, respectively. Time 0 represents the start-up of chemostat cultivation. Abbreviation: 6-APA, 6-aminopenicillanic acid; OPC, 6-oxopipeidine-2-carboxylic acid; o-OH-PAA, ortho-hydroxyphenyl acetic acid.

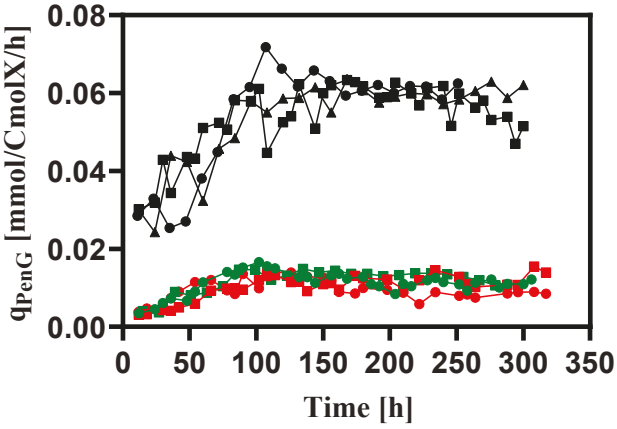

Figure 5. The biomass specific penicillin production rate during rapid feast/famine conditions throughout the chemostat phase. The symbols in black, red and green denote the results obtained from *Penicillium chrysogenum* Wisconsin 54-1255, *Penicillium chrysogenum* Δ*tps1* and *Penicillium chrysogenum* Δ*tps2*, respectively. Time 0 represents the start-up of chemostat cultivation.

In addition, Table 1 shows that the carbon and redox balances closed within 5% for all chemostat cultures, which suggests that marginal unknown compounds are formed during the cultivation.

Table 1. Comparison of the reconciled biomass-specific rates and relevant yields of different *Penicillium chrysogenum* strains on glucose obtained from feast/famine cultures at the average dilution rate of 0.05 h^{-1} in the time range of 100–200 h of cultivation. Measurements are given as average ± standard deviation of at least two individual experiments. Significant test was conducted * $p < 0.05$ vs. WT, by Student's *t*-test. Numbers marked with superscript a and b means significantly increased and decreased, respectively.

		Wisconsin 54-1255	***P. chrysogenum*-Δ*tps1***	***P. chrysogenum*-Δ*tps2***
μ	mCmolX/CmolX/h	50.03 ± 1.60	49.72 ± 1.60	49.50 ± 1.60
$-q_s$	mmol/CmolX/h	19.43 ± 0.46	25.19 ± 1.20 [a]	24.33 ± 1.20 [a]
$-q_{O_2}$	mmol/CmolX/h	67.42 ± 1.70	105.40 ± 6.90 [a]	100.86 ± 6.90 [a]
q_{CO_2}	mmol/CmolX/h	68.63 ± 1.70	106.21 ± 6.90 [a]	101.66 ± 6.90 [a]
$-q_{PAA}$	mmol/CmolX/h	0.63 ± 0.12	0.90 ± 0.23 [a]	0.91 ± 0.15 [a]
q_{PenG}	mmol/CmolX/h	0.063 ± 0.004	0.013 ± 0.002 [b]	0.011 ± 0.001 [b]
q_{OPC}	mmol/CmolX/h	0.66 ± 0.02	0.27 ± 0.06 [b]	0.055 ± 0.03 [b]
q_{6APA}	mmol/CmolX/h	0.136 ± 0.005	0.484 ± 0.09 [a]	0.562 ± 0.107 [a]
$q_{-OH-PAA}$	mmol/CmolX/h	0.208 ± 0.01	0.121 ± 0.02 [b]	0.153 ± 0.01 [b]
$Y_{X/S}$	CmolX/molS	2.57 ± 0.06	1.97 ± 0.07 [b]	2.03 ± 0.08 [b]
$Y_{O/S}$	$molO_2$/molS	3.47 ± 0.03	4.18 ± 0.19 [a]	4.15 ± 0.20 [a]
C balance	-	98.4 ± 1.88	98.61 ± 4.39	98.74 ± 4.56
γ balance	-	96.11 ± 1.03	95.56 ± 2.29	96.02 ± 2.22

3.2. Penicillin Production

A schematic overview of the penicillin synthesis pathway, including the byproduct mentioned in this study, can be seen in Figure 6. It is apparent that the biomass-specific rates for penicillin production (q_{PenG}) obtained for all cultivations reached a maximum value at about 100 h after the start-up of the chemostat phase, which suggests the typical behavior of the induction of the penicillin pathway enzymes because of the repression of the genes encoding these enzymes at high glucose concentrations in the batch phase [26]. Strikingly, the penicillin production capacity in terms of q_{PenG} was reduced by about 30%, 74% and 78% for *P. chrysogenum* Wisconsin 54-1255, *P. chrysogenum*-Δ*tps1* and *P. chrysogenum*-

Δ*tps2* strains under feast/famine conditions, respectively, relative to those under steady state conditions [24]. This can be anticipated because the cells under rapid feast/famine conditions will use multi-layered metabolic regulation mechanisms to maintain a balanced metabolic state at different omics levels (e.g., short-term stringent regulation, long-term repeatedly switched on/off of related genes, protein turnover, etc.), which is often at the expenditure of extra ATP and/or reducing equivalents [31–34]. Meanwhile, it was found that the absence of intact trehalose metabolism can aggravate the loss of the penicillin production capacity, which can be manifested by an almost 40% greater reduction in penicillin productivity for *P. chrysogenum*-Δ*tps1* and *P. chrysogenum*-Δ*tps2* strains under industrially relevant conditions as compared to the steady state conditions. Combining this with the findings from the steady state conditions as we reported elsewhere [24], it can therefore be concluded that trehalose plays an essential role in regulating penicillin production under both non-perturbed and perturbed conditions.

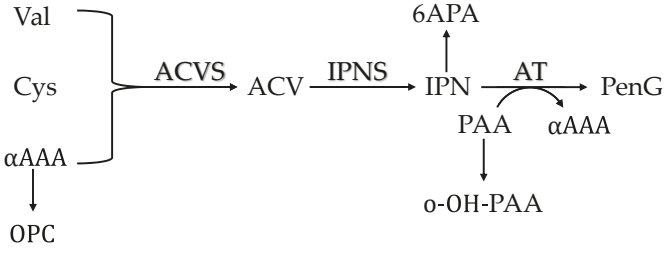

Figure 6. A schematic view of the penicillin biosynthesis pathway and the derived byproducts mentioned in this study. Precursors are L-α-amino adipic acid (αAAA), L-cysteine (Cys) and L-valine (Val). ACVS: L-α-(δ-aminoadipyl)-L-α-cysteinyl-D-α-valine synthase; IPNS: isopenicillin N synthase; AT: acyl-CoA:isopenicillin acyltransferase.

In spite of the reduced production performance under rapid feast/famine conditions, an interesting observation showed that the cells appeared to maintain their production capacity throughout the cultivation process (Figure 5), which was, however, not the case for the strains under steady state conditions, which unavoidably undergo strain degeneration (i.e., loss of production capacity) followed by the onset of the maximum q_{PenG} value [16,35]. This result is very consistent with previous reports by de Jonge et al. [16] and Wang et al. [8], and also suggests that there must be an unknown regulatory mechanism contributing to this non-declining phenomenon.

3.3. Stoichiometry

The biomass-specific rates and relevant yields are provided in Table 1, and the results shows that the absence of intact trehalose metabolism gives rise to significant changes in strain process performance. Notably, during the chemostat phase, the biomass-specific carbon dioxide evolution rates (q_{CO_2}) were increased by 55% and 48%, respectively, in *P. chrysogenum*-Δ*tps1* and *P. chrysogenum*-Δ*tps2* strains compared to the wild-type *P. chrysogenum* Wisconsin strain. This considerable increase in q_{CO_2} is mainly ascribed to the significant increase in specific glucose consumption rates (~90%) and the increase in PAA consumption rates (~6–7%). In the Wisconsin family strains, the reduced oxidative activity of a phenylacetate-oxidizing cytochrome P450 makes more PAA available for the production of PenG [36]. However, the PAA recoveries were not closed in the chemostat phase, leaving 90% or even more PAA catabolized towards the formation of o-OH-PAA, and further, to acetoacetate and fumarate, through the homogentisate pathway. In the engineered strains, more PAA was consumed while much less PenG and o-OH-PAA accumulated, which also pointed to the increased catabolism of PAA as the second carbon source (Table 1). In contrast with this, the PAA recoveries were very well closed during the early phase of the batch process before the initiation of the chemostat mode (Figure 7).

In the batch phase, no penicillin was produced, and the summation of the residual PAA concentration and the formed o-OH-PAA concentration was almost equal to the initial PAA concentration in the bioreactor. Nonetheless, the PAA concentration was gradually decreased during the late phase of the batch fermentation. Meanwhile, we observed that the glucose was rapidly consumed and reached a threshold value at the late stage, which then coincided with the PAA consumption. Combining this, the results indicated that the catabolism of PAA as the carbon source can only be activated under carbon-limited conditions rather than carbon-rich scenarios, which was proven to be controlled via carbon catabolite repression.

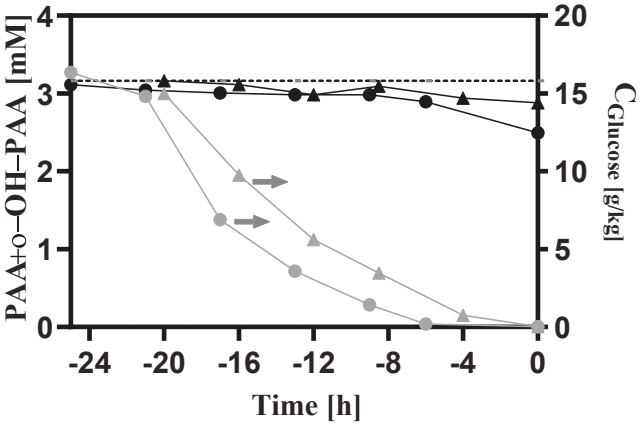

Figure 7. Measured concentrations of PAA, o-OH-PAA and glucose during the batch process. The dash line represents the initial PAA concentration in the bioreactor. The symbols in black, red and green denote the results obtained from *Penicillium chrysogenum* Wisconsin 54-1255, *Penicillium chrysogenum*Δ*tps1* and *Penicillium chrysogenum* Δ*tps2*, respectively. Time 0 represents the start-up of chemostat cultivation.

The other byproduct associated with penicillin production, such as 6APA and OPC, were also measured in this work. The results showed that as compared to the wild-type strain, the specific formation rates for 6APA and OPC were significantly increased and decreased, respectively. The formation of OPC was because of the spontaneous cyclization of one of the precursor amino acids, α-aminoadipic acid (αAAA), and thus the decreased excretion rate of OPC might be ascribed to the lower precursor demand for penicillin production, since the αAAA was not actually consumed during the PenG production. The five-fold lower q_{PenG} values in the engineered strains seem to corroborate this (Table 1). It has been reported that PenG can be formed via both isopenicillin acyltransferase (IAT) and acyl-CoA: 6APA acyltransferase (AAT), the two activities of the key enzyme, acyl-CoA: isopenicillin acyltransferase (AT), in the PenG biosynthesis. Besides this, the AT also has the activity of isopenicillin amidohydrolase (IAH), which converts isopenicillin N (IPN) into 6APA [37]. Recently, Deshmukh et al. estimated the enzyme capacity ratio of IAH:IAT:AAT, which was 250:1:6, and the results showed that the IAH-AAT route is a high-capacity but low-affinity route, while the IAT route is a low-capacity but high-affinity route [38]. In the present study, it was observed that the excretion of 6APA was about four-fold higher outside the cells in the engineered strains (Table 1), which makes it reasonable that IPN (not measured) and 6APA were the main end products when the productivity of PenG was reduced by 80%. In addition, this result also indicated that the IAH activity was less affected, while the IAT and the AAT activities become much more sensitive to rapid feast/famine conditions in the engineered strains than in the Wisconsin 54-1255 strain.

The relevant yields, i.e., $Y_{X/S}$ and $Y_{O/S}$, were also calculated in Table 1. Consistent with previous studies [7], the biomass yields under feast/famine conditions were reduced

by over 20% in the engineered strain as compared to the steady state values [24]. However, the biomass yield in the Wisconsin strain was not significantly varied between the conditions, which is consistent with the results of a high-yielding strain derived by de Jonge et al. [16]. This result showed that although trehalose takes up a small amount of the cell composition [24], it may be involved in maintaining the constant biomass yield under industrially relevant conditions. Meanwhile, the $Y_{O/S}$ value indicates the efficiency of glucose combustion by the cells. We have observed that as compared to the Wisconsin strain, the absence of trehalose metabolism in the *Penicillium chrysogenum* cells slightly increases the energy efficiency under the steady state conditions, which was reflected by the lower $Y_{O/S}$ values [24]. Contrary to the results under the steady state conditions, the $Y_{O/S}$ values for the *P. chrysogenum*-Δ*tps1* and *P. chrysogenum*-Δ*tps2* strains became 46% and 37% higher under dynamic conditions. However, the energy efficiency of the Wisconsin strain did not significantly change between the conditions. The substrate consumption by the *P. chrysogenum* strain can be described by the well-known Herbert–Pirt relation, i.e., $q_s = \alpha\mu + \beta q_p + m_s$, where the parameters α and β are the inverse values of the maximum biomass yield and product yield, respectively [39]. Under rapid feast/famine conditions, the q_s values for the *P. chrysogenum*-Δ*tps1* and *P. chrysogenum*-Δ*tps2* strains became 30% and 25% higher as compared to the Wisconsin strain, while the q_p values were much lowered. This result clearly indicated that the maintenance requirements for the engineered strains became 25–30% higher when the substrate distributed towards penicillin production was neglected (less than 0.5%). This increased maintenance for the engineered strain is very likely to be associated with the loss of the physiological role of trehalose. It has well been documented that trehalose is a multifunctional molecule, which can act as a carbon/energy reserve, as a stabilizer and protectant against adverse substances/environments, as a sensing compound and/or growth regulator, and as a structural component of the cell envelope [19]. More importantly, the flux branching off towards trehalose lies at the glucose-6-phosphate node, which is very close to the gate of glucose uptake, and hence the formation/mobilization of this compound can react immediately to the environmental perturbations, e.g., feast/famine conditions. For example, in a high-producing *P. chrysogenum* strain, de Jonge et al. showed that storage turnover is increased under dynamic cultivation conditions, and upon one cycle of repetitive glucose pulses, about 18% of the carbon entering the cell was recycled in the trehalose node [17]. Although this periodic formation and degradation of trehalose will generate extra ATP costs, the functional role of trehalose cycling can buffer the extracellular nutrient dynamics, and thus contribute to maintaining a balanced cellular state [23]. Based on this, we can hypothesize that the absence of trehalose could expose the cell to more severe intracellular dynamics, which often leads to forming futile cycles at the expense of extra ATP, and also could result in an increased protein turnover rate because the loss-of-function proteins would become higher, which may lead to one of the highest maintenance costs in trehalose-null *P. chrysogenum* strains [33].

3.4. Intracellular Metabolites

In addition to the above-mentioned comparison of the altered trehalose metabolism upon the physiological response of *Penicillium chrysogenum* strains from a macroscopic view, we also carried out a quantitative metabolomics study to investigate the change in the intracellular metabolite pools under industrially relevant conditions, i.e., the feast/famine setup. Moreover, the results from dynamic conditions were compared with those obtained under steady state conditions. As shown in Figures 8 and 9, sugar phosphates, organic acids, sugar alcohols as well as amino acids are measured. Obviously, the majority of the metabolites were significantly decreased under feast/famine conditions relative to steady state conditions. This phenomenon has already been observed in the high-yielding *P. chrysogenum* strain, DS 17690 [8,10], which is derived from the *P. chrysogenum* Wisconsin 54-1255 strain used in this study. This may be associated with metabolic adaptation, where the shrinkage of the metabolite pools can allow the cells to cope with rapid metabolite, flux

and growth rate responses to changes in substrate availability. For instance, in prolonged aerobic, glucose-limited chemostat cultures of *Saccharomyces cerevisiae*, the reduced metabolite pools and a partial loss of capacity (e.g., ATP regeneration, glycolytic enzymes) have been reported [40,41]. Such a decrease in the overcapacities in cells can be accompanied by the faster turnover of the metabolite pools, which results in the optimized metabolic productivity at the cost of metabolic flexibility.

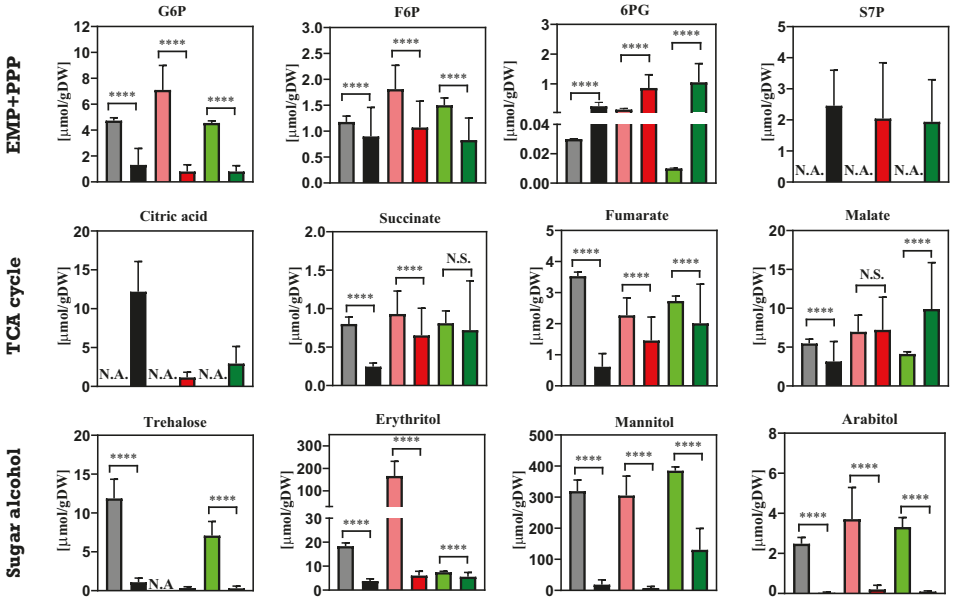

Figure 8. Intracellular amount of sugar phosphates, organic acids and sugar alcohols in *Penicillium chrysogenum* Wisconsin 54-1255, *Penicillium chrysogenum* Δ*tps1* and *Penicillium chrysogenum* Δ*tps2* strains under both steady state conditions and feast/famine conditions. Under steady state conditions, samples were taken at each residence time and datasets were collected from triplicate experiments, while under rapid feast/famine conditions, samples were rapidly taken within a feeding cycle time of 6 min twice for each experiment. The datasets are shown as average value ± standard deviation. The numbers of data points for the steady state conditions and feast/famine conditions are 30 and 32, respectively. A two-tail Student's *t*-test was conducted * $p < 0.05$ (significant) and **** $p < 0.01$ (extremely significant) versus WT using GraphPad Prism 8. N.A., not available. ▮ WT steady state conditions; ▮ WT feast/famine conditions; ▮ Δtps1 steady state conditions; ▮ Δ*tps1* feast/famine conditions ▮ Δ*tps2* steady state conditions; ▮ Δ*tps2* feast/famine conditions. The results from steady state conditions were obtained from Wang et al. (2019) [24]. Abbreviations: G6P, glucose-6-phosphate; F6P, fructose-6-phosphate; 6PG, 6-phosphogluconate; S7P, sedoheptulose-7-phosphate; EMP, Embden–Meyerhof–Parnas; PPP, Pentose phosphate; TCA, tricarboxylic acid.

The above results indicated that under feast/famine conditions there might be a large increase in maintenance requirements in the engineered strains, which suggests the rearrangement of metabolism. Evidence for such a rearrangement can be derived by comparing the mass action ratios (MARs) of near equilibrium reactions in the central metabolism. In this study, the mass action ratios for F6P/G6P and malate/fumarate were calculated for *P. chrysogenum* Wisconsin 54-1255, *P. chrysogenum*-Δ*tps1* and *P. chrysogenum*-Δ*tps2* strains (Table 2), which were (0.25, 1.56), (0.25, 3.07) and (0.33,1.51) for steady state conditions, while they were (0.68, 5.18), (1.34, 4.95) and (1.02, 4.93) for feast/famine conditions, respectively.

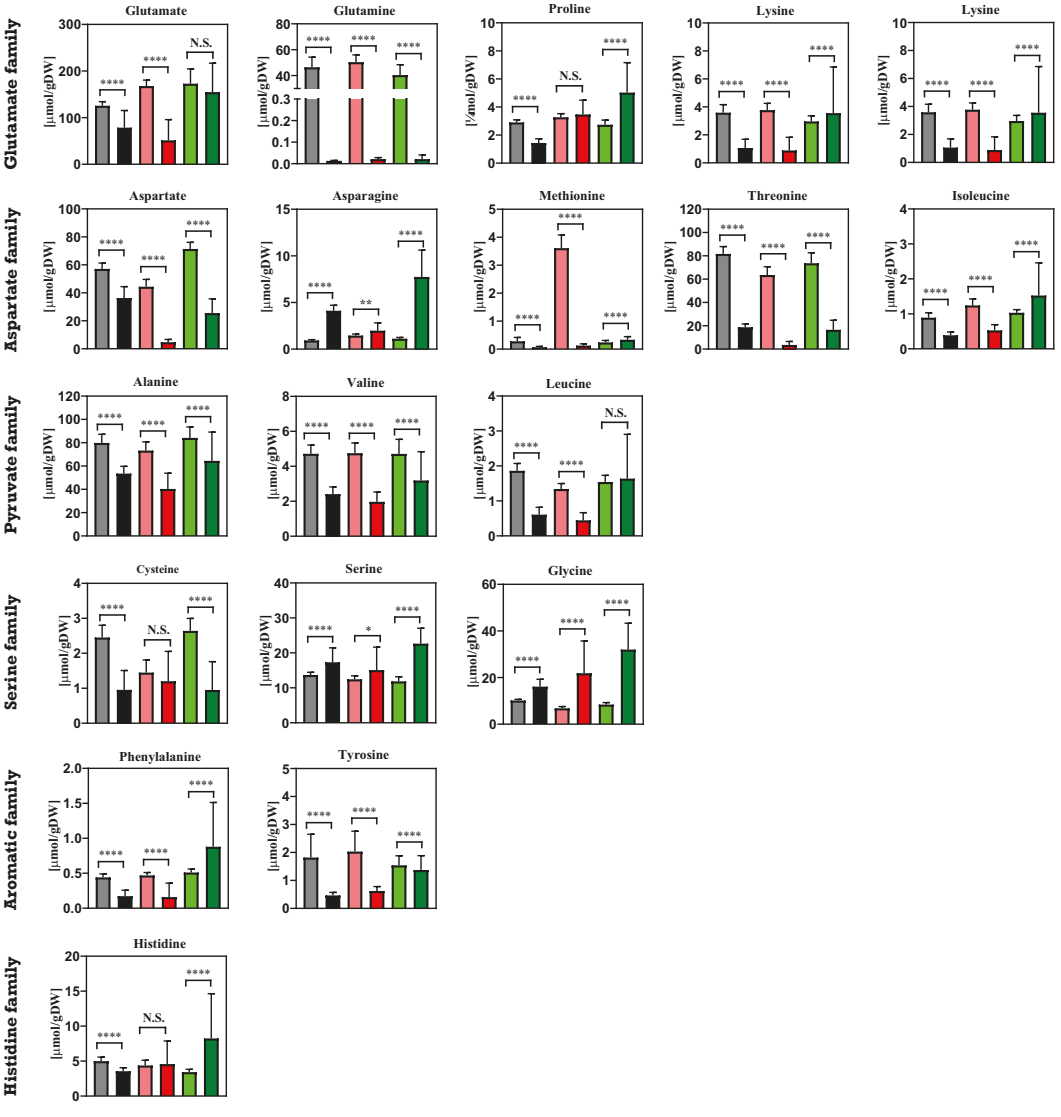

Figure 9. Intracellular amounts of amino acids in *Penicillium chrysogenum* Wisconsin 54-1255, *Penicillium chrysogenum* Δ*tps1* and *Penicillium chrysogenum* Δ*tps2* strains under both steady state conditions and feast/famine conditions. Amino acids were classified into six families, which are derived from the same precursors in the central carbon metabolism. Under steady state conditions, samples were taken at each residence time and datasets were collected from triplicate experiments, while under rapid feast/famine conditions, samples were rapidly taken within a feeding cycle time of 6 min twice for each experiment. The datasets are shown as average value ± standard deviation. The numbers of data points for steady state conditions and feast/famine conditions are 30 and 36, respectively. A two-tailed Student's *t*-test was conducted * $p < 0.05$ (significant) and **** $p < 0.01$ (extremely significant) vs. WT using GraphPad Prism 8. N.S., not significant; N.A., not available. ▮ WT steady state conditions; ▮ WT feast/famine conditions; ▮ Δ*tps1* steady state conditions; ▮ Δ*tps1* feast/famine conditions ▮ Δ*tps2* steady state conditions; ▮ Δ*tps2* feast/famine conditions. The results from steady state conditions were obtained from Wang et al. (2019) [24].

Table 2. Comparison of mass action ratios for phosphoglucose isomerase (PGI) and fumarase of different *Penicillium chrysogenum* strains obtained from both steady state conditions and feast/famine cultures at the average dilution rate of 0.05 h^{-1} in the time range of 100–200 h of cultivation. Measurements are given as average ± standard deviation of at least two individual experiments.

		Wisconsin 54-1255	***P. chrysogenum*-Δ*tps1***	***P. chrysogenum*-Δ*tps2***
Steady state conditions	F6P/G6P	0.25 ± 0.02	0.25 ± 0.02	0.33 ± 0.03
	malate/fumarate	1.56 ± 0.14	3.07 ± 0.55	1.51 ± 0.06
Feast/famine conditions	F6P/G6P	0.68 ± 0.05	1.34 ± 0.16	1.02 ± 0.22
	malate/fumarate	5.18 ± 0.21	4.95 ± 0.33	4.93 ± 0.78

The significant increase in these MARs indicated that the flux through these key nodes is reduced or even reversed under feast/famine conditions. This has also been reported in our previous work [8], which shows that the intracellular metabolite pool was first increased and then decreased during the feast/famine cycle. The MARs can be increased above their equilibrium values during the famine phase [8]. Nonetheless, under feast/famine conditions, the q_s values did not decrease but increased in the engineered strains (Table 1). Combining the above results, this indicated that there might be triggered an increased ATP-consuming futile cycling under feast/famine conditions through forming a cycling flux between the pentose phosphate (PP) pathway and the reversed Embden–Meyerhof–Parnas (EMP) pathway [9]. To corroborate this, the intracellular amounts of 6PG were significantly increased under feast/famine conditions, as compared to the steady state scenario. Furthermore, this futile cycling might become much more enhanced for the engineered *P. chrysogenum* strains lacking an intact trehalose storage pool and possessing a reduced pool size of other stored carbohydrates (Figure 8), e.g., mannitol, arabitol and erythritol, because upon the repetitive glucose pulses given by block-wise feeding there is no extra stored carbon pool to alleviate the perturbation of the whole metabolic system. As a result, more carbon and thus energy can be wasted in this futile cycling, which would lead to increased maintenance requirements and thus reduced biomass yield and productivity. In the future, this metabolic rearrangement should be confirmed by ^{13}C metabolic flux analysis.

4. Conclusions

In the present study, the physiological role of the trehalose metabolism has been explored by cultivating *P. chrysogenum* Wisconsin 54-1255 (wild type), *P. chrysogenum*-Δ*tps1* and *P. chrysogenum*-Δ*tps2* strains in the chemostat cultivation where the glucose feast/famine cycles were imposed. The results clearly showed that the absence of intact trehalose metabolism gave rise to a loss of penicillin production capacity under dynamic conditions, which might be caused by the enhanced maintenance requirement. Additionally, this increased maintenance cost may be caused by triggering a reversed EMP–PPP futile cycle. Meanwhile, the shrinkage of the metabolite pools and the partial loss of enzyme capacity under rapid feast/famine cycles might contribute as a generic mechanism to the metabolic productivity. Furthermore, we could thus conclude that trehalose is indispensable to maintaining the balanced metabolic state and thus high penicillin production capacity under both steady state and feast/famine conditions. However, one should be aware that the detailed physiological role of trehalose in this industrial-relevant *P. chrysogenum* strain should be further investigated via more cell physiology studies, e.g., in more sophisticated and representative scale-down simulators.

Author Contributions: Conceptualization, G.W.; methodology, G.W., J.X; formal analysis, G.W., and X.W.; investigation, X.W., J.Z., G.W.; writing—original draft preparation, G.W.; writing—review and editing, G.W.; visualization, G.W., X.W; supervision, G.W., J.C., Y.Z.; project administration, G.W., Y.Z., J.X.; funding acquisition, G.W., Y.Z. All authors have read and agreed to the published version of the manuscript.

Funding: This research was funded by the National Natural Science Foundation of China grant number [31900073, 21978085], the Science and Technology Commission of Shanghai Municipality grant number [19ZR1413600] and the 111 Project grant number [B18022].

Institutional Review Board Statement: Not applicable.

Informed Consent Statement: Not applicable.

Data Availability Statement: The data presented in this study are available on request from the corresponding author.

Conflicts of Interest: The authors declare no conflict of interest.

References

1. Guzman-Chavez, F.; Zwahlen, R.D.; Bovenberg, R.A.L.; Driessen, A.J.M. Engineering of the Filamentous Fungus *Penicillium chrysogenum* as Cell Factory for Natural Products. *Front. Microbiol.* **2018**, *9*, 2768. [CrossRef]
2. Nielsen, J.C.; Grijseels, S.; Prigent, S.; Ji, B.; Dainat, J.; Nielsen, K.F.; Frisvad, J.C.; Workman, M.; Nielsen, J. Global analysis of biosynthetic gene clusters reveals vast potential of secondary metabolite production in *Penicillium* species. *Nat. Microbiol.* **2017**, *2*, 17044. [CrossRef] [PubMed]
3. Wehrs, M.; Tanjore, D.; Eng, T.; Lievense, J.; Pray, T.R.; Mukhopadhyay, A. Engineering Robust Production Microbes for Large-Scale Cultivation. *Trends Microbiol.* **2019**, *27*, 524–537. [CrossRef] [PubMed]
4. Wang, G.; Haringa, C.; Tang, W.; Noorman, H.; Chu, J.; Zhuang, Y.; Zhang, S. Coupled metabolic-hydrodynamic modeling enabling rational scale-up of industrial bioprocesses. *Biotechnol. Bioeng.* **2020**, *117*, 844–867. [CrossRef] [PubMed]
5. Wang, G.; Haringa, C.; Noorman, H.; Chu, J.; Zhuang, Y. Developing a Computational Framework To Advance Bioprocess Scale-Up. *Trends Biotechnol.* **2020**, *38*, 846–856. [CrossRef]
6. Paul, K.; Herwig, C. Scale-down simulators for mammalian cell culture as tools to access the impact of inhomogeneities occurring in large-scale bioreactors. *Eng. Life Sci.* **2020**, *20*, 197–204. [CrossRef]
7. Lara, A.R.; Galindo, E.; Ramirez, O.T.; Palomares, L.A. Living with heterogeneities in bioreactors: Understanding the effects of environmental gradients on cells. *Mol. Biotechnol.* **2006**, *34*, 355–381. [CrossRef]
8. Wang, G.; Zhao, J.; Haringa, C.; Tang, W.; Xia, J.; Chu, J.; Zhuang, Y.; Zhang, S.; Deshmukh, A.T.; van Gulik, W.; et al. Comparative performance of different scale-down simulators of substrate gradients in *Penicillium chrysogenum* cultures: The need of a biological systems response analysis. *Microb. Biotechnol.* **2018**, *11*, 486–497. [CrossRef]
9. Wang, G.; Wu, B.; Zhao, J.; Haringa, C.; Xia, J.; Chu, J.; Zhuang, Y.; Zhang, S.; Heijnen, J.J.; van Gulik, W.; et al. Power input effects on degeneration in prolonged penicillin chemostat cultures: A systems analysis at flux, residual glucose, metabolite, and transcript levels. *Biotechnol. Bioeng.* **2018**, *115*, 114–125. [CrossRef]
10. Wang, G.; Chu, J.; Zhuang, Y.; van Gulik, W.; Noorman, H. A dynamic model-based preparation of uniformly-(13)C-labeled internal standards facilitates quantitative metabolomics analysis of *Penicillium chrysogenum*. *J. Biotechnol.* **2019**, *299*, 21–31. [CrossRef]
11. Vasilakou, E.; van Loosdrecht, M.C.M.; Wahl, S.A. *Escherichia coli* metabolism under short-term repetitive substrate dynamics: Adaptation and trade-offs. *Microb. Cell Fact.* **2020**, *19*, 116. [CrossRef] [PubMed]
12. Hakkaart, X.; Liu, Y.; Hulst, M.; El Masoudi, A.; Peuscher, E.; Pronk, J.; van Gulik, W.; Daran-Lapujade, P. Physiological responses of *Saccharomyces cerevisiae* to industrially relevant conditions: Slow growth, low pH, and high CO_2 levels. *Biotechnol. Bioeng.* **2020**, *117*, 721–735. [CrossRef] [PubMed]
13. Wright, N.R.; Wulff, T.; Palmqvist, E.A.; Jorgensen, T.R.; Workman, C.T.; Sonnenschein, N.; Ronnest, N.P.; Herrgard, M.J. Fluctuations in glucose availability prevent global proteome changes and physiological transition during prolonged chemostat cultivations of *Saccharomyces cerevisiae*. *Biotechnol. Bioeng.* **2020**. [CrossRef] [PubMed]
14. Kuschel, M.; Takors, R. Simulated oxygen and glucose gradients as a prerequisite for predicting industrial scale performance a priori. *Biotechnol. Bioeng.* **2020**, *117*, 2074–2088. [CrossRef] [PubMed]
15. Ankenbauer, A.; Schafer, R.A.; Viegas, S.C.; Pobre, V.; Voss, B.; Arraiano, C.M.; Takors, R. *Pseudomonas putida* KT2440 is naturally endowed to withstand industrial-scale stress conditions. *Microb. Biotechnol.* **2020**, *13*, 1145–1161. [CrossRef] [PubMed]
16. de Jonge, L.P.; Buijs, N.A.; ten Pierick, A.; Deshmukh, A.; Zhao, Z.; Kiel, J.A.; Heijnen, J.J.; van Gulik, W.M. Scale-down of penicillin production in *Penicillium chrysogenum*. *Biotechnol. J.* **2011**, *6*, 944–958. [CrossRef] [PubMed]
17. De Jonge, L.P.; Buijs, N.A.; Heijnen, J.J.; van Gulik, W.M.; Abate, A.; Wahl, S.A. Flux response of glycolysis and storage metabolism during rapid feast/famine conditions in *Penicillium chrysogenum* using dynamic (13) C labeling. *Biotechnol. J.* **2014**, *9*, 372–385. [CrossRef]
18. Zhao, Z.; Ten Pierick, A.; de Jonge, L.; Heijnen, J.J.; Wahl, S.A. Substrate cycles in *Penicillium chrysogenum* quantified by isotopic non-stationary flux analysis. *Microb. Cell Fact.* **2012**, *11*, 140. [CrossRef]
19. Elbein, A.D.; Pan, Y.T.; Pastuszak, I.; Carroll, D. New insights on trehalose: A multifunctional molecule. *Glycobiology* **2003**, *13*, 17r–27r. [CrossRef]
20. Wiemken, A. Trehalose in yeast, stress protectant rather than reserve carbohydrate. *Antonie Leeuwenhoek* **1990**, *58*, 209–217. [CrossRef]

21. Thevelein, J.M.; Hohmann, S. Trehalose synthase: Guard to the gate of glycolysis in yeast? *Trends Biochem Sci.* **1995**, *20*, 3–10. [CrossRef]
22. Teusink, B.; Walsh, M.C.; van Dam, K.; Westerhoff, H.V. The danger of metabolic pathways with turbo design. *Trends Biochem. Sci.* **1998**, *23*, 162–169. [CrossRef]
23. Van Heerden, J.H.; Wortel, M.T.; Bruggeman, F.J.; Heijnen, J.J.; Bollen, Y.J.; Planque, R.; Hulshof, J.; O'Toole, T.G.; Wahl, S.A.; Teusink, B. Lost in transition: Start-up of glycolysis yields subpopulations of nongrowing cells. *Science* **2014**, *343*, 1245114. [CrossRef] [PubMed]
24. Wang, G.; Zhao, J.F.; Wang, X.X.; Wang, T.; Zhuang, Y.P.; Chu, J.; Zhang, S.L.; Noorman, H.J. Quantitative metabolomics and metabolic flux analysis reveal impact of altered trehalose metabolism on metabolic phenotypes of *Penicillium chrysogenum* in aerobic glucose-limited chemostats. *Biochem. Eng. J.* **2019**, *146*, 41–51. [CrossRef]
25. Douma, R.D.; Deshmukh, A.T.; de Jonge, L.P.; de Jong, B.W.; Seifar, R.M.; Heijnen, J.J.; van Gulik, W.M.J.B. Novel insights in transport mechanisms and kinetics of phenylacetic acid and penicillin-G in *Penicillium chrysogenum*. *Biotechnol. Prog.* **2012**, *28*, 337–348. [CrossRef] [PubMed]
26. Douma, R.D.; Verheijen, P.J.; de Laat, W.T.; Heijnen, J.J.; van Gulik, W.M. Dynamic gene expression regulation model for growth and penicillin production in *Penicillium chrysogenum*. *Biotechnol. Bioeng.* **2010**, *106*, 608–618. [CrossRef]
27. Wang, G.; Wang, X.; Wang, T.; van Gulik, W.; Noorman, H.J.; Zhuang, Y.; Chu, J.; Zhang, S. Comparative Fluxome and Metabolome Analysis of Formate as an Auxiliary Substrate for Penicillin Production in Glucose-Limited Cultivation of *Penicillium chrysogenum*. *Biotechnol. J.* **2019**, *14*, e1900009. [CrossRef]
28. Li, C.; Shu, W.; Wang, S.; Liu, P.; Zhuang, Y.; Zhang, S.; Xia, J. Dynamic metabolic response of *Aspergillus niger* to glucose perturbation: Evidence of regulatory mechanism for reduced glucoamylase production. *J. Biotechnol.* **2018**, *287*, 28–40. [CrossRef]
29. Liu, X.; Sun, X.; He, W.; Tian, X.; Zhuang, Y.; Chu, J. Dynamic changes of metabolomics and expression of candicidin biosynthesis gene cluster caused by the presence of a pleiotropic regulator AdpA in Streptomyces ZYJ-6. *Bioproc. Biosyst. Eng.* **2019**, *42*, 1353–1365. [CrossRef]
30. Verheijen, P.J. Data reconciliation and error detection. In *The Metabolic Pathway Engineering Handbook*; CRC Press: Boca Raton, FL, USA, 2010; Volume 8, pp. 1–12.
31. Loffler, M.; Simen, J.D.; Jager, G.; Schaferhoff, K.; Freund, A.; Takors, R. Engineering *E. coli* for large-scale production—Strategies considering ATP expenses and transcriptional responses. *Metab. Eng.* **2016**, *38*, 73–85. [CrossRef]
32. Simen, J.D.; Loffler, M.; Jager, G.; Schaferhoff, K.; Freund, A.; Matthes, J.; Muller, J.; Takors, R.; RecogNice, T. Transcriptional response of *Escherichia coli* to ammonia and glucose fluctuations. *Microb. Biotechnol.* **2017**, *10*, 858–872. [CrossRef] [PubMed]
33. Lahtvee, P.J.; Seiman, A.; Arike, L.; Adamberg, K.; Vilu, R. Protein turnover forms one of the highest maintenance costs in *Lactococcus lactis*. *Microbiology* **2014**, *160*, 1501–1512. [CrossRef] [PubMed]
34. Chatterji, D.; Ojha, A.K. Revisiting the stringent response, ppGpp and starvation signaling. *Curr. Opin. Microbiol.* **2001**, *4*, 160–165. [CrossRef]
35. Douma, R.D.; Batista, J.M.; Touw, K.M.; Kiel, J.A.; Krikken, A.M.; Zhao, Z.; Veiga, T.; Klaassen, P.; Bovenberg, R.A.; Daran, J.M.; et al. Degeneration of penicillin production in ethanol-limited chemostat cultivations of *Penicillium chrysogenum*: A systems biology approach. *BMC Syst. Biol.* **2011**, *5*, 132. [CrossRef] [PubMed]
36. Rodriguez-Saiz, M.; Barredo, J.L.; Moreno, M.A.; Fernandez-Canon, J.M.; Penalva, M.A.; Diez, B. Reduced function of a phenylacetate-oxidizing cytochrome p450 caused strong genetic improvement in early phylogeny of penicillin-producing strains. *J. Bacteriol.* **2001**, *183*, 5465–5471. [CrossRef] [PubMed]
37. Alvarez, E.; Meesschaert, B.; Montenegro, E.; Gutiérrez, S.; Díez, B.; Barredo, J.L.; Martín, J.F. The isopenicillin-N acyltransferase of *Penicillium chrysogenum* has isopenicillin-N amidohydrolase, 6-aminopenicillanic acid acyltransferase and penicillin amidase activities, all of which are encoded by the single penDE gene. *Eur. J. Biochem.* **1993**, *215*, 323–332. [CrossRef]
38. Deshmukh, A.T.; Verheijen, P.J.; Seifar, R.M.; Heijnen, J.J.; van Gulik, W.M. In vivo kinetic analysis of the penicillin biosynthesis pathway using PAA stimulus response experiments. *Metab. Eng.* **2015**, *32*, 155–173. [CrossRef]
39. Van Gulik, W.M.; Antoniewicz, M.R.; deLaat, W.T.A.M.; Vinke, J.L.; Heijnen, J.J. Energetics of growth and penicillin production in a high-producing strain of *Penicillium chrysogenum*. *Biotechnol. Bioeng.* **2001**, *72*, 185–193. [CrossRef]
40. Jansen, M.L.; Diderich, J.A.; Mashego, M.; Hassane, A.; de Winde, J.H.; Daran-Lapujade, P.; Pronk, J.T. Prolonged selection in aerobic, glucose-limited chemostat cultures of *Saccharomyces cerevisiae* causes a partial loss of glycolytic capacity. *Microbiology* **2005**, *151*, 1657–1669. [CrossRef]
41. Wu, L.; Mashego, M.; Proell, A.; Vinke, J.; Ras, C.; Vandam, J.; Vanwinden, W.; Vangulik, W.; Heijnen, J. In vivo kinetics of primary metabolism in *Saccharomyces cerevisiae* studied through prolonged chemostat cultivation. *Metab. Eng.* **2006**, *8*, 160–171. [CrossRef]

processes

MDPI

Article

Synbiotic Fermented Milk with Double Fortification (Fe-Zn) as a Strategy to Address Stunting: A Randomized Controlled Trial among Children under Five in Yogyakarta, Indonesia

Siti Helmyati [1,2,*], Karina Muthia Shanti [3], Fahmi Tiara Sari [3], Martha Puspita Sari [3], Dominikus Raditya Atmaka [4], Rio Aditya Pratama [5], Maria Wigati [2], Setyo Utami Wisnusanti [1,2], Fatma Zuhrotun Nisa' [1,2] and Endang Sutriswati Rahayu [6]

[1] Department of Nutrition and Health, Faculty of Medicine, Public Health and Nursing, Universitas Gadjah Mada, Yogyakarta 55281, Indonesia; setyo.utami.w@ugm.ac.id (S.U.W.); fatma.znisa@gmail.com (F.Z.N.)
[2] Center for Health and Human Nutrition, Faculty of Medicine, Public Health and Nursing, Universitas Gadjah Mada, Yogyakarta 55281, Indonesia; maria.wigati@mail.ugm.ac.id
[3] Department of Biostatistics, Epidemiology and Population Health, Faculty of Medicine, Public Health and Nursing, Universitas Gadjah Mada, Yogyakarta 55281, Indonesia; karinamuthia.s@gmail.com (K.M.S.); fahmi.tiara.sari@gmail.com (F.T.S.); martha.puspita6@gmail.com (M.P.S.)
[4] Faculty of Public Health, Airlangga University, Surabaya 60115, Indonesia; dominikus.raditya@fkm.unair.ac.id
[5] Study Program of Public Health Science, Specialization of Health Informatics System, Faculty of Medicine, Public Health and Nursing, Universitas Gadjah Mada, Yogyakarta 55281, Indonesia; rioadityapratama@outlook.com
[6] Faculty of Agricultural Technology, Universitas Gadjah Mada, Yogyakarta 55281, Indonesia; endangsrahayu@ugm.ac.id
* Correspondence: siti.helmyati@gmail.com; Tel.: +62-274-547775

Citation: Helmyati, S.; Shanti, K.M.; Sari, F.T.; Sari, M.P.; Atmaka, D.R.; Pratama, R.A.; Wigati, M.; Wisnusanti, S.U.; Nisa', F.Z.; Rahayu, E.S. Synbiotic Fermented Milk with Double Fortification (Fe-Zn) as a Strategy to Address Stunting: A Randomized Controlled Trial among Children under Five in Yogyakarta, Indonesia. *Processes* **2021**, *9*, 543. https://doi.org/10.3390/pr9030543

Academic Editors: Maria Tufariello and Francesco Grieco

Received: 29 January 2021
Accepted: 25 February 2021
Published: 19 March 2021

Abstract: Stunting is one of the public health problems that has yet to be solved in Indonesia. This study developed synbiotic fermented milk with iron and zinc fortification that was then tested in a clinical setting. The product was made from skimmed milk and fructooligosaccharides (FOS) and fermented with *Lactobacillus plantarum*. A sample of 94 stunted children under five years old were randomly assigned to intervention or control groups. The intervention group received double-fortified synbiotic milk, while the control group drank non-fortified milk. After three months, the number of normal children in both groups, according to weight- or height-for-age z-score category, was found to be increasing. However, the difference between the two groups was not significant ($p > 0.05$). The study suggests that fermented milk may have a good effect on child growth. Further research is needed to deepen the potency of synbiotic fermented milk for stunted children.

Keywords: children; double fortification; fermented milk; iron and zinc; stunting; synbiotic

1. Introduction

Developing countries are known for their complex public health problems, including stunting. Globally, it is estimated that 171 million children under five are stunted. Although this number lowered to 149 million children in 2019, stunting remains one of the serious global health challenges that need to be solved. This problem is also happening in Indonesia as one of the developing countries [1–3]. The prevalence of stunting among Indonesian children under five reached 30.8% in 2018. This situation is highly varied in each of the 34 provinces—for example, in East Nusa Tenggara, the stunting prevalence has reached more than 40% [4]. This alarming number emphasizes the need for innovative approaches to combat stunting [5,6].

Stunting is marked by diminished nutritional status and quality of life. Prendergast and Humphrey [7] mentioned that stunting in children is associated with morbidity and mortality, low physical and economic capacity, and an increased risk of metabolic disease in

adulthood. This is supported by a study in Indonesia that showed stunting was associated with disease incidence, family income, and parental education [8]. It is estimated that stunting in developing countries costs 13.5% of Gross Domestic Product (GDP) per capita. A one-point increase of child stunting led to a 0.4% reduction of GDP per capita [9].

Stunting is closely related to inadequate nutritional intake. According to Blaney et al. [10], more than 50% of Indonesian children have low energy, likely due to poor iron, zinc, and calcium intake per AKG (*Angka Kecukupan Gizi* or Indonesian Nutrition Adequacy Rate). These are essential minerals that play key roles in human growth [11–13]. The combination of iron and zinc can increase height by 1.1 cm above the standard growth of children [14]. This is in accordance with a meta-analysis by Liu et al. [15] which provided evidence of the potency of zinc supplementation to prevent stunting. Zinc supplementation given after birth can increase height by 0.23 cm and when given to children above 2 years old can increase their height by 1.37 cm. On the other hand, iron supplementation is known to prevent iron deficiency anemia. Larson et al. [16] suggested a strong association between iron supplementation and increased hemoglobin levels and mental development among children. Research on the benefits of zinc and iron combination intake on children's growth is scarce. It is strategic to conduct a clinical trial on the effect of iron and zinc consumption on stunted children in the form of food fortification.

Food fortification is a cost-effective effort to tackle the problem of micronutrient deficiencies [17,18]. Cost-effectiveness is generally defined as the affordable cost to achieve a certain outcome. In this article, it means the cost to avert one case of stunting among children under five. It can also be calculated as the cost per disability-adjusted life-year (DALY) saved [18]. Cost-effectiveness is related to other types of interventions. An analysis in 48 countries showed that food fortification would cost between USD 1 and USD 134 per DALY saved [19].

We planned to develop functional foods by fortifying fermented milk with iron and zinc. Fermented milk was chosen as the vehicle to increase its nutritional value. A meta-analysis by Matsuyama et al. [20] revealed that fortified milk could lower the risk of anemia but could not increase height. On the other hand, several studies about fermented milk development showed its positive effects on health [21–24]. A clinical trial with 494 children in Indonesia demonstrated beneficial effects in that the consumption of probiotics modestly increased weight and height [25]. Onubi et al. [26] suggested that probiotic consumption is beneficial to improving child growth in developing countries. The fermentation process in milk is also essential since it will be fortified with iron and zinc. A higher intake of iron is associated with various side effects including diarrhea, increasing pathogens, and other inflammatory diseases in the gut [27,28]. Lin et al. [29] mentioned that consumption of probiotic and prebiotic could ameliorate those side effects. The presence of pre- and probiotics in diets, called synbiotic foods, which are good to the gut microbiota balance, can reduce the likelihood of micronutrient utilization by pathogenic bacteria in the colon and increase nutrients absorption [30].

Fermented milk with double fortification has potential as a functional food to promote children's growth. Bearing the complex causes of stunting among children under five, the innovation of food development is essential to support stunting management programs in the country. We carried out this research and aimed to determine the effect of synbiotic fermented milk with double fortification on the height and nutritional status of stunted children in Indonesia. We expected this research to give a novel evidence-based intervention for Indonesia and the other low- and middle-income countries which face the same problem, stunting.

2. Materials and Methods

2.1. Subjects and Design of the Study

The study was conducted between May 2017 and October 2018 among under-5-year-olds in Seyegan District, Yogyakarta Province, Indonesia. Informed consent was obtained from the parents or guardians of the children. The Medical and Health Ethics Committee of

the Faculty of Medicine, Public Health and Nursing, Universitas Gadjah Mada gave ethical permission with the reference no. KE/FK/0640/EC/2017. The study is also registered in ClinicalTrial.gov no NCT03495401.

The study used a double-blind, randomized, controlled trial design. There were three main parts: screening, intervention, and a follow-up phase. Screening was conducted with inclusion and exclusion criteria (n = 212). The inclusion criteria were children aged between 2 and 5 years old and categorized as stunted, according to the height-for-age z-score (HAZ < −2 standard deviation). Exclusion criteria were one or more congenital abnormalities, chronic disease, presence of edema or weight-for-height z-score (WHZ) below −3SD, and allergy to milk, iron, or zinc supplements. There were 7 children who refused to be measured, 101 who did not meet the inclusion criteria, and 10 who refused to participate. The subjects were then randomly divided into the intervention (n = 47) and control groups (n = 47). In the intervention phase, the researchers gave synbiotic fermented milk with double fortification (Fe-Zn) to the intervention group and the same milk without fortification to the control group for three months. In the middle of the study, nine subjects from the intervention group and four from the control group dropped out. Anthropometric measurements were conducted twice, namely before and after intervention. Dietary intake was assessed eight times throughout the intervention phase. The number of subjects who remained through the entire study were 38 children from the intervention group and 43 from the control group. The baseline characteristics can be seen in Table 1.

Table 1. Baseline sociodemographic characteristics.

Characteristics	Intervention Group n = 38	Control n = 43	*p*
Age (months) (n, %)			
24–35 months	18 (47)	20 (47)	
36–47 months	11 (29)	10 (23)	0.345 [a]
48–59 months	9 (24)	13 (30)	
Birth weight (gram) (n, %)			
<2500	10 (26)	4 (9)	0.347 [a]
≥2500	28 (74)	39 (91)	
Birth length (cm) (n, %)			
Unknown	0 (0)	1 (2)	
<48	14 (37)	11 (26)	0.700 [b]
≥48	24 (63)	31 (72)	
Sex (n, %)			
Male	21 (55)	22 (51)	0.712 [a]
Female	17 (45)	21 (49)	
Number of sibling (n, %)			
0–1	12 (31)	9 (21)	0.291 [a]
2–3	25 (66)	31 (72)	
≤4	1 (3)	3 (7)	
Mothers' educational level (n, %)			
Did not attend school	0 (0)	0 (0)	
Elementary school	3 (8)	2 (5)	
Junior high school	11 (29)	9 (20)	0.723 [a]
Senior high school	22 (58)	30 (70)	
Bachelor	2 (5)	2 (5)	

Table 1. *Cont.*

Characteristics	Intervention Group n = 38	Control n = 43	*p*
Fathers' educational level (n, %)			
Did not attend school	1 (3)	0 (0)	0.498 [b]
Elementary school	5 (13)	4 (9)	
Junior high school	10 (26)	10 (23)	
Senior high school	19 (50)	28 (65)	
Bachelor	3 (8)	1 (3)	
Household income (IDR) (n, %)			
<1,000,000	4 (10)	5 (12)	0.347 [b]
1,000,000–<1,500,000	17 (45)	13 (30)	
1,500,000–<2,000,000	6 (16)	14 (33)	
2,000,000–<2,500,000	3 (8)	7 (16)	
2,500,000–<3,000,000	2 (5)	0 (0)	
≤3,000,000	6 (16)	4 (9)	
Episode of illness (past 3 months) (n, %)			
0	8 (21)	9 (21)	0.853 [a]
1	15 (39)	16 (37)	
2	12 (32)	12 (28)	
3	3 (8)	6 (14)	
Illness duration (days) (n, %)			
0	8 (21)	9 (21)	0.482 [a]
1–5	11 (29)	16 (37)	
6–10	8 (21)	10 (23)	
11–15	6 (16)	4 (9)	
16–20	2 (5)	1 (2)	
<20	3 (8)	3 (7)	
Height-for-age z-score categories (HAZ) (n, %)			N/A
Stunted	38 (100)	43 (100)	
Normal	0 (0)	0 (0)	
Weight-for-age z-score categories (WAZ) (n, %)			0.246 [a]
Underweight	19 (50)	27 (63)	
Normal	19 (50)	16 (37)	

N/A, not available; [a] chi-squared test; [b] Fisher's exact test; significant if $p < 0.05$; intervention group, subjects given synbiotic fermented milk fortified with iron and zinc; control, subjects given synbiotic fermented milk without fortification.

2.2. Production of Synbiotic Fermented Milk with Double Fortification (Fe-Zn)

The researchers collaborated with CV Violla Foods to produce synbiotic fermented milk with and without fortification. Ingredients consisted of skim milk, sugar, probiotic *Lactobacillus plantarum* (*L. plantarum*), prebiotic fructooligosaccharides (FOS), iron fortificant (ferrous sulfate, Merck, Branchburg, NJ, USA), and zinc fortificant (zinc acetate, Merck). The skim milk (Lactona, Yogyakarta, Indonesia) and sugar (Gulaku, Lampung, Indonesia) were procured from the local public market in Yogyakarta, the probiotic was obtained from the Food and Nutrition Culture Collection at Universitas Gadjah Mada, and the prebiotic was from Beneo Orafti, Indonesia. Skim milk is commonly used as an ingredient for making fermentation products. Before we carried out this research, we conducted trials by comparing skim milk, whole milk, and ultra-high-temperature milk as the main ingredient. We concluded that using skim milk will have better consistency and sensory characteristics that the other two. In line with our trials, several studies mentioned the advantages of using skim milk including lower price and a positive relation with probiotic viability and fermented milk flavor [31–33].

The steps in the process to make synbiotic fermented milk were as follows: (1) dissolve sugar, skim milk, and add FOS and fortificants into water; (2) sterilize; (3) inoculate *L. plantarum*; and (4) incubate. CV Violla Foods had the authority to encode the milk, and the code was not known to the research team. The code was revealed only after the research ended. All types of milk were packed in 100 mL bottles and had the same color, flavor, and taste so that participants could not differentiate the products. Before the study began, we made sure that all subjects had received deworming medication to minimize the potential effects of worm infection. The participants consumed synbiotic fermented milk every day for three months. Considering the study subjects are children, we did not give rigid dietary rules but advised the parents to not change the dietary habits of their children during the study. Children were permitted to consume the milk at any meal each day. Each bottle of synbiotic fermented milk with double fortification contained 79.93 kcal energy, 2.26 g protein, 1.95 g fat, 13.67 g carbohydrate, 1.27 g crude fiber, 90 mg calcium, 2.26 mg iron, 1.22 mg zinc, and 3.23×10^8 CFU/mL *L. plantarum*. Synbiotic fermented milk without fortification contained 85.75 kcal energy, 2.05 g protein, 1.51 g fat, 16.44 g carbohydrate, 0.74 g crude fiber, 88 mg calcium, 0.73 mg iron, 0.18 mg zinc, and 3.19×10^8 CFU/mL *L. plantarum*.

2.3. Socio-Demographic Characteristics Assessment

Socio-demographic characteristics were collected from the parents or guardians of the subjects using questionnaires before the intervention began. The variables assessed were birth weight, birth length, sex, number of siblings, parents' educational levels, household income, illness frequency in the last three months, and illness duration. The variability of these factors between the two groups was assessed.

2.4. Anthropometry Measurements

Body weight and height were measured before and after the intervention phase using a standardized procedure [34]. The weights of the children were assessed using a digital weight scale (GEA Medical, Jakarta, Indonesia) with an accuracy of 0.1 kg; the height was measured using a microtoise with an accuracy of 0.1 cm. We assessed HAZ and WAZ to categorize the nutritional status of the subjects.

2.5. Dietary Intake Assessment

Dietary intake information was collected using 24-h food recall from the parents or guardians of the children. Trained enumerators conducted eight recalls in non-consecutive time with a range of 1–2 weeks for each assessment. The enumerators used a food model book to help with data collection. NutriSurvey software was used to analyze dietary data consumed by the subjects as energy, carbohydrates, protein, fat, iron, and zinc.

2.6. Statistical Analysis

Data were analyzed using STATA 13. Baseline characteristics were written as categorical data, then assessed using a chi-squared test or Fisher's exact test. A chi-square test was used to compare categorical data between the intervention and control groups; if the chi-square assumption could not be fulfilled (there is an expected value < 5 in the cell), then we used Fisher's Exact test [35]. Normality of the data was determined using the Shapiro–Wilk Test. Normally distributed data are presented as a mean ± standard deviation (SD) while abnormally distributed data are presented as a median (interquartile range). For normal data, the mean difference between the intervention and control groups was measured using an independent *t*-test. The mean difference between pre- and post-intervention was assessed using the paired *t*-test. For data that were not normally distributed, the Mann–Whitney U test was used instead of the independent *t*-test, and the Friedman test instead of the paired *t*-test. The differences in the nutritional status categories between the intervention and control groups were evaluated using the chi-squared test

or Fisher's exact test. Multiple linear regression was also used to assess the influence of several nutrients on subjects' nutritional status according to HAZ.

3. Results

Ninety-four (n = 94) children under five years of age were divided into two groups: intervention and control. Throughout the research, four subjects dropped out from the control group and nine dropped out from the intervention group. Subject characteristics were evenly distributed between the two groups. In the current study, the age of the subjects ranged from 24 to 59 months with the number of boys and girls nearly equal. More than 50% of the subjects had birth lengths of 48 cm and birth weights of more than 2500 g. The complete results can be seen in Table 1.

After drinking synbiotic fermented milk for three months, the heights and weights of the subjects remained nearly the same. Table 2 shows that there was no difference in nutritional status between the intervention and control groups ($p > 0.05$), according to their HAZ and WAZ data.

Table 2. Height-for-age z-score (HAZ) and Weight-for-age z-score (WAZ) category after intervention.

	Nutritional Status	Intervention Group	Control	*p*
Height-for-age z-score (HAZ)				
Post-intervention	Stunted	29 (76)	39 (91)	0.078 [a]
	Normal	9 (24)	4 (9)	
Weight-for-age z-score (WAZ)				
Post-intervention	Underweight	15 (39)	26 (60)	0.059 [a]
	Normal	23 (61)	17 (40)	

Data presented in frequency n (%); [a] chi-squared Test; * significant at $p < 0.05$; intervention group, given synbiotic fermented milk fortified with iron and zinc; control, given synbiotic fermented milk without fortification.

In the preliminary phase of the intervention group, all 38 subjects were categorized as stunted. When the subjects were measured again three months after intervention, nine were categorized as normal according to height-for-age ($p < 0.05$). Six months after the intervention, 11 subjects had dropped out. Of these children, four were categorized as stunted in the past two measurements, and two as severely stunted. Two more were severely stunted before the intervention but improved to stunted after the intervention. Three subjects who were stunted before the intervention were re-categorized as normal afterwards. Although four subjects in the control group were also categorized as normal after the intervention, it was not considered statistically significant.

Table 3 shows there was a significant difference of energy, carbohydrates, protein, fat, and iron intake between the intervention and control groups. The intake was higher in the control group than in the intervention group.

Table 3. Comparison of dietary intake between intervention and control group.

Dietary Intake	Intervention Group	Control	*p*
Energy [2] (kcal)	1005.37 ± 197.86	1118.08 ± 189.48	0.011 [b]
Carbohydrate [2] (g)	130.03 ± 32.34	143.95 ± 26.82	0.037 [b]
Protein [2] (g)	32.32 ± 6.62	36.59 ± 8.76	0.016 [b]
Fat [2] (g)	41.85 ± 8.60	47.09 ± 10.59	0.017 [b]
Iron [1] (mg)	5.10 (2.4)	5.23 (2.07)	0.011 [a]
Zinc [1] (mg)	3.43 (1.42)	3.61 (1.56)	0.116 [a]

[1] Data presented in median (IQR); [2] data presented in mean ± standard deviation (SD); [a] Mann–Whitney U test; [b] independent *t*-test; significant if $p < 0.05$.

4. Discussion

The research subjects were stunted young children aged 2–5 years. After the subjects were randomized, there were some who dropped out during the study. The drop-out rate in the intervention group was 19.1%, while in the control group, it was 8.5%. According to Dumville et al. [36], the stunting level of the dropouts did not bias the results of the study. Statistical test results also showed no significant difference between subjects in the control group and the intervention group.

Synbiotic fermented milk in this study was fortified with as much as 2.26 mg (28% AKG) of iron and 1.22 mg (30% AKG) of zinc per 100 mL serving per day. In this study, the amount of fortification complied with the WHO Recommended Dietary Allowance (RDA), which mentions requirements for dairy products and their preparations in the range of 15–30% [18]. A study by Sazawal et al. [37] and El Menchawy et al. [38] also used 30% RDA for the amount of fortification added to milk, which proved to have a positive impact on growth. Antagonistic interactions between iron and zinc in research can be minimized with a ratio of iron to zinc of 1.8:1. Another study noted that iron and zinc fortification in milk formula, with a ratio of 1.3:1, had no effect on reducing zinc absorption [39]. Iron and zinc content of 1:1, however, can cause interactions that reduce the concentration of iron in the plasma, while a $\geq$ 2:1 ratio inhibits the absorption of zinc in the intestine [40].

Three months after being given the product, the bodyweight of subjects in the intervention group increased by 0.7 kg, while height increased by 2.58 cm. Weight and height gains in the control group were 0.6 kg and 2.5 cm. Based on the WHO Child Growth Standards, the increase in body weight and height of children aged 2–5 years over the course of three months ranged from 0.5 to 0.6 kg and 1.5 to 2.5 cm, respectively [41]. This shows that the results in both groups equaled or exceeded normal growth. Growth velocity of body weight and height in stunted children exceeded the speed of growth of children with normal height after the phase of growth restriction [42]. Every 1 cm in height was associated with a lower growth rate of 0.03 cm, and each one-unit increase in HAZ was associated with a decrease in growth speed of 0.08 standard deviation (SD) per year [43].

Nutrition intake, health status, and biological systems interact with each other [44]. The mechanisms underlying this interaction occur locally as well as systemically. The phase of stunted growth causes a decrease in the speed of cell proliferation and molecular changes. Increased levels of pro-inflammatory cytokines in the body can inhibit growth-promoting protein [45]. After this phase is completed, there is an increase in the speed of proliferation at the growth plate, or non-skeletal organs, beyond the normal speed according to age, because the organ feels a growth that is not in accordance with age [46].

Comparisons between weight, height, HAZ, and WAZ of the intervention and control groups did not show a significant difference. Various studies show inconsistent results related to the effect of micronutrient fortification on growth and growth indicators. This was not in accordance with the research of [47], which showed a significant difference in all growth indicators—body weight, height, WAZ, WHZ, and HAZ—in the larger group of children aged 1–4 years, given milk fortified with iron, zinc, and several other micronutrients for one year.

The provision of micronutrients showed mixed results on the growth of children. A meta-analysis by Ramakrishnan et al. [48] noted that iron and zinc supplements affected young children's height and weight gains, though the effect size was minor. Lind et al. [49] said that in his group, giving iron and zinc supplements had no effect on the HAZ after 12 months of intervention. Fahmida et al. [14] found a significant increase in HAZ and height compared to those given placebos, as well as stunted children given zinc after just 10 mg iron and 10 mg zinc supplements for four months. Iron and zinc produce varying effects on children's growth, especially those aged < 24 months who are not iron-deficient but, on the contrary, experience iron repletion. Iron repletion is negatively related to growth because iron in this condition can be a pro-oxidant that increases the number of pathogenic microorganisms [50].

Sufficient energy intake (≥80% RDA) was found to affect the HAZ. Energy plays a role in the synthesis of new tissue to form normal body composition, including adipose tissue, lean tissue, and skeletal tissue. The existence of a positive energy balance in the body can increase weight and height [51]. Micronutrients alone cannot support growth; the adequacy of macronutrients in the body also plays an important role. The lack of significant differences in growth between the intervention and control groups could be caused by the synbiotic milk given to both. Synbiotic milk contains energy of around 80 kcal/serving/day, and protein of around 2 g/serving/day that can support growth.

The addition of synbiotics to milk influences growth. A study by Sazawal et al. [47] showed a significant difference in the speed of weight gain that was greater in children who were given the synbiotic milk *Bifidobacterium lactis* HN019 and oligosaccharides compared to children who were given normal milk. Agustina et al. [25] stated that children who were given milk supplemented with *Lactobacillus reuteri* DSM 17938 for six months experienced significantly faster growth in body weight and height, and a significantly higher WAZ than those without probiotic supplementation. Another strain, *Lactobacillus plantarum* FNCC 260 from Indonesia, also has microbial activity against pathogens that is beneficial for gut health [52].

This study had several limitations. First, the duration was only three months. Although it is appropriate to measure height changes due to an intervention, it is difficult to conclude whether the effects of the intervention will continue. Secondly, the study group only consisted of the intervention and control groups. Both groups were given synbiotic fermented milk; the only difference was the presence of fortified iron and zinc. This design left the researchers without an exact conclusion regarding whether the synbiotic milk has a truly beneficial effect on growth, since the two groups' results were almost identical.

This study introduces an innovation to address stunting using a food-based approach. This research serves as the beginning of further studies in Indonesia, where many local resources can be utilized to address the country's nutritional problems. As a contribution to society, the development of the product in this study has been following the Innovator Innovation Indonesia Expo (*Inovator Inovasi Indonesia Expo*) in 2018 and is in the process of commercialization with the name of "Forty Milk".

5. Conclusions

There were no significant differences in height between the intervention and the control groups after they were given synbiotic milk, with or without double fortification (Fe-Zn). Nutritional status improvement according to HAZ and WAZ tended to be higher in the intervention group than in the control. However, statistical analysis revealed no significant difference observed, which suggests that the consumption of synbiotic milk alone had a good effect on the nutritional status of the children. Further study to include a third group who are not given fermented milk is needed for better comparison.

Author Contributions: Conceptualization, S.H. and E.S.R.; Supervision, S.H. and F.Z.N.; investigation, K.M.S., F.T.S., and M.P.S.; formal analysis, K.M.S., F.T.S., M.P.S., S.H., and M.W.; project administration and validation, D.R.A., R.A.P., and S.U.W.; writing—original draft K.M.S. and M.W. All authors have read and agreed to the published version of the manuscript.

Funding: This research was funded by the Indonesian Ministry of Research and Higher Education throughout *Hibah Penelitian Terapan Unggulan Perguruan Tinggi* on behalf of SH, grant number 1964/UN1/DITLIT/DIT-LIT/LT/2018.

Institutional Review Board Statement: The study was conducted according to the guidelines of the Declaration of Helsinki, and approved by the the Medical and Health Ethics Committee of the Faculty of Medicine, Public Health and Nursing, Universitas Gadjah Mada (protocol code KE/FK/0640/EC/2017 in 6 June 2017 and was amended in 9 February 2018). The study is also registered in ClinicalTrial.gov no NCT03495401.

Informed Consent Statement: Informed consent was obtained from all subjects involved in the study.

Data Availability Statement: Data available on request due to privacy issues.

Acknowledgments: The authors want to acknowledge all participants who followed this study and Beneo Orafti who gave some materials needed to make the product. They also acknowledge Bapak Jumarko, a local community nutritionist; Dita, a local resident; and all enumerators who helped to coordinate with participants and conduct this research.

Conflicts of Interest: The authors declare no conflict of interest.

References

1. de Onis, M.; Blössner, M.; Borghi, E. Prevalence and trends of stunting among pre-school children, 1990–2020. *Public Health Nutr.* **2012**, *15*, 142–148. [CrossRef]
2. International Food Policy Research Institute. *Global Nutrition Report 2016: From Promise to Impact: Ending Malnutrition by 2030*; International Food Policy Research Institute: Washington, DC, USA, 2016.
3. UNICEF/ WHO/The World Bank. *Levels and Trends in Child Malnutrition*; World Health Organization: Washington, DC, USA, 2019; Available online: https://www.who.int/nutgrowthdb/jme-2019-key-findings.pdf (accessed on 1 February 2020).
4. Ministry of Health of Republic Indonesia. *Main Results of Basic Health Research 2018*; Ministry of Health of Republic Indonesia: Jakarta, Indonesia, 2018.
5. de Onis, M.; Borghi, E.; Arimond, M.; Webb, P.; Croft, T.; Saha, K.; Flores-Ayala, R. Prevalence thresholds for wasting, overweight and stunting in children under 5 years. *Public Health Nutr.* **2018**, *22*, 175–179. [CrossRef]
6. Rokx, C.; Subandoro, A.; Gallagher, P. *Aiming High: Indonesia's Ambition to Reduce Stunting*; The World Bank: Washington, DC, USA, 2018.
7. Prendergast, A.J.; Humphrey, J.H. The stunting syndrome in developing countries. *Paediatr. Int. Child Health* **2014**, *34*, 250–265. [CrossRef] [PubMed]
8. Soekatri, M.Y.E.; Sandjaja, S.; Syauqy, A. Stunting was associated with reported morbidity, parental education and socioeconomic status in 0.5–12-year-old Indonesian children. *Int. J. Environ. Res. Public Health* **2020**, *17*, 6204. [CrossRef] [PubMed]
9. Mary, S. How much does economic growth contribute to child stunting reductions? *Economies* **2018**, *6*, 55. [CrossRef]
10. Blaney, S.; Februhartanty, J.; Sukotjo, S. Feeding practices among Indonesian children above six months of age: A literature review on their potential determinants (part 2). *Asia Pac. J. Clin. Nutr.* **2015**, *24*, 16–27.
11. Bening, S.; Margawati, A.; Rosidi, A. Zinc deficiency as risk factor for stunting among children aged 2–5 years. *Universa Med.* **2017**, *36*, 11. [CrossRef]
12. Putri, A.R.; Anwar, A.; Chasanah, E.; Fawzya, Y.N.; Martosuyono, N.; Afifah, D.N. Analysis of iron, calcium and zinc contents in for-mulated fish protein hydrolyzate (FPH) complementary feeding instant powder. *Food Res.* **2020**, *4* (Suppl. 3), 63–66. [CrossRef]
13. Bhandari, N.; Bahl, R.; Taneja, S. Effect of micronutrient supplementation on linear growth of children. *Br. J. Nutr.* **2001**, *85* (Suppl. 2), S131–S137. [CrossRef]
14. Fahmida, U.; Rumawas, J.S.P.; Utomo, B.; Patmonodewo, S.; Schultink, W. Zinc-iron, but not zinc-alone supplementation, increased linear growth of stunted infants with low haemoglobin. *Asia Pac. J. Clin. Nutr.* **2007**, *16*, 301–309.
15. Liu, E.; Pimpin, L.; Shulkin, M.; Kranz, S.; Duggan, C.P.; Mozaffarian, D.; Fawzi, W.W. Effect of zinc supplementation on growth outcomes in children under 5 years of age. *Nutrients* **2018**, *10*, 377. [CrossRef] [PubMed]
16. Larson, L.M.; Kubes, J.N.; Ramírez-Luzuriaga, M.J.; Khishen, S.; Shankar, A.H.; Prado, E.L. Effects of increased hemoglobin on child growth, development, and disease: A systematic review and meta-analysis. *Ann. N. Y. Acad. Sci.* **2019**, *1450*, 83–104. [CrossRef] [PubMed]
17. Baltussen, R.; Knai, C.; Sharan, M. Iron fortification and iron supplementation are cost-effective interventions to reduce iron deficiency in four subregions of the world. *J. Nutr.* **2004**, *134*, 2678–2684. [CrossRef] [PubMed]
18. Allen, L.H.; de Benoist, B.; Dary, O.; Hurrell, R. *Guidelines on Food Fortification with Micronutrients*; World Health Organization: Geneva, Switzerland, 2006; Available online: https://www.who.int/nutrition/publications/micronutrients/guide_food_fortification_micronutrients.pdf (accessed on 2 February 2020).
19. Fiedler, J.L.; Macdonald, B. A strategic approach to the unfinished fortification agenda: Feasibility, costs, and cost-effectiveness analysis of fortification programs in 48 countries. *Food Nutr. Bull.* **2009**, *30*, 283–316. [CrossRef] [PubMed]
20. Matsuyama, M.; Harb, T.; David, M.; Davies, P.S.; Hill, R.J. Effect of fortified milk on growth and nutritional status in young children: A systematic review and meta-analysis. *Public Health Nutr.* **2016**, *20*, 1214–1225. [CrossRef]
21. Batista, A.; Silva, R.; Cappato, L.; Ferreira, M.; Nascimento, K.; Schmiele, M.; Esmerino, E.; Balthazar, C.; Silva, H.; Moraes, J.; et al. Developing a synbiotic fermented milk using probiotic bacteria and organic green banana flour. *J. Funct. Foods* **2017**, *38*, 242–250. [CrossRef]
22. Helmyati, S.; Rahayu, E.S.; Kandarina, B.J.I.; Juffrie, M. No difference between iron supplementation only and iron supplementation with synbiotic fermented milk on iron status, growth, and gut microbiota profile in elementary school children with iron deficiency. *Curr. Nutr. Food Sci.* **2020**, *16*, 220–227. [CrossRef]
23. Ahanchian, H.; Jafari, S.A.; Ansari, E.; Ganji, T.; Kiani, M.A.; Khalesi, M.; Momen, T.; Kianifar, H. A multi-strain synbiotic may reduce viral respiratry infections in asthmatic children: A randomized controlled trial. *Electron. Phys.* **2016**, *8*, 2833–2839.

24. Helmyati, S.; Sudargo, T.; Kandarina, B.I.; Yuliati, E.; Wisnusanti, S.U.; Puspitaningrum, V.A.D.; Juffrie, M. Tempeh extract fortified with iron and synbiotic as a strategy against anemia. *Int. Food Res. J.* **2016**, *23*, 2296–2299.
25. Agustina, R.; Bovee-Oudenhoven, I.M.J.; Kok, F.J.; Lukito, W.; Fahmida, U.; Van De Rest, O.; Zimmermann, M.B.; Firmansyah, A.; Wulanti, R.; Albers, R.; et al. Probiotics lactobacillus reuteri dsm 17938 and lactobacillus casei crl 431 modestly increase growth, but not iron and zinc status, among Indonesian children aged 1–6 years. *J. Nutr.* **2013**, *143*, 1184–1193. [CrossRef]
26. Onubi, O.J.; Poobalan, A.S.; Dineen, B.; Marais, D.; McNeill, G. Effects of probiotics on child growth: A systematic review. *J. Health Popul. Nutr.* **2015**, *34*, 1–15. [CrossRef] [PubMed]
27. Yilmaz, B.; Li, H. Gut microbiota and iron: The crucial actors in health and disease. *Pharmaceuticals* **2018**, *11*, 98. [CrossRef] [PubMed]
28. Jaeggi, T.; Kortman, G.A.M.; Moretti, D.; Chassard, C.; Holding, P.; Dostal, A.; Boekhorst, J.; Timmerman, H.M.; Swinkels, D.W.; Tjalsma, H.; et al. Iron fortification adversely affects the gut microbiome, increases pathogen abundance and induces intestinal inflammation in Kenyan infants. *Gut* **2015**, *64*, 731–742. [CrossRef] [PubMed]
29. Lin, F.; Wu, H.; Zeng, M.; Yu, G.; Dong, S.; Yang, H. Probiotic/prebiotic correction for adverse effects of iron fortification on intestinal resistance to Salmonella infection in weaning mice. *Food Funct.* **2018**, *9*, 1070–1078. [CrossRef] [PubMed]
30. Sazawal, S.; Dhingra, U.; Hiremath, G.; Sarkar, A.; Dhingra, P.; Dutta, A.; Black, R.E. Effects of *Bifidobacterium lactis* HN019 and prebiotic oli-gosaccharide added to milk on iron status, anemia, and growth among children 1 to 4 years old. *J. Pediatr. Gastroenterol. Nutr.* **2010**, *51*, 341–346. [CrossRef] [PubMed]
31. Akal, C.; Yetişemiyen, A. Use of whey powder and skim milk powder for the production of fermented cream. *Food Sci. Technol.* **2016**, *36*, 616–621. [CrossRef]
32. Hafiizha, A.; Kayaputri, I.L.; Tensiska, T.; Amalia, N.R. The effect of skim milk concentration on sensory quality and PH of probiotic yoghurt added with red dragon fruit (*Hylocereus polyrhizus*). *J. Ilmu dan Teknol. Has. Ternak* **2020**, *15*, 52–60. [CrossRef]
33. Maganha, L.C.; Rosim, R.; Corassin, C.H.; Cruz, A.G.; Faria, J.A.F.; Oliveira, C.A.F. Viability of probiotic bacteria in fermented skim milk produced with different levels of milk powder and sugar. *Int. J. Dairy Technol.* **2013**, *67*, 89–94. [CrossRef]
34. National Health and Nutrition Examination Survey. *Anthropometry Procedures Manual*; NHANES: Washington, DC, USA, 2004.
35. Kim, H.-Y. Statistical notes for clinical researchers: Chi-squared test and Fisher's exact test. *Restor. Dent. Endod.* **2017**, *42*, 152–155. [CrossRef]
36. Dumville, J.C.; Torgerson, D.J.; Hewitt, C.E. Reporting attrition in randomised controlled trials. *BMJ* **2006**, *332*, 969–971. [CrossRef]
37. Sazawal, S.; Habib, A.A.; Dhingra, U.; Dutta, A.; Dhingra, P.; Sarkar, A.; Husna, A.; Black, R.E. Impact of micronutrient fortification of yoghurt on micro-nutrient status markers and growth-a randomized double blind controlled trial among school children in Bangladesh. *BMC Public Health* **2013**, *13*, 514. [CrossRef]
38. El Menchawy, I.; El Hamdouchi, A.; El Kari, K.; Saeid, N.; Zahrou, F.E.; Benajiba, N.; El Harchaoui, I.; El Mzibri, M.; El Haloui, N.; Aguenaou, H. Efficacy of multiple micronutrients fortified milk consumption on iron nutritional status in Moroccan schoolchildren. *J. Nutr. Metab.* **2015**, *2015*, 690954. [CrossRef]
39. Haschke, F.; Ziegler, E.E.; Edwards, B.B.; Fomon, S.J. Effect of iron fortification of infant formula on trace mineral absorption. *J. Pediatr. Gastroenterol. Nutr.* **1986**, *5*, 768–773. [CrossRef]
40. Crofton, R.W.; Gvozdanovic, D.; Gvozdanovic, S.; Khin, C.C.; Brunt, P.W.; Mowat, N.; Aggett, P.J. Inorganic zinc and the intestinal absorption of ferrous iron. *Am. J. Clin. Nutr.* **1989**, *50*, 141–144. [CrossRef] [PubMed]
41. World Health Organization. *WHO Child Growth Standards*; WHO: Geneva, Switzerland, 2006.
42. Godoy, R.; Nyberg, C.; Eisenberg, D.T.; Magvanjav, O.; Shinnar, E.; Leonard, W.R.; Gravlee, C.; Reyes-García, V.; McDade, T.W.; Huanca, T.; et al. Short but catching up: Statural growth among native Amazonian Bolivian children. *Am. J. Hum. Biol.* **2009**, *22*, 336–347. [CrossRef]
43. Zhang, R.; Undurraga, E.A.; Zeng, W.; Reyes-García, V.; Tanner, S.; Leonard, W.R.; Behrman, J.R.; Godoy, R.A. Catch-up growth and growth deficits: Nine-year annual panel child growth for native Amazonians in Bolivia. *Ann. Hum. Biol.* **2016**, *43*, 304–315. [CrossRef] [PubMed]
44. Raiten, D.J.; Bremer, A.A. Exploring the nutritional ecology of stunting: New approaches to an old problem. *Nutrients* **2020**, *12*, 371. [CrossRef] [PubMed]
45. Millward, D.J. Nutrition, infection and stunting: The roles of deficiencies of individual nutrients and foods, and of inflammation, as determinants of reduced linear growth of children. *Nutr. Res. Rev.* **2017**, *30*, 50–72. [CrossRef]
46. Finkielstain, G.P.; Lui, J.C.; Baron, J. Catch-up growth: Cellular and molecular mechanisms. *World Rev. Nutr. Diet.* **2013**, *106*, 100–104. [CrossRef]
47. Sazawal, S.; Dhingra, U.; Dhingra, P.; Hiremath, G.; Sarkar, A.; Dutta, A.; Menon, V.P.; Black, R.E. Micronutrient fortified milk improves iron status, anemia and growth among children 1–4 years: A double masked, randomized, controlled trial. *PLoS ONE* **2010**, *5*, e12167. [CrossRef]
48. Ramakrishnan, U.; Nguyen, P.; Martorell, R. Effects of micronutrients on growth of children under 5 years of age. *Am. J. Clin. Nutr.* **2009**, *89*, 191–203. [CrossRef] [PubMed]
49. Lind, T.; Lönnerdal, B.; Stenlund, H.; Gamayanti, I.L.; Ismail, D.; Seswandhana, R.; Persson, L.Å. A community-based randomized controlled trial of iron and zinc supplementation in Indonesian infants: Effects on growth and development. *Am. J. Clin. Nutr.* **2004**, *80*, 729–736. [CrossRef] [PubMed]

50. Lönnerdal, B. Excess iron intake as a factor in growth, infections, and development of infants and young children. *Am. J. Clin. Nutr.* **2017**, *106*, 1681S–1687S. [CrossRef] [PubMed]
51. Golden, M.H. Proposed recommended nutrient densities for moderately malnourished children. *Food Nutr. Bull.* **2009**, *30*, S267–S342. [CrossRef] [PubMed]
52. Yogeswara, I.B.A.; Kittibunchakul, S.; Rahayu, E.S.; Domig, K.J.; Haltrich, D.; Nguyen, T.H. Microbial production and enzymatic biosynthesis of γ-aminobutyric acid (Gaba) Using lactobacillus plantarum fncc 260 isolated from Indonesian fermented foods. *Processes* **2020**, *9*, 22. [CrossRef]

processes

MDPI

Article

Microbial Production and Enzymatic Biosynthesis of γ-Aminobutyric Acid (GABA) Using *Lactobacillus plantarum* FNCC 260 Isolated from Indonesian Fermented Foods

Ida Bagus Agung Yogeswara [1,2,*,†], Suwapat Kittibunchakul [1,3,†], Endang Sutriswati Rahayu [4,5], Konrad J. Domig [6], Dietmar Haltrich [1] and Thu Ha Nguyen [1,*]

[1] Food Biotechnology Laboratory, Department of Food Science and Technology, University of Natural Resources and Life Sciences Vienna (BOKU), Muthgasse 18, 1190 Vienna, Austria; suwapat.kit@mahidol.ac.th (S.K.); dietmar.haltrich@boku.ac.at (D.H.)
[2] Nutrition Department, Faculty of Health, Science and Technology, Universitas Dhyana Pura, Dalung Kuta Utara 80361, Indonesia
[3] Institute of Nutrition, Mahidol University, 999 Phutthamonthon 4 Road, Nakhon Pathom 73170, Thailand
[4] Faculty of Agricultural Technology, Universitas Gadjah Mada, Jalan Flora No 1 Bulaksumur, Yogyakarta 55281, Indonesia; endangsrahayu@ugm.ac.id
[5] Center for Food and Nutrition Studies, Universitas Gadjah Mada, Jalan Teknika Utara, Barek, Yogyakarta 55281, Indonesia
[6] Department of Food Science and Technology, Institute of Food Science, University of Natural Resources and Life Sciences Vienna (BOKU), Muthgasse 18, 1190 Vienna, Austria; konrad.domig@boku.ac.at
* Correspondence: agungyogeswara@undhirabali.ac.id (I.B.A.Y.); thu-ha.nguyen@boku.ac.at (T.H.N.)
† First authorship.

Abstract: In the present study, we isolated and screened thirty strains of GABA (γ-aminobutyric acid)-producing lactic acid bacteria (LAB) from traditional Indonesian fermented foods. Two strains were able to convert monosodium glutamate (MSG) to GABA after 24 h of cultivation at 37 °C based on thin layer chromatography (TLC) screening. Proteomic identification and 16S rDNA sequencing using MALDI-TOF MS identified the strain as *Lactobacillus plantarum* designated as *L. plantarum* FNCC 260 and FNCC 343. The highest yield of GABA production obtained from the fermentation of *L. plantarum* FNCC 260 was 809.2 mg/L of culture medium after 60 h of cultivation. The supplementation of 0.6 mM pyridoxal 5′-phosphate (PLP) and 0.1 mM pyridoxine led to the increase in GABA production to 945.3 mg/L and 969.5 mg/L, respectively. The highest GABA production of 1226.5 mg/L of the culture medium was obtained with 100 mM initial concentration of MSG added in the cultivation medium. The open reading frame (ORF) of 1410 bp of the *gad*B gene from *L. plantarum* FNCC 260 encodes 469 amino acids with a calculated molecular mass of 53.57 kDa. The production of GABA via enzymatic conversion of monosodium glutamate (MSG) using purified recombinant glutamate decarboxylase (GAD) from *L. plantarum* FNCC 260 expressed in *Escherichia coli* was found to be more efficient (5-fold higher within 6 h) than the production obtained from fermentation. *L. plantarum* FNCC 260 could be of interest for the synthesis of GABA.

Keywords: GABA; Indonesian fermented foods; glutamate decarboxylase; lactic acid bacteria; *L. plantarum*

Citation: Yogeswara, I.B.A.; Kittibunchakul, S.; Rahayu, E.S.; Domig, K.J.; Haltrich, D.; Nguyen, T.H. Microbial Production and Enzymatic Biosynthesis of γ-Aminobutyric Acid (GABA) Using *Lactobacillus plantarum* FNCC 260 Isolated from Indonesian Fermented Foods. *Processes* **2021**, *9*, 22. https://dx.doi.org/10.3390/pr9010022

Received: 30 November 2020
Accepted: 21 December 2020
Published: 24 December 2020

1. Introduction

γ-aminobutyric acid (GABA), which is a non-protein amino acid and plays a major role as a suppressive neurotransmitter, is widely present in plants, microorganisms, and the mammalian brain [1–3]. GABA has been extensively studied due to its physiological and pharmacological effects including anti-depressant, hypotensive activity, anti-diabetic in humans [4–6]. Recently, GABA administration in fluoride-exposed mice showed protective effects against hypothyroidism and maintained lipid and glucose levels in vivo [4]. Furthermore, GABA-enriched foods have been developed [5–11]. GABA-rich chlorella

has been shown to significantly lower high blood pressure in hypertensive subjects [12]. A number of GABA-enriched foods such as soymilk [13], fermented milk [14], natto [15], green tea [16], and cheese [5] have been reported to suppress the elevation of blood pressure in spontaneously hypertensive rats (SHR) and hypertensive subjects.

GABA can be synthesized using chemical or biochemical means, of which the latter involves enzymatic conversion, whole-cell biocatalysts, or microbial fermentation. The chemical synthesis is considered hazardous due to corrosive nature of used reagents [17–19], hence the application in the food industry is limited. Moreover, the supplementation of synthetic GABA to food system is considered unnatural and unsafe [14]. Therefore, it is important to develop a natural and safe method to increase GABA in foods, since there are no side effects of natural GABA supplementation [16]. Recent studies showed that several strains of lactic acid bacteria (LAB) are promising candidates as GABA-producing bacteria [1–3,5] due to their GRAS (generally recognized as safe) status. A number of GABA-producing bacteria has been isolated from fermented foods such as *L. brevis* (from kimchi) [20], *L. rhamnosus* (from fermented pickles) [21], *L. plantarum* (from fermented dairy products) [22], *L. helveticus* (from koumis fermented milk) [23], *L. buchneri* (from kimchi) [24], *L. otakiensis* (from Pico cheese) [25], *L. namurensis* (from fermented green papaya) [11], and *L. paracasei* (from Italian cheese) [3]. These reports have shown that fermented foods are promising sources of GABA-producing bacteria. In addition, screening GABA-producing LAB from various fermented foods might open the possibilities to obtain newly isolated strains for the use as functional starter cultures in the food industry.

Several fermented foods from Indonesia namely *gatot*, *growol*, *tape ubi*, *bekasam*, and *tempoyak* are spontaneously fermented by LAB, which mainly involve the strains of the genera *Lactobacillus*, *Pediococcus*, and *Streptococcus* [26,27]. However, the potential of these LAB strains from Indonesian fermented foods to be used as GABA-producing bacteria as well as their relevant enzymes have not yet been studied. Therefore, the development of GABA-enriched foods using suitable LAB is a promising strategy, to bring new functional foods to the market. In addition, biosynthesis of GABA using LAB also provides advantageous effects including probiotic activity and extension of the shelf-life of food products [9].

The biosynthesis of GABA involves irreversible decarboxylation reaction of glutamate to GABA and carbon dioxide catalyzed by glutamate decarboxylase (GAD). GAD (EC 4.1.1.15) is a major enzyme for GABA synthesis and it requires pyridoxal 5′-phosphate (PLP) as a cofactor [28–30]. The GAD genes from various sources have been cloned, expressed and their biochemical properties have been characterized [20,31–34]. The use of purified GAD for the biosynthesis of GABA is also of interest because only simple downstream purification of GABA is required and yet, the process could overcome the limitation of microbial fermentation (i.e., GABA catabolism). In the present study, we describe the screening of GABA-producing LAB from Indonesian fermented foods (fermented soybeans, *growol*, *gatot*, *tempeh*, and *bekasam*) and GABA productions using microbial fermentation of the isolated strain and the purified GAD of this strain for the conversion of glutamate to GABA.

2. Materials and Methods

2.1. Screening of GABA-Producing LAB

Thirty isolates of *Lactobacillus* spp. were previously isolated from Indonesian fermented foods such as fermented soybeans, *growol*, *gatot*, *tempeh*, and *bekasam* (fermented fish) [35]. *Lactobacillus* spp. were the predominant genus according to cell morphology, Gram reactions and catalase tests. All strains were obtained and stored in the Food and Nutrition Culture Collection, Universitas Gadjah Mada (Yogyakarta, Indonesia). Prior to screening, all strains were grown in MRS broth containing 118 mM monosodium glutamate (MSG) (Ajinomoto, Tokyo, Japan) for 24–48 h at 37 °C under microaerophilic conditions. The cultures broth was then centrifuged at 8000× *g* for 5 min at 4 °C. GABA formation in the supernatant was analyzed using thin layer chromatography (TLC). Briefly, 0.5–1.0 µL of supernatants were spotted onto TLC plates Silica gel 60 F_{254} (Merck, Darmstadt, Germany).

The mobile phase consists of a mixture of 1-butanol: acetic acid: distilled water (5:2:2). Subsequently, the plates were sprayed with 0.5% ninhydrin and heated at 105 °C for 5 min to visualize the spots. GABA (Sigma Aldrich, St. Louis, MO, USA) was used as a standard, and the Rf values were calculated. LAB cultures showing the same Rf values as GABA standard were considered as positive GABA-producers. Positive GABA-producing strains were identified using proteomic and genotype techniques. Furthermore, the amount of GABA produced was determined by the GABase assay [36]. All chemicals were of the highest grade.

2.2. Identification of GABA-Producing LAB

Proteomic and genotype techniques were performed to identified GABA-producing LAB. Genomic DNA of GABA-producing LAB was extracted using peqGOLD Bacterial DNA Mini Kit (PeqLab, Erlangen, Germany) according to manufacturer's instructions. The extracted DNA was used as a template for partial 16S rDNA amplification. The amplifications of 16S rDNA were performed using forward primer bak4 (5′-AGGAGGTCATCCARC CGCA-3′) and reverse primer bak11w (5′-AGTTTGATCMTGGCTCAG-3′) [37], The PCR reaction mixtures consisted of 10× PCR buffer (Dynazyme buffer 10× Thermo scientific, Waltham, MA, USA), 10 nmol/μL dNTP mix (GE Healthcare Buckinghamshire, UK), 2 U/μL DNA polymerase (Dynazime II, Thermo scientific) and high-quality sterile water to a total volume of 25 μL. The conditions for PCR amplification were as follows: initial denaturation at 95 °C for 3 min, followed by 30 cycles of denaturation at 95 °C for 30 s, annealing at 56 °C for 30 s, extension 72 °C for 2 min, and a final extension at 72 °C for 7 min. After PCR amplification, the amplified products were visualized by gel electrophoresis. The gel was stained with GelRed Nucleic Acid (Biotium, Hayward, CA, USA) and subsequently visualized with an ultraviolet transilluminator (BioRad, Hercules, CA, USA). The PCR products were purified using QIAquick PCR purification Kit (Qiagen, Venlo, The Netherlands) and sent for sequencing (Eurofins MWG Operon, Ebersberg, Germany). Subsequently, the partial 16S rDNA sequence was compared with the National Center for Biotechnology Information (NCBI) sequence database using Basic Local Alignment Search Tool (BLAST) program.

Proteomic identification was performed using matrix-assisted laser desorption/ionizing time-of-flight mass spectrometry (MALDI-TOF MS). GABA-producing bacteria were identified by the extended direct transfer method. A single colony was directly spread onto a MALDI target plate. The spot was overlayed with 1 μL of 70% formic acid and allowed to dry at room temperature. Furthermore, 1 μL of 10 mg/μL HCCA (α-cyano-4-hydroxycinnamic acid) solution was then added to the spot and allowed to dry at room temperature. The target plate was immediately applied to MALDI-TOF MS and analyzed using Microflex LT bench-top mass spectrometer (Bruker Daltonics, Bremen, Germany) equipped with the FlexControl 3.4 software. A mass spectrum was processed using BioTyper software (version 3.0, Bruker Daltonics, Bremen, Germany). MALDI-TOF MS profiles were obtained from bacteria isolates and matched with a database containing 8223 reference MALDI-TOF MS profiles.

2.3. Determination of GABA Production and GAD Assay

The GABAse method was performed to determine GABA concentration in culture supernatants. Briefly, the culture broth was centrifuged at 8000× *g* for 5 min at 4 °C. 10 μL of supernatants were mixed with 140 μL of 100 mM $K_4P_2O_7$ buffer (pH 8.6), 30 μL of 4 mM $NADP^+$, 10 μL of 1 U/mL GABase (Sigma-Aldrich, St. Louis, MO, USA). The mixtures were dispensed into each well of 96-well plate. The initial absorbance was read at 340 nm in PerkinElmer plate reader (PerkinElmer, Buckinghamshire, UK). After the initial reading, 10 μL of 20 mM α-ketoglutarate were added and the mixtures were incubated for 1 h. The final absorbance was read after 1 h at the same wavelength. GABA concentrations were determined based on the difference of A_{340} values and the standard curve of GABA.

The GAD assay was carried out using colorimetric method [38]. The reaction mixtures consist of 200 mM Na_2HPO_4-citric acid buffer (pH 5.0), 20 mM L-MSG, 0.2 mM PLP, and 20 µL of purified GAD. The mixtures were thoroughly mixed and incubated at 37 °C for 1 h and then deactivated by boiling for 5 min. The reaction mixtures were used to determined GAD activity using the Berthelot reaction method, which was composed of 100 µL of reaction sample, 250 µL of H_2O, 50 µL of 200 mM sodium borate (pH 9.0), 250 µL of 6% phenol and 200 µL of 5% (*w*/*v*) sodium hypochlorite. Subsequently, the reaction mixtures were thoroughly mixed and boiled for 10 min until the blue color developed, then immediately placed on ice for 15 min. The mixtures were analyzed colorimetric at 630 nm to determine the absorption value. One unit of GAD activity was defined as the amount of enzyme that liberates 1 µmol of GABA per minute under activity assay conditions.

The concentrations of GABA formed in supernatants and after enzymatic conversions were confirmed using Ultra Performance Liquid Chromatography (UPLC Acquity H- Class, Waters Corporation, Milford, MA, USA) equipped with a PDA detector and an AccQ. Tag Ultra C18 column (1.7 µm particle, 2.1 × 100 mm). The samples were hydrolyzed using 6 N HCL and followed by derivatization of the samples and the GABA standard using AccQ-Tag ultra-derivatization kit (Waters, Milford, MA, USA) according to the manufacturer's instructions. For UPLC analysis, the derivatized samples were injected to Acquity UPLC H class [39]. The system was operated at a flow rate of 0.5 mL/min at 49 °C with a wavelength of 260 nm. The mobile phase used were AccQ. Tag Ultra Eluent A 100%; Accq. Tag Ultra Eluent B (Aquabides 90:10); Aquabides Eluent C; AccQ. Tag Ultra Eluent B 100%.

2.4. GABA Production

The MRS medium was inoculated with 5% inoculum of GABA-producing LAB and incubated at 37 °C for 108 h. The optical densities (OD_{600}) of the cultures were measured every 12 h. A concentration of MSG (25–100 mM) (Sigma Aldrich, St. Louis, MO, USA), pyridoxal 5-phosphate (PLP, 0.2 and 0.6 mM) and pyridoxine (vitamin B6, 0.1–0.3 mM) were added to the MRS medium and GABA production under these conditions was investigated subsequently.

2.5. Cloning of gadB Gene

The glutamate decarboxylase gene (*gad*) from *L. plantarum* FNCC260 was amplified using degenerated primers *gad*_FwdNdeI (5′-CATATGATGGCAATGTTRTAYGGTAAAC-3′) and *gad*_RevEcoRI (5′-GAATTCCAGTGTGTGAATMSGTATTTC-3′), which were designed based on the sequences of the *gad* genes of *Lactobacillus* spp. available in GenBank (Accession numbers JN248358.1, KU214639.1, AB986192.1, CP029349.1, AL935263.1, CP018209.1, CP028977.1, GU987102.1, JX545343.1).

The primers were supplied by VBC-Biotech Service (Vienna, Austria) and the appropriate endonuclease restriction sites were introduced in the forward and reverse primers (underlined sequences). The conditions for PCR reactions were as follows: initial denaturation at 98 °C for 20 s; 30 cycles of denaturation at 98 °C for 20 s, annealing at 58 °C for 20 s, extension at 72 °C for 1 min 45 s, and final extension at 72 °C for 2 min. The amplified PCR products were purified using the Monarch DNA Gel Extraction Kit (New England Biolabs, Ipswich, MA, USA), digested with *Nde*I and *Eco*RI and cloned into the pET 21(+a) vector (Novagen, Merck KGaA, Darmstadt, Germany) resulting in the plasmid pET21GAD. *E. coli* NEB5α was used as a host for obtaining the plasmids in sufficient amounts. The sequence of the insert was confirmed by DNA sequencing performed by a commercial provider (Microsynth, Vienna, Austria). The alignment tool (BLAST) from the National Center for Biotechnology Information BLAST website was used for the alignment of the nucleotide sequence of the *gad* gene from *L. plantarum* FNCC 260 with the available *gad* sequences from LAB. The comparison of glutamate decaroboxylases (GAD) from different LAB species was carried out using the program Clustal Omega (https://www.ebi.ac.uk/Tools/msa/clustalo/) [31,33].

2.6. Overexpression of GADLbFNCC260 in E. coli and Protein Purification

The expression vector of pET21GAD harboring the *gad* gene from *L. plantarum* FNCC 260 was transformed into *E. coli* T7 Express GRO carrying the plasmid pGRO7, which encodes the chaperones GroEL and GroES (Takara, Shiga, Japan). Subsequently, *E. coli* T7 Express GRO carrying the plasmid pET21GAD was cultivated in LB broth medium supplemented with 100 μg/mL ampicillin, 20 μg/mL chloramphenicol, and 1 mg/mL arabinose until OD_{600nm} of 0.6 was reached. Thereafter, the isopropyl β-D-1-thiogalactopyranoside (IPTG) was added to a final concentration of 0.5 mM for induction. The culture was further incubated at 18 °C for 20 h with shaking at 180 rpm. The cells were harvested, washed twice with 50 mM sodium phosphate buffer (pH 6.5), and resuspended in buffer A (50 mM NaH_2PO_4, 300 mM NaCl, and 10 mM imidazole, pH 7.0). The resuspended cells were disrupted using a French press (Aminco, Silver Spring, MD, USA) and centrifuged at 15,000× *g* for 20 min at 4 °C. The cell-free extracts were collected and loaded to a prepacked 1 mL HisTrap HP Ni-immobilized metal ion affinity chromatography (IMAC) column (GE Healthcare, Uppsala, Sweden) that was pre-equilibrated with buffer A (50 mM NaH_2PO_4, 300 mM NaCl, and 10 mM imidazole, pH 7.0). The His-tagged protein was eluted at a rate of 1 mL/min with a 15 mL linear gradient from 0 to 100% buffer B (20 mM NaH_2PO, 500 mM imidazole, 500 mM NaCl, pH 6.5). Active fractions were pooled, desalted, and concentrated by ultrafiltration using an Amicon Ultra centrifugal filter unit with a 30 kDa cut-off membrane (Millipore, Burlington, MA, USA). The purified enzyme was stored in 50 mM citrate-phosphate buffer (pH 5.0) for further characterization and enzymatic conversion. The molecular masses of purified GAD were determined by SDS-PAGE and Native PAGE. Protein bands were visualized by staining with Bio-safe Coomassie (Bio-Rad). The determination of protein mass was carried out using Unstained Precision plus Protein Standard (Bio-Rad, Hercules, CA, USA).

The size of the protein was also confirmed by LC-ESI-MS analysis. The proteins were S-alkylated with iodoacetamide and digested with Trypsin (Promega, Madison, WI, USA). The digested proteins were directly injected to LC-ESI-MS (LC: Dionex Ultimate 3000 LC). A gradient from 10 to 80% acetonitrile in 0.05% trifluoroacetic acid (using a Thermo ProSwiftTM RP-4H column (0.2 × 250 mm) at a flow rate of 8 μL/min was applied (30 min gradient time). Detection was performed with a Q-TOF instrument (Bruker maxis 4G, Billerica, MA, USA) equipped with standard ESI source in positive ion, MS mode (range: 400–3000 Da). Instrument calibration was performed using ESI calibration mixture (Agilent, Santa Clara, CA, USA). Data were processed using Data analysis 4.0 (Bruker) and the spectrum was deconvoluted by MaxEnt.

2.7. Enzymatic Synthesis of GABA

Batch conversion reactions were carried out in 2 mL scale with 0.64 U/mL purified GAD using 100 mM MSG in 50 mM citrate-phosphate buffer (pH 4.5) containing 0.2 mM of PLP as cofactor. Decarboxylation reactions were performed at 30 °C with 300 rpm agitation using a Thermomixer (Eppendorf, Hamburg, Germany). The samples were withdrawn at time intervals and the enzyme GAD was inactivated at 100 °C for 5 min. The samples were stored at −20 °C for subsequent analysis. GABA content in the reaction mixtures was determined using the GABase assay and confirmed with UPLC analysis as described in Section 2.3.

3. Results and Discussion

3.1. Screening and Identification of GABA-Producing LAB

Thirty isolates of *Lactobacillus* spp. from Indonesian fermented foods were screened for the formation of GABA in the culture medium using the TLC method and only two isolates showed clear spots on TLC plate (Figure 1), which have similar Rf value (0.78) as the GABA standard. These two isolates were FNCC 260 and FNCC 343 isolated from fermented cassava and fermented fish, respectively. The two strains FNCC 260 and FNCC 343 were cultivated in MRS broth containing 118 mM MSG for 48 h to determine the GABA

production in the culture medium, which was analyzed to be 352 mg and 328 mg of GABA per liter of culture medium, respectively. Based on morphological observation, these two strains were Gram positive, rod-shape, microaerophilic, and catalase negative.

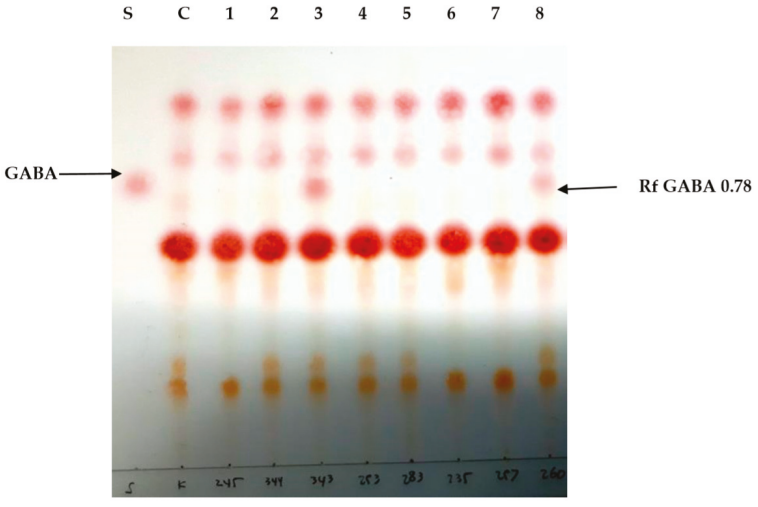

Figure 1. Thin layer chromatography (TLC) screening of GABA–producing LAB. Lane S: GABA standard, Lane C: MRS with 118 mM monosodium glutamate (MSG), Lane 1–8: the strains FNCC 245, FNCC 344, FNCC 343, FNCC 253, FNCC 283, FNCC 235, FNCC 257, and FNCC 260, respectively. All strains were cultivated in MRS broth supplemented with 118 mM MSG and incubated at 37 °C for 48 h.

Subsequently, these two GABA-producing LAB were identified using 16S rDNA and MALDI-TOF MS (Bruker Biotyper). Proteomic identification by MALDI-TOF MS was performed since this technique is very effective in identifying species and subspecies of LAB. A number of species and subspecies of LAB have been successfully identified using proteomic-based identification technique [40–43]. Based on MALDI-TOF MS identification, both strains FNCC 260 (2.15 log score) and FNCC 343 (2.12 log score) were identified to be *L. plantarum*, which matches with the strain in a reference database. The log scores also indicate the accuracy and reliability of MALDI-TOF MS identification. A log score between 2.00 and 2.30 indicates accurate identification to the genus and species level [44,45]. Subsequently, GABA-producing LAB were subjected to 16S rDNA sequencing.

Based on partial 16S rDNA sequencing (~1400 bp), both strains belong to the species *L. plantarum*, with 99.81% sequence identity with *L. plantarum* strain CIP 103,151 (accession number, NR_104573.1) for the strain FNCC 260, and 99.81% sequence identity with *L. plantarum* strain NBRC 15,891 (accession number, NR_113338.1) for the strain FNCC 343, respectively. The results confirmed that both strains FNCC 260 and FNCC 343 are indeed *L. plantarum*.

3.2. Time-Course of GABA Production by L. plantarum FNCC 260

L. plantarum FNCC 260 was cultivated in MRS medium supplemented with 118 mM MSG at 37 °C. The time courses of GABA production, the pH value and the growth profile of *L. plantarum* FNCC 260 are shown in Figure 2. GABA production started when cell growth reached the stationary phase after 12 h of cultivation. A slightly higher GABA production was obtained after 48 h (450 mg/L) compared to the GABA production mentioned above in the screening experiment (352 mg/L). This was due to different MSG used in these two experiments (see Materials and Methods). The highest GABA production was 809.2 mg/L

of cultivation medium after 60 h of cultivation, at which cell growth is still in the stationary phase. This observation agrees with previous reports in the literature. The maximum GABA production of *L. brevis* L-32 was observed between 36 to 72 h of cultivation and GABA was mainly produced during the stationary growth phase [46–48]. However, GABA production decreased when the cultivation time was prolonged further. This might be due to the activity of the enzyme GABA transaminase (GABA-T), which degrades GABA. This enzyme catalyzes GABA degradation to succinic semialdehyde by using either pyruvate or α-ketoglutarate as the amino acceptors and succinic semialdehyde is irreversibly oxidized to succinate by succinic semialdehyde dehydrogenase [46,49,50]. Interestingly, we observed that the cell growth did not show a decreasing trend when the cultivation time was extended up to 108 h since GABA is utilized as a nutrient during prolonged cultivation [49]. Ko et al. (2013) reported a similar observation of cell growth of *L. brevis* FPA 3709 during GABA synthesis when GABA production decreased [49].

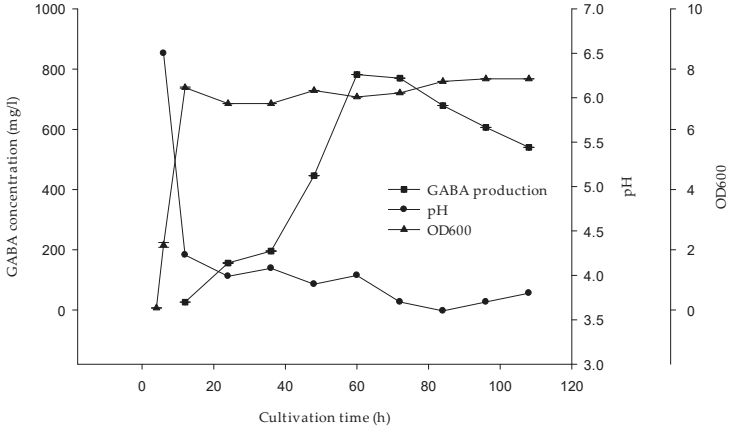

Figure 2. Time course of γ-aminobutyric acid (GABA) production, bacterial growth, and change in pH during cultivation of *L. plantarum* FNCC 260 strain in MRS broth supplemented with 118 mM MSG at 37 °C. Data shown as mean ±SD with SD less than 5%. The experiments were conducted at least in duplicates.

During GABA production, a decrease in pH of MRS medium was observed. The pH of the cultivation medium rapidly decreased from the initial pH 6.5 to pH 4.1 after 12 h of cultivation. The decrease in pH was due to lactic acid and acetic acid formation during the cultivation of the organism [50]. GABA production involves cytoplasmic decarboxylation, which results in extracellular proton consumption after the uptake of glutamate by its specific transporter [28]. This may lead to the removal of hydrogen ions and an increase of pH in the cytoplasm [51]. Apparently, we observed that the decrease in pH of the cultivation medium (to below pH 4.0) correlated with the increase in GABA production during cultivation of *L. plamtarum* FNCC 260. Similarly, the maximum GABA production of *L. buchnerii* was achieved when the pH of the cultivation medium decreased to pH 5.0 [24]. In this study, although GABA production started to decrease after 60 h of cultivation, which might be due to the activity of the enzyme GABA transaminase, the pH of the cultivation medium kept decreasing until 84 h of cultivation indicating that decarboxylation of glutamate still occurred.

3.3. The Effect of Cofactors on GABA Production and Cell Growth

Glutamate decarboxylase is a pyridoxal 5′-phosphate (PLP) dependent enzyme. Theoretically, the addition of PLP to the medium could increase GAD activity and GABA production [2,21,52,53]. PLP and pyridoxine were added into the medium at various

concentrations. As expected, the addition of 0.2 mM and 0.6 mM PLP led to the increase in GABA production, reaching 903.0 mg/L and 945.3 mg/L after 108 h of cultivation, respectively (Figure 3a). Furthermore, GABA was still produced when cultivation time was prolonged to 108 h. In contrast, GABA production in a medium without PLP rapidly decreased after 72 h. it was clear that the strain was able to utilize PLP to produced GABA. The addition of PLP to the medium did not inhibit cell growth during the cultivations (Figure 3b). Previous studies by Komatsuzaki et al. [2] and Yang et al. [53] reported that the addition of 0.1 mM and 0.02 mM PLP significantly enhanced GABA production and GAD activity in the culture media of *L. paracasei* NFRI 7451 and *S. thermophillus* Y2, respectively.

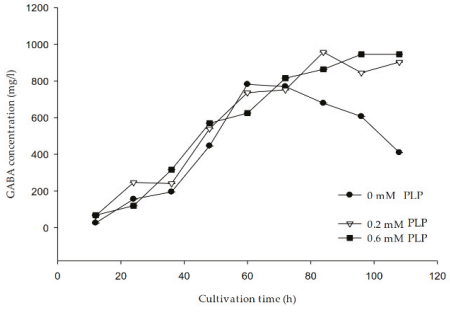

(**a**)

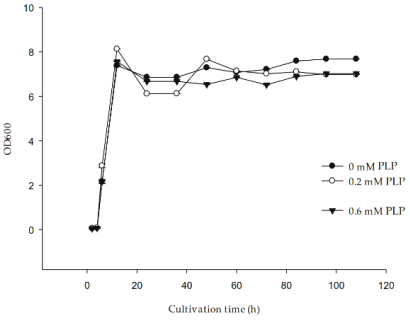

(**b**)

Figure 3. Effect of pyridoxal 5′-phosphate (PLP) on (**a**) GABA production and (**b**) cell growth during the cultivation of *L. plantarum* FNCC 260. The MRS medium were supplemented with 118 mM MSG and PLP at concentrations 0, 0.2 mM and 0.6 mM. The strain was incubated at 37 °C for 108 h. Data expressed as means ±SD with SD less than 5%. The experiments were conducted at least in duplicates.

Pyridoxine (vitamin B6) is a water-soluble vitamin that is ubiquitously found in nature. Pyridoxine can be taken by the cells at the plasma membrane and is subsequently phosphorylated to form PLP within the cytoplasm [52]. The utilization of pyridoxine could be an alternative to replace PLP since PLP is significantly more expensive with low availability. Therefore, we hypothesized that the addition of pyridoxine would improve GABA production. It is shown that the addition of 0.1 mM pyridoxine had a better enhancement on GABA production compared to higher concentrations of pyridoxine tested. The addition of 0.1 mM pyridoxine enhanced GABA production reaching 839.5 mg/L and 969.5 mg/L after 60 h and 96 h of cultivation, respectively (Figure 4a), which are higher compared to the cultivation without pyridoxine (754 mg/L and 606 mg/L, respectively). This observation

suggests that pyridoxine can be taken up by the cells and is phosphorylated to form PLP, which is essential for GAD activity. However, GABA production decreased to 878.8 mg/L after 108 h of cultivation (Figure 4a). This could be due to the degradation of pyridoxine during cultivation and hence it lost its activity as a cofactor [53]. The addition of pyridoxine did not have notable effects on cell growth during the cultivation of *L. plantarum* FNCC 260 (Figure 4b). In both cases of PLP and pyridoxine additions, we observed that the growth reached OD_{600} ~ 8 within 12 h and then maintained at OD ~ 6–7 during the entire cultivation time up to 108 h. Li et al. reported that the addition of cofactor did not improve or inhibit the cell growth of *L. brevis* NCL912 [28].

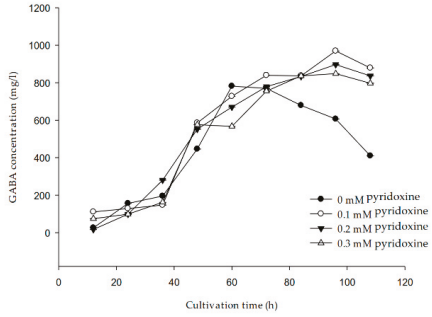

(**a**)

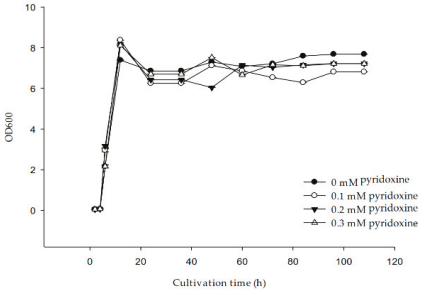

(**b**)

Figure 4. Effect of pyridoxine on (**a**) GABA production and (**b**) cell growth during the cultivation of *L. plantarum* FNCC 260. The MRS medium was supplemented with 118 mM MSG and various concentrations of pyridoxine 0, 0.1 mM, 0.2 mM, 0.3 mM. The strain was incubated at 37 °C for 108 h. Data expressed as mean ± SD with SD less than 5%. The experiments were conducted at least in duplicates.

3.4. The Effect of Monosodium Glutamate on GABA Production

The presence of MSG is a key factor in producing GABA. The optimal culture conditions for GABA production were determined by measuring the GABA content in the cultivation medium of *L. plantarum* FNCC 260 with different initial MSG concentrations in the MRS medium. As shown in Figure 5 increasing MSG concentrations increased GABA production (Figure 5a) and maintained cell viability (Figure 5b). The maximum GABA production was achieved at 1226 mg/L at 96 h in an MRS medium containing 100 mM MSG. It appears that a prolonged incubation time did not increase GABA productivity of the strain. A possible reason led to such circumstances was due to GABA catabolism,

resulting from GABA transaminase activity. The activity of GABA transaminase could decrease GABA production by converting GABA to succinic semi-aldehyde (SSA).

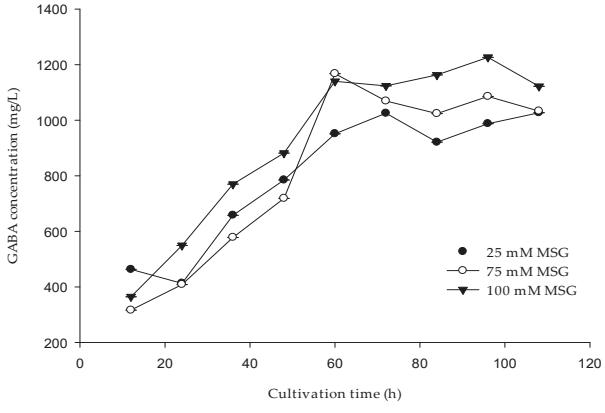

(**a**)

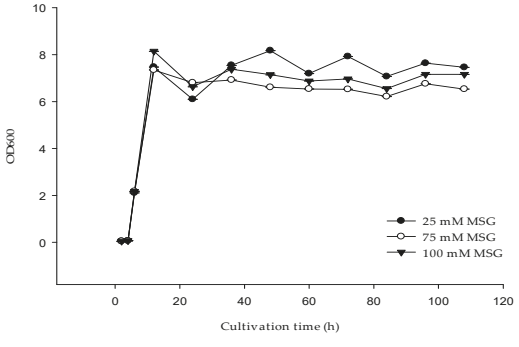

(**b**)

Figure 5. Effect of various MSG concentrations on (**a**) GABA production and (**b**) the growth of *L. plantarum* FNCC 260 cultivated in MRS medium at 37 °C. Data expressed as mean ± SD with SD less than 5%. The experiments were conducted at least in duplicates.

Similarly, high concentrations of MSG resulted in decreased GABA production of the strains *L brevis* CRL 1942, *S. thermophillus* Y2 and *L. paracasei* NFRI 7415 [2,54,55]. It was suggested that high glutamate concentrations become more toxic to some strains of LAB and suppressed the expression of *gad*B genes [56]. In this study, we observed that MSG concentration up to 100 mM did not have effects on bacterial growth (Figure 5b) indicating that GABA is consumed by the cells to maintain its viability during the cultivation period. However, as it was shown in Figure 2, when the initial concentration of MSG in cultivation medium was 118 mM, the production of GABA was significantly lower compared to the production obtained with 100 mM MSG. This suggests that the observations from previous studies [2,28,53] about the negative effects of high glutamate concentrations on bacterial growth of some LAB strains and the expression of *gad*B genes could be an explanation for a similar observation in our study.

3.5. Cloning, Expression of Glutamate Decarboxylase from L. plantarum FNCC 260 in E. coli and Purification of the Enzyme

The *gad*B gene from *L. plantarum* FNCC 260 was cloned and its complete open reading frame consists of 1410 bp, encoding 469 amino acids. The predicted molecular mass of GAD is 53. 57 kDa and the theoretical isoelectric point (pI) is 5.62 as calculated using ExPASy program (www.expasy.org). The GadB sequence from *L. plantarum* FNCC 260 shared 98% homology with the GadB from *L. futsaii* CS3 (accession number AB839950), *L. plantarum* Taj-Apis362 (accession number AHG59384) and *L. plantarum* WCFS1(accession number CCC80401.1).

The *gad*B gene was cloned into the expression vector pET-21a(+) (Novagen, Merck KGaA, Darmstadt, Germany). The resulting vector pET21Gad was subsequently transformed into *E. coli* T7 Express carrying the plasmid pGRO 7 for the enhanced expression of the chaperones GroEL/GroES (*E. coli* T7 Express GRO). *E. coli* cells were cultivated in LB medium and induced with 0.5 mM IPTG as described in Section 2. The obtained expression yield was 1.38 kU/L fermentation medium with a specific activity of 0.24 U/mg. The recombinant GAD was purified with a single-step purification using the His-trap HP column and the specific activity of the purified enzyme was 1.12 U/mg with a purification factor of 4.5. The apparent molecular mass as judged by SDS-PAGE and native PAGE was estimated to be ~51 kDa and ~140 kDa, respectively (Figure 6a,b). The size of the protein was also confirmed by LC-ESI-MS and it was determined to be 51.79 kDa (data not shown). Several bands were found in native PAGE with the largest band was ~140 kDa. The LC-ESI-MS analysis revealed that these bands on native PAGE contain components of the subunit. The first band represent the intact dimeric enzyme and the other bands with lower molecular masses result from degradation of the intact protein. It also suggested that GadB from *L. plantarum* FNCC 260 is a homodimeric enzyme. GadB from *L. plantarum* ATCC 14917 was also reported as a homodimer [56].

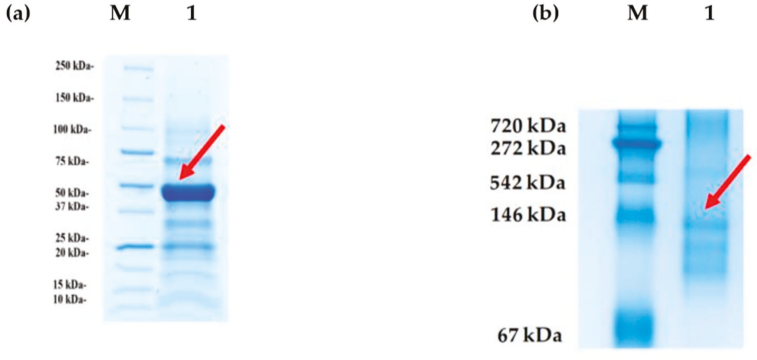

Figure 6. (**a**) SDS-PAGE analysis of purified recombinant GAD from *L. plantarum* FNCC 260 expressed in *E. coli.* Lane M; protein marker, 1; purified GAD. The arrow indicated GAD with molecular masses of approximately 53 kDa. (**b**) Native PAGE analysis of purified recombinant GAD. The molecular masses of GAD were estimated to be 140 kDa, Lane M; protein marker, 1; purified GAD.

The deduced amino acid sequence of *L. plantarum* FNCC 260 GAD contains a highly conserved catalytic domain that belongs to the PLP-dependent decarboxylase superfamily (Figure 7). A lysine residue (K280) is considered as the PLP-binding site for most bacterial GADs [51,56]. Lysine residue is also found in plant GADs since high homology between bacterial and plant GADs has been revealed [57,58]. In addition, the two residues T215 and D247 are crucial to promote decarboxylation [50]. Furthermore, the consensus sequence HVDAASGG is highly conserved in many bacterial GADs (Figure 7) and is also found in several GADs from Lactobacillus spp including *L. futsaii* CS3, *L. brevis* HYE1, *L. zymae*, and *L. paracasei* NFRI 7415 [19,34,36,51].

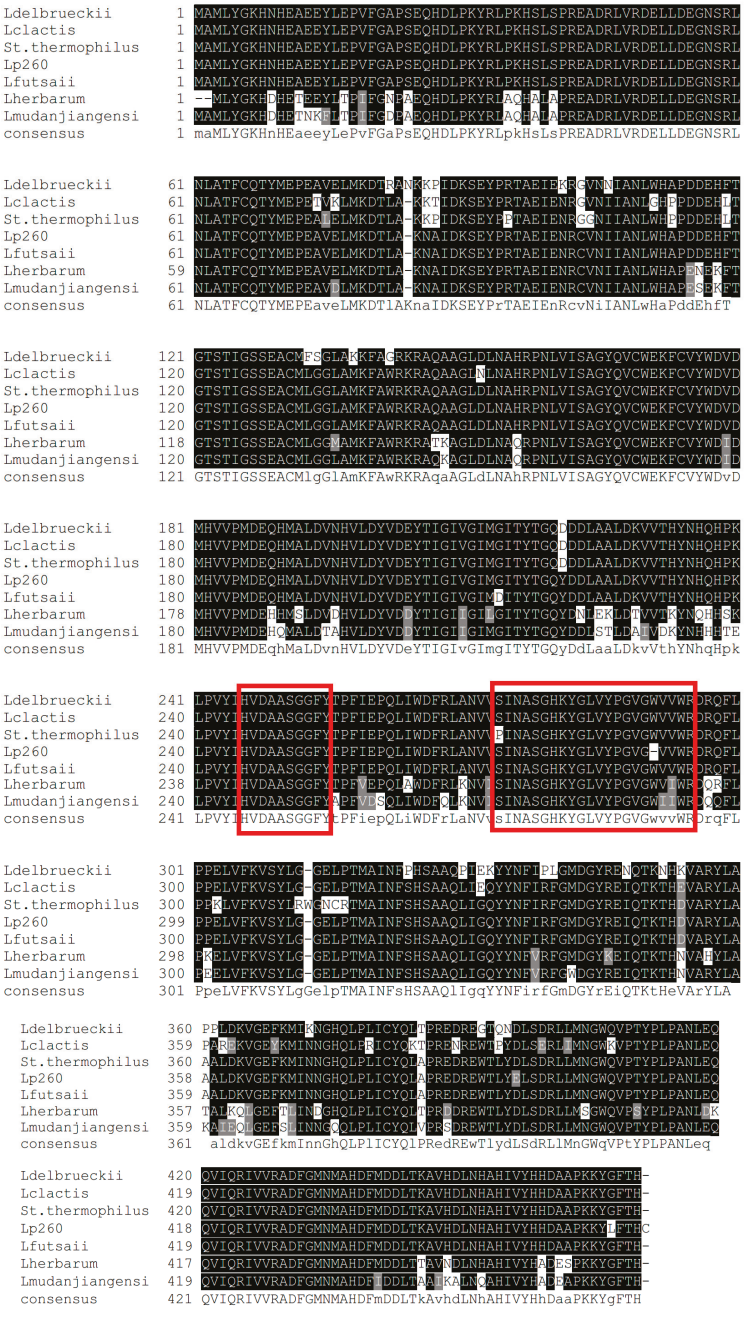

Figure 7. Alignment of amino acid sequences of GAD from *L. plantarum* FNCC 260 and six other GADs from LAB. The consensus sequence HVDAASGGF indicated by a smaller red box is highly conserved in GAD sequences. The sequence SINASGHKYGLVYPGVGWVVWR in the bigger red box is the PLP-binding domain [49]. GadB sequences shown are from *L. delbrueckii* (Ldelbrueckii), *Lactococcus lactis* (Lclactis), *S. thermophilus* (St. thermophilus), *L. plantarum* FNCC 260 (Lp260), *L. futsaii* (Lfutsaii), *L. herbarum* (Lherbarum), and *L. mudajiangensi* (Lmudanjiangensi).

3.6. GABA Synthesis by Recombinant Glutamate Decarboxylase from L. plantarum FNCC 260

For enzymatic GABA synthesis, we performed the conversion of MSG using 0.64 U/mL purified recombinant GAD in a 2-mL scale of reaction mixtures. Most GADs from *Lactobacillus* spp. have optimum activities at acidic pH values [33,36,57,58], and the recombinant GAD from *L. plantarum* FNCC 260 showed an optimum pH at pH 4.5 as expected (data not shown). MSG (100 mM) in 50 mM citrate-phosphate buffer (pH 4.5) containing 0.2 mM PLP was used as substrate and the reaction was performed at 30 °C. GABA synthesis reached its highest yield at 6450 mg/L (63 mM) within 6 h of reaction (Figure 8), and the enzyme retained 73% of its initial activity after 6 h of reaction. It was clear that the use of purified GAD was more efficient in terms of both GABA production and conversion time. Enzymatic synthesis of GABA using purified recombinant GAD from *L. plantarum* FNCC 260 showed 5 to 7-fold higher product concentrations than microbial fermentations in a significantly shorter time. This suggests that the use of purified GAD is crucial to overcome the limitations in GABA production due to GABA-degrading enzymes in the cells, slow reaction rate, and low production yield [28,53,59,60]. Furthermore, UPLC analysis was performed to confirm GABA production in both microbial fermentation and enzymatic conversion with a retention time of GABA at 8.5 min (Figure 9).

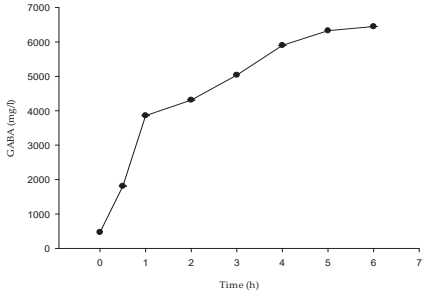

Figure 8. Enzymatic conversion of MSG to GABA using purified recombinant GAD from *L. plantarum* FNCC 260. The conversion was performed using 0.64 U/mL of GAD in 2 mL of 50 mM citrate-phosphate buffer (pH 4.5) containing 100 mM MSG and 0.2 mM PLP at 30 °C. Data expressed as mean ± SD with SD less than 5%. The experiments were conducted at least in duplicate.

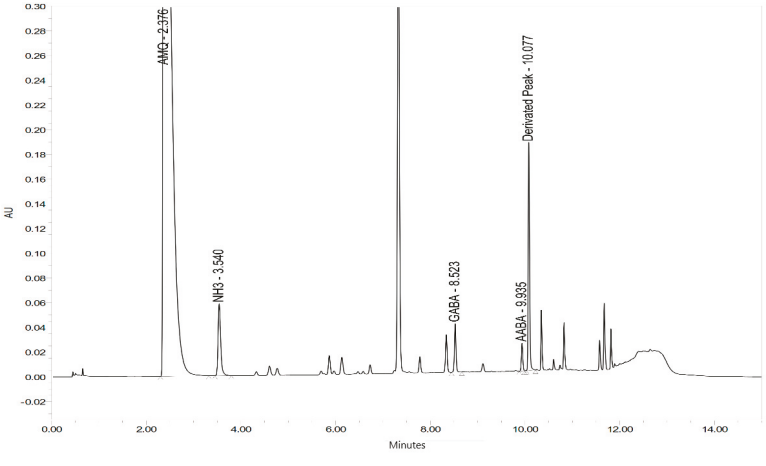

(**a**)

Figure 9. *Cont.*

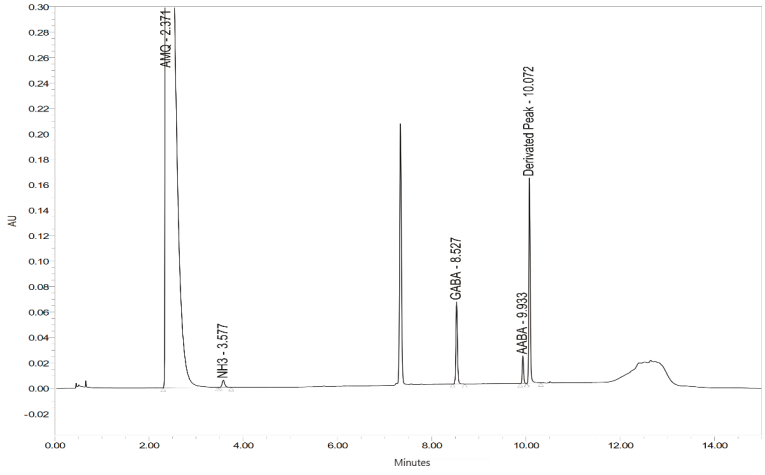

(**b**)

Figure 9. UPLC analysis of GABA in the culture medium of microbial fermentation (**a**) and in the reaction mixture of enzymatic conversion of MSG (**b**). The strain was cultivated in MRS broth containing 118 mM MSG and incubated at 37 °C for 48 h. The culture broth was centrifuged and the supernatans were collected (**a**). Enzymatic conversion was performed with 0.64 U/mL purified GAD using 100 mM MSG in 50 mM citrate-phosphate buffer (pH 4.5) containing 0.2 mM of PLP. The reactions were carried out at 30 °C with 300 rpm agitation (**b**). All samples (microbial fermentations and enzymatic conversion) were hydrolyzed and derivatized prior to UPLC analysis.

4. Conclusions

In the present study, we compared GABA synthesis between microbial fermentation of *L. plantarum* FNCC 260, which was isolated from Indonesian fermented cassava, and enzymatic conversion of glutamate using recombinant glutamate decarboxylase (GAD) from *L. plantarum* FNCC 260 expressed in *E. coli*. MSG, PLP, and pyridoxine were shown to positively affect GABA production during the cultivations of *L. plantarum* FNCC 260. Enzymatic synthesis of GABA using purified recombinant GAD from *L. plantarum* FNCC 260 showed at least 5-fold higher GABA titres than microbial fermentations in a significantly shorter time. The newly isolated GABA-producing LAB is of great interest to extend the area of applications. *L. plantarum* FNCC 260 should be considered as a potential candidate for GABA production via both fermentation and enzymatic synthesis and can be also developed as functional starter culture.

Author Contributions: Conceptualization, I.B.A.Y., E.S.R., D.H. and T.H.N.; methodology, I.B.A.Y., S.K., T.H.N. and D.H.; software, I.B.A.Y.; validation, I.B.A.Y., S.K. and T.H.N.; formal analysis, I.B.A.Y. and S.K.; investigation, I.B.A.Y., S.K. and T.H.N.; resources, I.B.A.Y.; data curation, I.B.A.Y. and S.K.; writing—original draft preparation, I.B.A.Y.; writing—review and editing, I.B.A.Y. and T.H.N., D.H., K.J.D.; visualization, I.B.A.Y.; supervision, T.H.N., D.H., K.J.D. and E.S.R.; project administration, I.B.A.Y.; funding acquisition, D.H. and T.H.N. All authors have read and agreed to the published version of the manuscript.

Funding: This research received no external funding.

Informed Consent Statement: This study did not involve any human/animal interventions.

Acknowledgments: This study was part of the project titled "GABA-producing lactic acid bacteria from Indonesian fermented foods and its development for functional foods ingredients and starter cultures". We are also grateful for the Indonesian Endowment Fund for Education (LPDP) under Beasiswa Unggulan Dosen Indonesia-Luar Negeri (BUDI-LN) batch I 2016 for funding this study (grant number PRJ-3607/LPDP.3/2016). S.K. is thankful for the Ernst Mach—ASEA Uninet scholar-

ship granted by the OeAD—Austrian Agency for International Cooperation in Education & Research and financed by the Austrian Federal Ministry of Science, Research and Economy. We would like to thank Clemens Grünwald-Gruber (Department of Chemistry, University of Natural Resources and Life Sciences-BOKU Wien) for his assistance in LC-ESI-MS analysis. The authors thank the EQ BOKU VIBT GmbH – Core facility for food and bio processing for providing the MALDI-TOF MS (Bruker Biotyper) for the identification of lactic acid bacteria.

Conflicts of Interest: The authors declare no conflict of interest.

References

1. Nomura, M.; Kimoto, H.; Someya, Y.; Furukawa, S.; Suzuki, I. Production of gamma-aminobutyric acid by cheese starters during cheese ripening. *J. Dairy Sci.* **1998**, *81*, 1486–1491. [CrossRef]
2. Komatsuzaki, N.; Shima, J.; Kawamoto, S.; Momose, H.; Kimura, T. Production of γ-aminobutyric acid (GABA) by *Lactobacillus paracasei* isolated from traditional fermented foods. *Food Microbiol.* **2005**, *22*, 497–504. [CrossRef]
3. Siragusa, S.; De Angelis, M.; Di Cagno, R.; Rizzello, C.G.; Coda, R.; Gobbetti, M. Synthesis of γ-aminobutyric acid by lactic acid bacteria isolated from a variety of Italian cheeses. *Appl. Environ. Microbiol.* **2007**, *73*, 7283–7290. [CrossRef]
4. Yang, H.; Xing, R.; Liu, S.; Yu, H.; Li, P. Analysis of the protective effects of γ-aminobutyric acid during fluoride-induced hypothyroidism in male Kunming mice Analysis of the protective effects of γ-aminobutyric acid during fluoride-induced. *Pharm. Biol.* **2019**, *57*, 29–37. [CrossRef]
5. Pouliot-Mathieu, K.; Gardner-Fortier, C.; Lemieux, S.; St-Gelais, D.; Champagne, C.P.; Vuillemard, J.C. Effect of cheese containing gamma-aminobutyric acid-producing lactic acid bacteria on blood pressure in men. *Pharma Nutr.* **2013**, *1*, 141–148. [CrossRef]
6. Zhang, Q.; Xiang, J.; Zhang, L.; Zhu, X.; Evers, J.; van der Werf, W.; Duan, L. Optimizing soaking and germination conditions to improve gamma-aminobutyric acid content in japonica and indica germinated brown rice. *J. Funct. Foods* **2014**, *10*, 283–291. [CrossRef]
7. Hagiwara, H.; Seki, T.; Ariga, T. The effect of pre-germinated brown rice intake on blood glucose and PAI-1 levels in streptozotocin-induced diabetic rats. *Biosci. Biotechnol. Biochem.* **2004**, *68*, 444–447. [CrossRef]
8. Brambilla, P.; Perez, J.; Barale, F.; Schettini, G.; Soares, J.C. GABAergic dysfunction in mood disorders. *Mol. Psychiatry* **2003**, *8*, 721–737. [CrossRef] [PubMed]
9. Ratanaburee, A.; Kantachote, D.; Charernjiratrakul, W.; Sukhoom, A. Selection of γ-aminobutyric acid-producing lactic acid bacteria and their potential as probiotics for use as starter cultures in Thai fermented sausages (Nham). *Int. J. Food Sci. Technol.* **2013**, *48*, 1371–1382. [CrossRef]
10. Song, H.Y.; Yu, R.C. Optimization of culture conditions for gamma-aminobutyric acid production in fermented adzuki bean milk. *J. Food Drug Anal.* **2018**, *26*, 74–81. [CrossRef] [PubMed]
11. Dalin, L.; Mayrhofer, S.; Yogeswara, I.B.A.; Nguyen, T.H.; Domig, K.J. Identification, classification and screening for gamma aminobutyric acid production in lactic acid bacteria from Cambodian fermented foods. *Biomolecules* **2019**, *9*, 768. [CrossRef]
12. Shimada, M.; Hasegawa, T.; Nishimura, C.; Kan, H.; Kanno, T.; Nakamura, T.; Matsubayashi, T. Anti-hypertensive effect of γ-aminobutyric acid (GABA)-rich chlorella on high-normal blood pressure and borderline hypertension in placebo-controlled double blind study. *Clin. Exp. Hypertens.* **2009**, *31*, 342–354. [CrossRef] [PubMed]
13. Tsai, J.S.; Lin, Y.S.; Pan, B.S.; Chen, T.J. Antihypertensive peptides and γ-aminobutyric acid from prozyme 6 facilitated lactic acid bacteria fermentation of soymilk. *Process Biochem.* **2006**, *41*, 1282–1288. [CrossRef]
14. Hayakawa, K.; Kimura, M.; Kasaha, K.; Matsumoto, K.; Sansawa, H.; Yamori, Y. Effect of a γ-aminobutyric acid-enriched dairy product on the blood pressure of spontaneously hypertensive and normotensive Wistar–Kyoto rats. *Br. J. Nutr.* **2004**, *92*, 411–417. [CrossRef]
15. Suwanmanon, K.; Hsieh, P.C. Effect of γ-aminobutyric acid and nattokinase-enriched fermented beans on the blood pressure of spontaneously hypertensive and normotensive Wistar-Kyoto rats. *J. Food Drug Anal.* **2014**, *22*, 485–491. [CrossRef]
16. Abe, Y.; Umemura, S.; Sugimoto, K.; Hirawa, N.; Kato, Y.; Yokoyama, N.; Yokoyama, T.; Iwai, J.; Ishii, M. Effect of green tea rich in γ-aminobutyric acid on blood pressure of Dahl salt-sensitive rats. *Am. J. Hypertens.* **1995**, *8*, 74–79. [CrossRef]
17. Huang, J.; Mei, L.H.; Hong, W.; Lin, D. Biosynthesis of γ-aminobutyric acid (GABA) using immobilized whole cells of *Lactobacillus brevis*. *World J. Microbiol. Biotechnol.* **2007**, *23*, 865–871. [CrossRef]
18. Lu, X.; Chen, Z.; Gu, Z.; Han, Y. Isolation of γ-aminobutyric acid-producing bacteria and optimization of fermentative medium. *Biochem Eng. J.* **2008**, *41*, 48–52. [CrossRef]
19. Komatsuzaki, N.; Nakamura, T.; Kimura, T.; Shima, J. Characterization of glutamate decarboxylase from a high gamma-aminobutyric acid (GABA)-producer, *Lactobacillus paracasei*. *Biosci. Biotechnol. Biochem.* **2008**, *72*, 278–285. [CrossRef]
20. Park, K.B.; Oh, S.H. Cloning, sequencing and expression of a novel glutamate decarboxylase gene from a newly isolated lactic acid bacterium, *Lactobacillus brevis* OPK-3. *Bioresour. Technol.* **2007**, *98*, 312–319. [CrossRef]
21. Lin, Q. Submerged fermentation of *Lactobacillus rhamnosus* YS9 for γ-aminobutyric acid (GABA) production. *Braz. J. Microbiol.* **2013**, *44*, 183–187. [CrossRef] [PubMed]
22. Das, D.; Goyal, A. Antioxidant activity and γ-aminobutyric acid (GABA) producing ability of probiotic *Lactobacillus plantarum* DM5 isolated from Marcha of Sikkim. *LWT Food Sci. Technol.* **2015**, *61*, 263–268. [CrossRef]

23. Sun, T.; Zhao, S.; Wang, H.; Cai, C.; Chen, Y.; Zhang, H. ACE-inhibitory activity and gamma-aminobutyric acid content of fermented skim milk by *Lactobacillus helveticus* isolated from Xinjiang koumiss in China. *Eur. Food Res. Technol.* **2009**, *228*, 607–612. [CrossRef]
24. Cho, Y.R.; Chang, J.Y.; Chang, H.C. Production of γ-aminobutyric acid (GABA) by *Lactobacillus buchneri* isolated from Kimchi and its neuroprotective effect on neuronal cells. *J. Microbiol. Biotechnol.* **2007**, *17*, 104–109. [PubMed]
25. Ribeiro, S.C.; Domingos-Lopes, M.F.P.; Stanton, C.; Ross, R.P.; Silva, I.A.C.G. Production of γ-aminobutyric acid (GABA) by *Lactobacillus otakiensis* and other *Lactobacillus* sp. isolated from traditional Pico cheese. *Int. J. Dairy Technol.* **2007**, *70*, 1–6. [CrossRef]
26. Rahayu, E.S.; Yogeswara, I.B.A.; Windiarti, L.; Utami, T.; Watanabe, K. Molecular characteristics of indigenous probiotic strains from Indonesia. *Int. J. Probiotics Prebiotics* **2015**, *10*, 1–8.
27. Rahayu, E.S. Lactic acid bacteria in fermented foods of Indonesian origin. *Agritech* **2003**, *23*, 75–84.
28. Li, H.; Qiu, T.; Huang, G.; Cao, Y. Production of gamma-aminobutyric acid by *Lactobacillus brevis* NCL912 using fed-batch fermentation. *Microb. Cell Fact.* **2010**, *9*, 85. [CrossRef]
29. Li, H.; Qiu, T.; Gao, D.; Cao, Y. Medium optimization for production of gamma-aminobutyric acid by *Lactobacillus brevis* NCL912. *Amino Acids* **2010**, *38*, 1439–1445. [CrossRef]
30. Dhakal, R.; Bajpai, V.K.; Baek, K.H. Production of GABA (γ-aminobutyric acid) by microorganisms: A review. *Braz. J. Microbiol.* **2012**, *43*, 1230–1241. [CrossRef]
31. Tajabadi, N.; Baradaran, A.; Ebrahimpour, A.; Rahim, R.A.; Bakar, F.A.; Manap, M.Y.A.; Mohammed, A.S.; Saari, N. Overexpression and optimization of glutamate decarboxylase in *Lactobacillus plantarum* Taj-Apis362 for high gamma-aminobutyric acid production. *Microb. Biotechnol.* **2015**, *8*, 623–632. [CrossRef] [PubMed]
32. Seo, M.J.; Nam, Y.D.; Lee, S.Y.; Park, S.L.; Yi, S.H.; Lim, S.I. Expression and characterization of a glutamate decarboxylase from *Lactobacillus brevis* 877G producing γ-aminobutyric acid. *Biosci. Biotechnol. Biochem.* **2013**, *77*, 853–856. [CrossRef] [PubMed]
33. Fan, E.; Huang, J.; Hu, S.; Mei, L.; Yu, K. Cloning, sequencing and expression of a glutamate decarboxylase gene from the GABA-producing strain *Lactobacillus brevis* CGMCC 1306. *Ann. Microbiol.* **2012**, *62*, 689–698. [CrossRef]
34. Lim, H.S.; Seo, D.H.; Cha, I.T.; Lee, H.; Nam, Y.D.; Seo, M.J. Expression and characterization of glutamate decarboxylase from *Lactobacillus brevis* HYE1 isolated from kimchi. *World J. Microbiol. Biotechnol.* **2018**, *34*, 1–10. [CrossRef] [PubMed]
35. Yogeswara, I.B.A.; Kusumawati, I.G.A.W.; Sumadewi, N.L.U.; Rahayu, E.S.; Indrati, R. Isolation and identification of lactic acid bacteria from Indonesian fermented foods as γ-aminobutyric acid-producing bacteria. *Int. Food Res. J.* **2018**, *25*, 1753–1757.
36. Park, J.Y.; Jeong, S.J.; Kim, J.H. Characterization of a glutamate decarboxylase (GAD) gene from *Lactobacillus zymae*. *Biotechnol. Lett.* **2014**, *36*, 1791–1799. [CrossRef]
37. Dasen, G.; Smutny, J.; Teuber, M.; Meile, L. Classification and identification of Propionibacteria based on ribosomal RNA genes and PCR. *Syst. Appl. Microbiol.* **1998**, *21*, 251–259. [CrossRef]
38. Yuan, H.; Wang, H.; Fidan, O.; Qin, Y.; Xiao, G.; Zhan, J. Identification of new glutamate decarboxylases from *Streptomyces* for efficient production of γ-aminobutyric acid in engineered *Escherichia coli*. *J. Biol. Eng.* **2019**, *13*, 24. [CrossRef]
39. Ohmori, T.; Tahara, M.; Ohshima, T. Mechanism of gamma-aminobutyric acid (GABA) production by a lactic acid bacterium in yogurt-sake. *Process Biochem.* **2018**, *74*, 21–27. [CrossRef]
40. Huang, C.; Huang, L. Rapid species and subspecies-specific level classification and identification of *Lactobacillus casei* group members using MALDI Biotyper combined with ClinProTools. *J. Dairy Sci.* **2018**, *101*, 979–991. [CrossRef]
41. Dec, M.; Urban-Chmiel, R.; Gnat, S.; Puchalski, A.; Wernicki, A. Identification of *Lactobacillus* strains of goose origin using MALDI-TOF mass spectrometry and 16S e 23S rDNA intergenic spacer PCR analysis. *Res. Microbiol.* **2014**, *165*, 190–201. [CrossRef] [PubMed]
42. Tanigawa, K.; Kawabata, H.; Watanabe, K. Identification and typing of *Lactococcus lactis* by matrix-assisted laser desorption ionization—Time of flight mass spectrometry. *Appl. Environ. Microbiol.* **2010**, *76*, 4055–4062. [CrossRef] [PubMed]
43. Lee, H.; Baek, H.; Bom, S.L.; Soo, J.H.; Shim, S.; Shin, S.Y.; Han, N.S.; Seo, J.H. Development of species-specific PCR primers and polyphasic characterization of *Lactobacillus sanfranciscensis* isolated from Korean sourdough. *Int. J. Food Microbiol.* **2015**, *200*, 80–86. [CrossRef] [PubMed]
44. Doan, N.T.L.; Van Hoorde, K.; Cnockaert, M.; De Brandt, E.; Aerts, M.; Thanh, B.L.; Vandamme, P. Validation of MALDI-TOF MS for rapid classification and identification of lactic acid bacteria with a focus on isolates from traditional fermented foods in Northern Vietnam. *Lett. Appl. Microbiol.* **2012**, *55*, 265–273. [CrossRef]
45. Dec, M.; Puchalski, A.; Urban-chmiel, R.; Wernicki, A. 16S-ARDRA and MALDI-TOF mass spectrometry as tools for identification of *Lactobacillus* bacteria isolated from poultry. *BMC Microbiol.* **2016**, *16*, 105. [CrossRef]
46. Cho, S.Y.; Park, M.J.; Kim, K.M.; Ryu, J.; Park, H.J. Production of high γ-aminobutyric acid (GABA) sour kimchi using lactic acid bacteria isolated from mukeunjee kimchi. *Food Sci. Biotechnol.* **2011**, *20*, 403–408. [CrossRef]
47. Kono, I.; Himeno, K. Changes in gamma-aminobutyric acid content during beni-koji making. *Biosci. Biotechnol. Biochem.* **2000**, *64*, 617–619. [CrossRef]
48. Shelp, B.J.; Bown, A.W.; Mclean, M.D. Metabolism and functions of gamma-aminobutyric acid. *Trends Plant Sci.* **1999**, *4*, 446–452. [CrossRef]
49. Ko, C.Y.; Lin, H.T.V.; Tsai, G.J. Gamma-aminobutyric acid production in black soybean milk by *Lactobacillus brevis* FPA 3709 and the antidepressant effect of the fermented product on a forced swimming rat model. *Process Biochem.* **2013**, *48*, 559–568. [CrossRef]

50. Han, S.H.; Hong, K.B.; Suh, H.J. Biotransformation of monosodium glutamate to gamma-aminobutyric acid by isolated strain *Lactobacillus brevis* L-32 for potentiation of pentobarbital-induced sleep in mice. *Food Biotechnol.* **2017**, *31*, 80–93. [CrossRef]
51. Sanchart, C.; Rattanaporn, O.; Haltrich, D.; Phukpattaranont, P.; Maneerat, S. *Lactobacillus futsaii* CS3, a New GABA-Producing Strain Isolated from Thai Fermented Shrimp (Kung-Som). *Indian J. Microbiol.* **2017**, *57*, 211–217. [CrossRef] [PubMed]
52. Su, L.; Huang, Y.; Wu, J. Enhanced production of recombinant *Escherichia coli* glutamate decarboxylase through optimization of induction strategy and addition of pyridoxine. *Bioresour. Technol.* **2015**, *198*, 63–69. [CrossRef] [PubMed]
53. Yang, S.Y.; Lu, F.X.; Lu, Z.X.; Bie, X.M.; Jiao, Y.; Sun, L.J.; Yu, B. Production of γ-aminobutyric acid by *Streptococcus salivarius* subsp. thermophilus Y2 under submerged fermentation. *Amino Acids* **2008**, *34*, 473–478.
54. Villegas, J.M.; Brown, L.; Savoy de Giori, G.; Hebert, E.M. Optimization of batch culture conditions for GABA production by *Lactobacillus brevis* CRL 1942, isolated from quinoa sourdough. *LWT Food Sci. Technol.* **2016**, *67*, 22–26. [CrossRef]
55. Jong, A.; Yong, C.C.; Oh, S. Bioconversion of gamma-aminobutyric acid from monosodium glutamate by *Lactobacillus brevis* Bmb5. *J. Microbiol. Biotechnol.* **2019**, *29*, 1745–1748. [CrossRef] [PubMed]
56. Shin, S.; Kim, H.; Joo, Y.; Lee, S.; Lee, Y.; Lee, S.J.; Lee, D.W. Characterization of glutamate decarboxylase from *Lactobacillus plantarum* and its C-terminal function for the pH dependance of activity. *J. Agric. Food Chem.* **2014**, *62*, 12186–12193. [CrossRef]
57. Sa, H.D.; Park, J.Y.; Jeong, S.J.; Lee, K.W.; Kim, J.H. Characterization of glutamate decarboxylase (GAD) from *Lactobacillus sakei* A156 isolated from jeot-gal. *J. Microbiol. Biotechnol.* **2015**, *25*, 696–703. [CrossRef]
58. Cotter, P.D.; Gahan, C.G.M.; Hill, C. A glutamate decarboxylase system protects *Listeria monocytogenes* in gastric fluid. *Mol. Microbiol.* **2001**, *40*, 465–475. [CrossRef]
59. Lee, S.J.; Lee, S.H.; Lee, W.D. Production of γ-aminobutyric acid using immobilized glutamate decarboxylase from *Lactobacillus plantarum*. *Microbiol. Biotechnol. Lett.* **2015**, *43*, 300–305. [CrossRef]
60. Lee, S.; Ahn, J.; Kim, G.Y.; Jung, K.J.; Lee, H.; Lee, G.E. Gamma aminobutyric acid production using immobilized glutamate decarboxylase followed by downstream processing with cation exchange chromatography. *Int. J. Microbiol. Sci.* **2013**, *14*, 1728–1739. [CrossRef]

processes

MDPI

Article

Antifungal Effect of Volatile Organic Compounds from *Bacillus velezensis* CT32 against *Verticillium dahliae* and *Fusarium oxysporum*

Xinxin Li [1,2,3], Xiuhong Wang [2,3], Xiangyuan Shi [2,3], Baoping Wang [1,2,3], Meiping Li [1], Qi Wang [1] and Shengwan Zhang [1,*]

1 School of Life Science, Shanxi University, Taiyuan 030006, China; lixinxin_215@163.com (X.L.); wangbp8409@163.com (B.W.); lmpmg@sxu.edu.cn (M.L.); wangqi@sxu.edu.cn (Q.W.)
2 Shanxi Institute of Organic Dryland Farming, Shanxi Agricultural University, Taiyuan 030031, China; wxhsxy75@163.com (X.W.); sxy75@yeah.net (X.S.)
3 Research Center of Modern Agriculture, Shanxi Academy of Agricultural Sciences, Taiyuan 030031, China
* Correspondence: zswan@sxu.edu.cn

Received: 2 November 2020; Accepted: 15 December 2020; Published: 18 December 2020

Abstract: The present study focuses on the inhibitory effect of volatile metabolites released by *Bacillus velezensis* CT32 on *Verticillium dahliae* and *Fusarium oxysporum*, the causal agents of strawberry vascular wilt. The CT32 strain was isolated from maize straw compost tea and identified as *B. velezensis* based on 16S rRNA gene sequence analysis. Bioassays conducted in sealed plates revealed that the volatile organic compounds (VOCs) produced by the strain CT32 possessed broad-spectrum antifungal activity against eight phytopathogenic fungi. The volatile profile of strain CT32 was obtained by headspace solid-phase microextraction (HS-SPME) coupled with gas chromatography-mass spectrometry (GC-MS). A total of 30 volatile compounds were identified, six of which have not previously been detected in bacteria or fungi: (Z)-5-undecene, decyl formate, 2,4-dimethyl-6-tert-butylphenol, dodecanenitrile, 2-methylpentadecane and 2,2′,5,5′-tetramethyl-1,1′-biphenyl. Pure compounds were tested in vitro for their inhibitory effect on the mycelial growth of *V. dahliae* and *F. oxysporum*. Decanal, benzothiazole, 3-undecanone, 2-undecanone, 2-undecanol, undecanal and 2,4-dimethyl-6-tert-butylphenol showed high antifungal activity, with benzothiazole and 2,4-dimethyl-6-tert-butylphenol being the most potent compounds. These results indicate that the VOCs produced by *B. velezensis* CT32 have the potential to be used as a biofumigant for management of vascular wilt pathogens.

Keywords: biocontrol; *Bacillus velezensis*; volatile organic compounds; vascular wilt pathogens

1. Introduction

Vascular wilt diseases, caused by *Verticillium dahliae* and *Fusarium oxysporum*, are devastating diseases of strawberry (*Fragaria* × *ananassa* Duch.) that severely affect the production of this crop. Due to the fact that the persistent resting structures produced by the pathogens are able to survive in the absence of hosts for long periods of time, vascular wilt diseases are particularly difficult to control [1,2]. Due to the lack of resistant strawberry cultivars, soil fumigation with methyl bromide is an effective way to manage vascular wilt diseases, but this fumigant has been withdrawn from routine use under the Montreal Protocol [3]. Non-chemical soil disinfections, such as steam sterilization and solarization, show potential in reducing soil inoculum levels, but these approaches may negatively impact soil microbial communities and associated functions [4]. Crop rotation is generally ineffective for Verticillium and Fusarium wilt of strawberry because of the wide host range of the pathogenic fungi. Therefore, the need to develop eco-friendly and highly efficient biocontrol agents (BCAs) for sustainable strawberry production is extremely urgent.

Over the past few decades, impressive progress has been made in the development, registration and commercialization of BCAs based on microbial antagonists. Members of the *Bacillus* genus are good candidates as BCAs because they form endospores that can be readily formulated into biopesticide products [5,6]. Moreover, they produce a vast array of bioactive molecules with strong inhibitory potential against plant pathogens, such as bacteriocins, lipopeptides, siderophores, polyketides and volatile compounds [7,8]. Among these metabolites, non-volatile substances have received considerable research attention, whereas volatile compounds are less frequently studied. Volatile organic compounds (VOCs) are low-molecular-weight (<300 Da) organic compounds that are characterized by a low boiling point, high vapor pressure and lipophilic character [9]. Several studies have demonstrated that the VOCs emitted by microbes may benefit plants by promoting growth, activating defence responses, and suppressing or eliminating potential pathogens [10–15]. Moreover, as naturally occurring chemicals, VOCs emitted by microorganisms are biodegradable. Therefore, microbial VOCs can be exploited as a sustainable strategy for use in crop enhancement and protection.

Muscodor albus, a biofumigant fungus, is the first commercially available BCA acting through its volatile emissions. In-package biofumigation with *M. albus* was shown to provide an effective control of fungal decay in grapes and extend their shelf life [16]. In addition, previous publications have shown the potential application of *M. albus* to protect building materials from biological damage and manage plant-parasitic nematodes of plants [17,18]. The successful application of *M. albus* inspired researchers to further explore the benefits of employing VOCs produced by antagonistic bacteria to control plant diseases.

Bacterial VOCs have been demonstrated to inhibit the growth and differentiation of numerous phytopathogenic fungi, suggesting that the complex mixtures of bacterial emissions represent a source of novel antifungal natural substances. For example, dimethyl disulfide (DMDS), a volatile sulphur compound frequently emitted by bacteria, has been shown to possess broad-range antifungal activities [19,20]. DMDS-containing products are used as novel soil fumigants. Recently, Zhang et al. [21] reported the inhibitory activity of 2,6-di-tert-butyl-4-methylphenol and 2,4-di-tert-butylphenol produced by *B. siamensis* G-3 against *Botrytis cinerea* and *Rhizopus stolonifer* both in vitro and in vivo. Given the diversity of microbes, only a small fraction of these volatile metabolites have been detected and studied, and more novel compounds with interesting bioactivities are yet to be discovered. A large number of phytopathogenic fungi have been used to investigate the antifungal potential of bacterial volatiles. However, the response of strawberry vascular wilt-causing agents to these volatile signals has largely been ignored in previous studies, despite the heavy losses they cause in strawberry production.

The objectives of this study were three-fold: (i) to investigate the response of two fungal vascular wilt pathogens to bacterial volatiles, (ii) to determine the chemical composition of bacterial VOCs, and (iii) to identify the bioactive compounds responsible for the antifungal effects. To achieve these aims, we isolated 73 strains of bacteria from maize straw compost tea and assessed their volatile-mediated effects on the mycelial growth of *V. dahliae* and *F. oxysporum*. From the above isolates, we selected *B. velezensis* CT32, which exhibited the highest antagonistic activity through the production of antifungal VOCs. Moreover, the VOCs produced by strain CT32 were qualitatively analysed by headspace solid-phase microextraction/gas chromatography-mass spectrometry (HS-SPME-GC-MS) and tested for their antifungal activity in vitro against *V. dahliae* and *F. oxysporum*.

2. Materials and Methods

2.1. Phytopathogenic Fungi and Culture Conditions

V. dahliae (ACCC 36196) and *F. oxysporum* f. sp. *cucumerinum* (ACCC 30220) were obtained from the Agricultural Culture Collection of China (ACCC), Beijing, China. *Glomerella cingulata* (CFCC 83279) and *Thanatephorus cucumeris* (CFCC 83233) were obtained from the China Forestry Culture Collection Center (CFCC). *F. oxysporum* f. sp. *fragariae* (FOF), *F. oxysporum* f. sp. *niveum*, *Botryosphaeria dothidea* and *Botrytis cinerea* were provided by the Research Center of Modern Agriculture, Shanxi Academy of

Agricultural Sciences. The plant pathogens were grown on potato dextrose agar (PDA) plates in the dark at 28 °C, except *B. cinerea*, which was incubated at 25 °C.

2.2. Isolation of Bacteria from Maize Straw Compost Tea

Maize straw compost tea samples for the isolation of antagonistic bacteria were prepared as described previously [22]. Briefly, 10 mL of the compost tea was added to 90 mL of sterile distilled water in a 250 mL Erlenmeyer flask and shaken at 180 rpm and 30 °C for 30 min on a rotary shaker. Serial 10-fold dilutions of the suspension were prepared in sterile distilled water, and aliquots (200 µL) of each dilution were spread-plated onto nutrient agar (NA). After 48 h of incubation at 30 °C, bacterial colonies with dissimilar morphologies were selected and further purified by streaking on NA plates. All isolates were routinely maintained on slants of NA at 4 °C until further use.

2.3. Screening for Bacteria Producing Antifungal Volatiles

Seventy-three bacterial isolates were tested for their volatile-mediated effect on the mycelial growth of *V. dahliae* and FOF using the sealed plate method. A Petri dish containing NA was inoculated by spreading 200 µL of cell suspension (1×10^7 cfu ml^{-1}) of bacterial strain and incubated at 28 °C for 24 h. A 5 mm diameter mycelial plug was taken from an actively growing culture of the tested pathogen and placed in the centre of a second Petri dish containing PDA. The lids of the two plates were removed. Subsequently, the plate inoculated with the mycelial plug was inverted and placed over the bacterial plate. The two plates were sealed with 3 turns of Parafilm. Sealed plates with only mycelial plugs growing in them served as controls. All plates were incubated at 28 °C until control plates were fully covered with mycelia of the tested pathogen. Three plates for each bacterial strain and control were used. The inhibition rate was calculated using the formula presented by Gao et al. [23]:

$$\text{Inhibition rate (\%)} = (D_{CK} - D_{TR})/(D_{CK} - 5\text{ mm}) \times 100$$

where D_{CK} is the colony diameter of the target pathogen in the control and D_{TR} is the colony diameter of the target pathogen in the treatment.

The broad-spectrum antifungal effect of the VOCs produced by the selected antagonistic bacterium, designated as CT32, against 8 plant pathogenic fungi was determined using the same method described above.

2.4. Analysis of Bacterial VOCs by HS-SPME-GC-MS

2.4.1. Sample Preparation

Three millilitres of melted NA culture medium was added into 20 mL headspace vials. The vials containing NA were sterilized at 121 °C for 20 min. Then, 90 µL of cell suspension of the strain CT32 (1×10^7 cfu ml^{-1}) was inoculated on the surface of the culture medium in sample vials. The vials were capped with polytetrafluoroethylene (PTFE)/silicone septa and incubated for 4 d at 28 °C in the dark. Three samples were prepared, and uninoculated vials containing only NA medium served as controls.

2.4.2. HS-SPME Procedure

An SPME fibre with 50/30 µm divinylbenzene/carboxen/polydimethylsiloxane (DVB/CAR/PDMS) coating (Supelco, Bellefonte, PA, USA) was conditioned following the manufacturer's instructions. The vials were positioned inside a water bath to equilibrate for 27 min at 74 °C, and then extraction was carried out by exposing the SPME fibre to the headspace of the vial for 53 min. The trapped compounds were desorbed for 4 min within the GC injector at 250 °C.

2.4.3. GC-MS Analysis

GC-MS analysis was performed on an Agilent 7890A GC coupled to a 5975C mass selective detector (MSD) (Agilent, Santa Clara, CA, USA). Chromatographic separation was carried out on

an HP-5MS capillary column (30 m × 0.25 mm ID, 0.25 μm film thickness). Helium flow rate was 1 mL min^{-1}. Injector temperature was maintained at 250 °C, and the splitless mode was chosen for injection. The oven programme was: initial 40 °C with a 2 min hold, ramped to 110 °C at 4 °C min^{-1}, ramped to 130 °C at 2 °C min^{-1} (held for 2 min), ramped to 150 °C at 2 °C min^{-1} (held for 2 min), ramped to 200 °C at 3 °C min^{-1}, ramped to 300 °C at 30 °C min^{-1} (held for 5 min). The total run time was 68.5 min. MSD settings: electron impact mode at 70 eV, full scan acquisition mode, scan range 33–500 *m*/*z*. Ion source temperature was 230 °C. Quadrupole temperature was 150 °C. The retention index (RI) of each volatile compound was calculated using *n*-alkanes (C_7-C_{40}) as reference compounds, as described by Bianchi et al. [24]. Identification of bacterial VOCs was accomplished by comparing the obtained mass spectra with those stored in the National Institute of Standards and Technology (NIST) Mass Spectral Library (version 11) as well as by comparing the determined RIs with those reported in the literature. The relative amounts (RA) of the detected volatile compounds were calculated by dividing the area data of each component by the summed total peak area of all components. The analysis of NA medium was performed under the same conditions.

2.5. Effect of Synthetic VOCs on Mycelial Growth of V. dahliae and FOF

Pure standards of 26 commercially available VOCs produced by strain CT32 and identified by GC-MS analysis were purchased from Sigma-Aldrich LLC (Saint Louis, USA), Aladdin Reagent Inc. (Shanghai, China), and Tokyo Chemical Industry Co., Ltd. (Tokyo, Japan). These VOC standards were tested to determine their effect against the mycelial growth of *V. dahliae* and FOF. A sterile filter paper disc containing 100 μL of each pure compound was placed inside a Petri dish. For solid standards, 100 mg of each solid alcohol was dissolved with 100 μL methanol, 100 mg of each solid ketone was dissolved with 100 μL acetone. The remaining solid standards were added directly to the filter paper. The lid of the Petri dish was replaced by the PDA plate previously inoculated with a 5 mm diameter mycelial plug of the target pathogen in the centre. The two plates were quickly sealed with Parafilm and incubated at 28 °C in the dark. The inhibition rate was calculated according to the formula previously described in Section 2.3. In the control plates, pure VOCs were substituted by an equivalent amount of sterile distilled water. The experiment was performed in triplicate.

2.6. Identification of Strain CT32

Strain CT32 was subjected to Gram staining. The spore formation and cell morphology of strain CT32 were observed under a transmission electron microscope as well as a light microscope. Then, 16S rRNA gene sequencing was conducted to assess the phylogenetic relationship of the unidentified bacterium to other related taxa. Genomic DNA was extracted using an Ezup Column Bacteria Genomic DNA Purification Kit (Sangon Biotech, Shanghai, China). Amplification was performed using the primer pair 27F (5′-AGTTTGATCMTGGCTCAG-3′) and 1492R (5′-GGTTACCTTGTTACGACTT-3′) under the conditions described by Zhang et al. [21]. The purified PCR product was sequenced by Sangon Biotech Co., Ltd. The 16S rRNA gene sequences of unknown bacterium and of closely related type strains were aligned using Clustal X (version 2.0). The phylogenetic tree was built using MEGA (version 6.0) via the neighbor-joining method.

2.7. Statistical Analysis

Statistical analyses of inhibition rates were performed using SPSS 21.0 software. Data were calculated and subjected to one-way ANOVA.

3. Results

3.1. Screening for Bacteria with Volatile-Mediated Antagonistic Activity

In total, 73 isolates of bacteria with distinct morphologies were isolated from maize straw compost tea. Among these isolates, five bacterial strains produced volatiles able to significantly ($p < 0.05$) inhibit

the mycelial growth of both *V. dahliae* and FOF (Table 1). One of these bacterial strains, designated as CT32, was found to have the highest antagonistic activity. Upon exposure to VOCs emitted by strain CT32, the mycelial growth of *V. dahliae* and FOF was reduced by 66.94% and 45.72%, respectively. Therefore, strain CT32 was selected for further investigation.

Table 1. Inhibitory effect of volatile compounds produced by antagonistic bacteria on the mycelial growth of *V. dahliae* and *F. oxysporum* f. sp. *fragariae* (FOF).

Bacterial Isolate	Colony Diameter of Control (mm)		Colony Diameter of Treatment (mm)		Inhibition Rate (%)	
	V. dahliae	FOF	*V. dahliae*	FOF	*V. dahliae*	FOF
CT11	81.22 ± 0.70	87.47 ± 0.64	56.12 ± 0.89	54.18 ± 2.58	32.93 ± 1.17 d [1]	40.36 ± 3.13 b
CT32	81.22 ± 0.70	87.47 ± 0.64	30.20 ± 1.57	49.77 ± 1.53	66.94 ± 2.06 a	45.72 ± 1.86 a
CT56	81.22 ± 0.70	87.47 ± 0.64	47.85 ± 0.60	68.55 ± 1.70	43.78 ± 0.79 b	22.94 ± 2.06 d
CT58	81.22 ± 0.70	87.47 ± 0.64	52.55 ± 2.19	65.37 ± 1.03	37.61 ± 2.87 c	26.80 ± 1.25 c
CT64	81.22 ± 0.70	87.47 ± 0.64	67.82 ± 1.26	79.38 ± 0.83	17.58 ± 1.65 e	9.80 ± 1.01 e

[1] Data are the mean ± standard deviation. In the same column, data with different lowercase letters are significantly different according to Duncan's multiple range test ($p < 0.05$).

3.2. In Vitro Antifungal Activity of VOCs Produced by Strain CT32

The VOCs emitted by strain CT32 significantly ($p < 0.05$) inhibited the mycelial growth of all tested pathogens, although with different inhibition extents (Figure 1). *V. dahliae* was the most susceptible fungus to VOCs emitted by strain CT32, and its mycelial growth was inhibited by 66.67%. In contrast, *T. cucumeris* showed the greatest resistance to bacterial volatiles. Additionally, the VOCs produced by strain CT32 significantly reduced the mycelial growth of *G. cingulata*, *B. cinerea*, *B. dothidea*, *F. oxysporum* f. sp. *niveum*, FOF and *F. oxysporum* f. sp. *cucumerinum*, with percentages of inhibition ranging from 19.76% to 55.02%. The suppressive effect of the VOCs emitted by strain CT32 on the in vitro growth of eight pathogenic fungi is presented in Figure 2.

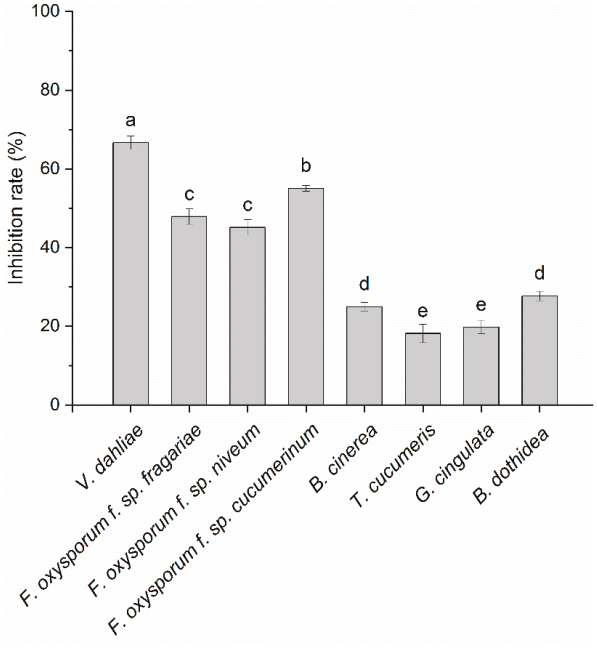

Figure 1. Inhibitory effect of volatile organic compounds (VOCs) produced by strain CT32 on the mycelial growth of 8 plant pathogenic fungi. Values with different lowercase letters are significantly different according to Duncan's multiple range test at the 0.05 level.

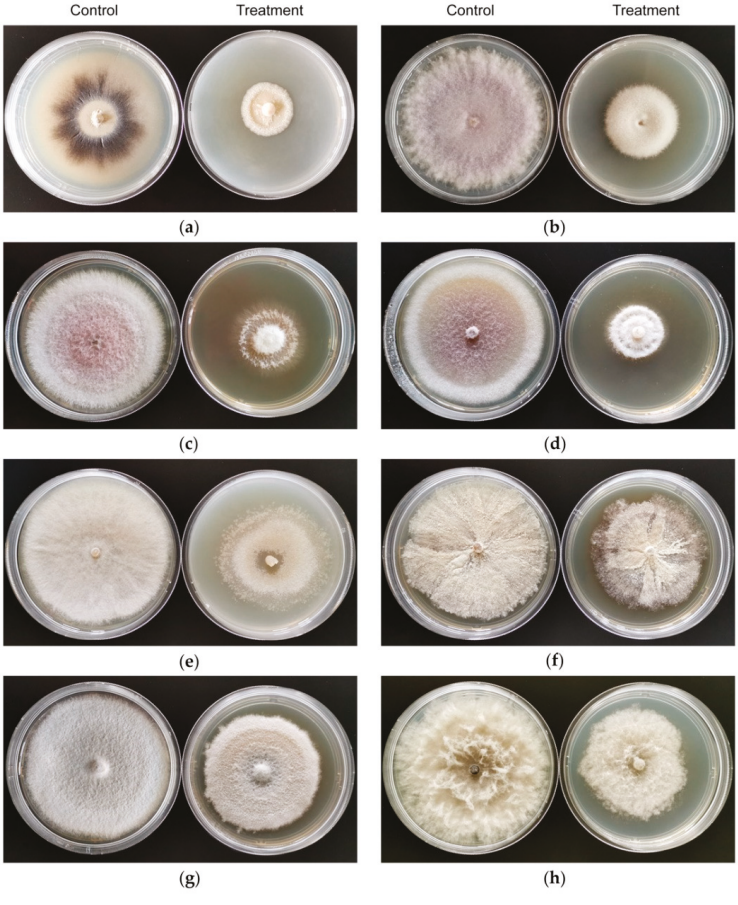

Figure 2. Effect of VOCs emitted by strain CT32 on the growth of 8 phytopathogenic fungi in vitro. In the sealed plates test, fungi in the control groups were cultured on potato dextrose agar (PDA) medium. The mycelial growth of fungi in the treatment groups was suppressed upon exposure to volatiles emitted by strain CT32. (**a**) *V. dahliae*; (**b**) *F. oxysporum* f. sp. *fragariae*; (**c**) *F. oxysporum* f. sp. *niveum*; (**d**) *F. oxysporum* f. sp. *cucumerinum*; (**e**) *B. cinerea*; (**f**) *T. cucumeris*; (**g**) *G. cingulata*; (**h**) *B. dothidea*.

3.3. HS-SPME-GC-MS Analysis of VOCs Produced by Strain CT32

The total ion chromatogram of VOCs emitted by strain CT32 is shown in Figure 3. A total of 30 volatile compounds derived from strain CT32, i.e., eight alkanes, six ketones, five alcohols, four aldehydes, two phenols, one alkene, one thiazole, one ester, one nitrogen compound and one biphenyl, were identified by GC-MS (Table S1). Alkanes, ketones, alcohols, and aldehydes were found to be the predominant VOCs emitted by strain CT32, which constituted 76.67% of the 30 detected compounds. The relative amounts of aldehydes, alcohols, ketones, and alkanes were calculated to account for 50.32%, 24.31%, 11.28% and 2.75% of the total volatile components, respectively. The most abundant volatile compound was dodecanal (48.56%), followed by 1-dodecanol (10.27%), 2-undecanol (8.46%), 2-undecanone (3.37%) and 2-dodecanol (3.24%).

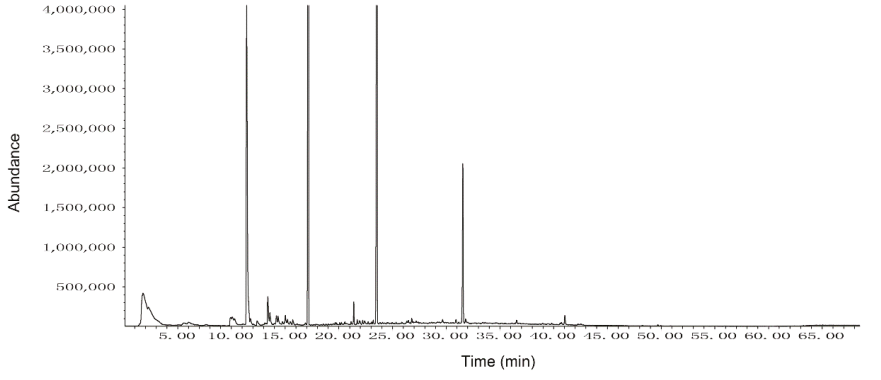

(**a**)

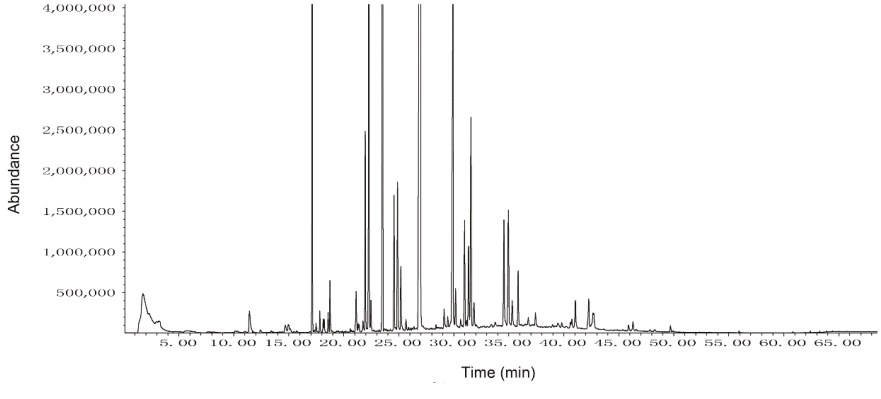

(**b**)

Figure 3. (**a**) Total ion chromatogram of VOCs from uninoculated nutrient agar (NA) medium; (**b**) total ion chromatogram of VOCs from strain CT32.

3.4. Antifungal Activity of Synthetic VOCs against V. dahliae and FOF

As shown in Table 2, 26 out of the 30 volatile compounds were commercially available and tested for their antifungal activities against *V. dahliae* and FOF in vitro. Benzothiazole significantly ($p < 0.05$) inhibited the mycelial growth of the two target pathogens. Furthermore, 2,4-dimethyl-6-tert-butylphenol proved highly suppressive against both fungi, showing an inhibition rate greater than 90%. The inhibition rates of dodecanenitrile were 51.10% against *V. dahliae* and 20.04% against FOF. All four aldehydes negatively impacted both pathogens, but the strength of their impact varied. Although dodecanal was the most abundant compound in the headspace of strain CT32, it exhibited significant but weak inhibitory activity. Decanal and undecanal possessed high antifungal activity against *V. dahliae* and FOF, but they were produced in low amounts. In general, FOF was more tolerant to alcohols than *V. dahliae*. The antifungal activity of alcohols was negatively correlated with the number of carbon atoms in the alcohols, and thus, 2-undecanol showed the highest inhibitory activity. Among the six ketones tested for bioactivity against *V. dahliae* and FOF, 2-undecanone showed the highest level of inhibition under the experimental conditions, followed by 3-undecanone and 2-dodecanone.

Table 2. Inhibitory effect of 26 synthetic VOCs on the mycelial growth of *V. dahliae* and FOF.

Compound	Colony Diameter of Control (mm)		Colony Diameter of Treatment (mm)		Inhibition Rate (%)	
	V. dahliae	FOF	*V. dahliae*	FOF	*V. dahliae*	FOF
Undecane	83.05 ± 0.83	87.75 ± 0.25	88.00 ± 0.00	88.00 ± 0.00	–p [1]	–o
Decanal	83.05 ± 0.83	87.75 ± 0.25	21.13 ± 1.21	35.03 ± 0.96	79.33 ± 1.54 d [2]	63.71 ± 1.16 c
Benzothiazole	83.05 ± 0.83	87.75 ± 0.25	5.00 ± 0.00	5.00 ± 0.00	100.00 ± 0.00 a	100.00 ± 0.00 a
3-Undecanone	83.05 ± 0.83	87.75 ± 0.25	32.75 ± 1.75	42.85 ± 0.41	64.45 ± 2.24 f	54.26 ± 0.49 e
2-Undecanone	83.05 ± 0.83	87.75 ± 0.25	25.47 ± 2.87	40.62 ± 1.62	73.78 ± 3.67 e	56.96 ± 1.95 d
2-Undecanol	83.05 ± 0.83	87.75 ± 0.25	24.42 ± 1.23	41.83 ± 1.15	75.12 ± 1.58 e	55.49 ± 1.40 de
Undecanal	83.05 ± 0.83	87.75 ± 0.25	12.05 ± 0.91	49.25 ± 1.09	90.97 ± 1.17 c	46.53 ± 1.32 f
2-Dodecanone	83.05 ± 0.83	87.75 ± 0.25	54.47 ± 1.50	55.35 ± 2.93	36.62 ± 1.92 h	39.15 ± 3.54 g
2-Dodecanol	83.05 ± 0.83	87.75 ± 0.25	43.75 ± 2.41	64.22 ± 1.55	50.35 ± 3.09 g	28.44 ± 1.87 h
2,4-Dimethyl-6-tert-butylphenol	83.05 ± 0.83	87.75 ± 0.25	8.45 ± 0.43	12.33 ± 0.38	95.58 ± 0.55 b	91.14 ± 0.46 b
Tetradecane	83.05 ± 0.83	87.75 ± 0.25	86.75 ± 0.87	88.00 ± 0.00	–nop	–o
Dodecanal	83.05 ± 0.83	87.75 ± 0.25	61.75 ± 1.24	80.58 ± 1.28	27.29 ± 1.59 i	8.66 ± 1.55 j
1-Dodecanol [4]	83.05 ± 0.83	87.75 ± 0.25	59.55 ± 1.50	71.25 ± 1.91	30.11 ± 1.93 i	19.94 ± 2.31 i
Dodecanenitrile	83.05 ± 0.83	87.75 ± 0.25	43.17 ± 2.36	71.17 ± 1.61	51.10 ± 3.03 g	20.04 ± 1.94 i
2-Tridecanone [3]	83.05 ± 0.83	87.75 ± 0.25	82.52 ± 0.23	84.13 ± 1.04	0.68 ± 0.29 m	4.37 ± 1.26 kl
Pentadecane	83.05 ± 0.83	87.75 ± 0.25	86.92 ± 1.01	88.00 ± 0.00	–op	–o
2-Tridecanol [4]	83.05 ± 0.83	87.75 ± 0.25	67.47 ± 1.73	84.33 ± 0.38	19.97 ± 2.22 j	4.13 ± 0.46 klm
Butylated Hydroxytoluene	83.05 ± 0.83	87.75 ± 0.25	76.13 ± 0.81	85.40 ± 0.26	8.86 ± 1.04 l	2.84 ± 0.31 lmn
2-Tetradecanone [3]	83.05 ± 0.83	87.75 ± 0.25	84.42 ± 0.88	88.00 ± 0.00	–mno	–o
2-Tetradecanol [4]	83.05 ± 0.83	87.75 ± 0.25	71.77 ± 1.67	85.95 ± 0.51	14.46 ± 2.13 k	2.18 ± 0.61 lmn
Hexadecane	83.05 ± 0.83	87.75 ± 0.25	86.37 ± 0.64	88.00 ± 0.00	–nop	–o
Tetradecanal	83.05 ± 0.83	87.75 ± 0.25	75.28 ± 1.34	82.50 ± 1.32	9.95 ± 1.71 l	6.34 ± 1.60 k
2,2′,5,5′-Tetramethyl-1,1′-biphenyl	83.05 ± 0.83	87.75 ± 0.25	83.30 ± 0.72	88.00 ± 0.00	–m	–o
Heptadecane	83.05 ± 0.83	87.75 ± 0.25	84.72 ± 0.80	86.68 ± 0.70	–mno	1.29 ± 0.85 no
2-Hexadecanone [3]	83.05 ± 0.83	87.75 ± 0.25	84.58 ± 1.01	86.18 ± 0.28	–mno	1.89 ± 0.34 mno
Octadecane	83.05 ± 0.83	87.75 ± 0.25	84.33 ± 1.26	85.88 ± 0.81	–mn	2.26 ± 0.98 lmn

[1] "–" indicates no antifungal activity. [2] Data are the mean ± standard deviation ($n = 3$). In the same column, data with different lowercase letters are significantly different according to Duncan's multiple range test ($p < 0.05$). [3] Compound was dissolved with acetone. [4] Compound was dissolved with methanol.

3.5. Identification of Antagonistic Bacterium CT32

The cells of strain CT32 are Gram-positive rods, (0.5–0.7) × (1.5–4.2) μm, occurring singly and occasionally in pairs. Endospores are ellipsoidal and lie in subterminal positions in non-swollen sporangia (Figure 4). The 16S rRNA gene sequence of strain CT32 (GenBank accession number MT509863) comprised 1381 nucleotides. A BLAST search of GenBank revealed that the unidentified bacterium was a member of the genus *Bacillus*. A neighbor-joining tree depicting the phylogenetic affinity of the unidentified strain CT32 is shown in Figure 5. Tree analysis showed that strain CT32 was most closely related to *B. velezensis* CBMB205^T. Pairwise comparison revealed approximately 99% sequence similarity between bacterial strain CT32 and the CBMB205^T and FZB42^T type strains of *B. velezensis*. Thus, strain CT32 was identified as *B. velezensis*.

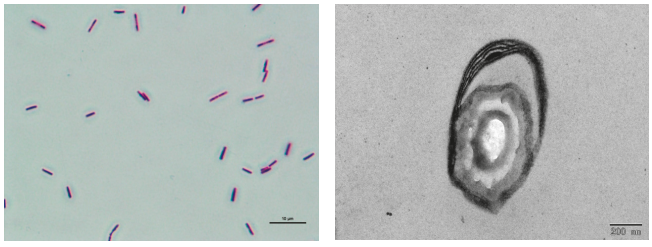

(**a**) (**b**)

Figure 4. (**a**) Light micrograph of strain CT32 cell morphology; (**b**) transmission electron microscopy image of strain CT32 endospore.

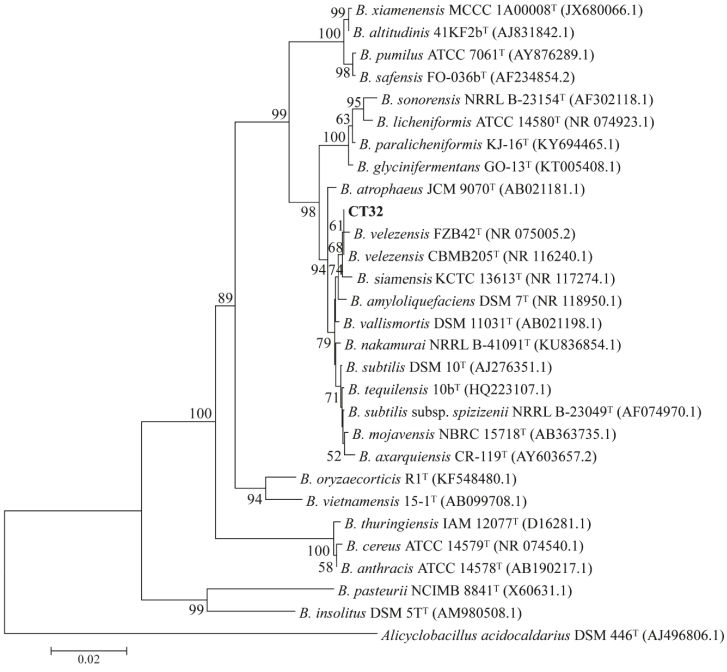

Figure 5. Neighbor-joining (NJ) tree based on 16S rRNA gene sequences, highlighting the phylogenetic relationship of strain CT32 to other strain types of the genus *Bacillus*. Bootstrap values (1000 replications) greater than 50% are given at branch points. Scale bar = 0.02 substitutions per nucleotide position.

4. Discussion

Vascular wilts are devastating plant diseases that cause major economic losses in strawberry production globally. The present work aims to address this issue by isolating potential bacterial antagonists that can be integrated into disease management strategies. In this study, 73 strains of bacteria were isolated from maize straw compost tea and screened for their ability to produce VOCs with antifungal activity against *V. dahliae* and FOF. One of the most effective isolates, designated as CT32, was identified as *B. velezensis*. Members of the species *B. velezensis* are well known for their ability to promote plant growth and to synthesize of a diverse array of secondary metabolites, such as bacillomycin D, plantazolicin and amylocyclicin, that can inhibit the growth of plant pathogens [25–28]. Our results provide evidence that VOC production can play an essential role in the biocontrol activity of *B. velezensis* CT32 against vascular wilt pathogens.

A broad-spectrum antifungal effect was exhibited by VOCs emitted by strain CT32, even though the inhibition rate was low for some pathogenic fungi. The experimental data revealed that the extent of inhibition varied greatly depending on the fungal species. This is consistent with the results obtained by Che et al. [29], who reported that the volatiles from *Lysinibacillus* sp. FJAT-4748 did not affect the growth of all pathogenic fungi to the same extent. The observed differences in fungal susceptibilities to bacterial VOCs may be explained by differences in the action site or in the ability of fungal pathogens to detoxify the volatiles [30]. In addition, considering that different isolates of each pathogen type vary in terms of their physiological properties and pathogenicity, the inhibitory effect on one pathogen isolate observed in our study may not represent the responses of all isolates of the species to bacterial volatiles. Notably, the VOCs produced by strain CT32 were particularly active in inhibiting the mycelial growth of *V. dahliae* and *F. oxysporum*. Similarly, previous studies have reported the in vitro growth inhibition of tomato vascular wilt pathogens by VOCs released from *Bacillus* spp.; however, they did not identify the bioactive compounds responsible for the inhibition [31,32].

To identify the volatile compounds composing the natural emissions of strain CT32, HS-SPME-GC-MS was employed. In comparison with other sampling techniques, HS-SPME allows the volatile metabolites in the headspace of the bacterial cultures to be preconcentrated prior to analysis by GC-MS [33]. In fact, HS-SPME-GC-MS has been used for profiling VOCs from various microbial samples without contaminating the culture or causing damage to living cells [34–36]. The results of this study show that the volatile blend produced by strain CT32 comprised 30 individual compounds. To the best of our knowledge, six of the 30 identified volatiles have not previously been reported to be produced by bacteria or fungi: (Z)-5-undecene, decyl formate, 2,4-dimethyl-6-tert-butylphenol, dodecanenitrile, 2-methylpentadecane and 2,2′,5,5′-tetramethyl-1,1′-biphenyl. The predominant classes of compounds detected in the headspace of strain CT32 were alkanes, ketones, alcohols, and aldehydes. However, Dhouib et al. [31] reported that terpenes, alcohols, and alkanes were the major classes of compounds released from the endophytic *B. velezensis* strain C2. This discrepancy may be explained by the different methods applied to collect and detect VOCs. It needs to be recognized that bacterial VOC profiles are greatly influenced by the sample preparation method as well as the extraction and chromatographic procedures, such as the choice of culture media, duration of incubation, choice of capillary column and selection of SPME fibres, all of which can lead to inconsistent results and hinder the comparison between different studies.

To investigate the precise contribution of 26 commercially available compounds identified in the headspace of strain CT32 to the previously observed volatile-mediated inhibition of mycelial growth, we assessed their antifungal activity against *V. dahliae* and FOF. The majority of the tested compounds showed low to moderate fungistatic effects, while benzothiazole exhibited 100% inhibition against the two tested pathogens. Benzothiazole is widely found in the volatiles produced by *Paenibacillus polymyxa*, *Bacillus* spp., *Ensifer adhaerens*, *Stenotrophomonas maltophilia*, *Sporosarcina ginsengisoli* and *Arthrobacter nitroguajacolicus* [37,38]. This sulphur-containing heterocyclic compound has been shown to display a wide range of pharmacological and biological properties, such as antifungal, anticancer, antidiabetic and antimicrobial activities [39]. A previous study based on

transcriptomic and proteomic analyses has suggested that benzothiazole has antimicrobial activity against *Phytophthora capsici* by suppressing detoxification and stress responses as well as by inducing apoptosis [40]. In the present study, 2,4-dimethyl-6-tert-butylphenol showed excellent growth inhibition towards all of the fungi tested in vitro (reaching > 90% inhibition), and thus this phenolic antioxidant can be considered a potential inhibitor of phytopathogenic fungi. Dodecanenitrile is an important fragrance ingredient widely used in consumer products such as detergents and cosmetics, but its effect on fungal growth has so far not been reported. In the present study, this nitrogen-containing compound greatly hindered the mycelial growth of *V. dahliae* and FOF.

According to the mVOC 2.0 database, almost 70% of the recorded VOCs produced by *Bacillus* spp. are fatty acid derivatives, for example, alkenes, alcohols, ketones, and aldehydes, which make them the most important group of volatile metabolites [41]. Alcohols have long been known to display broad antimicrobial activity and are utilized as preservatives or disinfectants [42]. All five alcohols assayed in this study showed antifungal activity against both pathogens. In addition, we found that the antifungal activity of alcohols was negatively correlated with the number of carbon atoms in the alcohols, and thus, 2-undecanol showed the highest level of inhibition. As proposed by Yuan et al. [43], the antifungal activities of ketones towards *F. oxysporum* f. sp. *cubense* decreased in the following order: 2-undecanone > 2-dodecanone > 2-tridecanone. In this work, when individual compounds were tested on *V. dahliae* and FOF, this order was also observed. In addition, 3-undecanone was proven to be effective against the two target pathogens. The antimicrobial properties of aldehydes have been demonstrated in previous studies, for example, the in vitro inhibition of *Sclerotinia sclerotiorum* by decanal and nonanal [44] and the in vitro inhibition of *P. infestans* by undecanal and tridecanal [45]. Similarly, decanal and undecanal showed high antifungal activity against the mycelial growth of *V. dahliae* and FOF, but they were produced in low amounts. In contrast, dodecanal was the most abundant compound in the headspace of strain CT32, but it had a weak effect on the mycelial growth of the two target pathogens. The results presented here indicate that the inhibition of *V. dahliae* and FOF observed with the natural emissions of strain CT32 is probably not caused by one or a few of these compounds but is most likely the result of synergistic or additive actions of various components of the complex mixture.

However, our study was performed in vitro, which differs from that under natural conditions as most of the volatiles evaporate easily under greenhouse and field conditions. Nevertheless, field applications of bacterial VOCs have been reported recently, and some showed promising results. For example, drench application of 2-butanone emitted from *Bacillus* spp. on cucumber seedlings consistently triggered a higher resistance against bacterial pathogens, decreased the *Myzus persicae* population, as well as increased the number of ladybird beetles, even under open-field conditions [46]. Further studies are needed to develop appropriate application techniques and formulations for the effective usage of bacterial VOCs.

5. Conclusions

The data obtained confirmed the antifungal activity of *B. velezensis* CT32 towards eight plant pathogens and indicated the pivotal role of VOC production in antagonist–pathogen interactions. GC-MS analysis of the bacterial volatile profile suggested the contribution of ketones, alcohols, aldehydes, phenols, nitrogen compound and thiazole to the antifungal property of strain CT32 emissions, which was verified by in vitro assays where individual chemical compounds were tested against the mycelial growth of *V. dahliae* and FOF. Among these compounds, benzothiazole and 2,4-dimethyl-6-tert-butylphenol showed the strongest antifungal activity. These findings will hopefully provide lead compounds for the development of new antifungal agents. Although further studies are required to evaluate the efficacy of the volatile-producing strain CT32 for the protection of strawberry plants, it shows potential to be used as a biofumigant for the control of vascular wilt diseases.

Supplementary Materials: The following are available online at http://www.mdpi.com/2227-9717/8/12/1674/s1, Table S1: Volatile compounds identified in the headspace of strain CT32 by HS-SPME-GC-MS.

Author Contributions: Conceptualization, X.L. and S.Z.; methodology, X.W.; validation, B.W., Q.W. and M.L.; formal analysis, X.L.; investigation, M.L.; resources, S.Z.; data curation, Q.W.; writing—original draft preparation, X.L.; writing—review and editing, S.Z.; supervision, X.S.; project administration, B.W.; funding acquisition, X.L. All authors have read and agreed to the published version of the manuscript.

Funding: This research was funded by the Key Research and Development Program of Shanxi Province, grant number 201703D211022; the Postdoctoral Foundation of Shanxi Academy of Agricultural Sciences, grant number YCX2018D2BH1 and the Agricultural Science and Technology Innovation Programs of Shanxi Academy of Agricultural Sciences, grant number YGC2019TD07, YCX2020YQ24.

Acknowledgments: The authors would like to acknowledge everyone who has provided helpful guidance.

Conflicts of Interest: The authors declare no conflict of interest.

References

1. Eljounaidi, K.; Lee, S.K.; Bae, H. Bacterial endophytes as potential biocontrol agents of vascular wilt diseases—Review and future prospects. *Biol. Control* **2016**, *103*, 62–68. [CrossRef]
2. Yadeta, K.A.; Thomma, B.P.H.J. The xylem as battleground for plant hosts and vascular wilt pathogens. *Front. Plant Sci.* **2013**, *4*, 97. [CrossRef]
3. Bell, C. Fumigation in the 21st century. *Crop. Prot.* **2000**, *19*, 563–569. [CrossRef]
4. Roux-Michollet, D.; Czarnes, S.; Adam, B.; Berry, D.; Commeaux, C.; Guillaumaud, N.; Le Roux, X.; Clays-Josserand, A. Effects of steam disinfestation on community structure, abundance and activity of heterotrophic, denitrifying and nitrifying bacteria in an organic farming soil. *Soil Biol. Biochem.* **2008**, *40*, 1836–1845. [CrossRef]
5. Emmert, E.A.B.; Handelsman, J. Biocontrol of plant disease: A (Gram-) positive perspective. *FEMS Microbiol. Lett.* **1999**, *171*, 1–9. [CrossRef]
6. Ongena, M.; Jacques, P. Bacillus lipopeptides: Versatile weapons for plant disease biocontrol. *Trends Microbiol.* **2008**, *16*, 115–125. [CrossRef]
7. Fira, D.; DimkiC, I.; Beric, T.; Lozo, J.; Stankovic, S. Biological control of plant pathogens by Bacillus species. *J. Biotechnol.* **2018**, *285*, 44–55. [CrossRef]
8. Kai, M.; Haustein, M.; Molina, F.; Petri, A.; Scholz, B.; Piechulla, B. Bacterial volatiles and their action potential. *Appl. Microbiol. Biotechnol.* **2009**, *81*, 1001–1012. [CrossRef]
9. Effmert, U.; Kalderás, J.; Warnke, R.; Piechulla, B. Volatile Mediated Interactions Between Bacteria and Fungi in the Soil. *J. Chem. Ecol.* **2012**, *38*, 665–703. [CrossRef]
10. Farag, M.A.; Zhang, H.; Ryu, C.-M. Dynamic Chemical Communication between Plants and Bacteria through Airborne Signals: Induced Resistance by Bacterial Volatiles. *J. Chem. Ecol.* **2013**, *39*, 1007–1018. [CrossRef]
11. Fincheira, P.; Quiroz, A. Microbial volatiles as plant growth inducers. *Microbiol. Res.* **2018**, *208*, 63–75. [CrossRef] [PubMed]
12. Kanchiswamy, C.N.; Emalnoy, M.; Maffei, M.E. Chemical diversity of microbial volatiles and their potential for plant growth and productivity. *Front. Plant Sci.* **2015**, *6*, 151. [CrossRef] [PubMed]
13. Lee, B.; Farag, M.A.; Park, H.B.; Kloepper, J.W.; Lee, S.H.; Ryu, C. Induced Resistance by a Long-Chain Bacterial Volatile: Elicitation of Plant Systemic Defense by a C13 Volatile Produced by Paenibacillus polymyxa. *PLoS ONE* **2012**, *7*, e48744. [CrossRef]
14. Ryu, C.-M.; Farag, M.A.; Hu, C.-H.; Reddy, M.S.; Kloepper, J.W.; Pare, P.W. Bacterial Volatiles Induce Systemic Resistance in Arabidopsis. *Plant Physiol.* **2004**, *134*, 1017–1026. [CrossRef] [PubMed]
15. Ryu, C.-M.; Farag, M.A.; Hu, C.-H.; Reddy, M.S.; Wei, H.-X.; Paré, P.W.; Kloepper, J.W. Bacterial volatiles promote growth in Arabidopsis. *Proc. Natl. Acad. Sci. USA* **2003**, *100*, 4927–4932. [CrossRef] [PubMed]
16. Mercier, J.; Lego, S.F.; Smilanick, J.L. In-package use of Muscodor albus volatile-generating sachets and modified atmosphere liners for decay control in organic table grapes under commercial conditions. *Fruits* **2010**, *65*, 31–38. [CrossRef]
17. Mercier, J.; Jiménez, J.I. Potential of the volatile-producing fungus Muscodor albus for control of building molds. *Can. J. Microbiol.* **2007**, *53*, 404–410. [CrossRef]
18. Riga, E.; Lacey, L.A.; Guerra, N. Muscodor albus, a potential biocontrol agent against plant-parasitic nematodes of economically important vegetable crops in Washington State, USA. *Biol. Control* **2008**, *45*, 380–385. [CrossRef]

19. Wang, C.; Wang, Z.; Qiao, X.; Li, Z.; Li, F.; Chen, M.; Wang, Y.; Huang, Y.; Cui, H. Antifungal activity of volatile organic compounds fromStreptomyces alboflavusTD-1. *FEMS Microbiol. Lett.* **2013**, *341*, 45–51. [CrossRef]
20. Zhou, J.; Zhao, X.; Dai, C. Antagonistic mechanisms of endophytic Pseudomonas fluorescens against Athelia rolfsii. *J. Appl. Microbiol.* **2014**, *117*, 1144–1158. [CrossRef]
21. Zhang, X.; Gao, Z.; Zhang, X.; Bai, W.; Zhang, L.; Pei, H.; Zhang, Y. Control effects of Bacillus siamensis G-3 volatile compounds on raspberry postharvest diseases caused by Botrytis cinerea and Rhizopus stolonifer. *Biol. Control* **2020**, *141*, 104135. [CrossRef]
22. Li, X.; Wang, X.; Shi, X.; Wang, Q.; Li, X.; Zhang, S. Compost tea-mediated induction of resistance in biocontrol of strawberry Verticillium wilt. *J. Plant Dis. Prot.* **2019**, *127*, 257–268. [CrossRef]
23. Gao, Z.; Zhang, B.; Liu, H.; Han, J.; Zhang, Y. Identification of endophytic Bacillus velezensis ZSY-1 strain and antifungal activity of its volatile compounds against Alternaria solani and Botrytis cinerea. *Biol. Control* **2017**, *105*, 27–39. [CrossRef]
24. Bianchi, F.; Careri, M.; Mangia, A.; Musci, M. Retention indices in the analysis of food aroma volatile compounds in temperature-programmed gas chromatography: Database creation and evaluation of precision and robustness. *J. Sep. Sci.* **2007**, *30*, 563–572. [CrossRef] [PubMed]
25. Fan, B.; Wang, C.; Song, X.; Ding, X.; Wu, L.; Wu, H.; Gao, X.; Borriss, R. Bacillus velezensis FZB42 in 2018: The Gram-Positive Model Strain for Plant Growth Promotion and Biocontrol. *Front. Microbiol.* **2018**, *9*, 2491. [CrossRef] [PubMed]
26. Meng, Q.; Jiang, H.; Hao, J. Effects of Bacillus velezensis strain BAC03 in promoting plant growth. *Biol. Control* **2016**, *98*, 18–26. [CrossRef]
27. Scholz, R.; Molohon, K.J.; Nachtigall, J.; Vater, J.; Markley, A.L.; Süssmuth, R.D.; Mitchell, D.A.; Borriss, R. Plantazolicin, a Novel Microcin B17/Streptolysin S-Like Natural Product from Bacillus amyloliquefaciens FZB42. *J. Bacteriol.* **2010**, *193*, 215–224. [CrossRef]
28. Scholz, R.; Vater, J.; Budiharjo, A.; Wang, Z.; He, Y.; Dietel, K.; Schwecke, T.; Herfort, S.; Lasch, P.; Borriss, R. Amylocyclicin, a Novel Circular Bacteriocin Produced by Bacillus amyloliquefaciens FZB42. *J. Bacteriol.* **2014**, *196*, 1842–1852. [CrossRef]
29. Che, J.; Liu, B.; Liu, G.; Chen, Q.; Lan, J. Volatile organic compounds produced by Lysinibacillus sp. FJAT-4748 possess antifungal activity against Colletotrichum acutatum. *Biocontrol Sci. Technol.* **2017**, *27*, 1349–1362. [CrossRef]
30. Chaves-López, C.; Serio, A.; Gianotti, A.; Sacchetti, G.; Ndagijimana, M.; Ciccarone, C.; Stellarini, A.; Corsetti, A.; Paparella, A. Diversity of food-borne Bacillus volatile compounds and influence on fungal growth. *J. Appl. Microbiol.* **2015**, *119*, 487–499. [CrossRef]
31. Dhouib, H.; Zouari, I.; Ben Abdallah, D.; Belbahri, L.; Taktak, W.; Triki, M.A.; Tounsi, S. Potential of a novel endophytic Bacillus velezensis in tomato growth promotion and protection against Verticillium wilt disease. *Biol. Control* **2019**, *139*, 104092. [CrossRef]
32. Jangir, M.; Pathak, R.; Sharma, S.; Sharma, S. Biocontrol mechanisms of Bacillus sp., isolated from tomato rhizosphere, against Fusarium oxysporum f. sp. lycopersici. *Biol. Control* **2018**, *123*, 60–70. [CrossRef]
33. A Farag, M.; Song, G.C.; Park, Y.; Audrain, B.; Lee, S.; Ghigo, J.-M.; Kloepper, J.W.; Ryu, C.-M. Biological and chemical strategies for exploring inter- and intra-kingdom communication mediated via bacterial volatile signals. *Nat. Protoc.* **2017**, *12*, 1359–1377. [CrossRef] [PubMed]
34. Castillo, M.; da Silva, E.; Câmara, J.S.; Khadem, M. Molecular identification and VOMs characterization of Saccharomyces cerevisiae strains isolated from madeira region winery environments. *Processes* **2020**, *8*, 1058. [CrossRef]
35. Ghader, M.; Shokoufi, N.; Es-Haghi, A.; Kargosha, K. Headspace solid-phase microextraction (HS-SPME) combined with GC–MS as a process analytical technology (PAT) tool for monitoring the cultivation of C. tetani. *J. Chromatogr. B* **2018**, *1083*, 222–232. [CrossRef] [PubMed]
36. Romoli, R.; Papaleo, M.C.; De Pascale, D.; Tutino, M.L.; Michaud, L.; Logiudice, A.; Fani, R.; Bartolucci, G. Characterization of the volatile profile of Antarctic bacteria by using solid-phase microextraction-gas chromatography-mass spectrometry. *J. Mass Spectrom.* **2011**, *46*, 1051–1059. [CrossRef]
37. Zhao, L.-J.; Yang, X.-N.; Li, X.-Y.; Mu, W.; Liu, F. Antifungal, Insecticidal and Herbicidal Properties of Volatile Components from Paenibacillus polymyxa Strain BMP-11. *Agric. Sci. China* **2011**, *10*, 728–736. [CrossRef]

38. Zou, C.-S.; Mo, M.-H.; Gu, Y.-Q.; Zhou, J.; Zhang, K.-Q. Possible contributions of volatile-producing bacteria to soil fungistasis. *Soil Biol. Biochem.* **2007**, *39*, 2371–2379. [CrossRef]
39. Agarwal, S.; Gandhi, D.; Kalal, P. Benzothiazole: A Versatile and Multitargeted Pharmacophore in the Field of Medicinal Chemistry. *Lett. Org. Chem.* **2017**, *14*, 729–742. [CrossRef]
40. Mei, X.; Liu, Y.; Huang, H.; Du, F.; Huang, L.; Wu, J.; Li, Y.; Zhu, S.; Yang, M. Benzothiazole inhibits the growth of Phytophthora capsici through inducing apoptosis and suppressing stress responses and metabolic detoxification. *Pestic. Biochem. Physiol.* **2019**, *154*, 7–16. [CrossRef]
41. Caulier, S.; Nannan, C.; Gillis, A.; Licciardi, F.; Bragard, C.; Mahillon, J. Overview of the Antimicrobial Compounds Produced by Members of the Bacillus subtilis Group. *Front. Microbiol.* **2019**, *10*, 302. [CrossRef] [PubMed]
42. Ingram, L.O.; Buttke, T.M. Effects of Alcohols on Micro-Organisms. *Adv. Microb. Physiol.* **1985**, *25*, 253–300. [CrossRef]
43. Yuan, J.; Raza, W.; Shen, Q.; Huang, Q. Antifungal Activity of Bacillus amyloliquefaciens NJN-6 Volatile Compounds against Fusarium oxysporum f. sp. cubense. *Appl. Environ. Microbiol.* **2012**, *78*, 5942–5944. [CrossRef] [PubMed]
44. Fernando, W.G.D.; Ramarathnam, R.; Krishnamoorthy, A.S.; Savchuk, S.C. Identification and use of potential bacterial organic antifungal volatiles in biocontrol. *Soil Biol. Biochem.* **2005**, *37*, 955–964. [CrossRef]
45. De Vrieze, M.; Pandey, P.; Bucheli, T.D.; Varadarajan, A.R.; Ahrens, C.H.; Weisskopf, L.; Bailly, A. Volatile Organic Compounds from Native Potato-associated Pseudomonas as Potential Anti-oomycete Agents. *Front. Microbiol.* **2015**, *6*, 1295. [CrossRef]
46. Song, K.C.; Ryu, C.-M. Two Volatile Organic Compounds Trigger Plant Self-Defense against a Bacterial Pathogen and a Sucking Insect in Cucumber under Open Field Conditions. *Int. J. Mol. Sci.* **2013**, *14*, 9803–9819. [CrossRef] [PubMed]

processes

MDPI

Article

High Cell Density Cultivation of *Saccharomyces cerevisiae* with Intensive Multiple Sequential Batches Together with a Novel Technique of Fed-Batch at Cell Level (FBC)

Kwanruthai Malairuang [1,2,3], Morakot Krajang [1], Jatuporn Sukna [1,2,3], Krongchan Rattanapradit [3,4,*] and Saethawat Chamsart [1,2,3,*]

1 Biological Science Program, Faculty of Science, Burapha University, Chon Buri 20131, Thailand; pinsor_17@hotmail.com (K.M.); morakoto_2@hotmail.com (M.K.); jatuporn08@gmail.com (J.S.)
2 Department of Biology, Faculty of Science, Burapha University, Chon Buri 20131, Thailand
3 Biochemical Engineering Pilot Plant, Faculty of Science, Burapha University, Chon Buri 20131, Thailand
4 Department of Biotechnology, Faculty of Science, Burapha University, Chon Buri 20131, Thailand
* Correspondence: krongchan@buu.ac.th (K.R.); saethawa@buu.ac.th (S.C.); Tel.: +6663-941-5993 (K.R.); +6696-887-3878 (S.C.)

Received: 28 August 2020; Accepted: 14 October 2020; Published: 21 October 2020

Abstract: High cell density cultivation (HCDC) is developed for the production of microbial biomasses and their products. They must be produced from high concentrations of substrate, e.g., glucose or sucrose. In batch culture, a high concentration of those sugars >40–50% (*w/v*) cannot efficiently be utilized because of a dissolved O_2 limitation causing the Crabtree effect that produces toxic by-products, i.e., ethanol and/or acetate, that inhibit cell growth. To prevent this effect, the HCDC is conducted with the fed-batch strategies. However, it has many disadvantages, i.e., complicated operations. To overcome those problems, this study was designed to use a new, efficient C-source (carbon source) substrate, namely dextrin, an oligomer of glucose. It can be utilized by yeast at a very high concentration of ~100 g/L although using just batch cultivation. As it is gradually hydrolyzed to release glucose molecules and gradually assimilated into the cells as "fed-batch at the cell level" (FBC), it prevents the yeast cell system from undergoing the Crabtree effect. In this research, the types of medium, the types of sugar compared with dextrin, and the concentrations of yeast extract (YE) were studied. The batch production medium (BPM) with dextrin and YE performed very good results. The concentrations of dextrin for yeast cultivation were studied in the aerobic batch 5-L bioreactors. Its optimum concentration was at 90 g/L with 9 g/L of YE in 3× BPM. It was operated at 3 W/kg energy dissipation rate per unit mass ($\overline{\varepsilon}_T$) and 3 vvm airflow rate. Further, the intensive multiple sequential batch (IMSB) technique of high intensities of agitation speed and airflow was developed to achieve higher yield and productivity. The maximum values of cell biomass, specific growth rate, yield coefficient, productivity, and efficiency were at 55.17 g/L, 0.21 h^{-1}, 0.54 g/g, 2.30 g/L/h, and 98.18%, respectively. The studies of cell growth kinetics, biochemical engineering mass balances, and fluid dynamics for the design of impeller speeds of the 5-L bioreactors during the cultivations of yeast using dextrin at the high concentrations were successful. The results can be used for the scale-up of bioreactor for the industrial production of yeast cell biomass at high concentrations.

Keywords: high cell density cultivation (HCDC); intensive multiple sequential batch (IMSB); cell cultivation; fed-batch at cell level (FBC); *S. cerevisiae*; dextrin; bioreactor

1. Introduction

Since the end of the 19th century to 2020, the addition of exogenous yeast biomass to produce bread, beer, wine, and industrial ethanol has become a common practice. Wineries started using exogenous yeast inoculants in the 1950s. In the 1960s, yeast biomass-producing plants contributed to the technology of producing large amounts of active dry yeast (ADY) or yeast cell biomass, and its use rapidly spread to European, North America, Asian, and other countries. Nowadays, modern industries require very large amounts of selected yeasts to obtain high-quality reproducible products and to ensure fast, complete cultivations. Efficient and profitable factory-scale processes have been developed to produce yeast biomass. The standard process was empirically optimized to obtain the highest yield by increasing biomass and decreasing production costs [1]. The ADY or yeast cell biomass is a yeast product that is dehydrated and dried from the fresh yeast. The dry yeast products are mainly used in the bakery, brewery, winery, feeds, pharmaceuticals, and ethanol industries, etc. The global production of ADY increased from 589.70 MT (metric tons) in 2010 to 862.50 MT in 2014, with an annual average growth rate of 7.91% [2]. It is estimated to a value of 1544.74 MT in 2024.

Saccharomyces cerevisiae is the most prominent in the yeast group. *S. cerevisiae* is a species of the budding yeasts in a group of unicellular fungi. It is a free-living organism with rapid growth and is simple for cultivation under a defined condition. As profound knowledge of its genetics, functional genomics, biochemistry, physiology, etc. of this yeast is presently available, it is widely used as a model eukaryote for certain studies [3], e.g., fermentation, aerobic cell cultivation, and molecular biology. It is a particularly suitable organism for biological studies and is generally regarded as safe status (GRAS). Moreover, it can produce a wide range of biological products of both wild types, e.g., single cell proteins and β-glucans [4], and recombinant products, e.g., viral vaccines and certain proteins [5]. More than 47 natural bioproducts have been produced in yeasts [6]. For those reasons, it was used herein as the model yeast for this study.

High cell density cultivation (HCDC) is a potential technique that has been developed to produce microbial cell biomasses at high concentrations and subsequently to gain relatively high product concentrations. It is used in various bioprocesses to achieve the cost-effective production of desired products. HCDC can be applied to produce a variety of biological products from microbial cells, such as cell biomasses, probiotics, single cell proteins, amino acids, organic acids, bioplastics, biochemicals, pharmaceuticals, etc. HCDC is a relative term with no exact concentration of dry cell weight value. In general, a cell concentration of more than those achieved in conventional cultivation has been considered as the high cell density. Most experiments have dry cell weights ranging from 20 to 40 g/L, and if they are higher than 100 g/L they are designated as having a high cell density concentration (modified from [7]). They are normally operated with the fed-batch mode. There has not been any batch cultivation to achieve a high cell concentration at a high productivity by using high concentration of dextrin or oligomer as a carbon source (C-source), but we have successfully done this. This is unlike an anaerobic SSF (simultaneous saccharification and fermentation), a fermentation method using maltodextrin as a substrate at high titer without the problem of oxygen requirement. The HCDC is principally designed as the fed-batch mode to control the carbon substrate feeding in order to avoid cell growth inhibition due to too high a concentration of substrate and the accumulation of toxic by-products. The substrate feeding strategies are implemented to eliminate the problems of using high concentrations of substrates, especially glucose and sucrose, that effect to the biosynthesis of growth inhibitory by-products due to the Crabtree effect [8]. The fed-batch HCDC development often studies the optimum conditions of two main factors, i.e., medium feeding and cultivation strategies.

A defined medium is generally used to obtain a high cell density concentration because the nutrient amounts are known and can be controlled during cultivation while complex medium can vary in composition and quality making fermentation less reproducible. However, semi-defined or complex media are sometimes necessary to boost cell growth and product formation. The use of a defined medium with a single or a few amino acids to achieve high cell biomass and/or recombinant proteins would be attractive [9]. Although the fed-batch method is complicated, the results of some

research works using fed-batch cultivations to produce yeast cell biomass have been reported. The dry cell weights and productivities of 187.63 g/L and 1.71 g/L/h were obtained from [10], 120 g/L and 1.84 g/L/h [11], 95.7 g/L and 1.20 g/L/h [12], and 63.30–96.10 g/L and 1.33–1.99 g/L/h [13].

For aerobic cultivation, using sugar as a substrate at a high concentration usually causes the Crabtree effect. Although glycerol is generally used to minimize this effect, it can be utilized by microorganisms at a limited concentration, though its advantage generates a higher degree of reduction per carbon atom when compared to other sugars [14]. As a result, in this study, dextrin, an oligomer of glucose from cassava starch liquefaction was used as the major C-source substrate. It can efficiently be used at a high concentration. So far, there have not been any other research reports using dextrin or other oligomers as the potential C-source to prevent the system from oxygen limitation, especially for the aerobic batch cultivation operation to achieve a high cell density. Our new finding herein essentially explains that the dextrin oligomer regulates gradual glucose assimilation into the yeast cells, as so-called the "fed-batch at cell level" (FBC). It also plays a key role in a reserved C-source in the cultivation system when it is in the mixture of glucose.

Both fed-batch and continuous techniques usually: (i) require more types and units of equipment and (ii) complicated process steps; (iii) entail a high cost of operation, (iv) long time cultivation and time-consuming both in up-stream and down-stream processes, and (v) induce the Crabtree effect problem to inhibit cell growth because of using glucose and sucrose at high concentrations. Here, in order to achieve a high cell density concentration at a high production rate, these problems can be overcome by: (i) the use of aerobic batch mode with (ii) the use of a simple-defined minimal medium, (iii) the ability to use high concentrations of C-source substrate, (iv) the cultivation with a short time course, (v) with the intensive multiple sequential batches, (vi) the use of dextrin, oligomer of glucose from cassava starch liquefaction as the major substrate; (vii) the control of "fed-batch at cell level", and (viii) the prevention of the yeast cultivation system from the Crabtree effect to achieve these system balances, operating at the high intensities of (ix) aeration rates and (x) impeller agitation speeds, both proportional to the high concentrations of the C-source dextrin and the BPM (batch production medium).

These are the objectives of this research work in order to achieve high cell density cultivation of the model yeast at a high productivity with comprehensive and profound explanations of the details of all aspects, from culture medium design, new cultivation technique, kinetics of cell growth, and biochemical engineering mass balance models of substrate utilizations to regulate the fed-batch at cell level (FBC), through fluid dynamics, and reactor scale-up for the industries.

This study isolates the problem of the efficient operation of *S. cerevisiae* cultivation in bioreactors focusing only on the need for high cell density cultures. On this basis, the novelty of the FBC technique is proposed. It has been explained in principles and details of the cultivation technique, the potential substrate dextrin, the mechanism of substrate utilization to regulate the FBC, the FBC kinetics, and material balances, through the bioreactor design and scale-up.

2. Materials and Methods

2.1. Yeast Strain and Preparations of Inoculants and Culture Media

The stock of *Saccharomyces cerevisiae* S3, a strain of model yeasts was from the Microbiology Department, Faculty of Science, Burapha University, Thailand. It was maintained in YPD (Yeast Peptone Dextrose) medium, (composed of 10 g/L of yeast extract, 10 g/L of peptone, and 20 g/L of dextrose) at pH 4.5, then mixed with a cryo-protective agent of glycerol at 15% (*v/v*) and stored in 2-mL cryo-tubes at −40 °C as the stocks. Before use, they were activated by defrosting at a room temperature of 28–30 °C and then transferred into the 10-mL YPD contained in the 50-mL Erlenmeyer flasks. The cultures were incubated at 30 °C in a rotary incubator shaker at a speed of 200 rpm overnight. Then, 5-mL volumes were transferred into the 20-mL YPD contained in the 50-mL baffled flasks and cultured at the same conditions (i.e., pH, temperature, and shaker speed above) for 18 h. Further,

10-mL volumes were transferred into the 100-mL YPD contained in the 500-mL baffled flasks and again cultured at the same conditions for 18 h to use as the inoculants for further cultivation experiments in the 5-L fermenters of Topic 2.6. They had an optical density ($OD_{600\ nm}$) of about 8–10. To increase the inoculum concentration at an $OD_{600\ nm}$ of ~15–18, the cultures were grown for 24 h. This was used for the initial batch of the intensive multiple sequential batch cultivation in Topic 2.7.

The batch production medium (BPM) [15], the minimal synthetic defined medium containing (L^{-1}) of 2.2 g $(NH_4)_2SO_4$, 1.5 g KH_2PO_4, 1.8 g Na_2HPO_4, 0.2 g $MgSO_4.7H_2O$, and 1.0 mL of trace element solution, was composed of (L^{-1}) of 10.0 g $CaCl_2.2H_2O$, 6.0 g $(NH_4)_5[Fe(C_6H_4O_7)_2]$, 0.2 g $CoCl_2.6H_2O$, 0.3 g H_3BO_3, 0.1 g $ZnSO_4.7H_2O$, 0.03 g $MnCl_2.4H_2O$, 0.03 g $Na_2MoO_4.2H_2O$, 0.02 g $NiSO_4.7H_2O$, and 0.01 g $CuSO_4.5H_2O$. The BPM is designed for use as the main medium for high cell density cultivation because of its simplicity, low cost (~0.035–0.045 US $ per liter), and high potential for industrial applications at the commercial scale of cell cultivation for the productions of varieties of bioproducts, from cell biomasses to fine biochemicals, e.g., pharmaceuticals. When compared to a laboratory medium, it costs ~0.85 US $ per liter which is ~25 times higher.

2.2. Preparations of Carbon Sources, Dextrin from Cassava Starch Liquefaction and Glucose from Further Saccharification of Dextrin

It is important that an industrial application practice was implemented, in terms of potential raw material use and its preparation with in-house technologies. As plenty of a major C-source substrate, dextrin solution with a DE (dextrose equivalent) value of 25–40 was prepared by our own liquefaction method [16] using the in-house design and fabrication of a 200-L stirred-tank enzymatic hydrolysis bioreactor in the controlled optimum conditions. A 40% (*w/v*) of cassava starch powder (3-Elephant Heads Brand (Chorchiwat Industry Co., Ltd. (CCW), Thailand) was suspended in distilled water and subsequently added with 0.1% (*v/w*) of α-amylase (Spezyme Alpha, thermostable α-amylase from *Bacillus licheniformis* with a minimum activity of 13,775 Units/g protein; DuPont Industrial Biosciences, Shanghai, China) per dry starch basis. The mixture was controlled at 85–90 °C, pH 6.5, and agitated with 2-Ekato Intermig, high-efficiency impellers at a speed of 125 rpm for 3 h [17]. The desired concentrations of dextrin were adjusted by dilutions depending on each experimental condition.

A glucose solution with a DE of 95 was prepared by further hydrolysis called saccharification of the above dextrin solution. After liquefaction, the slurry of dextrin solution was cooled to 65 °C and subsequently supplemented with a glucoamylase at 0.2% (*v/w*) (Distillase ASP, a blend of enzymes produced by *B. licheniformis* and *Trichoderma reesei* with a minimum activity of 580 units/g protein; DuPont Industrial Biosciences, Shanghai, China). The mixture was controlled at 65 °C, pH 4.5, and agitated at 100 rpm for 20 h. The desired concentrations of glucose were adjusted by dilutions on each experimental condition.

2.3. The Effective BPM for Aerobic Batch Cultivation of S. cerevisiae

The effective BPM for aerobic cultivation of *S. cerevisiae* was determined. The cultivations were undertaken in the 500-mL baffled flasks contained 100 mL of BPM with 20 g/L of glucose supplemented with YE at a concentration of 0.3% (*w/v*) and another without the YE. They were compared with cultivation in the YPD medium. The initial pH of the three media was adjusted to 4.5 with 4 N NaOH and 4 N HCl. After autoclaving and leaving to a temperature of 30 °C, the 5-mL inoculant volumes (from Section 2.1) were inoculated into those culture media and incubated at 30 °C in a rotary incubator shaker at a speed of 200 rpm for 36 h. The culture broth samples of 5 mL of each treatment were withdrawn every 6 h, put on ice for 20 min to suddenly drop the temperature to 2 °C to stop cell activities before keeping at 5–10 °C in a refrigerator for further analyses of the $OD_{600\ nm}$, cell biomass, and reducing sugar concentrations.

2.4. The Addition of Yeast Extract as the Supplement in BPM

From the above experimental result, in order to enhance more efficient utilization of BPM by *S. cerevisiae*, yeast extract (Hi-media, India), the major source of complex nutrients was supplemented into the BPM of 20 g/L of glucose. The experiment was conducted using 500-mL baffled flasks contained 100 mL of BPM supplemented with YE at concentrations of 0, 0.3, 0.6, and 0.9% (*w/v*). The initial pH of the media was adjusted to 4.5 with 4 N NaOH and 4 N HCl. After autoclaving and leaving to a temperature of 30 °C, the 5-mL inoculant volumes (from Section 2.1) were inoculated into the four cultivation media and incubated at 30 °C in a rotary incubator shaker at a speed of 200 rpm for 36 h. The culture broth samples of 5 mL were withdrawn every 6 h for the first 24 h and after that every 12 h. They were put on ice for 20 min to suddenly drop the temperature to 2 °C to stop cell activities before keeping them at 5–10 °C for further analyses.

2.5. The Comparison of Different Carbon Sources

This was to compare the efficient utilization, by *S. cerevisiae*, of different C-sources, i.e., dextrin from cassava starch liquefaction, glucose from further dextrin saccharification (from Section 2.2), and the commercial pure glucose (D-glucose, Sigma-Aldrich). The experiment was conducted using 500-mL baffled flasks contained with 100 mL of BPM added with those C-sources at the same concentration of 20 g/L. The initial pH of the media was adjusted to 4.5. After autoclaving and leaving to a temperature of 30 °C, the 5-mL inoculant volumes (from Section 2.1) were inoculated into those three media. The cultivation conditions and the sample collections were undertaken with the same as above in Section 2.4. Noted, the concentrations of dextrin and glucose from dextrin saccharification were calculated from the initial concentration of starch hydrolysis at 40% (*w/v*). For stoichiometry, one gram of starch produces 1.11 g of glucose, thus the factor of 1.11 is used for the calculation of using glucose to meet the equimolar concentration of using dextrin at 20 g/L. So, glucose at a concentration of 22.22 g/L should be used. When the starch hydrolysis is considered at 90% (based on 90% (*w/w*) pure starch content in cassava starch), the equimolar concentration of glucose to use is 19.98 g/L. This means that a 20 g/L of dextrin from starch when completely hydrolyzed will produce 19.98 g/L of glucose. This proves that the 20 g/L of the three C-sources are comparable as they are all the same equimolar concentration of 111 mM (millimolar) as the glucose at 20 g/L (calculated from $(20/180.156) \times 1000 = 111$ mM).

2.6. The High Concentrations of Dextrin for S. cerevisiae Cultivation in the 5-L Bioreactors

The larger-scale cell cultivation in the accurate control conditions using bioreactor makes the results approaching more scalability. The 5-L bioreactors of 0.15 m in diameter and 0.35 m height fit with 2 Rushton turbine impellers of 0.065 m were operated. This experiment was carried out to investigate the optimal-high concentration of dextrin to use as the C-source instead of glucose by *S. cerevisiae* cultivation in the 5-L bioreactor with 3-L working volume. This experiment was carefully developed from a normal batch procedure to the intensive batch cultivation technique using four intense parameters: (i) high concentrations of BMP, (ii) high concentrations of dextrin, (ii) high agitation rates, and (iv) high aeration rates. They were proportionally increased when the concentrations of dextrin used were increasingly changed (Table 1). This experiment was designed to achieve high cell biomass yield related to stoichiometry. The higher the concentrations of BPM and dextrin, the higher the intensities of aeration and agitation were operated with the optimum cultivation conditions that could produce the higher biomass yields. Those parameters effect efficient mass transfers and balance the uses of substrates, i.e., carbon and nitrogen sources; O_2 and inorganic salts to produce cell biomass at high-density concentrations. This is superior to the conventional fed-batch technique in many ways as mentioned before.

Table 1. The designed experimental parameters and conditions for normal batch and intensive multiple sequential batches for cultivations of *S. cerevisiae* in 5-L bioreactors to produce cell biomass at high density concentrations. # Molar concentrations of dextrin were calculated on the basis of 90% (*w/w*) glucose content of them.

Treatments	Dextrin Conc. (g/L)	# Glucose Conc. (mM)	Yeast Extract (g/L)	BPM Conc.	Agitation Rates by Controlling Power Input (W/kg)	Agitation Speeds (rpm)	Aeration Rates (vvm)
Normal	30	150	3	1×	1	500	1
Intensive I	60	300	6	2×	2	600	2
Intensive II	90	450	9	3×	3	700	3
Intensive III	120	600	12	4×	4	800	4

A 3 L of BPM was prepared at a concentration of 1×, put into a 5-L bioreactor, and sterilized at 121 °C under 15 lb/in^2 pressure for 25 min in an autoclave. A dextrin solution of 40% (*w/v*) from cassava starch liquefaction was separately sterilized at 110 °C under 15 lb/in^2 for 10 min. Its 225 mL was added into the bioreactor to the designed concentration of 30 g/L (equivalent to a concentration of 150 mM of glucose content) and YE was added at a concentration of 3 g/L. The cultivation conditions were set and controlled at 30 °C, pH of 4.5 by 4 N HCl and 4 N NH_4OH solutions, 1 vvm airflow rate, and 1 W/kg of power input, $\overline{\varepsilon}_T$ at an impeller speed of 500 rpm throughout the run. After they were well controlled and reached the designed conditions, a 150 mL of *S. cerevisiae* inoculum (from Section 2.1) was inoculated into the bioreactor (at a concentration of 5% *v/v*). For other treatments, the concentrations of dextrin in the cultures were at 60, 90, and 120 g/L (equivalent to concentrations of 300, 450, and 600 mM of glucose content, respectively). The YE was added at the concentrations of 6, 9, and 12 g/L, respectively giving the same YE/dextrin fraction with a value of 0.1. They were proportional to the increase in BPM concentration, agitation speed, and aeration rate as in Table 1. to achieve higher biomass yields. During cultivations, the culture broth samples of 10 mL of each treatment were withdrawn every 6 h for 30 h. Again, they were put on ice for 20 min to suddenly drop the temperature to 2 °C and stop cell activities before keeping at −20 °C for further analyses.

2.7. The Development from Batch to the Intensive Multiple Sequential Batch (IMSB) Technique to Achieve High Cell Density Concentration

This experiment was developed from a single batch to the intensive multiple sequential batches (see [17]) to achieve a high cell biomass with a high productivity. A 3 L of BPM was prepared at a concentration of 3× put into a 5-L bioreactor and sterilized at 121 °C under 15 lb/in^2 pressure for 25 min. A dextrin solution of 40% (*w/v*) was separately sterilized as above and its 675 mL was added into the bioreactor to the designed concentration of 90 g/L for 3-L working volume. The cultivation conditions were controlled at 30 °C and pH 4.5; 3 vvm airflow rate and 3 W/kg $\overline{\varepsilon}_T$ at the impeller speed of 700 rpm. After they were well controlled and reached the designed conditions. To increase the growth rate higher than the experiment in Section 2.6 (30 h of cultivation time course), a higher concentration of inoculum culture was used. A 150 mL of *S. cerevisiae* inoculum of an $OD_{600\,nm}$ of ~15–20 from 24 h culture was inoculated into the bioreactor (at a concentration of 5% *v/v*) and grown for 24 h of the initial (first) batch.

Following the first batch, the intensive multiple sequential batch operations were further continually repeated for four more cycles without newly batch up and sterilization. When each batch was completed, a major culture broth was discharged using a peristaltic pump, leaving only a 150 mL to be the starter inoculum for the next batch (at 5% *v/v*). Unlike the initial batch, the inoculants of the batch cycles 2–5 were the high cell density starters (the culture broths left from the prior batches).

During the time of the first batch cultivation, a further 3000 mL of the fresh medium of the same components and concentration was prepared. Dextrin solution was again prepared. It was sterilized separately and then newly added into the same bioreactor after the first culture broth withdrawal. The second cultivation process was again restarted under the same controlled conditions.

The cultivation process was continually repeated for five cycles. Along with the five cultivations, the culture broth samples of 10 mL were withdrawn every 6 h for 24 h. They were put on ice for 20 min for the same reason above and kept at −20 °C for further analyses.

2.8. Cell Growth Determination by Measuring Optical Density (OD) and Dry Cell Weight (DCW)

The growth during the cultivations of *S. cerevisiae* was determined by measuring absorbance and cell biomass concentration. For the former, a 1 mL of each culture broth sample was diluted 10 or 100 times with distilled water at an appropriate concentration and measured the absorbance at an optical density of 600 nm ($OD_{600\,nm}$) using a spectrophotometer. For the latter, a 1.5 mL of each culture broth sample was put into the micro-centrifuge tube and centrifuged at 10,000 rpm for 10 min. The supernatant was decanted and then the tube was added with a more 1.0 mL distilled water and re-centrifuged to wash the cells. The cell samples were dried at 80 °C for 24 h and weighed. Both methods were used in order to recheck each other for confident reliability.

2.9. Reducing Sugar Analysis

Glucose concentrations of the culture broth samples during cultivations were analyzed as the reducing (residual) sugar (G_l) quantities in the culture using the DNS method [18]. The 1-mL volumes of DNS reagent were added to test tubes each contained a 1 mL of 1/10 diluted culture broth sample. The mixtures were incubated in a boiling water bath at 95 °C for 5 min and then transferred into a cold bath at 5 °C for 5 min to stop the reaction. Then, each tube was added with a 10 mL of distilled water and mixed well before measuring the absorbance at 520 nm by a spectrophotometer. The quantities of reducing sugar were measured as the glucose concentration by comparison with the standard plot of known glucose concentrations of 0, 0.2, 0.4, 0.6, 0.8, and 1.0 g/L reacted with the DNS reagent and following the same procedure to measure the absorbance.

To verify the DNS assay method is significantly accurate. The concentrations of glucose standard solutions from 0 to 1.0 g/L as above were analyzed both by the DNS assay and by the High Performance Liquid Chromatography (HPLC) method. The HPLC (KNAUER Smartline, Berlin, Germany) with a refractive index (RI) detector (KNAUER Smartline 2300, Berlin, Germany) and a Eurokat H vertex column (KNAUER, Berlin, Germany) was used. Eluent of 0.01 N sulfuric acid solution at a flow rate of 0.8 mL/min was utilized. The analyses were performed at 60 °C. The samples were 10-fold diluted, filtered through 0.45-μm filters, and injected into the column with an amount of 20 μL. The results of both methods were compared and given no significant difference. The two might deviate from each other with a value of ≤5% deviation. Thus, the DNS method was used to quantify the concentration of glucose along with the yeast cell cultivations.

2.10. Total Sugar Analysis

Total sugars (S_T) mean all the concentrations of C-sources, i.e., free residual glucose (G_l) plus dextrin (Dx) left in the culture of which dextrin in the mixture of cell culture was completely hydrolyzed by a strong acid to release all glucose molecules, and then glucose from both sources in the same mixture was measured as the total sugar or total glucose. Thus S_T is the glucose from hydrolyzed Dx plus G_l. The total sugar of culture broth during cell growth was analyzed by sulfuric acid hydrolysis method modified from [16]. The 1-mL samples of culture broth in micro-tubes were centrifuged at 10,000 rpm for 10 min. The supernatants of 0.5 mL were transferred into 20-mL test tubes. Then 2-mL volumes of 2 N H_2SO_4 solution were added, mixed well, and capped. Test tubes with the mixture were boiled in a water bath at 95 °C for 30 min. The neutralizations were done with the addition of 4 N NaOH and re-centrifugation to precipitate the residues. The supernatants were used to measure the total sugar by the DNS method.

2.11. Quantitative Analyses of Total Sugar and Reducing Sugar (glucose) during Cell Cultivations

Again, total sugar (S_T) means the amount of dextrin (Dx) plus residual glucose or glucose left (G_l), $S_T = Dx + G_l$ in the cultures during cell cultivation. Thus, the concentration of dextrin in culture broth is S_T minus G_l, as $Dx = S_T - G_l$. As we know the initial concentration of C-source, (C_i), thus we know the concentration and the utilization rate of G_l, and also know those of the S_T. As a result, we know the concentration and the degradation rates Dx. So, we know the rates of change of all the carbon components in the culture system through the cultivation time course (Section 2.12). We obviously see gradual hydrolysis or degradation of the dextrin oligomer to release free glucose molecules continuously into the culture and subsequently gradual assimilation of glucose into the yeast cells. This phenomenon essentially regulates the fed-batch strategy at the cell level. So, we have herein invented the new technical term "fed-batch at cell level" (FBC). The FBC importantly prevents the cell cultivation system from the Crabtree effect. As a result, it promotes cell growth at a high rate, and enables the use of a very high concentration of C-source with just the aerobic batch mode whilst in principle this cannot be done using glucose and/or sucrose. In the laboratories to the pilot scales, many researchers increased the nutrients, i.e., proteins, minerals, growth factors, etc. in the media and increased the impeller speeds and the airflow rates, but they exceeded the economically scalable values.

2.12. Engineering Mass Balances' Method to Quantify the Unknown Values of Dextrin and Glucose Uptake

This is the "state-of-the-art" method. As a limitation of the HPLC method to analyze the quantities of dextrin oligomer at a time of such a wide range of Dp (Degree of polymerization of carbon atoms), e.g., from C_{18}, C_{17}, C_{16} … C_{10}, C_9, C_8, C_7 … to C_1, thus we use the Biochemical Chemical Engineering mass balances' technique. In Section 2.11, with the use of the mass balances' model from the overall mass balance equation, $C_i = G_u + S_T$ …. (Equation (1)), where G_u is the total glucose uptake, and the component mass balances of $S_T = Dx + G_l$ …. (Equation (2)), the concentrations of all the components can be calculated. Furthermore, the utilization rates, r, of each component can also be calculated as, $rS_T = \frac{dS_T}{dt}$ is the rate of total sugar degradation; $rG_u = \frac{dG_u}{dt}$ is the rate of overall glucose uptake; $rG_l = \frac{dG_l}{dt}$, is the rate of residual glucose utilization; $rDx = \frac{dDx}{dt}$ is the rate of dextrin degradation. Significantly, this biochemical engineering mass balance model, $rS_T = rG_u = rG_l + rDx$ … (Equation (3)). This clearly again proves and confirms the "fed-batch at cell level", the FBC phenomenon.

2.13. Statistical Analysis

The statistical analyses were done with the one-way analysis of variance (ANOVA) and the differences of the treatment mean values from three replications (each experiment was done in 3 replicates) were compared with the Tukey's range test method at p-value ≤0.05 using a software Minitab version 17. All the experimental result data were presented as the graphical plots using the mean values together with the error bars of standard deviations. The kinetic results are presented in the tables.

2.14. Growth Kinetic Parameters' Calculations

The five growth kinetic parameters were calculated using experimental data, i.e., cultivation time, t (h), cell biomass concentration, x (g/L), and substrate use, s (g/L). (i) The specific growth rate, μ (h^{-1}) is calculated from, $\mu = \frac{dlnx}{dt}$, where the differential natural log of x is divided by the time change. (ii) The productivity or production rate of cell biomass, r_x (g/L/h) is $r_x = \frac{dx}{dt}$. (iii) The utilization rate of substrate, r_s (g/L/h) is from $r_s = \frac{ds}{dt}$, where s can be all types of the sugar components, i.e., total sugar (S_T), glucose uptake (G_u), glucose residual (G_l), and dextrin (Dx), (iv) The cell yield coefficient, $Y_{x/s}$ (g/g) is from $Y_{x/s} = \frac{\Delta x}{\Delta s}$, where Δx is the cell biomass produced (g/L) and Δs is the substrate utilized (g/L). (v) The production efficiency, Ef (%) is from $Ef = \frac{Y_{x/s}}{Y'_{x/s}} \times 100$, where $Y_{x/s}$ is from the experiment and $Y'_{x/s}$ is from the theoretical yield coefficient or stoichiometry [15,19]. One gram of commercial glucose or glucose from dextrin could produce a cell biomass of 0.53 g, ($Y_{x/s_{glu}} = 0.53$ g/g) and one gram of

YE could additionally produce a cell biomass of ~0.6–0.7 g, ($Y_{x/s_{YE}} = 0.6 - 0.7$ g/g). When they are mixed in the medium, the $Y'_{x/s}$ was calculated based on the fraction of their components.

2.15. Calculation of the Designed Impeller Speeds

For fluid dynamics in a stirred-tank bioreactor [19–21], the power P (W) is calculated from $P = nPo_g\rho N^3D^5$, where n is the number of impellers of 2 for 5-L bioreactor, Po_g is the power number of 2.4, (no unit or dimensionless) for fluid with air sparging of Rushton turbine impeller in the bioreactor, ρ is the culture broth density (kg/m^3), N is the impeller speed (rps), and D is the impeller diameter of 0.065 (m). The power input or energy dissipation rate per unit mass, $\overline{\varepsilon}_T$ (W/kg) is calculated from $\overline{\varepsilon}_T$ or $\frac{P}{\rho V} = \frac{nPo_g\rho N^3D^5}{\rho V}$, where V is the culture broth volume (m^3). Thus, the designed impeller speeds, N of the power inputs 1, 2, 3, and 4 (W/kg) are calculated from $N = \left(\frac{\overline{\varepsilon}_T V}{nPo_g D^5}\right)^{1/3}$. These both kinetic and fluid dynamic parameters from the laboratory experiments are very crucial for the scale-up of further microbial cell cultivations both at the pilot and especially at the industrial scales. That is the foreseen reason why we designed the impeller speeds based on the power input rather than just the speed in rpm (Table 1).

3. Results and Discussion

3.1. The Effective BPM for S. cerevisiae Cultivation

A batch production medium (BPM) is a chemically defined minimal medium formulated here by our laboratory as a high potential medium for high cell density cultivation in the industry. The effectiveness of the BPM supplemented with YE was higher than that of the standard YPD complex medium for *S. cerevisiae* cultivation (Figure 1). At all the same glucose concentration of 20 g/L (111 mM), the BPM with 0.3 % (*w/v*) of YE significantly produced yeast cell biomass at a concentration of 7.67 g/L, the YPD medium produced it at 6.93 g/L, while the BPM without YE could produce it at only 3.30 g/L. The sole BPM is the lowest effective medium because it is the defined minimal medium containing only the satisfied defined nutrients, inorganic salts, and some trace elements. It lacks necessary nutrients, i.e., proteins, minerals, and growth factors, i.e., vitamins. As the microorganism growth requires major nutritive components, i.e., carbohydrate as an energy C-source and proteins as the cell components, they additionally still require peptides, amino acids, fatty acids and lipids, nucleic acids, inorganic salts, trace elements, and vitamins which are the precursors for numerous co-factors [22]. So, when the YE was added into the BPM, it importantly promotes *S. cerevisiae* cell growth and biomass production. It was observed from the increase in cell biomass at the final concentration of 7.67 g/L, which was higher than those of the two (Figure 1).

Yeast extract contains abundant components (% *w/w*) of carbohydrates and derivatives (~10–35%), proteins (~45–50%) and free amino acids (~8–15%), vitamin derivatives (~5–10%), minerals and trace elements (~5–10%), nucleotides (~5–15%), and fat (~3–10%), which are necessary for microbial cell growth [23]. The BPM defined medium added with the YE is actually called "semi-defined medium". The medium was mostly composed of the defined components with only one or two complex nutrients [24]. In this research work, it was the effective medium for yeast cell cultivation because it enhanced higher cell biomass concentration than that of the standard medium (YPD). The BPM can be both defined and semi-defined medium that has many advantages to be used both in the laboratory and at the industrial scale. It is much cheaper (~0.035–0.045 US $ per liter), when compared to a laboratory medium of ~0.85 US $ per liter which is ~25 times higher. The BPM is simpler to be produced and easier to be controlled in fermentation and downstream processes effecting lower cost of investment [25].

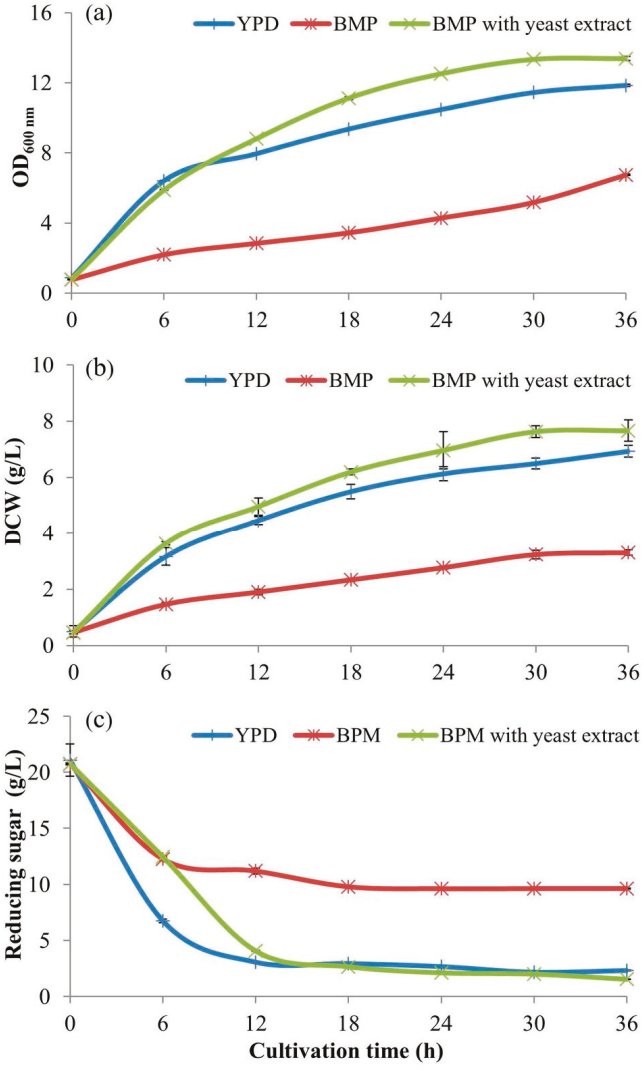

Figure 1. Growth (**a**) $OD_{600\ nm}$; (**b**) dry cell weight, and (**c**) glucose (reducing sugar) used during cultivations of *S. cerevisiae* in shake flasks with different media, YPD (Yeast Peptone Dextrose) a standard medium for yeast culture, BPM (Batch Production Medium) with yeast extract (YE) and BPM without YE as a control treatment. The BPM was formulated here for economic reasons and potent industrial use. Note: As standard deviation values are very small, error bars in Figures (**a**) and (**b**) are somewhat invisible.

3.2. The Addition of Yeast Extract as the Supplement to Improve the BPM for Yeast Cell Cultivation

As yeast extract significantly promotes yeast cell growth, its minimal optimum concentration herein for aerobic cultivation of *S. cerevisiae* is at 0.3% (*w/v*) (Figure 2). This treatment produced cell biomass at a concentration of 10.96 g/L at 18 h with a specific growth rate, μ at 0.15 h^{-1}, a cell yield coefficient, $Y_{x/s}$ of 0.53 g/g, a cell biomass production rate, r_x at 0.61 g/L/h, and a substrate consumption rate, r_s at 0.94 g/L/h with an efficiency of 95.98%. This also reduced cultivation time and increased

cell biomass when compared to the control treatment of the cultivation without the addition of YE (0% *w/v*). However, the increase in YE concentrations at 0.6% and 0.9% (*w/v*) performed no significant difference in biomass concentration (x) and specific growth rate (μ), while the yield coefficient ($Y_{x/s}$) and the cultivation efficiency (Ef) of 0.3% (*w/v*) YE addition were higher (Table 2).

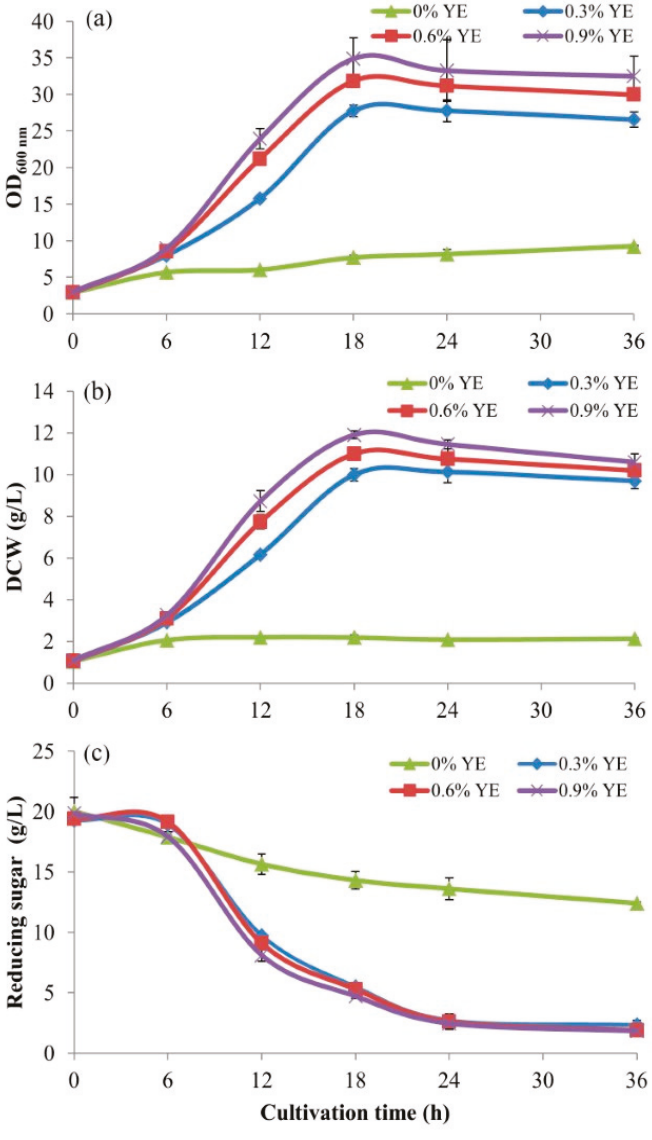

Figure 2. Growth (**a**) $OD_{600\,nm}$; (**b**) dry cell weight, and (**c**) glucose utilization during cultivations of *S. cerevisiae* in shake flasks using BPM with 20 g/L of glucose, supplemented with yeast extract (YE) at different concentrations (% *w/v*).

Normally, both anabolic and catabolic pathways of *S. cerevisiae* require amino acids such as Ser, Gly, Cys, Tyr, Trp, and others in certain concentrations which are sufficient but not excessive. These are present in YE. These results suggest that the BPM lacks amino acids, essential nutrients, and other

growth factors. The addition of YE at 0.3% (*w*/*v*) can supply those essential sources for yeast cell growth to produce cell biomass at a high concentration. Although more increasing it to concentrations of 0.6% and 0.9% (*w*/*v*) did not result in the increasing cell biomass, but these concentrations did not exceed the inhibiting value to yeast cells. Although it was reported that peptone and YE did not have any significant effect on cell growth or sugar consumption [26]; however, with the supplement of YE at a concentration of 6 g/L into the medium, ethanol concentration was slightly higher than those of the supplements of YE at 3 and 9 g/L [27].

Table 2. Growth kinetic parameters of *S. cerevisiae* cultivations in shake flasks using BPM medium with 20 g/L glucose and supplemented with yeast extract at different concentrations.

YE Conc.	YE/Glucose	x	μ	$Y_{x/s}$	r_x	r_s	Efficiency
(%)	Fraction	(g/L)	(h^{-1})	(g/g)	(g/L/h)	(g/L/h)	(%)
0.0	0.00	2.19 ^{b}	0.11 ^{c}	0.29 ^{c}	0.18 ^{c}	0.36 ^{c}	54.72 ^{d}
0.3	0.15	10.96 ^{a}	0.15 ^{ab}	0.53 ^{a}	0.61 ^{b}	0.94 ^{b}	95.98 ^{a}
0.6	0.30	11.42 ^{a}	0.17 ^{a}	0.48 ^{b}	0.63 ^{ab}	1.12 ^{b}	84.32 ^{b}
0.9	0.45	11.91 ^{a}	0.17 ^{a}	0.44 ^{b}	0.66 ^{a}	1.35 ^{a}	75.50 ^{c}

Statistic comparisons of those mean values within their own columns (among yeast extract concentrations) at *p*-values of ≤0.05 show different characters, a, b, and c, which indicate statistically significant differences.

3.3. Different Carbon Sources for the Yeast Cultivation

Type and concentration of C-sources in culture media effect to cell biomass and product formation especially for high cell density cultivation. Each microorganism requires and has some limitations on the type and its concentration. In general, glucose and sucrose are used for aerobic batch cultivations of microorganisms in bioreactors of every scale at a limited concentration of ≤40–50 g/L [17]. Glucose is very effective and is the most popular C-source because it supports fast growth as it is a single molecule and easy to consumption first. It is the initial substrate and the precursor of the main pathways. However, glucose cannot be used at too a high concentration as it is easily assimilated into the cells, causing its accumulation and congestion. This usually causes the Crabtree effect that inhibits cell growth. Because of the insufficiency of dissolved oxygen concentration, and the limitation of the bioreactor operation, the yeast cells produce ethanol and the bacterial cells produce acetate, the toxic by-products, instead of going through ATP-producing pathways. In this situation, cells stop growing and consequently producing low cell biomass. Glycerol is an alternative popular C-source because of its advantages, e.g., a high degree of reduction (4.67) per carbon when compared to that of glucose with a value of 4 [14] and prevention of cell system from the Crabtree effect [19]. There was a study on recombinant *S. cerevisiae* cultivation to obtain high cell density using glycerol as a substrate in the fed-batch mode with a feeding strategy based on an online response of the culture pH to the glycerol consumption [28].

Actually, yeast *S. cerevisiae* can utilize many different C-sources, such as glucose, fructose, galactose, mannose, and other alternative sources of the disaccharide, e.g., maltose and sucrose [29,30]. Glucose is the most popular C-source for yeast cultivation for the production of biological products as it provides fast growth other than other sugars. It is consumed first in sugar mixtures. However, it causes some limitations and problems as discussed above. To overcome those limitations, this research was challenged to the use of dextrin, the oligomer of glucose, the primary hydrolysate from cassava starch liquefaction as a new potential C-source to substitute glucose for *S. cerevisiae* cultivation.

Figure 3 and Table 3 show that yeast *S. cerevisiae* could not use sole dextrin as a C-source because it lacks hydrolase enzyme to degrade dextrin oligomer and release free glucose molecules. It could produce cell biomass at a concentration of only 4.52 g/L. When a glucoamylase enzyme was added together with dextrin into the BPM, dextrin was hydrolyzed to release glucose, and glucose was subsequently utilized by the yeast. This treatment produced cell biomass at a concentration of 9.51 g/L within 24 h at a specific growth rate, μ of 0.11 h^{-1}, a cell yield coefficient, $Y_{x/s}$ of 0.47 g/g, a cell biomass

production rate at 0.40 g/L/h and a substrate utilization rate at 0.74 g/L/h with an efficiency of 85.12%. These values are close to those of the cultivation with glucose (Table 3).

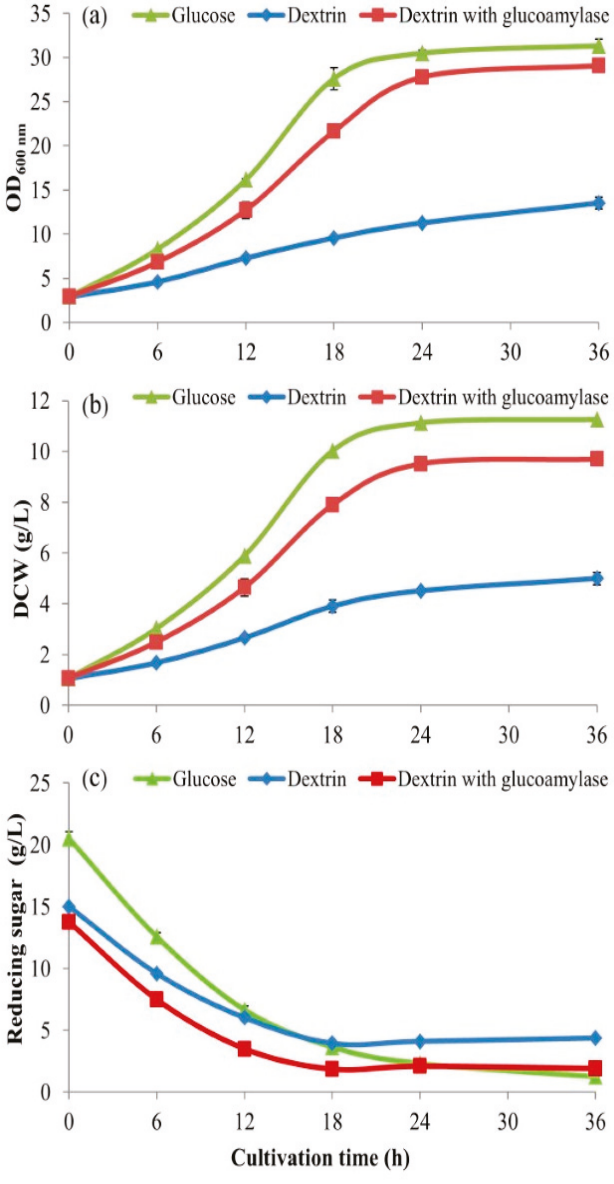

Figure 3. Growth (**a**) $OD_{600\ nm}$; (**b**) dry cell weight, and (**c**) substrates utilized during cultivations of *S. cerevisiae* in shake flasks using BPM with 20 g/L of different carbon sources, each supplemented with 0.3% (*w/v*) of yeast extract to compare with the use of glucose and select the most potential C-source for larger-scale and industrial cultivations; Note: As standard deviation values are very small, error bars in Figures might be invisible.

Table 3. Growth kinetic parameters of *S. cerevisiae* cultivations in shake flasks using BPM medium with 20 g/L of different carbon sources (at the same equimolar concentration of 111 mM), each supplemented with yeast extract at 0.3% (*w/v*).

Carbon Sources	x	μ	$Y_{x/s}$	r_x	r_s	Efficiency
	(g/L)	(h^{-1})	(g/g)	(g/L/h)	(g/L/h)	(%)
Glucose	11.13 [a]	0.12 [a]	0.55 [a]	0.46 [a]	0.76 [a]	99.61 [a]
Dextrin	4.52 [c]	0.07 [b]	0.22 [c]	0.19 [c]	0.66 [b]	39.84 [c]
Dextrin with glucoamylase	9.51 [b]	0.11 [a]	0.47 [b]	0.40 [b]	0.74 [a]	85.12 [b]

Statistic comparisons of those mean values within their own columns (among carbon sources) at *p*-values of ≤0.05 show different characters, a, b, and c, which indicate statistically significant differences.

The enzyme's optimum temperature and pH of our own study were at 65 °C and 4.5, respectively giving a maximum activity, u_{max} at a rate of 0.0073 g/g/L/min [16]. However, the external glucoamylase supplemented was also active in the same conditions of cell cultivation at a temperature of 30 °C and a pH of 4.5, respectively. (In this in vitro condition, the u_{max} was at a rate of 0.0037 g/g/L/min). The glucoamylase gradually degraded at the ends of dextrin chains to slowly release glucose monomers for gradual assimilation and consumption by the yeast. So, we suggest that the dextrin oligomer from cassava starch liquefaction here is a very effective potential C-source for *S. cerevisiae* cultivation when the enzyme is added at an appropriate concentration of 0.1–0.2% (*v/w*). Starch hydrolyses, liquefaction and saccharification, in a 10-L stirred tank lysis reactor and their kinetics have been profoundly studied by our group [16]. As dextrin is gradually hydrolyzed by the addition of glucoamylase, a continual gradual release of free glucose molecules occurs at an appropriate rate. Thus, the glucose molecules are proportionally assimilated into the yeast cells without accumulation, congestion, and inhibition.

3.4. The Use of High Concentrations of Dextrin for S. cerevisiae Cultivation in the 5-L Bioreactors

To produce experimental results approaching practicable scalability, the larger scale cell cultivations using 5-L bioreactors with fully controlled conditions were carefully undertaken. The optimum concentration of C-sources is very important to enhance cell growth and product formation. The lower the concentration of C-source affects the lower the cell biomass and productivity. When there is an increase in a maximum C-source concentration with appropriate conditions, i.e., sufficient nutrients, dissolved O_2, and mixing intensity, etc., the yield and productivity could be proportionally increased and maximized. The excessive C-sources especially for glucose and sucrose affect cell metabolisms and inhibit cell growth and consequential product formation. However, with our strategies here, the cell cultivations with very high concentrations of C-source can be achieved although using just the aerobic batch mode.

The experimental results showed that the effective maximum concentration of dextrin used by *S. cerevisiae* for aerobic batch cultivation without substrate repression problem inhibiting cell growth was at 90 g/L in 3× BPM with 0.9% (*w/v*) of YE. It produced the maximum cell biomass within 30 h. A dry cell weight, x at 53.63 g/L, a specific growth rate, μ at 0.18 h^{-1}, a cell yield coefficient, $Y_{x/s}$ of 0.54 g/g, a rate of cell biomass production, r_x at 1.79 g/L/h, and a rate of substrate utilization, r_s at 3.16 g/L/h with 99.00% efficiency were obtained (Table 4 and Figure 4). Clearly, when compared to those of other concentrations, this treatment shows efficient growth performances in terms of: (i) cell biomass growth profile and concentration. (ii) efficient use of C-source dextrin with the optimum concentration, and (iii) rates of biomass production and substrate utilization.

Table 4. Growth kinetic parameters of *S. cerevisiae* cultivations in 5-L bioreactors using BPM with dextrin at different concentrations and operating at the impeller speeds of 500, 600, 700, and 800 rpm, (equivalent to $\overline{\varepsilon}_T$ = 1, 2, 3, and 4 W/kg) with the airflow rates at 1, 2, 3, and 4 vvm where they were proportional to the concentrations of dextrin.

BPM Conc. with (Dextrin Conc.)	x	μ	$Y_{x/s}$	r_x	r_s	Efficiency
	(g/L)	(h^{-1})	(g/g)	(g/L/h)	(g/L/h)	(%)
1× (30 g/L)	11.17 ^{d}	0.15 ^{bc}	0.35 ^{b}	0.38 ^{d}	0.97 ^{d}	64.17 ^{b}
2× (60 g/L)	23.60 ^{c}	0.16 ^{b}	0.36 ^{b}	0.98 ^{c}	2.07 ^{c}	66.00 ^{b}
3× (90 g/L)	53.63 ^{a}	0.18 ^{a}	0.54 ^{a}	1.79 ^{a}	3.16 ^{a}	99.00 ^{a}
4× (120 g/L)	42.40 ^{b}	0.13 ^{c}	0.32 ^{c}	1.41 ^{b}	2.95 ^{b}	57.70 ^{c}

Statistic comparisons of those mean values within their own columns (among dextrin concentrations) at p-values of ≤0.05 show different characters, a, b, c, and d, which indicate statistically significant differences.

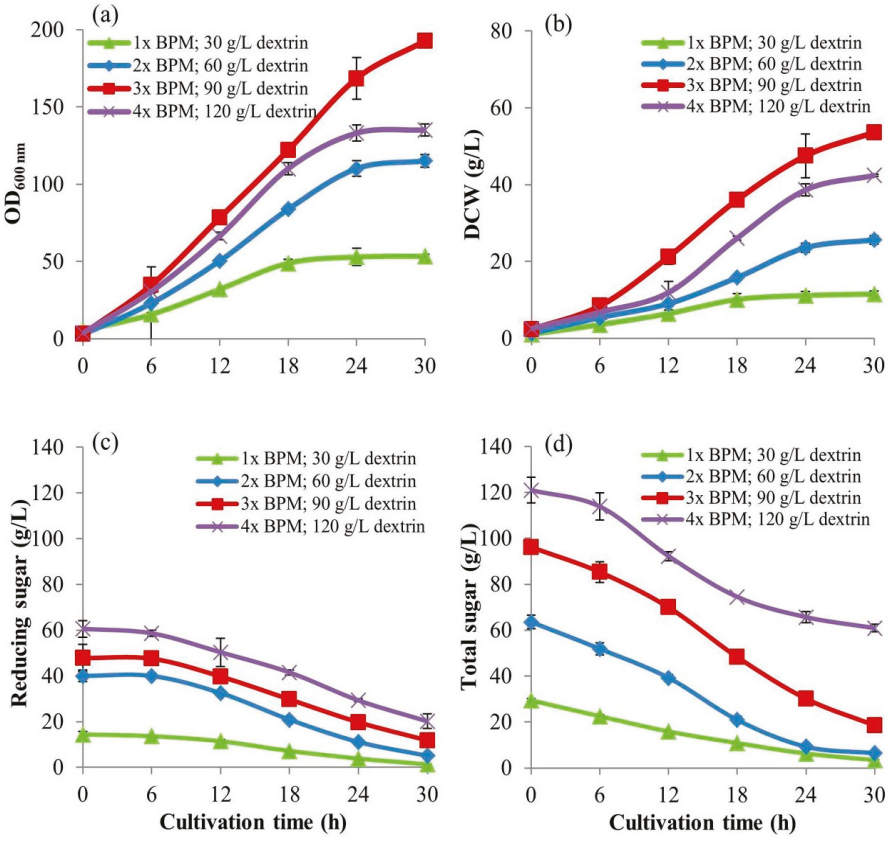

Figure 4. Growth (**a**) $OD_{600\ nm}$ and (**b**) dry cell weight; substrate utilizations (**c**) reducing sugar (residual glucose) and (**d**) total sugar, during cultivations of *S. cerevisiae* in 5-L bioreactors using BPM medium with dextrin at different concentrations of 30, 60, 90, and 120 g/L, and operating at the impeller speeds of 500, 600, 700, and 800 rpm, (equivalent to $\overline{\varepsilon}_T$ = 1, 2, 3, and 4 W/kg) with the airflow rates at 1, 2, 3, and 4 vvm where they were proportional to the concentrations of dextrin, respectively.

As dextrin is a longer molecule, *S. cerevisiae* cannot immediately import it into the cells for consumption with the normal pathway, but its need is to be shortened to release glucose and maltose molecules. However, *S. cerevisiae* cannot do by itself, so external glucoamylase added at an appropriate

concentration will act as gradually cutting at the ends of their chains and releasing free glucose molecules. Therefore, the amount of glucose released into the culture does not exceed the concentration of using glucose as a direct C-source. There is an explanation that glucoamylase is an exoamylase which cleaves 1,4-α-glycosidic bonds from the non-reducing ends of the glycosidic chains releasing D-glucose, thus increases the content of fermentable carbohydrates and reduces the non-fermentable dextrin [31]. Yeasts will gradually import glucose and maltose molecules into their cells in the right amount without accumulation until inhibiting the cell growth.

This "dextrin culture" is similar to an SSF (simultaneous scarification and fermentation) for ethanol production from maltodextrin by yeast, but it is not exactly the same herein because aerobic cell cultivation with "starch pre-product" called dextrin at a high concentration has a more difficulty in sufficient-dissolved O_2 supply. This problem is overcome by gradually cleaving the dextrin chains to release free glucose molecules gradually instead of the direct use of bulk glucose. As a consequence, they are gradually assimilated into yeast cells without accumulation and congestion to inhibit cell growth. This is a novel technique called "fed-batch at cell level" or FBC. It enhances the utilization of a high concentration of C-source oligomer to boost the production of a high cell biomass. As it is an oligomer, although the aerobic batch cultivation, it can be used at a concentration of ≥3-4 times higher than that of glucose and sucrose. Thus, it is superior to the conventional fed-batch cultivation techniques (Table 5) of which glucose and sucrose at high concentrations must be fed using fed-batch strategies with much longer time courses and complexities.

Table 5. Results of dry cell weight, production rate, and yield coefficient from *S. cerevisiae* cultivations using fed-batch techniques with different C-sources and cultivation time courses to compare with the result of our research work here.

Cultivation Techniques	Carbon Sources	Substrates Conc. (g/L)	Cultivation Time (h)	DCW (g/L)	Productivity (g/L/h)	$Y_{x/s}$ (g/g)	Ref.
Fed-batch	Molasses and corn steep liquor	Sucrose (85) Protein (225)	110	187.63 [Np]	1.71	0.60	[10]
Fed-batch	Glucose	Glucose (230)	65	120.00	1.84	0.52	[11]
Fed-batch	Molasses	Sucrose (250)	80	95.70	1.32	0.38	[12]
Fed-batch	Glucose	Glucose (200) YE (15)	50	63.3–96.10	1.30–1.99	0.4–0.48	[13]
Batch	**Dextrin**	**Dextrin (90) YE (9)**	**24**	**53.72**	**2.24**	**0.55**	**This study**

[Np]: not practical because of too high a titer of protein used beyond the industrial scalability and profitability.

3.5. The Intensive Multiple Sequential Batch Technique to Achieve High cell density Concentration Superior to the Fed-Batch Technique

"Intensive" means the use of very high concentrations of C-source together with proportionally high intensities of operations, i.e., agitation speed and airflow rate. HCDC is mainly based on the fed-batch technique with the development of different nutrient feeding strategies, e.g., pH-stat, chemo-stat, exponential feed, etc. They are complicated and use a lot of equipment, time, and investment cost at every scale [32]. Batch cultivation is not popular to implement for high cell density cultivation due to a limitation of using high level of C-source which could inhibit cell growth. However, our study recognizes the advantages of batch cultivation, i.e., ease of operation, and preparation of equipment and medium. We have developed the special batch cultivation strategies to compete with the convention fed-batch technique to produce yeast cell biomass at high density concentrations. By finding the effective C-source, formulating a potential minimal medium, operating intense agitation and airflow, and together with the repeating batches without preparations of new equipment, the experiments were done successfully by the so-called "intensive multiple sequential batch" technique. This implementation enables yeast cells to grow continuously at a high rate. It as well as helps reduce difficulties, time, cost, and labor, especially when implemented in the industrial processes.

In this experiment, the initial batch cultivation was operated with the same optimum conditions as in Section 3.4 above. The 3× BPM with 90 g/L dextrin and 0.9% (*w/v*) of YE was used. The optimum conditions, i.e., at pH of 4.5, temperature of 30 °C, impeller speed of 700 rpm, and aeration rate of 3 vvm were controlled through 24 h of cultivation. The next four consecutive batches with the same operations were repeated. Table 6 and Figure 5 show the results of *S. cerevisiae* cultivations with intensive multiple sequential batch technique of five-cycle batch runs for a total time course of 120 h. The biomass concentrations at 24 h in each batch from 1 to 5 were 53.13, 55.17, 53.03, 53.77, and 53.50 g/L, respectively with an average value at 53.72 g/L. From all the five sequential batches, the average values, i.e., a specific growth rate, μ at 0.16 h^{-1}, a yield coefficient, $Y_{x/s}$ of 0.50 g/g, a cell productivity, r_x at 2.24 g/L/h, and a substrate utilization rate, r_s at 4.05 g/L/h (80.93 mmol/L/s), with an overall efficiency of 90.55% were obtained. These values are higher than some of those results from the fed-batch cultures in the literature (Table 5).

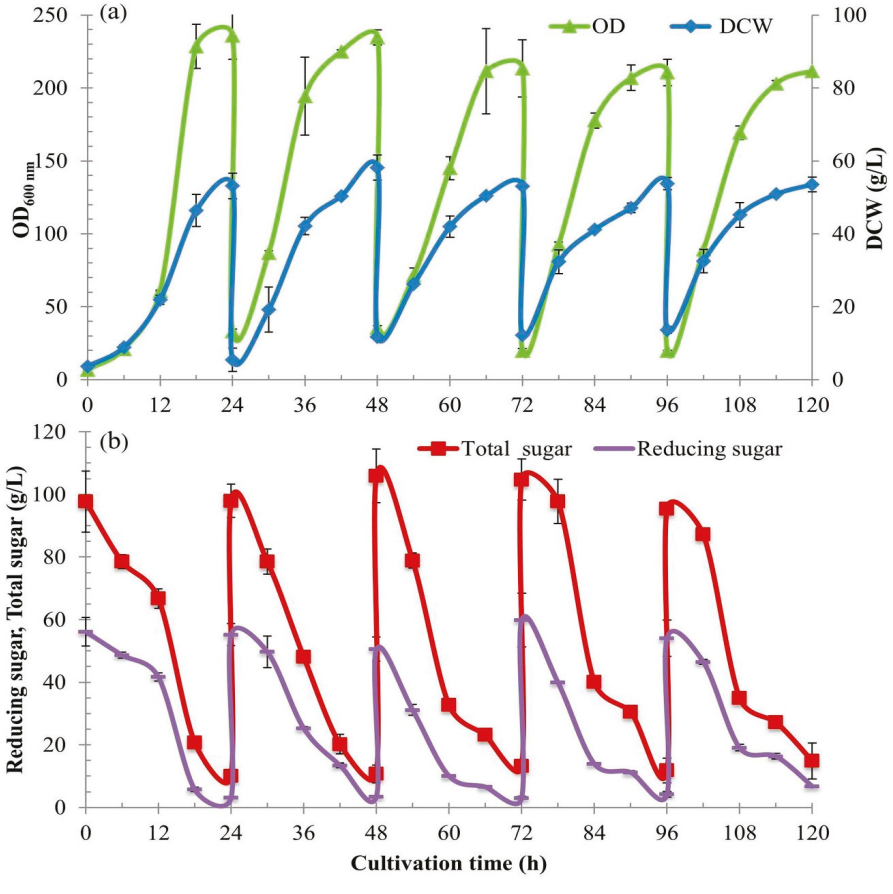

Figure 5. Growth (**a**) $OD_{600\ nm}$ and dry cell weight; (**b**) substrate utilizations, reducing sugar (residual glucose), G_l and total sugar, S_T during cultivations of *S. cerevisiae* with the intensive multiple sequential batches for 5-cycle runs using 3× BPM with 90 g/L of dextrin and 9 g/L (0.9% *w/v*) of yeast extract, operating at the impeller speed of 700 rpm ($\bar{\varepsilon}_T$ = 3 W/kg) with the airflow rate at 3 vvm.

Table 6. Growth kinetic parameters of *S. cerevisiae* cultivations with the intensive multiple sequential batches for 5-cycle runs using 3× BPM with 90 g/L of dextrin and 9 g/L (0.9% *w/v*) of yeast extract operating at the impeller speed of 700 rpm ($\bar{\varepsilon}_T$ = 3 W/kg) with the airflow rate at 3 vvm.

(Intensive Sequential Batches)	x	μ	$Y_{x/s}$	r_x	r_s	Efficiency
	(g/L)	(h^{-1})	(g/g)	(g/L/h)	(g/L/h)	(%)
Batch I	53.13 ^{b}	0.15 ^{b}	0.55 ^{a}	2.21 ^{b}	4.02 ^{b}	100.00 ^{a}
Batch II	55.17 ^{a}	0.21 ^{a}	0.54 ^{a}	2.30 ^{a}	4.01 ^{b}	98.18 ^{a}
Batch III	53.03 ^{b}	0.13 ^{b}	0.45 ^{c}	2.21 ^{b}	4.23 ^{a}	81.82 ^{c}
Batch IV	53.77 ^{b}	0.16 ^{b}	0.45 ^{c}	2.24 ^{b}	4.25 ^{a}	81.82 ^{c}
Batch V	53.50 ^{b}	0.14 ^{b}	0.50 ^{b}	2.23 ^{b}	3.73 ^{c}	90.91 ^{b}
Mean	53.72	0.16	0.50	2.24	4.05	90.55

Statistic comparisons of those mean values within their own columns (among sequential batch runs) at *p*-values of ≤0.05 show different characters, a, b, and c, which indicate statistically significant differences.

These values are comparable with those of the other high cell density cultivations using the fed-batch strategies. A high cell density cultivation of *S. cerevisiae* using a fed-batch technique was done with feeding the mixture of molasses: corn steep liquor in a ratio of 80: 20% (*w/v*). They obtained the maximum cell biomass at 187.63 g/L over 110 h with a productivity of 1.71 g/L/h [10]. A high cell density cultivation with the direct feedback control of glucose using an online ethanol concentration monitor in fed-batch cultivation technique for ergosterol production by *S. cerevisiae* was conducted and obtained a yeast dry weight at 120 g/L and the ergosterol yield reached 1500 mg/L within 65 h with a cell productivity of 1.84 g/L/h [11]. The cultivations of *S. cerevisiae* were used to produce β-glucan from molasses and corn steep liquor with batch and fed-batch techniques. A cell biomass in batch culture was at 36.5–39.3 g/L while the maximum biomass in fed-batch culture was at 95.7 g/L within 80 h (2.4-folds higher) with a low productivity of 1.20 g/L/h [12]. The yeast cell productivity of our work here is 2.24 g/L/h, which is higher than those of the other research works although they used the fed-batch strategies.

Furthermore, it has been repeatedly stated that the so-called "fed-batch at cell level-FBC" technique is superior to the conventional fed-batch cultivation strategy. However, this statement might have not been sufficiently proved in this study. When a comparison of experimental data on process performance (i.e., biomass productivity, yield coefficient, and concentration), operating under the FBC technique (this study) and the fed-batch cultivation strategies (literature data in Table 5) was attempted, it was shown that the FBC technique prevails over the fed-batch strategies in terms of productivity (due to the faster cultivation), resulting a notably lower dry cell concentration (Table 5). However, when they are considered, i.e., (53.7 g/L vs. 187.6 g/L, 120 g/L, or 95.7 g/L), it is correct, but not true. So, they are not comparable; i.e., 53.7 g/L/24 h vs. 187.6 g/L/110 h, 120 g/L/65 h, or 95.7 g/L/80 h. This is correct and true. So, they are comparable. In fact, the FBC technique is superior to the conventional fed-batch cultivation in terms of (i) less operation complexities, a number of equipment, cost, time, contamination risk, etc. (ii) production mass at a specific time course. For example, if a 20,000-L working volume of cell culture is produced in an industrial bioreactor at a rate of 95.70 g/L/80 h, a cell biomass of 1914 kg will be obtained. For the FBC, if a 20,000-L working volume of cell culture is produced using the same industrial bioreactor at a rate of 53.72 g/L/24 h, a cell biomass of 1074 kg will be obtained. By using the same time course of 80 h for operation and the FBC is run with the intensive multiple sequential batch technique, the number of batch cycle is 80/24 = 3.33. Thus, a cell biomass of 3576.42 kg will be obtained. That is the reason why the FBC of a high productivity must be operated together with the multiple sequential batch technique. Actually, the FBC can be operated at up to ≥7 cycles (data not shown). Moreover, we have successfully cultivated certain bacteria, i.e., *E. coli* and *Bacillus megatherium*, implementing the FBC technique, and much higher productivities at 3.50 and 3.92 g/L/h, respectively have been achieved (results not shown here).

However, if we think that the lower the culture density, the more reduced the separation efficiency and the greater the required energy, and in the case of industrial bioreactors the processed culture volume is of the order of several thousands of liters or cubic meters, then the advantages of this IMSB technique should be carefully studied. In the industry, all the issues, such as selected technologies, types and sizes of unit operations, investment cost, labor, time, etc. must be considered. They have to be compromised to meet the desired economic values.

3.6. Sugar Components' Analysis during High Cell Density Cultivation and the Proof of "Fed-Batch at Cell Level" (FBC)

3.6.1. Biochemical Engineering Mass Balances

The overall mass balance equation,

$$C_i = G_u + S_T \tag{1}$$

where

$$S_T = Dx + G_l \tag{2}$$

Thus, the component mass balances,

$$G_u = C_i - S_T \tag{3}$$

and when substitute (2) in (3) then,

$$G_u = C_i - (Dx + G_l) \tag{4}$$

So, the dextrin concentration, Dx is

$$Dx = C_i - (G_u + G_l) \tag{5}$$

where C_i is the initial carbon source (dextrin from cassava starch liquefaction), S_T is the total sugar left in the system during cell cultivation, G_u is the overall glucose which has been taken up into the cells, thus Dx and G_l are the dextrin left and glucose residue in the system, respectively.

For the overall rates' balances:

From Table 7, the overall rates' balance is

$$\frac{dG_l}{dt} + \frac{dDx}{dt} = \frac{dG_u}{dt} = \frac{dS_T}{dt} \tag{6}$$

thus,

$$rG_l + rDx = rG_u = rS_T \tag{7}$$

where each "r" represents the rates of each component by which each rate is calculated from the changes (reductions, i.e., G_l, Dx, S_T, or increase, i.e., G_u) of each component divided by cultivation times.

From cell cultivation experiments and analyses, as we know (i) C_i, the initial concentration of C-source used, e.g., 90 g/L, (ii) S_T, the total sugar concentration analyzed by complete acid hydrolysis and (iii) G_l the glucose left in the system as the reducing sugar by DNS assay. Thus, all those equations can be balanced and found the unknown values of G_u and Dx (Table 7 and Figures 5–7). This essentially proves that there is continually gradual hydrolysis of dextrin oligomer to release free glucose which is, at the same time, gradually assimilated into the cells proportionally. This importantly supports cell growth with the technique, "fed-batch at cell level" (FBC). Moreover, from Table 7 and Equations (6) and (7), an overall rates' balance equation can be derived as $rG_l + rDx = rG_u = rS_T$, where rG_l is the rate of residual glucose utilization and rDx is the rate of dextrin degradation to release free glucose, by which both of them are the sum of total glucose assimilation rate of rG_u. Both terms of $rG_l + rDx$ and rG_u are the same rate of the total sugar utilization, rS_T. As there is an amount of residual glucose in the

system, it is assimilated into the cells at a rate of almost proportional to the rate of dextrin hydrolysis, rG_l: rDx, in a ratio of 1: 0.72 g/g/L/h to a sum of the total glucose assimilation rate. Besides the technique of gradual hydrolysis of dextrin, it is a compromised utilization of glucose from both sources efficiently to prevent the yeast cell system from glucose accumulation and subsequent congestion to cause the Crabtree effect inhibiting cell growth. Again, this phenomenon importantly proves the mechanism of "fed-batch at cell level". Essentially, dextrin plays key roles both in the regulation of the FBC and in the reserved C-source.

Table 7. Concentrations and utilization rates of total sugars, glucose uptake, residual glucose, and dextrin during cultivations of *S. cerevisiae* with the intensive multiple sequential batches for 5-cycle runs using 3× BPM with 90 g/L of dextrin and 9 g/L (0.9% *w/v*) of yeast extract, operating at the impeller speed of 700 rpm ($\overline{\varepsilon}_T$ = 3 W/kg) with the airflow rate at 3 vvm. This is to show the rates of each sugar component and that of dextrin, the overall rates and its balance equation is to prove the "fed-batch at cell level" (FBC) phenomenon.

Continual Sequential Batch Runs	Time (h) Each Batch	Time (h) Accumulative	Initial C-Source C_i (g/L)	Total Sugar S_T (g/L)	Glucose Uptake G_u (g/L)	Glucose Residue G_l (g/L)	Dextrin Degraded Dx (g/L)
I	0	0	97.71	97.71	0.00	56.13	41.59
	6	6		78.51	19.20	48.65	29.90
	12	12		66.73	31.00	41.68	25.00
	18	18		20.72	77.00	5.72	15.05
	24	24		10.12	87.60	3.08	7.00
	Rate (g/L/h)			3.65 ^{b}	3.65 ^{b}	2.21 ^{b}	1.44 ^{c}
II	0	24	98.71	97.91	0.00	55.20	42.70
	6	30		78.49	19.20	49.71	29.00
	12	36		48.10	49.60	25.31	23.00
	18	42		20.21	77.50	13.45	7.00
	24	48		10.69	87.00	3.46	7.40
	Rate (g/L/h)			3.63 ^{b}	3.63 ^{b}	2.16 ^{b}	1.47 ^{c}
III	0	48	105.94	105.94	0.00	50.59	55.40
	6	54		78.87	27.10	31.12	47.70
	12	60		32.73	73.20	10.06	22.70
	18	66		23.15	82.80	6.58	16.60
	24	72		13.30	92.60	3.03	10.30
	Rate (g/L/h)			3.86 ^{a}	3.86 ^{a}	1.98 ^{c}	1.88 ^{a}
IV	0	72	104.71	104.71	0.00	59.87	44.83
	6	78		97.72	7.00	39.92	57.80
	12	84		40.05	64.70	13.96	26.10
	18	90		30.56	74.20	11.23	19.30
	24	96		11.82	92.90	4.19	7.60
	Rate (g/L/h)			3.87 ^{a}	3.87 ^{a}	2.32 ^{a}	1.55 ^{b}
V	0	96	95.40	95.40	0.00	54.09	41.30
	6	102		87.18	8.20	46.50	40.70
	12	108		34.98	60.40	19.09	15.90
	18	114		27.27	68.10	16.35	10.90
	24	120		14.86	80.50	6.73	8.10
	Rate (g/L/h)			3.35 ^{c}	3.35 ^{c}	1.97 ^{c}	1.38 ^{d}
	Overall rates			rS_T = 3.67	rG_u = 3.67	rG_l = 2.13	rDx = 1.54
	Overall rates' balance equation,			$rS_T = rG_u = rG_l + rDx$			

Statistic comparisons of those mean values within their own columns (among sequential batch runs) at p-values of ≤0.05 show different characters, a, b, c, and d, which indicate statistically significant differences.

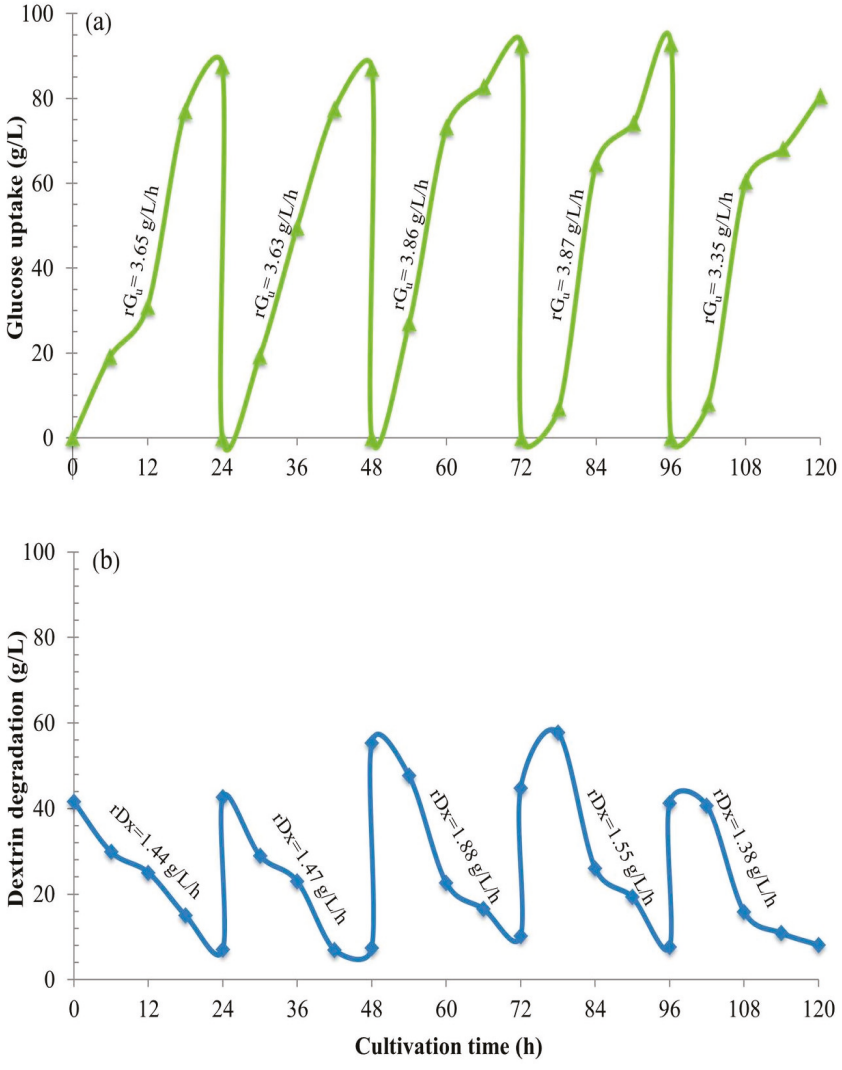

Figure 6. (**a**) Glucose uptake into the cells (green line) and (**b**) dextrin hydrolysis to release glucose (blue line), and their rates (slopes of $rG_u = dG_u/dt$ and $rDx = dDx/dt$) during cultivation of *S. cerevisiae* with the intensive multiple sequential batches for 5-cycle runs using 3× BPM with 90 g/L of dextrin and 9 g/L (0.9% *w/v*) of yeast extract, operating at the impeller speed of 700 rpm ($\bar{\varepsilon}_T$ = 3 W/kg) with the airflow rate at 3 vvm.

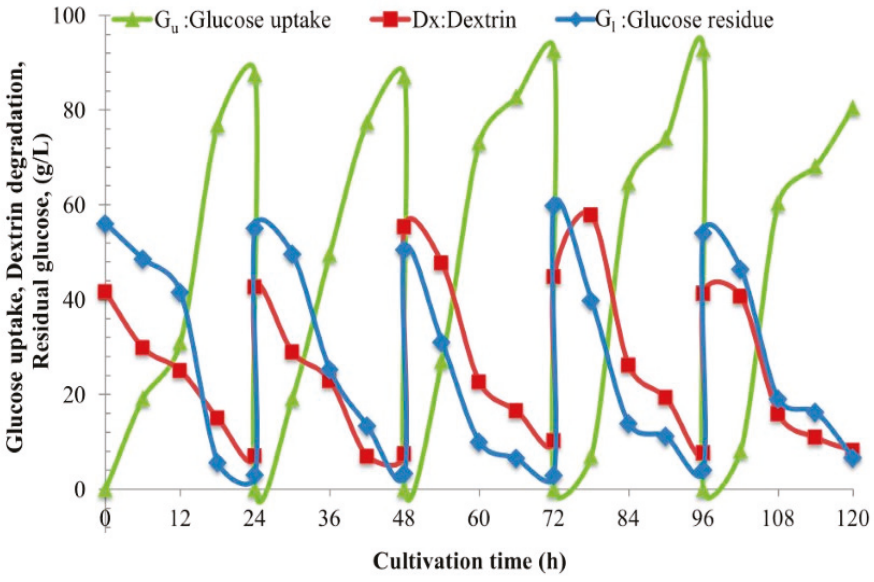

Figure 7. The relationship of the three sugar components during the cultivations of *S. cerevisiae* with the multiple sequential batches for 5-cycle runs; in each batch, the glucose uptake (G_u) is the sum of dextrin (Dx) hydrolyzed to release glucose plus residual glucose (G_l) in the culture system. Thus, $G_u = Dx + G_l$. This obviously shows the "fed-batch at cell level" (FBC) phenomenon. It is the compromised utilization of glucose from both sources during the gradual hydrolysis of dextrin to release glucose.

3.6.2. Proportional Relationship of the Three Sugar Components during the cultivation of *S. cerevisiae* Controls Fed-Batch at the Cell Level

Figure 7 and Table 7 show a relationship of the three sugar components in the culture system during the cultivation of *S. cerevisiae* with the intensive multiple sequential batches for five-cycle runs. In each batch, the total amount of glucose uptake ($G_{u)}$ is the sum of dextrin (Dx) hydrolyzed to release glucose plus (residual) glucose (G_l). Thus, it is $G_u = Dx + G_l$. Figure 7 is the figurative plot and Table 7 is the constructive numerical approach. They were fabricated to explain this phenomenon in each batch and overall the 5 batches. There are two components of carbon sources, i.e., glucose and dextrin in the culture system in bioreactor. "Glucose is ready to use, but dextrin is to use when ready". Dextrin cannot be utilized directly, but it needs to be hydrolyzed by a supplemented external glucoamylase to release free glucose which is subsequently assimilated into yeast cells. However, glucose from both sources is in the culture system as the mixture, thus it is simultaneously assimilated together into the cells as the glucose uptake (G_u). The concentrations of both glucose and dextrin gradually reduce in a certain proportional ratio. As well as the utilization rates of both C-sources are significantly proportional to a ratio of 1: 0.72 g/g/L/h (dG_l/dt:dDx/dt = *2.13:1.54* g/g/L/h) where the sum is equal to the glucose uptake rate of dG_u/dt = *3.67* g/L/h. This characteristic evidently shows the compromised use of both carbon sources by yeast cells efficiently in order to prevent the cells from glucose accumulation which will cause the Crabtree effect. In Figure 7, the reduction of glucose line (diamond) means that the major carbon source is utilized by the cells directly while the reduction of dextrin line (square) means that it is gradually hydrolyzed, to reduce the molecular lengths by freeing glucose, and also the reduction of its concentration as it is being utilized. Dextrin plays a key role in being the reserved C-source as it is hydrolyzed when needed. This state-of-the-art technique is very essential to regulate the gradual glucose uptake into the yeast cells at an appropriate rate like "fed-batch at cell level" (FBC). Unlike the control of feed rates of glucose solution into the fermenter in

conventional fed-batch technique, the FBC here has greater efficiency and many advantages which have been listed in Section 5.

3.7. The Proposed Scale-Up Strategies for High Cell Density Production

The scale-up strategies [19] for the high cell density production from the 5-L laboratory bioreactors to the larger pilot scales and up to the industrial scales are on the basis of fluid dynamic principles in the Section 2.15, where they were used to design the required impeller speeds (N) and given the result in the Table 1, based on the designed variables, called the power input or energy dissipation rate per unit mass, $\overline{\varepsilon}_T$ (W/kg). At the industrial-scale aerobic cell cultivation using C-source at a concentration of ~30 g/L, the designed $\overline{\varepsilon}_T$ value is ~1 (W/kg) [19–21]. Thus, if the C-source concentrations are 60, 90, and 120 g/L, the desired $\overline{\varepsilon}_T$ values are ~2, 3, and 4 (W/kg), respectively. So, if a designed $\overline{\varepsilon}_T$ value is fixed, all the geometries, parameters, and the designed operating impeller speed of a larger-scale bioreactor can be calculated using the equation,

$$\overline{\varepsilon}_T = \frac{nPo\rho N^3 D^5}{\rho V} \tag{8}$$

where n is the number of impellers of 3 for a larger-scale bioreactor, Po_g is 2.4 for the power number of Rushton turbine in fluid with air sparging, ρ is ~1050 (kg/m^3) for culture broth density, N is the impeller speed (rps), and D is the impeller diameter = 1/3 (m) of the bioreactor diameter, T (m), V is the designed volume of the reactor (m^3) such as 1–200 m^3. It is very important to note that the aspect ratio, H/T must be between 1–2, preferably 1–1.5, where H is the bioreactor or fluid height in bioreactor (m). Also, for other stirred-tank reactors using this type of impeller without air sparging, the Po_g changes to Po with its another value of 5 [19–21]. Also, other types of impellers with and without air sparging can be designed using the same principles.

Furthermore, for the design of the motor power to drive the three Rushton turbine impellers at a range of the designed speeds, the power of the motor, P (W) is calculated from

$$P = nPo_g\rho N^3 D^5 \tag{9}$$

This bioreactor design and scale-up strategies are very practical and have been used for the design of both pilot-scale bioreactors of 75-L, 200-L, and 750-L volumes and industrial bioreactors of 2000 L and 100,000 L successfully by the major corresponding author (results not shown here). Thus, it is practicable for the design of bioreactors for the high cell density production of yeast biomass.

4. Conclusions

The BPM with 90 g/L of dextrin C-source supplemented with YE at 0.9% (*w/v*) as a source of nutrients is very effective for the high cell density cultivation of *S. cerevisiae.* This medium enhances excellent cell growth for the production of yeast biomasses and/or their products. As the BPM is very simple and cheap, it is suitable for industrial applications. *S. cerevisiae* can efficiently use glucose from the gradual hydrolysis of dextrin. Dextrin from cassava starch liquefaction, the major C-source in BPM is more efficient than using commercial pure glucose for the production of yeast cell biomass at high density. It can substitute the major popular C-sources like glucose and/or sucrose which often cause the Crabtree effect inhibiting cell growth. Dextrin can be added into the BPM at a high concentration of ≥90 g/L for aerobic batch cultivation without the problem of too high a C-source concentration, as it regulates the assimilation of glucose at the cell level (FBC). The single 5-L batch cultivation provided the highest values of cell concentration (x), specific growth rate (μ), cell yield coefficient ($Y_{x/s}$), cell productivity (r_x), and efficiency (Ef), at 55.17 g/L, 0.21 h^{-1}, 0.54 g/g, 2.30 g/L/h, and 98.18%, respectively. To achieve higher yields, the intensive multiple sequential batches (IMSB) cultivation was designed and operated for five sequential batch runs. It showed very good results of those average values at 53.72 g/L, 0.16 h^{-1}, 0.50 g/g, 2.24g/L/h, and 90.55%, respectively. With the

studies of cell growth kinetics, biochemical engineering mass balances, and fluid dynamics in the bioreactors during cultivations, the production of yeast cell biomass at high density using dextrin at high concentrations can be scaled-up to the industries.

5. The Advantages

Again, we concluded that the advantages of this research work are as follows: (i) BPM, a minimal defined medium with YE, has a very high potential in terms of cost and efficient use for the production of *S. cerevisiae* biomass at a high density concentration with just an aerobic batch mode rather than using the fed-batch technique with a more complicated operation and longer time course. (ii) Dextrin, an oligomer of glucose from cassava starch liquefaction, is one of the best C-sources for aerobic batch cultivation to produce yeast cell biomass at a high concentration other than using the commercial glucose or/and sucrose. (iii) Dextrin can be used at a very high concentration ≥100 g/L with an aerobic batch mode without the Crabtree effect whereas glucose and sucrose cannot be done. With gradual hydrolysis, it regulates the gradual assimilation of glucose into the yeast cells like "fed-batch at cell level" (FBC), so no glucose accumulation and congestion in the cells will cause O_2 deficiency, enhancing the production of toxic by-products, i.e., ethanol in yeasts and acetate in bacteria, to inhibit cell growth. (iv) The intensive multiple sequential batch technique (IMSB) achieves high cell density concentration superior to the fed-batch technique, but it has fewer complications. (v) The kinetics of cell growth, substrate use, and product formation can be utilized to monitor, predict, validate, and control the cultivation to achieve high cell biomass. (vi) As a limitation of HPLC, the biochemical engineering mass balances of our work here are a key model of a very powerful tool implemented to quantify the unknown C-source components, i.e., dextrin and glucose uptake, both in terms of concentration and rate. (vii) Using fluid dynamics in biochemical engineering principles, the stirred-tank bioreactors at every scale can be designed and scaled-up to the industries. (viii) All (v), (vi), and (vii) are very crucial for the production of yeast and other microbial cell biomasses and their products at high concentrations in all scales of operations throughout the industries.

Author Contributions: Conceptualization, K.M. and M.K.; methodology, investigation, analysis, and writing—original draft preparation, J.S.; resources, validation, visualization, and data curation, S.C. and K.R.; writing—review and editing, validation, visualization, supervision, project administration, and funding acquisition. All authors have read and agreed to the published version of the manuscript.

Funding: A research grant, Grant No. 90/2559, was from The National Research Council of Thailand. This work was also supported by the Biochemical Engineering Pilot Plant, Biological Science Graduate Program, and Department of Biology, Faculty of Science, Burapha University, Chon Buri, Thailand.

Acknowledgments: The authors would like to sincerely thank Siripong Premjet, Daungjai Ochaikul, and Patcharanan Amornrattanpan, for their suggestions to the experimental report, and Kanyawe Kukam who supported her ideas, labor, and help in some experiments of this study.

Conflicts of Interest: The authors declare no conflict of interest. The funder had no role in the design of this study, analyses, or interpretation of data; in writing of the manuscript, or the decision to publish the experimental results.

References

1. Gómez-Pastor, R.; Pérez-Torrado, R.; Garre1, E.; Matallana, E. Recent advances in yeast biomass production. In *Biomass—Detection, Production and Usage*; InTech: Rijeka, Croatia, 2011; pp. 202–222. [CrossRef]
2. WFMJ. *Global Active Dry Yeast Market 2020 Size, Share, Growth, Trends and Forecast 2024, BUSINESS Opportunities and Future Investments*; WFMJ Press Release: Youngstown, OH, USA, 2020.
3. Forster, J.; Famili, I.; Fu, P.; Palsson, B.; Nielsen, J. Genome-scale reconstruction of the *Saccharomyces cerevisiae* metabolic network. *Genome Res.* **2003**, *13*, 244–253. [CrossRef] [PubMed]
4. Parapouli, M.; Vasileiadis, A.; Afendra, A.S.; Hatziloukas, E. *Saccharomyces cerevisiae* and its industrial applications. *Aims Microbiol.* **2020**, *6*, 1–31. [PubMed]
5. Peris, D.; Pérez-Torrado, R.; Hittinger, C.T. On the origins and industrial applications of *Saccharomyces cerevisiae* × *Saccharomyces kudriavzevii hybrids*. *Yeast* **2018**, *35*, 51–69. [PubMed]

6. Chen, R.; Yang, S.; Zhang, L.; Zhou, Y.J. Advanced strategies for production of natural products in yeast. *Cell Press Reviews Isc.* **2020**, *23*, 1–23. [CrossRef] [PubMed]
7. Subramaniam, R. High-density cultivation in the production of microbial products. *Chem. Biochem. Eng. Q.* **2019**, *32*, 451–464. [CrossRef]
8. Falco, F.; Landi, C.; Paciello, L.; Zueco, J.; Parascandola, P. Fed-batch production of endoglucanase with a recombinant industrial strain of the yeast *Saccharomyces cerevisiae*. *Chem. Eng. Trans.* **2014**, *38*, 379–384.
9. Panda, K.; Khan, R.H.; Mishra, S.; Rao, K.B.C.A.; Totey, S.M. Influences of yeast extract on specific cellular yield of ovine growth hormone during fed-batch fermentation of *E. coli*. *Bioprocess Eng.* **2000**, *22*, 379–383. [CrossRef]
10. Vu, L.; Hanh, V.; Kim, K. High-cell-density fed-batch culture of *Saccharomyces cerevisiae* kv-25 using molasses and corn steep. *J. Microbiol. Biotechnol.* **2009**, *19*, 1603–1611. [CrossRef]
11. Shang, F.; Wen, S.; Wang, X.; Tan, T. High-cell-density fermentation for ergosterol production by *Saccharomyces cerevisiae*. *J. Biosci. Bioeng.* **2006**, *101*, 38–41. [CrossRef]
12. Kim, H.Y.; Kang, S.W.; Lee, J.H.; Chang, H.I.; Yum, C.W.; Paik, H.D.; Kang, C.; Kim, S.W. High-cell-density fermentation of *Saccharomyces cerevisiae* JUL3 in fed-batch culture for the production in bata-glucan. *J. Ind. Eng. Chem.* **2007**, *13*, 153–158.
13. Lorenz, E.; Schmacht, M.; Stahl, U.; Senz, M. Enhanced incorporation yield of cysteine for glutathione overproduction by fed-batch fermentation of *Saccharomyces cerevisiae*. *J. Biotechnol.* **2015**, *216*, 131–139. [CrossRef] [PubMed]
14. Xiberras, J.; Klein, M.; Nevoigt, E. Glycerol as a substrate for *Saccharomyces cerevisiae* based bioprocesses—Knowledge gaps regarding the central carbon catabolism of this "non-fermentable" carbon source. *Biotechnol. Adv.* **2019**, *37*, 1–15. [CrossRef] [PubMed]
15. Malairuang, K. High-cell-density cultivation of three model microogranisms with intensively multiple sequential batch technique. Ph.D. Thesis, Faculty of Science, Burapha University, Chon Buri, Thailand, 2019.
16. Sawangwan, C. Starch Hydrolysis in a Stirred-Tank Lysis Reactor. Master of Science Thesis, Burapha University, Chon Buri, Thailand, 2005.
17. Malairuang, K.; Krajang, M.; Rotsattarat, R.; Chamsart, S. Intensive multiple sequential batch simultaneous saccharification and cultivation of *Kluyveromyces marxianus* SS106 thermotolerant yeast strain for single-step ethanol fermentation from raw cassava starch. *Process. Spec. Issue Adv. Microb. Ferment. Process.* **2020**, *8*, 898. [CrossRef]
18. Miller, G.L. Use of dinitrosalicylic acid reagent for determination of reducing sugar. *Anal. Chem.* **1959**, *31*, 426–428. [CrossRef]
19. Chamsart, S. A Cell Lysis Reactor for the Production of Plasmid DNA from Recombinant *E. coli* for Gene Therapy. Ph.D. Thesis, School of Chemical Engineering, The University of Birmingham, Birmingham, UK, 2001.
20. Chamsart, S.; Patel, H.; Hanak, J.A.J.; Hitchcock, A.G.; Nienow, A.W. The impact of fluid-dynamic-generated stresses on chDNA stability during alkaline cell lysis for gene therapy. *Biotechnol. Bioeng.* **2001**, *75*, 387–392. [CrossRef] [PubMed]
21. Nienow, A.W. *Bioreactor and Bioprocess Fluid Dynamics (British Hydromechanics Research Group (REP))*, 1st ed.; Wiley: London, UK, 1997; ISBN 13-978-1860580901.
22. Rouf, A.; Kanojia, V.; Naik, H.R.; Naseer, B.; Qadri, T. An overview of microbial cell culture. *J. Pharmacogn. Phytochem.* **2017**, *6*, 1923–1928.
23. Diederichs, S.; Korona, A.; Staaden, A.; Kroutil, W.; Honda, K.; Ohtake, H.; Büchs, J. Phenotyping the quality of complex medium components by simple online-monitored shake flask experiments. *Microb. Cell Factories* **2014**, *13*, 149. [CrossRef]
24. Zhang, G.; Mills, D.A.; Block, D.E. Development of chemically defined media supporting high-cell-density growth of *Lactococci*, *Enterococci*, and *Streptococci*. *Appl. Environ. Microbiol.* **2009**, *75*, 1080–1087. [CrossRef]
25. Tripathi, N.K.; Sathyaseelan, K.; Jana, A.M.; Rao, P.V.L. High yield production of heterologous proteins with *Escherichia coli*. *Def. Sci. J.* **2009**, *59*, 137–146.
26. Mezule, L.; Delecka, B. Adjustment of yeast growth media for the fermentation of lignocellulosic sugar. *Chem. Eng. Trans.* **2017**, *57*, 25–30.

27. Charoensapharat, K.; Wechgama, K. Effect of initial cells, yeast extract, and sugar concentrations on ethanol production from molasses by thermotolerant yeast *Saccharomyces cerevisiae* RMU Y-10. *Asia Pac. J. Sci. Technol.* **2019**, *24*, 1–6.
28. Raj, E.A.; Kumar, S.H.S.; Kumar, S.U.; Misra, M.C.; Ghildyal, N.P.; Karanth, N.G. High-cell-density fermentation of recombinant *Saccharomyces cerevisiae* using glycerol. *Biotechnol. Prog.* **2002**, *18*, 1130–1132.
29. Turcotte, B.; Liang, X.B.; Robert, F.; Soontorngun, N. Transcriptional regulation of non-fermentable carbon utilization in budding yeast. *Fed. Eur. Microbiol. Soc.* **2010**, *10*, 2–13.
30. Daran, L.P.; Jansen, M.L.A.; Daran, J.M.; van Gulik, W.; de Winde, J.H.; Pronk, J.T. Role of transcriptional regulation in controlling fluxes in central carbon metabolism of *Saccharomyces cerevisiae*: A chemostat culture study. *J. Biol. Chem.* **2004**, *279*, 9125–9138. [CrossRef] [PubMed]
31. Trono, D. Recombinant enzymes in the food and pharmaceutical. *Ind. Adv. Enzym. Technol.* **2019**, *20*, 349–387.
32. Boos, W.; Shuman, H. Maltose and maltodextrin system of *Escherichia coli*: Transport, metabolism and regulation. *Microbiol. Mol. Biol. Rev.* **1998**, *62*, 204–229. [CrossRef]

processes

MDPI

Article

Morphological Differentiation of *Streptomyces clavuligerus* Exposed to Diverse Environmental Conditions and Its Relationship with Clavulanic Acid Biosynthesis

Jeferyd Yepes-García, Carlos Caicedo-Montoya, Laura Pinilla, León F. Toro and Rigoberto Ríos-Estepa *

Group of Bioprocesses, Chemical Engineering Department, University of Antioquia UdeA, Calle 70 No. 5221, Medellín 050010, Colombia; jeferyd.yepesg@udea.edu.co (J.Y.-G.); candres.caicedo@udea.edu.co (C.C.-M.); laura.pinilla@udea.edu.co (L.P.); lfelipe.toro@udea.edu.co (L.F.T.)

* Correspondence: rigoberto.rios@udea.edu.co

Received: 7 July 2020; Accepted: 28 July 2020; Published: 25 August 2020

Abstract: Clavulanic acid (CA) is a potent inhibitor of class A β-lactamase enzymes produced by *Streptomyces clavuligerus (S. clavuligerus)* as a defense mechanism. Due to its industrial interest, the process optimization is under continuous investigation. This work aimed at identifying the potential relationship that might exist between *S. clavuligerus* ATCC 27064 morphology and CA biosynthesis. For this, modified culture conditions such as source, size, and age of inoculum, culture media, and geometry of fermentation flasks were tested. We observed that high density spore suspensions (1×10^7 spores/mL) represent the best inoculum source for *S. clavuligerus* cell suspension culture. Further, we studied the life cycle of *S. clavuligerus* in liquid medium, using optic, confocal, and electron microscopy; results allowed us to observe a potential relationship that might exist between the accumulation of CA and the morphology of disperse hyphae. Reactor geometries that increase shear stress promote smaller pellets and a quick disintegration of these in dispersed secondary mycelia, which begins the pseudosporulation process, thus easing CA accumulation. These outcomes greatly contribute to improving the understanding of antibiotic biosynthesis in the *Streptomyces* genus.

Keywords: clavulanic acid; *Streptomyces clavuligerus*; cell morphology; shear stress

1. Introduction

Clavulanic acid (CA) is a potent inhibitor of beta-lactamase enzymes, produced by the filamentous gram (+) bacterium *Streptomyces clavuligerus* (*S. clavuligerus*). Due to its industrial interest, diverse optimization strategies have been developed so as to overcome production drawbacks and low titers [1–3].

During its cell cycle in solid media, the *Streptomyces* genus has the capacity to form vegetative and reproductive mycelium, similar to filamentous fungi, and to produce spores at the extreme of the reproductive mycelium, once it undergoes starvation [4]. In liquid medium, the presence of compartmentalized (primary) mycelium (MI) has been observed, from which the multinuclear (secondary) mycelium (MII) emerges, prior to the sporulation process [5–7]. Special attention has been placed on the likely relationship that might exist between product accumulation and cell morphology or lifecycle stage [8–10]; for example, the synthesis of prodigiosin and actinorhodin by *S. coelicolor* has been related to the appearance and formation of secondary mycelium (MII) [7]. Moreover, production of erythromycin by *S. erythraea* is favored by the presence of larger clumps of mycelium [8,11]. In contrast, virginiamycin, an antibiotic produced by *S. virginiae*, is apparently not related to cell morphology [9].

The relationship between morphology and secondary metabolism is complex, considering that mycelium differentiation is one of the factors that triggers secondary metabolism and antibiotic production [7,12,13]. For the case of the *Streptomyces* morphology, research has shown that the presence of mycelial grouping in the medium (pellets and clumps of primary and secondary mycelium) affects product biosynthesis [7,14–16]. Moreover, authors have reported on specific genes involved in the morphological differentiation that affects secondary metabolism, such as *adpA*, which is a regulatory gene immersed in the morphogenesis and spore formation pathway in *S. clavuligerus* [17].

Production of CA has been performed at the lab and industrial scales [18]. Previous studies were aimed at attaining larger CA titers by using complex media containing olive oil, isolated soy protein, soy flour, and sunflower oil [2,19–21]. Product biosynthesis is also affected by biomass concentration and its physiological state at the beginning of the cell suspension culture; hence, inoculum concentration impacts CA production [10,21]. According to Saudagar et al., during inoculum preparation, the presence of healthy and abundant metabolically active biomass (3–10% *v/v*) must be considered along with its morphological conditions, in an attempt to avoid a prolonged lag phase during cultivation [1].

Neves et al. observed an increase of 22% in CA titers when the age and percentage of inoculum (mycelia) was 24 h and 14% of the bioreactor volume, respectively [21]; in addition, CA production appears to be related to spore-based inoculum concentration [22]. Similar results were found for erythromycin biosynthesis: A 3.5-fold reduction in antibiotic production was observed when spore concentration was changed from 1×10^6 to 1×10^3 spores/mL, at the beginning of cultivation [8,11].

Oxygen supply is another important factor in *Streptomyces* cell suspension culture for secondary metabolite production [23]. Concentration of dissolved oxygen strongly depends on the reactor geometry and homogenization system. Marín-Palacio et al. found a 2.5-fold increase in *S. lividans* biomass production along with a recombinant protein synthesis, when cells were grown in baffled Erlenmeyer flasks instead of flasks equipped with helical springs. Baffled Erlenmeyer flasks provide a higher interfacial area between gas and liquid, and, consequently, larger mass transfer coefficients [16,24].

Although morphological differentiation and its association with secondary metabolite production has been studied in some *Streptomycetes* model organisms, e.g., *S. coelicolor* and *S. virginiae* [6,9], similar investigations have been scarcely undertaken in *S. clavuligerus;* most of these studies aimed at understanding the relationship that might exist between the life cycle and CA production at flask scale, using mutant strains and a proteomic analysis [15,17]. However, flask geometries and their effect on CA production by *S. clavuligerus* have not been explored. In this contribution, we expose cells of *S. clavuligerus* ATCC 27064 to different environmental conditions to cause high and low shear stress forces so as to induce varied morphological phenotypes; it is expected that the study of these phenotypes could provide insights into the potential relationships that might exist between diverse mechanical stress conditions, the developed morphological states, and CA biosynthesis.

2. Materials and Methods

2.1. Microorganism and Culture Media

S. clavuligerus ATCC 27064 was used throughout this work. To activate the strain, mycelium samples of 500 µL, previously stored in glycerol 40% (*v/v*) at −80 °C, were cultured on plates with TSA (Trypticase Soy Agar, Acumedia–Neogen®, Lansing, MI 48912, USA), during 48 h at 28 °C. After growth, plates were stored at 4 °C for a time interval smaller than 8 weeks.

A complex culture medium was used during all the experiments that included CA production and quantification, e.g., those described in Sections 2.3 and 2.5. The composition of the medium was as follows (in g/L): glycerol, 15; yeast extract, 1; malt extract, 10; K_2HPO_4, 2.5; isolated soy protein, 10; 3-(*N*-morpholino)propanesulfonic acid (MOPS), 21; $MgSO_4 \cdot 7H_2O$, 0.75; $FeSO_4 \cdot 7H_2O$, 0.001; $MnCl_2 \cdot 4H_2O$, 0.001; $ZnSO_4 \cdot 7H_2O$, 0.001. Likewise, a TSB preculture (Trypticase Soy Broth, Merck®, Darmstadt 64293, Germany), with 50 mL of broth at a concentration of 30 g/L, in a 250 mL baffled

Erlenmeyer, was performed prior to the experiments, detailed in Sections 2.3 and 2.5. Conditions of the preculture, such as inoculum source, inoculum size, and running time, were selected according to the assays proposed in Sections 2.2 and 2.3.

For spores stock preparation, glycerol-preserved cells were transferred and cultivated in the GYM (glucose, yeast extract, and malt extract [25]) medium at 30 °C. After 14 days of culture, spore suspensions were obtained as described by Ghojavand et al. [8], and maintained at –20 °C in 20% sterile glycerol. Spore counting was performed as described by Hopwood et al. [26]. The stock of mycelium used for experiments carried out in Section 2.2 was obtained from a colony from the glycerol-preserved stock of spores, inoculated into a 50 mL TSB medium (250 mL Erlenmeyer) and incubated for 36 h at 28 °C and 220 rpm (rotary agitator New Brunswick). Aliquots of 500 µL were then transferred to 1.5 mL Eppendorf tubes containing 500 µL of 40% (*v/v*) sterile glycerol solution and stored at –20 °C. Average biomass concentration was calculated as 5.5 ± 0.5 g/L, using the dry weight technique [2].

2.2. Inoculum Studies

S. clavuligerus inoculum sources were studied to identify differences in the associated culture growth rate and performance. For this, three different sources were explored: (i) spore suspension, (ii) mycelium stock, and (iii) 5-day old colonies, obtained from agar plates with the GYM medium (5 days is the time required by *S. clavuligerus* to develop primary mycelium on this medium). TSB (50 mL of broth at a concentration of 30 g/L, in a 250 mL baffled Erlenmeyer) was used as culture medium. Inoculation was as follows: (a) 500 µL spore suspension (1×10^3–1×10^7 spores/mL), (b) 1 mL of mycelium stock and (c) 25 mm^2 colonies growing on solid medium. All experiments were run by triplicates (80 h, 220 rpm, 28 °C, and pH 6.8).

Statistically significant differences in cell density, specific growth rate (μ), and doubling time (t_d) for the different treatment (inoculum sources) were analyzed through variance analysis (ANOVA) with a value significance threshold of 0.05 (Software R, R–3.2.2). A least significant difference (LSD) test was performed to differentiate among means, and superscripts a, b, c, and d were used to identify every group generated (the same letter on a different inoculum source means no significant differences between them, for either μ or t_d). The inoculum source with a larger μ and lower statistical variation was selected for further experiments.

2.3. Combined Effect of Age and Inoculum Concentration on Cell Growth and CA Production

A three-level full factorial design 3^2 was used to identify the effect of volume (*v/v*), and incubation time (h) on CA concentration (mg/L) (response variable). For each assay, baffled Erlenmeyer flasks were used with 50 mL of production medium (220 rpm, 28 °C). Culture conditions were set as follows: incubation time 36–72 h; inoculum percentage 2.5–7.5% (*v/v*). A statistical analysis (R version R–3.2.2) was performed using the response surface methodology (RSM) following a second order model:

$$\hat{y} = b_0 + \sum b_i x_i + \sum b_{ii} x_i^2 + \sum b_{ij} x_i x_j, \quad (1)$$

where $\hat{y}$ is CA production; x_i and x_j are the lineal or individual factors (incubation time and inoculum concentration); ${x_i}^2$ is the quadratic factors; and b_0, b_i, b_{ii}, and b_{ij} are the coefficients of each effect.

2.4. Cell Cycle and Morphology Changes in S. Clavuligerus

For *S. clavuligerus* cell cycle studies starting from spores, 500 µL of spores suspension (1×10^7 spores/mL) were inoculated into 50 mL of TSB medium (250 mL baffled Erlenmeyer) and incubated at 28 °C, pH 6.8, 220 rpm, during 120 h. Sampling (20 µL) was carried out every twelve hours, and cell morphology was also observed, even at nutritional stress conditions. Cell cycle dynamics was observed using an optical Motic® BA 310 microscope equipped with Moticam® 5MP (Kowloon Bay, Hong Kong, China), and Software Images Plus 2.0.

Conformation and pellet structure were analyzed using propidium iodide (PI) and fluorescein diacetate (FDA) as probes. For this, 1 mL of the medium was centrifuged (10,000 rpm, 10 min, 25 °C); the obtained pellet was suspended in 1 mL staining solution (Table 1). The processed samples were incubated in darkness (10 min) and centrifuged; isolated pellets were suspended in fresh culture medium and analyzed in an Olympus IX81 confocal microscope.

Table 1. Staining solution components and excitation/emission wave lengths for confocal microscopy.

Component/Probe	Concentration	Volume Added	Wavelength (Excitation)	Wavelength (Emission)
Culture medium	30 g/L	5 mL	-	-
PI *	5 mg/mL	10 µL	470 nm	520 nm
FDA **	20 mg/mL	20 µL	534 nm	618 nm

* PI stock solution was prepared by dissolving 20 mg of PI in 1 mL Phosphate-buffered saline (PBS) (stored at 4 °C).
** FDA stock solution was obtained by dissolving 5 mg of FDA in 1 mL acetone (stored at –20 °C).

Additionally, in order to study the relationship between CA production and cell morphology, biomass (pellets morphology), grown in the TSB seed medium, was inoculated in the chemically defined medium GSPA (Glycerol-Sucrose-Proline-Asparagine) and in the production (complex) culture medium (50 mL, pH 6.2, 220 rpm, baffled Erlenmeyer) [27]. Samples were taken starting at 72 h of fermentation to analyze morphology changes through optic microscopy and scanning electron microscopy (SEM).

SEM was used for morphological changes studies; this technique has been previously selected for detailing differences at the filament surface level, in diverse *Streptomyces* species [28]. For this, a 120 µL medium was fixed on a glass plaque and submerged on glutaraldehyde (2.5% *v/v*) for two hours. Then, plaques were washed with distilled water and dehydrated by immersion in ethanol solutions (59, 75, 90, and 100% *v/v*) during 15 min. Finally, samples were exposed to drying until the critical point was reached [29].

2.5. Effect of Mechanical Stress on Biomass Growth and CA Production

Mechanical stress was induced in three ways: (i) by a baffled Erlenmeyer (250 mL), (ii) by a helical spring (80/20 Nickel/Chrome, 0.5 cm external diameter) placed on the bottom of a standard Erlenmeyer (250 mL), and (iii) by 0.4 mm diameter glass beads submerged into a standard Erlenmeyer (250 mL). A standard smooth Erlenmeyer was used as a negative control (Figure 1).

Cell suspension cultures, previously grown in TSB, were run during 184 h (28 °C and 220 rpm) using the production (complex) culture medium; samples (1 mL) were taken daily, starting at the 72 h of culture, for CA and biomass quantification, and for image analysis through optical and SEM microscopes, as previously described. Statistically significant differences in biomass growth and CA biosynthesis were estimated, as described in Section 2.2 for inoculum studies.

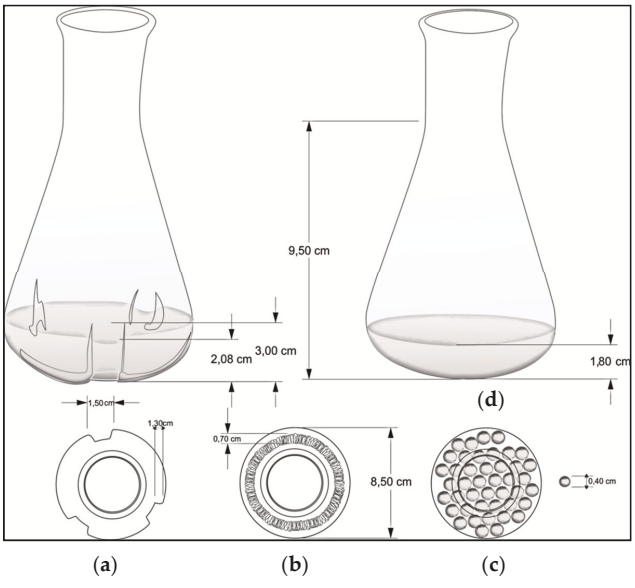

Figure 1. Flask geometries used to evaluate the mechanical stress effect on growth rate and clavulanic acid (CA) production: (**a**) baffled Erlenmeyer; (**b**) helical spring; (**c**) glass beads; and (**d**) smooth Erlenmeyer (control).

2.6. Analytical Techniques

Culture samples were centrifuged at 14,000 rpm for 10 min at 4 °C and filtered through a 0.22 µm membrane. CA was determined by High Performance Liquid Chromatography (HPLC) Agilent 1200 (Agilent Technologies, Waldbrom, Germany) equipped with a diode array detector (Agilent Technologies, Palo Alto, CA, USA) at 312 nm, using a reverse phase ZORBAX Eclipse XDB-C_{18} column (4.6 × 150 mm, 18 µm Agilent Technologies, Palo Alto, CA, USA). The mobile phase consisted of a KH_2PO_4 buffer (pH 3.2; 50 mM) and HPLC grade methanol with a flow rate of l mL/min. Likewise, the volume injection was 25 µL, and the running time was 10 min. Due to the fact that CA is poorly retained in C-18 columns, a derivative procedure described by Foulstone and Reading was followed, using imidazole at a ratio of 1:3; the reaction was kept at 30 °C for 30 min [30,31]. This method has been validated for linearity, LOD, and LLOQ (see Supplementary Material, Figure S1) as previously described by Anurag et al. [32].

For biomass quantification the dry cell weight method was used; 1 mL of cell culture was periodically taken and centrifuged at 10,000 rpm, rinsed, and later dried at 105 °C for 24 h [2].

For biomass quantification the dry cell weight method was used; 1 mL of cell culture was periodically taken and centrifuged at 10,000 rpm, rinsed, and later dried at 105 °C for 24 h [2].

3. Results and Discussion

3.1. Inoculum Studies

Inoculum size and age have been reported as important process parameters on which a significant part of the cultivation success lies. Many authors agree that the physiological and genetic state of the filamentous bacteria influences secondary metabolite production since the phase of formation of this kind of metabolites depends on the optimal growth during previous stages [8,10,21,22].

Figure 2 shows the dynamics of biomass production for all inoculum sources tested. For the case of mycelium and petri dish sources, a low reproducibility was observed; a particular case was

the difficulty to control cell morphological state and quantity, as well as the uncertainty of having a mycelium at the onset of cell death and/or fragmentation [21]. Further, mycelium from petri dishes was grown in a GYM solid medium, which could cause an extension of lag phase, after the transfer to the TSB medium. Under these circumstances, the microorganism required extra time to adapt its metabolic machinery to take advantage of the TSB nutrients.

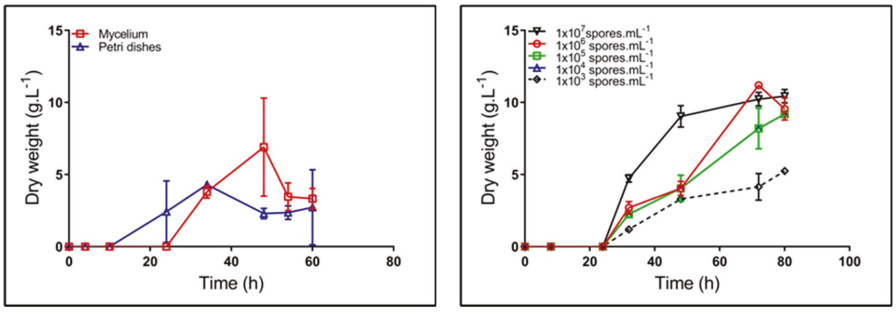

(**a**) (**b**)

Figure 2. Kinetics of biomass synthesis of *Streptomyces clavuligerus* grown in a Trypticase soy broth (TSB) medium, using different inoculum sources: (**a**) mycelium (square) and petri dishes (triangle); (**b**) spore suspensions at concentrations between 1×10^3 and 1×10^7 spores/mL.

The highest concentration of spore suspension shows high reproducibility for the different assays (std. dev. 0.1) (Figure 2), the largest formation rate, and the greatest biomass concentration (Table 2). Based on the ANOVA results (data not shown), the inoculum source has a significant effect on μ and t_d; the lower spore dilution showed the higher specific growth rate. Therefore, the spore suspension 10^7 spores/mL became the best alternative for starting cultures, which is in accordance with the results of Ghojavand et al., in *S. erythraea* [8].

Table 2. Kinetic parameters for *Streptomyces clavuligerus* cultivation according to different inoculum sources.

Inoculum Source	μ (1/h)	t_d (h)
Petri dishes	0.038 ^{ab}	19.17 ^{cd}
Mycelium	0.032 ^{abc}	23.12 ^{bcd}
1×10^7 spores/mL	0.041 ^{a}	16.86 ^{d}
1×10^6 spores/mL	0.030 ^{bcd}	23.18 ^{bcd}
1×10^5 spores/mL	0.029 ^{bcd}	23.64 ^{bc}
1×10^4 spores/mL	0.026 ^{cd}	27.02 ^{b}
1×10^3 spores/mL	0.020 ^{d}	33.89 ^{a}

Note: Superscripts a, b, c, and d indicate the groups generated through the least significant difference test (LSD). The same letter on different inoculum source means no significant differences among them, either for μ (specific growth rate) or t_d (doubling time).

Results from this work contrast those in which inoculum generation is carried out from stored mycelium under frozen conditions [10,21]. Apparently, the reactivated mycelium for starting fermentations, used by Neves et al. and Pinto et al., promotes the formation of secondary metabolites due to its high activity, despite its large variability (during the maximum CA production stages, the variability reached values close to 20%, at reactor scale [10,21]). For further cultivations, the spore suspension 1×10^7 spores/mL was used as the most favorable inoculum source; our results offered further support for the hypothesis that this condition provided uniform biomass generation.

3.2. Effect of Inoculum Age and Concentration on Cell Growth and CA Production

To establish the interactions between inoculum size and age on CA production, a factorial experimental design 3^2 was proposed (variables: size (*v*/*v*) and age of inoculums (h); response variable: CA concentration). Results allowed for fitting a second order model, wherein the factor accounting for the interaction between variables was not significant. In contrast, the quadratic factors did show significance on CA biosynthesis (p-value < 0.05) (see Supplementary Material, Table S1). Consequently, optimal values for larger CA production were estimated as 5.32% (*v*/*v*) for the inoculum size and 56.32 h for age, thus rendering about 29.73 ± 4.44 mg/L of CA. Further, both the coefficient of determination (r^2) and the adjusted-by-degree-of-freedom coefficient of determination ($r_a{}^2$) rendered evident the low predictability of the estimated model, which agrees with the variability of the maximum CA production during cultivations (central points for the experimental design) (see Supplementary Material, Table S1 and Figure S2). The large variability of the maximum CA titers agrees with the work of Neves et al., who observed a 20% variability (80–100 mg/L) [21]. Reducing such variation requires control and monitoring of cultivation variables, such as dissolved oxygen and CO_2 levels, inoculum and/or substrate concentration. Sánchez and Braña pointed out that the rapid activation of the CA biosynthetic pathway was favored by high inoculum cell density, in experiments using active spores [22]. In contrast, in this study, it was observed that increments in inoculum concentrations, above 5% (*v*/*v*), did not favor CA biosynthesis, which is consistent with other reports [1,22,33]. Accordingly, there must exist a regulatory mechanism that triggers biosynthetic pathways as a function of cell density. Thus, antibiotic production represents a response of bacteria population as a whole, and not a single property of each cell, which coincides with the nonessential nature of secondary metabolites, such as CA [22].

During inoculum preparation, cell density and age may also contribute to the premature onset of nutritional stress once the stationary phase is reached. Carbon, nitrogen, and/or phosphate deprivation renders a starving condition for the cell that may trigger the expression of genes related with programmed cell death, thus making it difficult to generate new cell material prior to cultivation using the production medium [34].

Neves et al. and Pinto et al. observed a 10% increment in CA production using stirred tank reactors, inoculated with cells at a late exponential phase (24 h) [10,21]. These authors used mycelium having a complete active enzymatic/metabolic machinery. In contrast, in this study, the need for obtaining larger preculture longevity was related with inoculum generation from nonactive *S. clavuligerus* spores. The lag/adaptation phase for spore growth increases prior to carbon, nitrogen, and/or phosphate catabolic activities for energy generation and cell constituents' formation. Nevertheless, from the experimental design, it was observed that the best conditions for inoculum formation were stablished at 54 h and 5% (*v*/*v*), starting from a spore suspension of 1×10^7 spores/mL.

3.3. Cell Cycle and Morphology Changes in Streptomyces Clavuligerus Cell Culture

In liquid medium, *S. clavuligerus* life cycle reaches an observable differentiation between primary and secondary mycelium, though without accomplishing complete sporulation (Figure 3) [4].

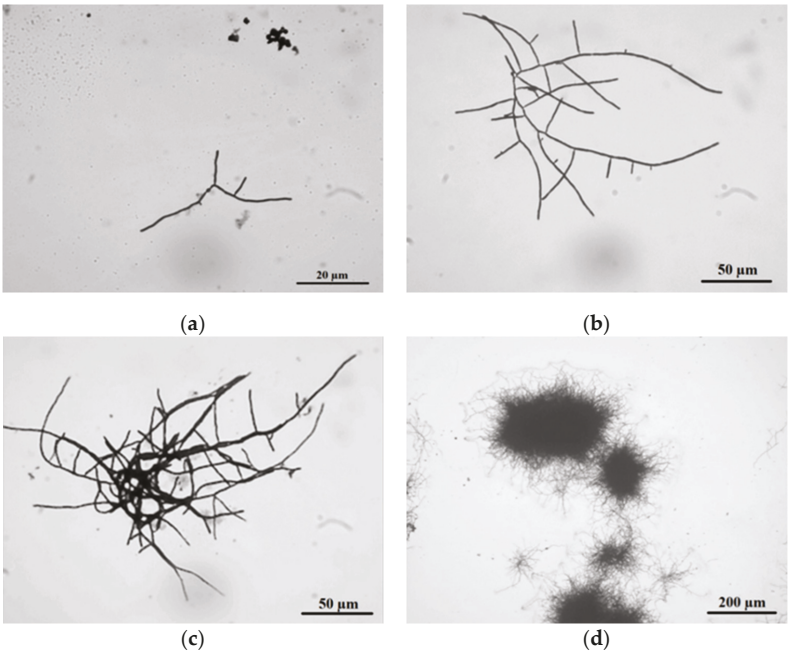

Figure 3. The life cycle of *Streptomyces clavuligerus* ATCC 27064 grown in TSB medium: (**a**) spore germination at 24 h; (**b**) branched hyphae at 28 h; (**c**) clump formation at 36 h; (**d**) pellet establishment at 45 h.

In TSB medium, at 24 h, the cell cycle started with spore germination followed by hyphae growing in apical and ramified forms (Figure 3a). These results match those observed in earlier studies where, prior to germination, three different stages were described using phase-contrast microscopy: First, darkening involved changes from bright to dark phase, followed by swelling, where spore diameter doubles its size, and changes in cell wall thickness were noticed, finally ending with the emergence of germ tubes [35].

Moreover, abundant hyphae ramification and apical growth were observed at 28 h of culture. According to Rioseras et al., these hyphae correspond to primary mycelium (MI), which exhibited compartments formed by single nucleus hyphae and divided by internal septa, and formed a right angle with the hyphae wall [7]. The observed MI thickness in *S. clavuligerus* was 2 ± 0.1 µm, comparable with those values reported for *S. coelicolor* [7].

At 36 h culture, MI clumps of about 600 µm diameter were observed (Figure 3c); this is an intermediate state prior to pellet formation [6]. After 45 h of culture, pellet formation occurs, reaching 700 µm of diameter (Figure 3d). Pellets are formed by two mycelium types: MI, which grows towards the pellet internal side since it was firstly developed, and secondary mycelium MII, localized towards the external part of the pellet. MII is apparently formed in a process similar to eukaryotic apoptosis where, under stress conditions, MI is dismantled and its components are reused for MII formation [4]. MII is a multinuclear mycelium; it does not possess compartments, and hyphae are composed of large multinuclear cells. MII thickness was about 0.6 ± 0.1 µm. Formerly, MII was known as vegetative mycelium in solid medium; it is a precursor of spore formation since it is further coated with a hydrophobic layer, thus rendering the aerial mycelium [7]. Species such as *S. venezuelae*, *S. griseus*, *S. antibioticus*, *S. chrysomallus*, *S. albidoflavus*, *S. brasiliensis*, *S. acrimycini*, and *S. albus*, have the capacity of forming the hydrophobic layer even in submerged fermentations. Nonetheless, there are no related reports for *S. clavuligerus* [1,33].

The confocal microscopy analysis of pellets allowed for identifying a structure within which the mycelium, in its most internal part, shows a compromised membrane. The PI probe (red) penetrates cells with altered cellular permeability (Figure 4a). In contrast, cells found in the pellet peripheral side show presence of the FDA probe (green), where only viable cells with intact membrane are able to metabolize the probe employing their enzymatic machinery [36]. Yagüe et al. studied this cellular conformation using the PI and SYTO9 probes [37]. The authors demonstrated the presence of two types of mycelium in the pellet structure. The cells at the pellet interior belong to primary mycelium, formed after spore germination, and are the nutrient source for secondary mycelium, which is observed in the pellet most external area [4,7,37]. This structure limits the nutrient transport towards MI, e.g., oxygen causing death and favoring MII formation, which is related to antibiotic production [6]. Pellet morphology is considered not appropriate for CA production in submerged cultures, since a larger proportion of MI is present [4,38]. The transition between MI and MII is characterized by a high genomic material degradation; although currently there is not known mechanisms involved in the regulation of apoptosis, the gene *ftsZ* (a gen required for cell division and establishment of MI) might participate in this transition, as it was reported in *S. coelicolor* [39].

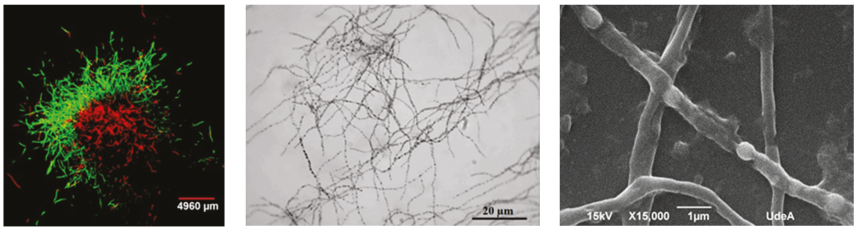

(**a**) (**b**) (**c**)

Figure 4. Observations of *Streptomyces clavuligerus* morphology: (**a**) Fluorescent staining of mycelia in TSB medium after 48 h of cultivation with FDA (green) and propidium iodide (red); (**b**) optical micrograph of mycelia at 120 h of culture in isolated soy protein based medium; (**c**) scanning electron microscopy of hyphae having separated compartments after 120 h of culture in isolated soy protein based medium.

Lastly, at 72 h culture, pellet disintegration was observed (see Supplementary Material, Figure S3) thus giving rise to disperse hyphae with no ramifications. Hyphae without branches showed septa that might suggest stages of programmed cell death. After 120 h cultivation, there was a biomass reduction, and the culture medium seemed more viscous. According to Kim and Kim, a layer of sticky extracellular polymers and insoluble substrates appears after pellet development, increasing medium viscosity, which is an indicator of appearance of the death phase [40].

Once pellets were transferred from TSB media, disperse nonramified MII hyphae were observed in GSPA and isolated soy protein media (120 h). Hyphae did show separated compartments because of subcompartmentalized sporulation guided by events of programmed cell dead; this pattern has been previously reported in *S. clavuligerus* by Pinilla et al. (Figure 4b) [41]. Further, membrane and cell wall residues, limiting hyphae (MII) formation, were evident (Figure 4c). This condition can be observed in *Streptomyces*, under starving conditions for which no sporulation in liquid media is present [14,42–46].

Morphological conditions at maximum CA production were analyzed for selected experiments. From this, Figure 4b,c display dispersed hyphae and subcompartmentalized sporulation (pseudo sporulation), which were continuously observed [39]. As a consequence, a relationship between the presence of disperse hyphae (MII) during pseudo sporulation and the cultivation time for the maximum CA production was established; under this condition, cells were exposed to a substrate deprivation condition for which genes involved in programmed cell death might be activated [7]. Some authors have found essential for antibiotic biosynthesis the presence of MII and the active expression of regulatory genes, e.g., *adpA*, and the genes related to amino acid and lipid metabolism [47,48]. In this

work, we did not analyze the expression of regulatory genes; however, the increase in the viscosity of the culture media due to protein (amino acids) catabolism, the emergence of intracellular compartments (programmed cell death), and the biosynthesis of CA (secondary metabolite) might indicate that genes such as *bldG*, *bldA*, and some Sigma factors were expressed, as suggested by Ferguson et al. [15]. Nevertheless, the pseudosporulation has not been correlated with secondary metabolite production as for CA.

It has been suggested there is no direct relationships between cell morphology and CA production in *S. clavuligerus* [10,49,50]. Notwithstanding, regulatory genes involved in morphological differentiation are also important for CA biosynthesis, e.g., *relA*, *adpA*, *bldA*, and some sigma factors [15,17,51]. Specifically, for the case of *adpA*, a gene related to regulation of sporulation and morphogenesis, López-García et al. demonstrated that the *adpA*-deleted mutant of *S. clavuligerus* decreased a 10% its CA accumulation, compared to the wild type [17]. These observations underpin those of Pinilla et al., who found that the gene *adpA* was highly expressed when *S. clavuligerus* was grown in a culture medium that favored CA production; late genes associated to CA biosynthesis, such as *ccaR* and *claR*, were also overexpressed [41]. The former scenario might indicate a connection between morphological differentiation and CA biosynthesis, suggesting a high protease activity, reported during programmed cell death [39,41]. Furthermore, the use of image analysis, assisted with fluorescent probes, has not been sufficient for identifying a potential relationship between morphology and CA production [10,52,53]. Interestingly, results from this work show that between 96–120 h of cultivation, pseudosporulation was present because of nutritional stress, which coincided with the time for maximum CA production. Conversely, Gómez-Ríos et al. pointed out that the prevalent form of mycelia during CA maximum productivity corresponds to a thinner and dispersed mycelium, which is favored by the continuous fragmentation and high shear forces presented in a stirred tank reactor [54]. Gómez-Ríos et al. ran their experiments in fed-batch cultivations using a chemically defined medium [54]. This kind of system completely changes the CA-production dynamics, shear stress, and nutrients transport, i.e., the peak for larger CA production, which was founded by Gómez-Ríos et al., was after 130 h of cultivation, while results from this work show that CA biosynthesis reached its maximum peak at 120 h of cultivation [54]. Therefore, further studies that involve gene expression analysis and morphology might be useful for deciphering the interaction between global and/or pathway regulatory genes and secondary metabolites biosynthesis.

3.4. The Effect of Mechanical Stress on Cell Growth and Product Biosynthesis

The effect of shear stress on cell growth, morphology, and secondary metabolism in the *Streptomyces* genus has been widely studied [1,55,56]. Authors have observed that the scale, culture medium composition, flask and/or reactor geometry, among others, are conditioning factors that somehow modulate the shear stress influence on CA accumulation [10,23,54,57].

The effect of mechanical stress on cell growth was studied using three geometries: baffled Erlenmeyer, Erlenmeyer with a helical spring on the bottom, Erlenmeyer with spherical beads; a smooth Erlenmeyer was used as a negative control. Figure 5 shows the maximum levels of CA and biomass concentration obtained from cultures using different geometries. As observed, geometries that, by some means, provide strong mechanical stress did favor CA biosynthesis, i.e., baffled geometries, spherical beads, and the use of a helical string. The presence of baffles provides the most favorable conditions for product biosynthesis. No difference in CA production was observed when Erlenmeyer with spherical beads and helical springs were used.

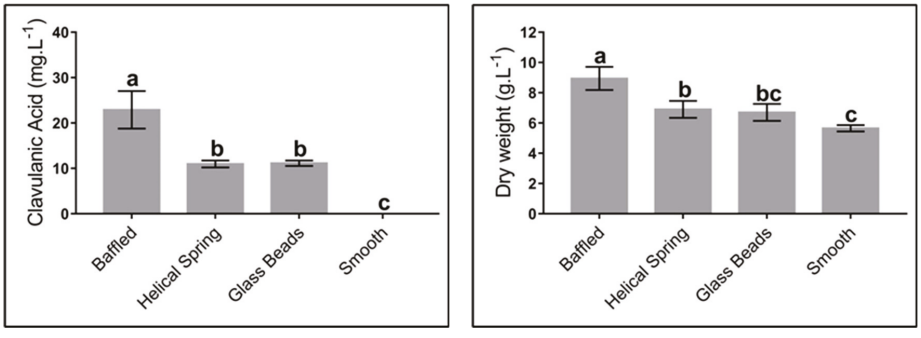

(**a**) (**b**)

Figure 5. Effect of different flask geometries on the maximum clavulanic acid (CA) and biomass concentration in *Streptomyces clavuligerus* cultivations, using the complex culture medium: (**a**) CA; (**b**) biomass. All experiments were carried out under similar conditions. Letters a, b, and c indicate the groups generated through the least significant difference test (LSD). The same letter above bars means no significant differences among sources of mechanical stress.

The absence of any form of mechanical stress significantly contributes to the loss of productivity. In the presence of baffles the liquid medium spreads all over the baffle surface, thus enhancing local velocity and energy dissipation and contributing with a better mixing and larger mass transfer [16,24,58]. The present study did consider neither monitoring nor control of dissolved oxygen in the culture medium; however, Li et al. showed that the presence of baffles in flasks rendered volumetric mass transfer coefficient (k_{La}) values as large as twice the value without baffles, no matter what the filling volume for the Erlenmeyer was [58]. In contrast, geometries that included the submerged helical spring or the spherical glass beads did not provide a beneficial environment for mass transfer, perhaps due to the lack of an appropriate mixing environment and low turbulence; for a defined agitation condition, both the spring and the beads follow the direction of the fluid and have the same velocity. Consequently, k_{La} values for flasks containing these geometries are lower than those for the baffled Erlenmeyer.

Our findings indicate that in smooth flasks no production of clavulanic acid was reached, while the concentration of this metabolite increased up to 20 mg/L when baffled flasks were used. These results are similar to those of Pinilla et al., who obtained 24 mg/L of CA using similar culture conditions [41]. Other authors have reached a production of CA up to 100 mg/L using either baffled Erlenmeyers or stirred tanks [20,55]. The low CA titers obtained in this work are associated with the different cultures media we used. Although these titters are moderate, they were high enough to be correlated (or not) to different shear stress sources and the associated diverse morphological responses.

Although we carried out all our experiments in Erlenmeyer flasks, we propose an extension of the present study to a laboratory bioreactor scale where culture conditions can be controlled. The presence of multiple devices and sensors allows for a faster shift of environmental conditions and, with them, the potential morphological changes that might exist during the *S. clavuligerus* life cycle. These changes would eventually be associated with shear stress and/or oxygen supply.

At the morphological level, the biosynthesis of metabolites, nonassociated to energy production in filamentous microorganisms, is greater with dispersed hyphae or smaller mycelia, when compared to pellet structure; this is caused by the mass transfer limitations inside the pellet [8,59]. For the case of baffled flasks, shear stress is considerably higher in contrast to smooth flasks [24,58]. There are differences between flow patterns and velocity fields; this causes a greater heterogeneity in turbulence intensity. Consequently, pellets in baffled flasks have a smaller diameter and show a faster disintegration and further formation at a higher proportion of dispersed secondary mycelia, which finally will favor the production of secondary metabolites, i.e., CA [16].

For the case of filamentous microorganisms, e.g., *S. lividans* and *S. clavuligerus*, oxygen is highly demanded for metabolite biosynthesis, not related with energy production [60,61]. During trophophase, cells proliferate at their maximum rate, giving rise to pellets as the predominant morphology; accordingly, diffusion of oxygen to the center of this morphology becomes limiting for secondary metabolite biosynthesis, e.g., CA [16,23,62]. Therefore, oxygen may become the substrate that limits production since some steps of the biosynthetic pathway of CA require oxygen, e.g., the reactions involving the clavaminate synthase enzyme [63]. Nevertheless, according to Gómez-Ríos et al., under conditions of high oxygen transfer (k_La values above 43 h^{-1}) in rocking-motion single-use bioreactors, CA biosynthesis may not be favored; in contrast, despite the damage caused on the mycelium by high values of shear stress (τ_{max} values above 1.4 Pa) when *S. clavuligerus* is cultivated in stirred tanks, shear stress seems to be necessary for triggering metabolic responses related with antibiotic production [54].

Commonly, promoting oxygen transfer through pellet morphology requires increasing the agitation rate and consequently increasing shear stress. Such a mechanical perturbation might induce a physiological response that ends up in cell wall and membrane disintegration, thereby triggering programmed cell death [50,64]. However, fragmentation caused by shear stress may lead to the formation of short hyphae capable of growing and reproducing, and thus producing antibiotics as long as some conditions are given in the stirred culture system; among others, a tip speed below 800 rpm, a carbon, phosphorus, and nitrogen availability, and a threshold value of dissolved oxygen between 20 and 80% during cultivation must be secured; the former condition is sufficiently provided by the baffled or even helical spring flasks used in this work [23,54,57].

Figure 6 shows the mycelium morphology as a response to the mechanical stress caused by different geometries; samples were taken after 72 h of cultivation for analysis under scanning electron microscopy. Micrographs show a strong affectation on the mycelial cell wall in experiments wherein baffled Erlenmeyer were used (Figure 6a), represented by a nonregular surface and lack of continuity of the filament which might indicate cell break. In contrast, in smooth Erlenmeyer (Figure 6d), mycelium appears continuous in its cell wall (nonbroken), which denotes cell integrity and viability. In the case of helical spring or glass beads (Figure 6b,c), cell damage does not seem evident, compared to smooth flasks, although it is possible to identify some slight discontinuity zones on the filament. Pinto et al., Roubos et al., and Belmar-Beiny and Thomas showed the high sensitivity of *S. clavuligerus* mycelium to different sources of mechanical stress, including agitation [10,49,50]. For *S. erythraea*, it has been shown that the predominance of the loosely grouping mycelium without specific shape—a clump structure—contributes to erythromycin biosynthesis, because of the favorable conditions for nutrients transport through filaments, as well as nystatin production (antifungal antibiotic). Jonsbu et al. reported that the increasing of pellet size over a critical value (not determined) discourages nystatin accumulation and cell growth, given the difficulty for metabolic activities at the center of the pellet [65].

The presence of secondary mycelium is indispensable for antibiotic production, when utilizing the *Streptomyces* species [5–7]. However, there is no consensus about a morphological nature that determines secondary metabolites accumulation. Such is the case of rapamycin (antibiotic) and avermectin (insecticide and pesticide) biosynthesis using *S. hygroscopicus* and *S. avermitilis*, respectively. Unlike this work, the authors found that pellet morphology promotes secondary metabolites excretion. In *S. hygroscopicus* and *S. avermitilis*, the growth of longer filaments and a high frequency of mycelia branching at the pellet periphery were present [66,67].

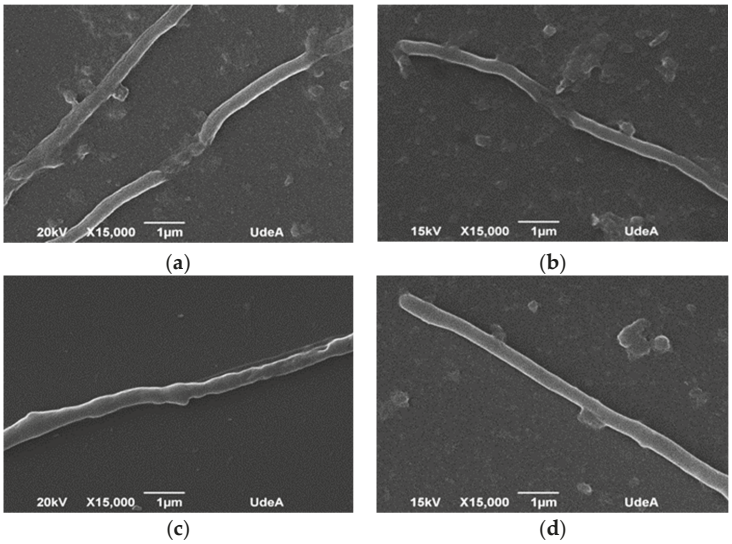

Figure 6. Scanning electron microscopy of *Streptomyces clavuligerus* at 72 h culture in: (**a**) baffled flask, (**b**) flask with helical spring on the bottom, (**c**) flasks with submerged glass beads, and (**d**) smooth flask.

4. Conclusions

This work aimed at identifying a potential relationship that might exist between *S. clavuligerus* ATCC 27064 morphology and CA biosynthesis. For this, modified culture conditions such as size and age of inoculum, and geometry of the fermentation flasks, were tested.

Primarily, the results provide clear evidence that high density spore suspensions (1×10^7 spores/mL) represent the best inoculum source for *S. clavuligerus* cell suspension culture. Under this condition, the highest specific growth rate and high reproducibility were attained, which is consistent with reports from other filamentous microorganisms, e.g., *S. erythraea* [8]. Inoculum concentration and age play an important role in CA biosynthesis. An inoculum equivalent to 5% as well as a 54 h incubation is recommended from the present research; in addition, this investigation suggests that 120 h of cultivation and a culture medium based on isolated soy protein are appropriate settings for CA biosynthesis.

Further, *S. clavuligerus* follows a cell cycle comparable to other *Streptomyces* species, such as *S. coelicolor* and *S. hygroscopicus* [13,66]. *S. clavuligerus* can reach the pellet conditions after going through the clump morphology. During its cell cycle, the cells form two mycelial types that differ in the order of synthesis, thickness, and relationship with CA biosynthesis. The pellet morphology presents a primary mycelium formation within the pellet and secondary mycelium in the periphery, similarly to *S. coelicolor* [7].

The study shows that as long as dispersed secondary mycelium of *S. clavuligerus* is in a pseudosporulation stage (hyphae with separated compartments), which is reached by programmed cell death and nutrient starvation [34,38,59], higher titers of CA are achieved; this phenomenon was observed in all experiments and was independent of flask geometry.

Although it is documented that *S. clavuligerus* is susceptible to shear stress generated by agitation and aeration [10,24,54,57], its response to different flask geometries, which characterizes the mechanical stress, has not been studied. In this work, differences regarding bacterial morphology and CA production were evident while using different mechanical stress sources. Baffled Erlenmeyer, helical springs, and circular glass beads did provide diverse mechanical stress conditions and favorable environmental conditions necessary for CA biosynthesis. The most suitable condition was the baffled

Erlenmeyer since it allows for better mixing conditions and an improved capacity for mass transfer; the above stems from *S. clavuligerus* having the ability to generate pellets, where diffusion of nutrients, e.g., oxygen, towards their core is critical for CA biosynthesis. Consequently, geometries that increase shear stress, e.g., baffled or coiled flasks, promote smaller pellets and a quick disintegration of these in dispersed secondary mycelia, which begins the pseudosporulation process, easing CA accumulation, as documented in the present work. These outcomes greatly contribute to improving the understanding of antibiotic biosynthesis in the *Streptomyces* species.

Supplementary Materials: The following are available online at http://www.mdpi.com/2227-9717/8/9/1038/s1, Figure S1: Calibration curve for quantification of clavulanic acid, Figure S2: Three-dimensional response surface plot showing the simultaneous effects of inoculum and size on CA concentration, Figure S3: Pellet disintegration of *Streptomyces clavuligerus* ATCC 27064 grown in TSB medium after 72 h of culture, Table S1. Analysis of variance applied to the regression model used for the clavulanic acid concentration.

Author Contributions: J.Y.-G.: conceived the study, designed, and performed all the experiments, and drafted the manuscript. C.C.-M., L.P. and L.F.T.: developed and executed statistical tests, and carried out image analysis for all the microscopies. R.R.-E.: supervised the research work, interpreted the results, corrected and wrote the manuscript, and serve as corresponding author. All authors have read and approved the final manuscript.

Funding: This work was supported by *Departamento Administrativo de Ciencia, Tecnología e Innovación–COLCIENCIAS*-Colombia (Grant Number 111566945929).

Acknowledgments: L.F.T and L.P. thank COLCIENCIAS-Colombia for scholarships.

Conflicts of Interest: The authors declare no conflict of interest regarding the publication of this paper.

References

1. Saudagar, P.S.; Survase, S.A.; Singhal, R.S. Clavulanic acid: A review. *Biotechnol. Adv.* **2008**, *26*, 335–351. [CrossRef] [PubMed]
2. Gouveia, E.R.; Baptista-Neto, A.; Azevedo, A.G.; Badino-jr, A.C.; Hokka, C.O. Improvement of clavulanic acid production by *Streptomyces clavuligerus* in medium containing soybean derivatives. *Microbiol. Biotechnol.* **1999**, *15*, 623–627. [CrossRef]
3. Higgens, C.E.; Kastner, R.E. *Streptomyces clavuligerus* sp. nov., a β-lactam antibiotic producer. *Syst. Bacteriol.* **1971**, *21*, 326–331. [CrossRef]
4. Manteca, A.; Sanchez, J. Streptomyces developmental cycle and secondary metabolite production. In *Current Research, Technology and Education Topics in Applied Microbiology and Microbial Biotechnology*, 1st ed.; Méndez-Vilas, A., Ed.; FORMATEX: Bajadoz, Spain, 2010; Volume 2, pp. 560–566, ISBN 978-84-614-6195-0.
5. Yagüe, P.; Rodríguez-García, A.; López-García, M.T.; Martín, J.F.; Rioseras, B.; Sánchez, J.; Manteca, Á. Transcriptomic analysis of *Streptomyces coelicolor* differentiation in solid sporulating cultures: First compartmentalized and second multinucleated mycelia have different and distinctive transcriptomes. *PLoS ONE* **2013**, *8*, 1–14. [CrossRef] [PubMed]
6. Manteca, A.; Sánchez, J.; Jung, H.R.; Schwämmle, V.; Jensen, O.N. Quantitative proteomics analysis of *Streptomyces coelicolor* development demonstrates that onset of secondary metabolism coincides with hypha differentiation. *Mol. Cell. Proteom.* **2010**, *9*, 1423–1436. [CrossRef] [PubMed]
7. Rioseras, B.; López-García, M.T.; Yagüe, P.; Sánchez, J.; Manteca, Á. Mycelium differentiation and development of *Streptomyces coelicolor* in lab-scale bioreactors: Programmed cell death, differentiation, and lysis are closely linked to undecylprodigiosin and actinorhodin production. *Bioresour. Technol.* **2014**, *151*, 191–198. [CrossRef]
8. Ghojavand, H.; Bonakdarpour, B.; Heydarian, S.M.; Hamedi, J. The inter-relationship between inoculum concentration, morphology, rheology and erythromycin productivity in submerged cultivation of *Saccharopolyspora erythraea*. *Braz. J. Chem. Eng.* **2011**, *28*, 564–574. [CrossRef]
9. Yang, Y.K.; Morikawa, M.; Shimizu, H.; Shioya, S.; Suga, K.I.; Nihira, T.; Yamada, Y. Image analysis of mycelial morphology in virginiamycin production by batch culture of *Streptomyces virginiae*. *J. Ferment. Bioeng.* **1996**, *81*, 7–12. [CrossRef]
10. Pinto, L.S.; Vieira, L.M.; Pons, M.N.; Fonseca, M.M.R.; Menezes, J.C. Morphology and viability analysis of *Streptomyces clavuligerus* in industrial cultivation systems. *Bioprocess Biosyst. Eng.* **2004**, *26*, 177–184. [CrossRef]

11. Stocks, S.M.; Thomas, C.R. Viability, strength, and fragmentation of *Saccharopolyspora erythraea* in submerged fermentation. *Biotechnol. Bioeng.* **2001**, *75*, 702–709. [CrossRef]
12. Manteca, Á.; Fernandez, M.; Sanchez, J. Mycelium development in *Streptomyces antibioticus* ATCC 11891 occurs in an orderly pattern which determines multiphase growth curves. *BMC Microbiol.* **2005**, *5*, 1–11. [CrossRef] [PubMed]
13. Manteca, A.; Alvarez, R.; Salazar, N.; Yagüe, P.; Sanchez, J. Mycelium differentiation and antibiotic production in submerged cultures of *Streptomyces coelicolor*. *Appl. Environ. Microbiol.* **2008**, *74*, 3877–3886. [CrossRef] [PubMed]
14. Kim, J.; Hancock, I.C. Pellet forming and fragmentation in liquid culture of *Streptomyces griseus*. *Biotechnol. Lett.* **2000**, *22*, 189–192. [CrossRef]
15. Ferguson, N.L.; Peña-Castillo, L.; Moore, M.A.; Bignell, D.R.D.; Tahlan, K. Proteomics analysis of global regulatory cascades involved in clavulanic acid production and morphological development in *Streptomyces clavuligerus*. *J. Ind. Microbiol. Biotechnol.* **2016**, *43*, 537–555. [CrossRef] [PubMed]
16. Marín-Palacio, L.D.; Gamboa-Suasnavart, R.A.; Valdez-Cruz, N.A.; Servín-González, L.; Córdova-Aguilar, M.S.; Soto, E.; Klöckner, W.; Büchs, J.; Trujillo-Roldán, M.A. The role of volumetric power input in the growth, morphology, and production of a recombinant glycoprotein by *Streptomyces lividans* in shake flasks. *Biochem. Eng. J.* **2014**, *90*, 224–233. [CrossRef]
17. López-García, M.T.; Santamarta, I.; Liras, P. Morphological differentiation and clavulanic acid formation are affected in a *Streptomyces clavuligerus adpA*-deleted mutant. *Microbiol* **2010**, *156*, 2354–2365. [CrossRef]
18. Cho, H.S.; Jo, J.C.; Shin, C.H.; Lee, N.; Choi, J.S.; Cho, B.K.; Roe, J.H.; Kim, C.W.; Kwon, H.J.; Yoon, Y.J. Improved production of clavulanic acid by reverse engineering and overexpression of the regulatory genes in an industrial *Streptomyces clavuligerus* strain. *J. Ind. Microbiol. Biotechnol.* **2019**, *46*, 1205–1215. [CrossRef]
19. Salem-Bekhit, M.M.; Alanazi, F.K.; Alsarra, I.A. Improvement and enhancement of clavulanic acid production in *Streptomyces clavuligerus* using vegetable oils. *Afr. J. Biotechnol.* **2010**, *9*, 6806–6812.
20. Maranesi, G.L.; Baptista-Neto, A.; Hokka, C.O.; Badino, A.C. Utilization of vegetable oil in the production of clavulanic acid by *Streptomyces clavuligerus* ATCC 27064. *World J. Microbiol. Biotechnol.* **2005**, *21*, 509–514. [CrossRef]
21. Neves, A.A.; Vieira, L.M.; Menezes, J.C. Effects of preculture variability on clavulanic acid fermentation. *Biotechnol. Bioeng.* **2001**, *72*, 628–633. [CrossRef]
22. Sánchez, L.; Braña, A.F. Cell density influences antibiotic biosynthesis in *Streptomyces clavuligerus*. *Microbiology* **1996**, *142*, 1209–1220. [CrossRef] [PubMed]
23. Rosa, J.C.; Neto, A.B.; Hokka, C.O.; Badino, A.C. Influence of dissolved oxygen and shear conditions on clavulanic acid production by *Streptomyces clavuligerus*. *Bioprocess Biosyst. Eng.* **2005**, *27*, 99–104. [CrossRef] [PubMed]
24. Peter, C.P.; Suzuki, Y.; Rachinskiy, K.; Lotter, S.; Büchs, J. Volumetric power consumption in baffled shake flasks. *Chem. Eng. Sci.* **2006**, *61*, 3771–3779. [CrossRef]
25. Manteca, A.; Ye, J.; Sánchez, J.; Jensen, O.N. Phosphoproteome analysis of *Streptomyces* development reveals extensive protein phosphorylation accompanying bacterial differentiation. *J. Proteome Res.* **2011**, *10*, 5481–5492. [CrossRef]
26. Hopwood, D.A.; Bibb, M.J.; Chater, K.F.; Kieser, T.; Bruton, C.J.; Kieser, H.M.; Lydiate, D.J.; Smith, C.P.; Ward, J.M.; Schrempf, H. *Genetic Manipulation of Streptomyces: A Laboratory Manual*, 1st ed.; The John Innes Foundation: Norwich, UK, 1985; pp. 1–356, ISBN 0-7084-0036-0.
27. Romero, J.; Liras, P.; Martín, J.F. Utilization of ornithine and arginine as specific precursors of clavulanic acid. *Appl. Environ. Biotechnol.* **1986**, *52*, 892–897. [CrossRef]
28. Kofroňová, O.; Nguyen, L.D.; Weiser, J.; Benada, O. *Streptomycetes* cultured on glass beads: Sample preparation for SEM. *Microsc. Res. Tech.* **2002**, *58*, 111–113. [CrossRef]
29. Bray, D. Critical point drying of biological specimens for scanning electron microscopy. In *Methods in Biotechnology: Supercritical Fluid Methods and Protocols*, 1st ed.; Williams, J.R., Clifford, A.A., Eds.; Humana Press: Totowa, NJ, USA, 2000; Volume 13, pp. 235–243, ISBN 978-0-89603-571-3.
30. Foulstone, M.; Reading, C. Assay of amoxicillin and clavulanic acid, the components of augmentin, in biological fluids with high-performance liquid chromatography. *Antimicrob. Agents Chemother.* **1982**, *22*, 753–762. [CrossRef]

31. Ramirez-Malule, H.; Junne, S.; López, C.; Zapata, J.; Sáez, A.; Neubauer, P. An improved HPLC-DAD method for clavulanic acid quantification in fermentation broths of *Streptomyces clavuligerus*. *J. Pharm. Biomed. Anal.* **2016**, *120*, 241–247. [CrossRef]
32. Anurag, M.; Gurumurthy, M.; Mishra, A.; Shukla, R. Development and method validation on stress degradation studies of cefpodoxime proxetil and clavulanic acid in dosage form by HPLC method. *Der Pharma. Lett.* **2015**, *7*, 81–92.
33. Ser, H.L.; Law, J.W.F.; Chaiyakunapruk, N.; Jacob, S.A.; Palanisamy, U.D.; Chan, K.G.; Goh, B.H.; Lee, L.H. Fermentation conditions that affect clavulanic acid production in *Streptomyces clavuligerus*: A systematic review. *Front. Microbiol.* **2016**, *7*, 522. [CrossRef]
34. Yagüe, P.; López-García, M.T.; Rioseras, B.; Sánchez, J.; Manteca, Á. Pre–sporulation stages of *Streptomyces* differentiation: State-of-the-art and future perspectives. *FEMS Microbiol. Lett.* **2013**, *342*, 79–88. [CrossRef] [PubMed]
35. Elliot, M.A.; Flärdh, K. *Streptomycete Spores*; John Wiley and Sons Ltd.: Hoboken, NJ, USA, 2012; pp. 1–9.
36. Fontvieille, D.A.; Outaguerouine, A.; Thevenot, D.R. Fluorescein diacetate hydrolysis as a measure of microbial activity in aquatic systems: Application to activated sludges. *Environ. Technol.* **1992**, *13*, 531–540. [CrossRef]
37. Yagüe, P.; Rodríguez–García, A.; López–García, M.T.; Rioseras, B.; Martín, J.F.; Sánchez, J. Transcriptomic analysis of liquid non-sporulating *Streptomyces coelicolor* cultures demonstrates the existence of a complex differentiation comparable to that occurring in solid sporulating cultures. *PLoS ONE* **2014**, *9*, 1–13. [CrossRef] [PubMed]
38. Yagüe, P.; Rioseras, B.; Sanchez, J.; Manteca, A. New insights on the development of *Streptomyces* and their relationships with secondary metabolite production. *Curr. Trends Microbiol.* **2012**, *8*, 65–73.
39. Yagüe, P.; Willemse, J.; Koning, R.I.; Rioseras, B.; López-García, M.T.; Gonzalez-Quiñonez, N.; Lopez-Iglesias, C.; Shliaha, P.V.; Rogowska-Wrzesinska, A.; Koster, A.J.; et al. Subcompartmentalization by cross-membranes during early growth of *Streptomyces* hyphae. *Nat. Commun.* **2016**, *7*, 1–11. [CrossRef]
40. Kim, Y.M.; Kim, J.H. Formation and dispersion of mycelial pellets of *Streptomyces coelicolor* A3(2). *J. Microbiol.* **2004**, *42*, 64–67.
41. Pinilla, L.; Toro, L.F.; Laing, E.; Alzate, J.F.; Ríos-Estepa, R. Comparative transcriptome analysis of *Streptomyces clavuligerus* in response to favorable and restrictive nutritional conditions. *Antibiotics* **2019**, *8*, 96. [CrossRef]
42. Kendrickt, K.E.; Ensign, J.C. Sporulation of *Streptomyces griseus* in submerged culture. *J. Bacteriol.* **1983**, *155*, 357–366. [CrossRef]
43. Glazebrook, M.A.; Doull, J.L.; Stuttard, C.; Vining, L.C. Sporulation of *Streptomyces Venezuelae* in submerged cultures. *J. Gen. Microbiol.* **1990**, *136*, 581–588. [CrossRef]
44. Gottlieb, D.; Legator, M. The growth and metabolic behavior of *Streptomyces Venezuelae* in liquid culture. *Mycol. Soc. Am.* **1953**, *45*, 507–515. [CrossRef]
45. Bradley, S.G.; Ritzi, D. Composition and ultrastructure of *Streptomyces Venezuelae*. *J. Bacteriol.* **1968**, *95*, 2358–2364. [CrossRef] [PubMed]
46. Hobbs, G.; Frazer, C.M.; Gardner, D.C.J.; Cullum, J.A.; Oliver, S.G. Dispersed growth of *Streptomyces* in liquid culture. *Appl. Microbiol. Biotechnol.* **1989**, *31*, 272–277. [CrossRef]
47. Manteca, A.; Jung, H.R.; Schwaömmle, V.; Jensen, O.N.; Sanchez, J. Quantitative proteome analysis of *Streptomyces coelicolor* nonsporulating liquid cultures demonstrates a complex differentiation process comparable to that occurring in sporulating solid cultures. *J. Proteome Res.* **2010**, *9*, 4801–4811. [CrossRef] [PubMed]
48. Beites, T.; Oliveira, P.; Rioseras, B.; Pires, S.D.S.; Oliveira, R.; Tamagnini, P.; Moradas-Ferreira, P.; Manteca, Á.; Mendes, M.V. Streptomyces natalensis programmed cell death and morphological differentiation are dependent on oxidative stress. *Sci. Rep.* **2015**, *5*, 1–15.
49. Belmar-Beiny, M.T.; Thomas, C.R. Morphology and clavulanic acid production of *Streptomyces clavuligerus*: Effect of stirrer speed in batch fermentations. *Biotechnol. Bioeng.* **1990**, *37*, 456–462. [CrossRef]
50. Roubos, J.A.; Krabben, P.; Luiten, R.G.M.; Verbruggen, H.B.; Heijnen, J.J. A quantitative approach to characterizing cell lysis caused by mechanical agitation of *Streptomyces clavuligerus*. *Biotechnol. Prog.* **2001**, *17*, 336–347. [CrossRef]
51. Ryu, Y.G.; Jin, W.; Kim, J.Y.; Kim, J.Y.; Lee, S.H.; Lee, K.J. Stringent factor regulates antibiotics production and morphological differentiation of *Streptomyces clavuligerus*. *J. Microbiol. Biotechnol.* **2004**, *14*, 1170–1175.

52. Sebastine, I.M.; Stocks, S.M.; Cox, P.W.; Thomas, C.R. Characterisation of percentage viability of *Streptomyces clavuligerus* using image analysis. *Biotechnol. Tech.* **1999**, *13*, 419–423. [CrossRef]
53. Nurmohamadi, M.; Pourghassem, H. Clavulanic acid production estimation based on color and structural features of *Streptomyces clavuligerus* bacteria using self-organizing map and genetic algorithm. *Comput. Methods Programs Biomed.* **2014**, *114*, 337–348. [CrossRef]
54. Gómez-Ríos, D.; Junne, S.; Neubauer, P.; Ochoa, S.; Ríos-Estepa, R.; Ramírez-Malule, H. Characterization of the metabolic response of *Streptomyces clavuligerus* to shear stress in stirred tanks and single-use 2D rocking motion bioreactors for clavulanic acid production. *Antibiotics* **2019**, *8*, 168. [CrossRef]
55. Neto, A.B.; Hirata, D.B.; Cassiano Filho, L.C.M.; Bellão, C.; Júnior, A.C.B.; Hokka, C.O. A study on clavulanic acid production by *Streptomyces clavuligerus* in batch, fed-batch and continuous processes. *Braz. J. Chem. Eng.* **2005**, *22*, 557–563. [CrossRef]
56. Sánchez Pérez, J.A.; Rodríguez Porcel, E.M.; Casas López, J.L.; Fernández Sevilla, J.M.; Chisti, Y. Shear rate in stirred tank and bubble column bioreactors. *Chem. Eng. J.* **2006**, *124*, 1–5. [CrossRef]
57. Cerri, M.O.; Badino, A.C. Shear conditions in clavulanic acid production by *Streptomyces clavuligerus* in stirred tank and airlift bioreactors. *Bioprocess Biosyst. Eng.* **2012**, *35*, 977–984. [CrossRef]
58. Li, C.; Xia, J.Y.; Chu, J.; Wang, Y.H.; Zhuang, Y.P.; Zhang, S.L. CFD analysis of the turbulent flow in baffled shake flasks. *Biochem. Eng. J.* **2012**, *70*, 140–150. [CrossRef]
59. Gamboa-Suasnavart, R.A.; Valdez-Cruz, N.A.; Cordova-Dávalos, L.E.; Martínez-Sotelo, J.A.; Servín-González, L.; Espitia, C.; Trujillo-Roldán, M.A. The O-mannosylation and production of recombinant APA (45/47 KDa) protein from *Mycobacterium tuberculosis* in *Streptomyces lividans* is affected by culture conditions in shake flasks. *Microb. Cell Fact.* **2011**, *10*, 1–11. [CrossRef] [PubMed]
60. Zacchetti, B.; Smits, P.; Claessen, D. Dynamics of pellet fragmentation and aggregation in liquid-grown cultures of *Streptomyces lividans*. *Front. Microbiol.* **2018**, *9*, 1–10. [CrossRef]
61. Gamboa-Suasnavart, R.A.; Valdez-Cruz, N.A.; Gaytan-Ortega, G.; Reynoso-Cereceda, G.I.; Cabrera-Santos, D.; López-Griego, L.; Klöckner, W.; Büchs, J.; Trujillo-Roldán, M.A. The metabolic switch can be activated in a recombinant strain of *Streptomyces lividans* by a low oxygen transfer rate in shake flasks. *Microb. Cell Fact.* **2018**, *17*, 1–12. [CrossRef]
62. Yegneswaran, P.K.; Gray, M.R.; Thompson, B.G. Effect of dissolved oxygen control on growth and antibiotic production in *Streptomyces clavuligerus* fermentations. *Biotechnol. Prog.* **1991**, *7*, 246–250. [CrossRef]
63. Martínez-Burgo, Y.; Álvarez-Álvarez, R.; Rodríguez-García, A.; Liras, P. The pathway specific–regulator *ClaR* of *Streptomyces clavuligerus* has a global effect on the expression of genes for secondary metabolism and differentiation. *Appl. Environ. Microbiol.* **2015**, *81*, 6637–6648. [CrossRef]
64. Olmos, E.; Mehmood, N.; Haj Husein, L.; Goergen, J.L.; Fick, M.; Delaunay, S. Effects of bioreactor hydrodynamics on the physiology of *Streptomyces*. *Bioprocess Biosyst. Eng.* **2013**, *36*, 259–272. [CrossRef]
65. Jonsbu, E.; McIntyre, M.; Nielsen, J. The influence of carbon sources and morphology on nystatin production by *Streptomyces noursei*. *J. Biotechnol.* **2002**, *95*, 133–144. [CrossRef]
66. Qi, H.; Zhao, S.; Fu, H.; Wen, J.; Jia, X. Coupled cell morphology investigation and metabolomics analysis improves rapamycin production in *Streptomyces hygroscopicus*. *Biochem. Eng. J.* **2014**, *91*, 186–195. [CrossRef]
67. Yin, P.; Wang, Y.H.; Zhang, S.L.; Chu, J.; Zhuang, Y.P.; Chen, N.; Li, X.F.; Wu, Y.B. Effect of mycelial morphology on bioreactor performance and avermectin production of *Streptomyces avermitilis* in submerged cultivations. *J. Chin. Inst. Chem. Eng.* **2008**, *39*, 609–615. [CrossRef]

processes

MDPI

Article

Influence of Different Smoking Procedures on Polycyclic Aromatic Hydrocarbons Formation in Traditional Dry Sausage *Hercegovačka kobasica*

Krešimir Mastanjević [1,*], Brankica Kartalović [2], Leona Puljić [3], Dragan Kovačević [1] and Kristina Habschied [1]

[1] Faculty of Food Technology Osijek, Josip Juraj Strossmayer University of Osijek, F. Kuhača 20, 31000 Osijek, Croatia; dragan.kovacevic@ptfos.hr (D.K.); kristinahabschied@gmail.com (K.H.)
[2] Scientific Veterinary Institute Novi Sad, Rumenački put 20, 21000 Novi Sad, Serbia; brankica@niv.ns.ac.rs
[3] The Faculty of Agriculture and Food Technology (APTF), University of Mostar, Biskupa Čule bb, 88000 Mostar, Bosnia and Herzegovina; leonapuljic224@gmail.com
* Correspondence: kmastanj@ptfos.hr; Tel.: +385-31-224-300

Received: 1 July 2020; Accepted: 24 July 2020; Published: 2 August 2020

Abstract: The concentrations of 16 polycyclic aromatic hydrocarbons (PAH) in smoked dry sausage *Hercegovačka kobasica* were investigated. The sausages were stuffed in two different casings (collagen and natural) and smoked in traditional and industrial smokehouses. The highest concentration of PAH 16 were detected in sausages in natural casings smoked in the traditional manner. The samples smoked in the industrial chamber stuffed in collagen casing showed the lowest PAH 16 content. The content of PAH 4 in sausage smoked in the traditional way and stuffed in natural casing averaged 24.46 μg/kg, which is more the double of maximum prescribed concentration of 12 μg/kg. The concentration of cancerogenic benzo[a]pyrene averaged 7.79 μg/kg in sausage stuffed in natural casing and smoked in the traditional way, which is almost four times the legislative prescribed values (2 μg/kg). Sausage smoked in the traditional manner and stuffed in collagen casing showed lower values for PAH 4 (13.88 μg/kg) and benzo[a]pyrene (4.97 μg/kg), but these values were also above the legislative prescribed values.

Keywords: smoking with open fire; PAH; industrial smoking

1. Introduction

Hercegovačka kobasica is a dry sausage produced in Herzegovina, a part of Bosnia and Herzegovina. It is a pork meat product with paprika, hot paprika, and garlic added as spices, stuffed traditionally into pig colon. Today's consumers want to return to the original and traditional products that are produced by small, family businesses and usually sold at the city markets. The specific taste and aroma are a result of the traditional production that includes smoking with an open fire. This can, however, lead to the formation of potential polycyclic aromatic hydrocarbon (PAH) accumulation [1–3]. This process is conditioned by the duration of smoking, temperature of wood combustion, type of wood, moisture of wood, and casing type [4–7]. Wood combustion results with different volatiles that end up in the air and can accumulate in the smoked meat products. The smoking process serves as one of the food preservation methods and includes the penetration of volatile compounds through the casing (natural or collagen) into the stuffing. This results in meat products with a characteristic aroma, color, and taste, which are very appealing to the consumers [8]. Incomplete wood combustion usually results in the formation of different PAHs, some of which are denoted as hazardous to human health when found in food. PAHs contain one or more condensed benzene rings, while some display carcinogenic and mutagenic properties [9–11].

PAHs are soluble in organic solvents, solids at room temperature, and lipophilic. This is why they can be found in meat and meat products which have been exposed to smoking [12].

The US Environmental Protection Agency (EPA) designated 16 polycyclic aromatic hydrocarbons [naphthalene (NA), acenaphthylene (ACL), acenaphthene (AC), fluorene (FL), anthracene (AN), phenanthrene (PHE), fluoranthene (FA), benz[a]anthracene (BaA), pyrene (PY), chrysene (CHR), benzo[b]fluoranthene (BbFA), benzo[k]fluoranthene (BkFA), benzo[a]pyrene (BaP), dibenz[a,h]anthracene (DBahA), benzo[ghi]perylene (BghiP) and indeno[1,2,3-cd]pyrene (IP)] (PAH16) as priority environmental pollutant [13]. As a reference for the determination of PAHs in food, the European Food Safety Authority (EFSA) concluded that the concentrations of BaP, as well as the sum of the concentrations of four PAHs BaP, BaA, BbFA, and CHR (PAH4) [14], would show the practical value of food safety. European legislation (European Commission (EU) Regulation no. 835/2011 [15] allows the 2 μg/kg as the maximum permissible concentration of BaP in meat products; the sum PAH4 concentrations should not exceed 12 μg/kg. Bosnia and Herzegovina's legislation leans toward these values [16].

The sausage were produced from pig meat, pig fat, red hot paprika powder, red sweet paprika powder, and garlic stuffed into natural (pig colon) and artificial (collagen) casings. The intention of this paper was to examine the effect of industrial and traditional smoking procedure and to compare the effect of casing on PAH concentrations in *Hercegovačka kobasica*.

2. Materials and Methods

2.1. Samples Production and Preparation

Traditional recipe was used for sausage manufacturing. *Hercegovačka kobasica* was produced from pork meat (75%) and pork fat (25%). The meat and fat is then ground through a grinding plate with holes of 6 to 8 mm in diameter. The ground meat and pork fat is then mixed with salt in the amount of 2%, red paprika in the amount of 1%, hot paprika in the amount of 0.7%, and garlic in the amount of 0.2%. The stuffing is then stuffed into a natural casing (pig's colon) or a collagen casing (500 mm long; 50 mm in diameter). The two groups were then further divided and subjected to two types of smoking.

The traditional smoking lasted for 30 days. Smoking was scheduled for 2–3 h every day for the first 6 days and every other day for the next 24 days. The sausages were hung three meters from the open fire. The combustion of dry hard wood (beech, hornbeam, and oak) and its sawdust was used to generate smoke. The conditions of production (temperature and relative humidity) were not controlled, but influenced by the atmospheric conditions. The temperature ranged from 3.5 to 11.2 °C (average 6.9 °C) and relative humidity from 61.3 to 90.5% (average 74.2%).

For industrial smoking, the industrial chamber (Mauting, Czech Republic) was employed. The smoke (25.0 °C) was produced using a heating plate on which beech and oak sawdust was placed; this resulted in indirect smoking of the samples. Smoking conditions were monitored and controlled with the average temperature of 18.9 °C and relative humidity of 74.49%. Samples were subjected to smoking for 4 h a day (8 × 30 min) for a total of three days.

Three batches of four groups were prepared and three samples from each group were excluded at the end of smoking in order to conduct the analysis. After the sampling, the casings were peeled from the sausages and stored in the same way as the stuffing; the samples were homogenized and stored in the freezer (−30 °C) in glass jars previously treated with acetone. All the analyses were carried out in triplicate.

2.2. PAHs Determination and Quantification

Extraction was done in the following manner: 3 g of samples were transferred into the centrifuge tube where a mixture of 3 mL of acetonitrile (ACN, Sigma-Aldrich, St. Louis, MO, USA) and 3 mL of water was added. The sample was vortexed for 1 min, followed by the addition of 3 g of anhydrous magnesium sulfate (MgSO4; Merck, Darmstadt, Germany) and 1 g of anhydrous sodium acetate.

The sample was then centrifuged for 5 min at 3000 rpm. 1 mL of upper layer of the acetonitrile extract, along with 150 mg of anhydrous magnesium sulfate, 100 mg of Primary and Secondary Amine (PSA) (Merck, Darmstadt, Germany), and 50 mg of C18 (Merck, Darmstadt, Germany) (Anastassiades, Lehotay, Stajnbaher, & Schenck, n.d.), was then transferred to 5 mL tubes. Centrifugation was applied for 5 min at 3000 rpm to ensure clear and pure extract. At the end, 0.5 mL of the extract was subjected to evaporation under nitrogen gas and reconstituted with hexane, resulting in a sample ready for the analysis on GC-MS (Agilent 7890B/5977A, Santa Clara, CA, USA).

Chromatographic separation of 16 PAHs of interest was performed by gas chromatography in combination with a mass detector (GC-MS), according to Mastanjević et al. (2019) [16]. In short, standard solutions of PAHs were prepared with PAH mix of 16 polycyclic aromatic hydrocarbons (Ultra Scientific, North Kingstown, RI, USA), 500 ± 0.2 μg/mL. Method validation and calibration through matrix blank sample was also performed. Samples were prepared using QuEChERS method (quick, easy, cheap, effective, rugged, and safe preparation) [16]. GC-MS parameters were adjusted as described (Supplementary Material) and reported by Mastanjević et al. 2019 [17]. All analyses were performed in triplicate.

2.3. Statistical Analysis

Data were subjected to the analysis of variance (ANOVA) with significance defined at $p < 0.05$ (Fisher's Least Significant Difference (LSD) test.). Statistica 13.1. (TIBCO Software Inc., Palo Alto, CA, USA) was used for statistical analysis.

3. Results and Discussion

The analysis of stuffing for *Hercegovačka kobasica* production revealed only 2.26 μg/kg for naphthalene and other 15 PAHs were below the quantification threshold. This is in agreement with previous research on similar samples [18,19].

The concentrations of 16 PAHs in natural and collagen casing used for *Hercegovačka kobasica* production are presented in Table 1. AC and IP were not quantified in any of the sample groups. The highest concentration was quantified for PHE and it from 1181.39 μg/kg in traditional smoking in natural casing, to <limit of quantification (LOQ) in industrial smoking in collagen casing samples. CHR, BbFA, BkFA, and DBahA were detected and quantified only in samples stuffed in natural casings and subjected to traditional smoking. The samples of casings subjected to industrial smoking, both collagen and natural, showed significantly ($p < 0.05$) lower PAH concentrations in comparison to casings subjected to traditional smoking. NA was found in higher concentrations in the samples exposed to industrial smoking and, moreover, the natural casings seem to bind NA more efficiently than collagen casing. From the other 15 PAHs, only ACL was quantified in both casings derived from industrial smoking. PHE was found only in natural casing in samples subjected to industrial smoking.

Cancerogenic BaP was quantified in both casings subjected to traditional smoking, with natural at 7.79 μg/kg and collagen at 4.98 μg/kg. For natural casing, this is almost four-fold the legally prescribed concentration (2 μg/kg); it is almost 2.5 times higher than the legally prescribed concentration for collagen. On the other hand, BaP was not quantified in industrial smoked casings.

PAH4 concentration was quantified only in traditionally smoked casings; it amounted to 44.86 μg/kg in natural casing and 21.46 μg/kg in collagen casings. The legally prescribed limit for PAH4 is 12 μg/kg, which makes the analyzed samples abundant with this group of PAHs.

PAH16 amounted to 2028.20 μg/kg in traditional smoked natural casing, while traditional smoked collagen casing showed almost ten-fold lower values (255.14 μg/kg). Casings smoked in the industrial manner showed significantly lower values ($p < 0.05$), resulting in 167.47 μg/kg for natural casing and 94.31 μg/kg for collagen casing.

PAH concentrations in *Hercegovačka kobasica* content are presented in Table 2. In the industrial smoked samples, similar as in casings, only NA and ACL were quantified. NA concentration amounted to 113.05 μg/kg in the industrially smoked sausages in natural casing and 44.40 μg/kg in collagen

casing. This is significantly higher than the levels in samples smoked in the traditional manner. Similar as for the casing, the most dominant PAH in traditional smoked samples was PHE, resulting in 79.24 μg/kg in natural casing and 31.59 μg/kg in collagen. AC, CHR, DBahA, and IP were not quantified in any of the samples. BaP amounted to 7.79 μg/kg in traditional smoked sausages in natural casings and 4.98 μg/kg in collagen. In the industrially smoked samples, the BaP content was below the quantification. The BaP content in traditionally smoked sausages was worryingly high; only a few studies of traditionally smoked Estonian and Swedish smoked meat products showed higher BaP concentrations [9,20]. Studies for Spanish, Portuguese, Italian, and Croatian smoked dry sausages reported lower values for BaP [4,5,17,21–25].

Table 1. Polycyclic aromatic hydrocarbons (PAH) contents (μg/kg) in *Hercegovačka kobasica* casings.

PAH	Traditional Smoking—Natural Casing	Traditional Smoking—Collagen Casing	Industrial Smoking—Natural Casing	Industrial Smoking—Collagen Casing
NA	54.17 ^{ab} ± 1.03	26.11 ^{b} ± 1.50	66.23 ^{a} ± 1.91	51.41 ^{ab} ± 0.80
ACL	351.24 ^{a} ± 5.71	65.77 ^{b} ± 2.11	84.31 ^{b} ± 1.94	42.91 ^{b} ± 0.81
AC	<LOQ	<LOQ	<LOQ	<LOQ
FL	133.10 ^{a} ± 2.27	20.33 ^{b} ± 0.32	<LOQ	<LOQ
AN	282.05 ^{a} ± 7.21	15.95 ^{b} ± 3.29	<LOQ	<LOQ
PHE	1108.39 ^{a} ± 6.061	79.4 ^{b} ± 4.06	15.21 ^{c} ± 1.35	<LOQ
FA	233.63 ^{a} ± 2.04	8.96 ^{b} ± 0.45	<LOQ	<LOQ
BaA	22.10 ^{a} ± 0.13	13.43 ^{b} ± 0.14	<LOQ	<LOQ
PY	177.67 ^{a} ± 2.33	5.57 ^{b} ± 0.17	<LOQ	<LOQ
CHR	21.38 ^{a} ± 0.73	<LOQ	<LOQ	<LOQ
BbFA	10.17 ^{a} ± 0.46	<LOQ	<LOQ	<LOQ
BkFA	12.38 ^{a} ± 0.15	<LOQ	<LOQ	<LOQ
BaP	5.06 ^{a} ± 0.11	7.79 ^{a} ± 0.17	<LOQ	<LOQ
DBahA	7.54 ^{a} ± 0.67	<LOQ	<LOQ	<LOQ
BghiP	5.46 ^{a} ± 0.19	0.76 ^{b} ± 0.20	<LOQ	<LOQ
IP	<LOQ	<LOQ	<LOQ	<LOQ
∑PAH4	44.86 ^{a} ± 2.16	21.46 ^{b} ± 0.93	<LOQ	<LOQ
∑PAH16	2028.20 ^{a} ± 12.55	255.14 ^{b} ± 5.34	167.47 ^{b} ± 5.48	94.31 ^{b} ± 3.26

$^{a–c}$ Means ± standard deviation within rows with different superscripts are significantly different ($p < 0.05$); LOQ—limit of quantification.

Similar to BaP, the PAH4 content was only quantified in traditionally smoked samples. The recorded concentrations for BaP in traditionally smoked samples is worryingly high, amounting to almost four times above the legally prescribed concentration. In traditionally smoked collagen samples, the BaP concertation was significantly lower than for the traditional, but still almost 2.5 times higher than the legally prescribed concentration. The sum of PAH4 was 21.46 μg/kg for natural casings and significantly lower for collagen casings, at 13.88 μg/kg. The legally prescribed values for PAH4 are 12 μg/kg; traditionally smoked samples showed almost two-fold higher concentrations. The samples in the collagen casing showed significantly lower values for PAH4, but it was still above the legally prescribed level. Thus, worryingly high concentrations of PAH4 were exceeded those in most Spanish, Croatian, Serbian, and Portuguese traditionally smoked dry sausages [3,4,11,17,19,21,22]. The higher PAH4 values were reported by Roserio et al. (2012) for Portuguese smoked blood sausage Moura of "Trás-os-Montes" (271.83 μg/kg) [24] and Wretling et al. (2010) for sauna smoked Swedish ham (209 μg/kg) [20].

Skaljac et al. (2018) [26] reported similar lower values for PAH4 and PAH16 in samples of Serbian sausage smoked in industrial conditions and in samples stuffed in artificial casing. A similar reduction of PAH content with the use of artificial casing were reported for frankfurter types, Spanish, Portuguese, and Croatian smoked dry sausages [7,18,27,28]. The sum of PAH16 was higher in natural casings

for both smoking procedures (traditional at 245.19 μg/kg and industrial at 145.48 μg/kg). However, in industrially smoked samples, the concentrations of BaP and PAH4 were not quantified and thus made them less harmful for human consumption. This may be related to the high porosity of natural casings. High concentrations for BaP, PAH4, and PAH16 may be the result of prolonged smoking in traditional procedures (30 days). Similar results, with the increase of PAH concertation in smoked meat products with an increase of smoking time, were reported Hitzel et al. (2013) [29], Pohlmann et al. (2012) [30], and Fraqueza et al. (2020) [31]. On the other hand, the PAH formation in smoked meat products may be related to the type of wood used for smoke generation [32–35]. The worryingly high concentrations of BaP, PAH4, and PAH16 in traditionally smoked sausages in this investigation may also be related to the use of oak wood to generate smoke; similarly high concentrations of BaP and PAH4 were reported by Reserio et al. (2012) [24] for Portuguese sausages smoked with oak wood.

Table 2. PAH contents (μg/kg) in *Hercegovačka kobasica*.

PAH	Traditional Smoking—Natural Casing	Traditional Smoking—Collagen Casing	Industrial Smoking—Natural Casing	Industrial Smoking—Collagen Casing
NA	26.11 ^{b} ± 0.51	<LOQ	113.05^{a} ± 1.84	44.40 ^{b} ± 0.53
ACL	65.77 ^{a} ± 0.25	23.55 ^{c} ± 0.17	32.83 ^{b} ± 0.59	22.05 ^{c} ± 0.56
AC	<LOQ	<LOQ	<LOQ	<LOQ
FL	23.33 ^{a} ± 0.43	<LOQ	<LOQ	<LOQ
AN	15.95 ^{a} ± 0.23	5.91 ^{b} ± 0.37	<LOQ	<LOQ
PHE	79.24 ^{a} ± 1.24	31.59 ^{b} ± 0.31	<LOQ	<LOQ
FA	8.95 ^{a} ± 0.14	6.10 ^{b} ± 0.22	<LOQ	<LOQ
BaA	13.43 ^{a} ± 0.40	8.40 ^{b} ± 0.19	<LOQ	<LOQ
PY	5.56 ^{a} ± 0.28	3.50 ^{b} ± 0.19	<LOQ	<LOQ
CHR	<LOQ	<LOQ	<LOQ	<LOQ
BbFA	0.23 ^{b} ± 0.08	0.51^{a} ± 0.10	<LOQ	<LOQ
BkFA	1.06 ^{a} ± 0.10	<LOQ	<LOQ	<LOQ
BaP	7.79 ^{a} ± 0.45	4.98^{b} ± 0.55	<LOQ	<LOQ
DBahA	<LOQ	<LOQ	<LOQ	<LOQ
BghiP	0.76 ^{a} ± 0.16	<LOQ	<LOQ	<LOQ
IP	<LOQ	<LOQ	<LOQ	<LOQ
∑PAH4	21.46 ^{a} ± 0.75	13.88 ^{b} ± 0.61	<LOQ	<LOQ
∑PAH16	245.19 ^{a} ± 2.93	84.54 ^{c} ± 0.82	145.48 ^{b} ± 1.17	64.46 ^{c} ± 1.25

$^{a–c}$ Means ± standard deviation within rows with different superscripts are significantly different ($p < 0.05$); LOQ—limit of quantification.

4. Conclusions

The results of this study indicate that traditional smoking and the use of natural casings can result in elevated and potentially harmful BaP and PAH4 concentrations in *Hercegovačka kobasica*. Producers who utilize the traditional smoking method should pay attention to smoking duration and wood combustion temperature. The potential use of smoke filters and smoking time reduction are also options that may help reduce the formation of PAHs in traditionally smoked sausages. Samples in collagen casings showed significantly lower values for PAHs, meaning that the smoking manner (industrial or traditional) plays a crucial role in PAH formation. The industrially smoked samples, both collagen and natural casings, had <LOQ concentrations of PAH4 and BaP.

Supplementary Materials: The following are available online at http://www.mdpi.com/2227-9717/8/8/918/s1, Table S1: The average values for precision, reproducibility, accuracy, linearity, LOQ and LOD for PAH method validation.

Author Contributions: Conceptualization, K.M.; methodology, B.K.; software, K.M.; validation, B.K.; investigation, L.P. and D.K.; data curation, K.H. and D.K.; writing—original draft preparation, K.M.; writing—review and editing, K.H.; supervision, K.M.; All authors have read and agreed to the published version of the manuscript.

Funding: This research received no external funding.

Conflicts of Interest: The authors declare no conflict of interest.

References

1. Ledesma, E.; Rendueles, M.; Diaz, M. Contamination of meat products during smoking by polycyclic aromatic hydrocarbons: Processes and prevention. *Food Control* **2016**, *60*, 64–87. [CrossRef]
2. Simko, P. Factors affecting elimination of polycyclic aromatic hydrocarbons from smoked meat foods and liquid smoke flavorings. *Mol. Nutr. Food Res.* **2005**, *49*, 637–647. [CrossRef] [PubMed]
3. Garcia-Falcon, M.S.; Simal-Gandara, J. Determination of polycyclic aromatic hydrocarbons in alcoholic drinks and the identification of their potential sources. *Food Addit. Contam.* **2005**, *22*, 791–797. [CrossRef] [PubMed]
4. Santos, C.; Gomes, A.; Roseiro, L.C. Polycyclic aromatic hydrocarbons incidence in Portuguese traditional smoked meat products. *Food Chem. Toxicol.* **2011**, *49*, 2343–2347. [CrossRef]
5. Roseiro, L.C.; Gomes, A.; Santos, C. Influence of processing in the prevalence of polycyclic aromatic hydrocarbons in a Portuguese traditional meat product. *Food Chem. Toxicol.* **2011**, *49*, 1340–1345. [CrossRef]
6. Skaljac, S.; Petrovic, L.; Tasic, T.; Ikonic, P.; Jokanovic, M.; Tomovic, V.; Dzinic, N.; Sojic, B.; Tjapkin, A.; Skrbic, B. Influence of smoking in traditional and industrial conditions on polycyclic aromatic hydrocarbons content in dry fermented sausages (Petrovska klobasa) from Serbia. *Food Control* **2014**, *40*, 12–18. [CrossRef]
7. Garcia-Falcon, M.S.; Simal-Gandara, J. Polycyclic aromatic hydrocarbons in smoke from different woods and their transfer during traditional smoking into chorizo sausages with collagen and tripe casings. *Food Addit. Contam.* **2005**, *22*, 1–8. [CrossRef]
8. Stumpe-Viksna, I.; Bartkevics, V.; Kukare, A.; Morozovs, A. Polycyclic aromatic hydrocarbons in meat smoked with different types of wood. *Food Chem.* **2008**, *110*, 794–797. [CrossRef]
9. Reinik, M.; Tamme, T.; Roasto, M.; Juhkam, K.; Tenno, T.; Kiis, A. Polycyclic aromatic hydrocarbons (PAHs) in meat products and estimated PAH intake by children and the general population in Estonia. *Food Addit. Contam.* **2007**, *24*, 429–437. [CrossRef]
10. Fontcuberta, M.; Arques, J.F.; Martinez, M.; Suarez, A.; Villalbi, J.R.; Centrich, F.; Serrahima, E.; Duran, J.; Casas, C. Polycyclic aromatic hydrocarbons in food samples collected in Barcelona, Spain. *J. Food Prot.* **2006**, *69*, 2024–2028. [CrossRef]
11. Fasano, E.; Yebra-Pimentel, I.; Martinez-Carballo, E.; Simal-Gandara, J. Profiling, distribution and levels of carcinogenic polycyclic aromatic hydrocarbons in traditional smoked plant and animal foods. *Food Control* **2016**, *59*, 581–590. [CrossRef]
12. Abdel-Shafy, H.I.; Mansour, M.S.M. A review on polycyclic aromatic hydrocarbons: Source, environmental impact, effect on human health and remediation. *Egypt. J. Pet.* **2016**, *25*, 107–123. [CrossRef]
13. US EPA National Center for Environmental Assessment; Murphy, P. EPA's Report on the Environment (ROE) (2008 Final Report). Available online: https://cfpub.epa.gov/ncea/risk/recordisplay.cfm?deid=190806 (accessed on 30 October 2019).
14. Aguilar, F.; Autrup, H.; Barlow, S.; Castle, L.; Crebelli, R.; Dekant, W.; Engel, K.-H.; Gontard, N.; Gott, D.M.; Grilli, S.; et al. Risk assessment of the scientific panel on food additives, flavourings, processing aids and materials in contact with food (Afc) on the smoke flavouring primary product-FF-B (question number EFSA-Q-2005-260) at its 22nd meeting the panel concluded the risk assessment and agreed the final text on 7 June 2007 by written procedure. *EFSA J.* **2007**, *5*, 1–12. [CrossRef]
15. Commission regulation (EU) No 835/2011 of 19 August 2011 amending regulation (EC) No 1881/2006 as regards maximum levels for polycyclic aromatic hydrocarbons in foodstuffs Text with EEA relevance. *Off. J. Eur. Union* **2011**, *215*, 1–5.
16. Službeni List—Pregled Dokumenta. Available online: http://www.sluzbenilist.ba/page/akt/zUp8Jgztz5k76kjn45hB4GvE= (accessed on 24 June 2020).
17. Mastanjević, K.M.; Kartalović, B.D.; Vranešević, J.M.; Novakov, N.J.; Habschied, K.J. Polycyclic aromatic hydrocarbons in traditionally smoked Slavonska kobasica. *Food Addit. Contam. Part B* **2020**, *13*, 82–87. [CrossRef] [PubMed]
18. Mastanjevic, K.; Kartalovic, B.; Petrovic, J.; Novakov, N.; Puljic, L.; Kovacevic, D.; Jukic, M.; Lukinac, J.; Mastanjevic, K. Polycyclic aromatic hydrocarbons in the traditional smoked sausage Slavonska kobasica. *J. Food Compos. Anal.* **2019**, *83*, 103282. [CrossRef]

19. Skaljac, S.; Jokanovic, M.; Tomovic, V.; Ivic, M.; Tasic, T.; Ikonic, P.; Sojic, B.; Dzinic, N.; Petrovic, L. Influence of smoking in traditional and industrial conditions on colour and content of polycyclic aromatic hydrocarbons in dry fermented sausage "Petrovska klobasa". *LWT Food Sci. Technol.* **2018**, *87*, 158–162. [CrossRef]
20. Wretling, S.; Eriksson, A.; Eskhult, G.A.; Larsson, B. Polycyclic aromatic hydrocarbons (PAHs) in Swedish smoked meat and fish. *J. Food Compos. Anal.* **2010**, *23*, 264–272. [CrossRef]
21. Lorenzo, J.M.; Purrinos, L.; Bermudez, R.; Cobas, N.; Figueiredo, M.; Garcia Fontan, M.C. Polycyclic aromatic hydrocarbons (PAHs) in two Spanish traditional smoked sausage varieties: "Chorizo gallego" and "Chorizo de cebolla". *Meat Sci.* **2011**, *89*, 105–109. [CrossRef]
22. Lorenzo, J.M.; Purrinos, L.; Garcia Fontan, M.C.; Franco, D. Polycyclic aromatic hydrocarbons (PAHs) in two Spanish traditional smoked sausage varieties: "Androlla" and "Botillo". *Meat Sci.* **2010**, *86*, 660–664. [CrossRef]
23. Ledesma, E.; Rendueles, M.; Diaz, M. Spanish smoked meat products: Benzo (a) pyrene (BaP) contamination and moisture. *J. Food Compos. Anal.* **2015**, *37*, 87–94. [CrossRef]
24. Roseiro, L.C.; Gomes, A.; Patarata, L.; Santos, C. Comparative survey of PAHs incidence in Portuguese traditional meat and blood sausages. *Food Chem. Toxicol.* **2012**, *50*, 1891–1896. [CrossRef]
25. Purcaro, G.; Moret, S.; Conte, L.S. Optimisation of microwave assisted extraction (MAE) for polycyclic aromatic hydrocarbon (PAH) determination in smoked meat. *Meat Sci.* **2009**, *81*, 275–280. [CrossRef] [PubMed]
26. Skaljac, S.; Petrovic, L.; Jokanovic, M.; Tasic, T.; Ivic, M.; Tomovic, V.; Ikonic, P.; Sojic, B.; Dzinic, N.; Skrbic, B. Influence of collagen and natural casings on the polycyclic aromatic hydrocarbons in traditional dry fermented sausage (Petrovska klobasa) from Serbia. *Int. J. Food Prop.* **2018**, *21*, 667–673. [CrossRef]
27. Poehlmann, M.; Hitzel, A.; Schwaegele, F.; Speer, K.; Jira, W. Influence of different smoke generation methods on the contents of polycyclic aromatic hydrocarbons (PAH) and phenolic substances in Frankfurter-type sausages. *Food Control* **2013**, *34*, 347–355. [CrossRef]
28. Gomes, A.; Santos, C.; Almeida, J.; Elias, M.; Roseiro, L.C. Effect of fat content, casing type and smoking procedures on PAHs contents of Portuguese traditional dry fermented sausages. *Food Chem. Toxicol.* **2013**, *58*, 369–374. [CrossRef]
29. Hitzel, A.; Poehlmann, M.; Schwaegele, F.; Speer, K.; Jira, W. PAH contents in smoked meat products—Influence of different types of wood and smoking spices on the contents of polycyclic aromatic hydrocarbons (PAH) and phenolic substances. *Fleischwirtschaft* **2013**, *93*, 92–97.
30. Pöhlmann, M.; Hitzel, A.; Schwägele, F.; Speer, K.; Jira, W. Contents of polycyclic aromatic hydrocarbons (PAH) and phenolic substances in Frankfurter-type sausages depending on smoking conditions using glow smoke. *Meat Sci.* **2012**, *90*, 176–184. [CrossRef]
31. Fraqueza, M.J.; Laranjo, M.; Alves, S.; Fernandes, M.H.; Agulheiro-Santos, A.C.; Fernandes, M.J.; Potes, M.E.; Elias, M. Dry-Cured meat products according to the smoking regime: Process optimization to control polycyclic aromatic hydrocarbons. *Foods* **2020**, *9*, 91. [CrossRef]
32. Hitzel, A.; Poehlmann, M.; Schwaegele, F.; Speer, K.; Jira, W. Polycyclic aromatic hydrocarbons (PAH) and phenolic substances in meat products smoked with different types of wood and smoking spices. *Food Chem.* **2013**, *139*, 955–962. [CrossRef]
33. Malarut, J.; Vangnai, K. Influence of wood types on quality and carcinogenic polycyclic aromatic hydrocarbons (PAHs) of smoked sausages. *Food Control* **2018**, *85*, 98–106. [CrossRef]
34. Ledesma, E.; Rendueles, M.; Diaz, M. Benzo (a) pyrene penetration on a smoked meat product during smoking time. *Food Addit. Contam. Part A* **2014**, *31*, 1688–1698. [CrossRef] [PubMed]
35. Skrbic, B.; Durisic-Mladenovic, N.; Macvanin, N.; Tjapkin, A.; Skaljac, S. Polycyclic aromatic hydrocarbons in smoked dry fermented sausages with protected designation of origin Petrovska klobasa from Serbia. *Maced. J. Chem. Chem. Eng.* **2014**, *33*, 227–236. [CrossRef]

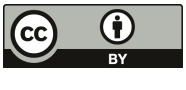

processes

MDPI

Article

Intensive Multiple Sequential Batch Simultaneous Saccharification and Cultivation of *Kluyveromyces marxianus* SS106 Thermotolerant Yeast Strain for Single-Step Ethanol Fermentation from Raw Cassava Starch

Kwanruthai Malairuang [1], Morakot Krajang [1], Rapeepong Rotsattarat [2] and Saethawat Chamsart [3,*]

[1] Biological Sciences Program, Faculty of Science, Burapha University, Chonburi 20131, Thailand; pinsor_17@hotmail.com (K.M.); morakoto_2@hotmail.com (M.K.)
[2] Department of Biotechnology, Faculty of Science, Burapha University, Chonburi 20131, Thailand; rapeepong_dome@hotmail.com
[3] Department of Biology, Faculty of Science, Burapha University, Chonburi 20131, Thailand
* Correspondence: saethawa@buu.ac.th; Tel.: +6696-887-3878

Received: 29 June 2020; Accepted: 20 July 2020; Published: 27 July 2020

Abstract: We developed the intensive multiple sequential batch simultaneous saccharification and cultivation of the selected thermotolerant yeast strain for single-step ethanol production. The selection and high-cell-density inoculum production of thermotolerant yeast able to produce ethanol under the optimal conditions for single-step ethanol fermentation has become a necessity. In this study, the newly isolated *Kluyveromyces marxianus* SS106 could tolerate high temperatures (35–45 °C) and grow under a wide range of pH values (3.0–5.5), which are the optimum conditions of raw cassava starch hydrolyzing enzyme used in single-step ethanol fermentation. The high-cell-density concentration of *K. marxianus* SS106 was produced by a single batch and an intensive multiple sequential batch process in a 5-L stirred tank bioreactor using the simultaneous saccharification and cultivation (SSC) method. The single SSC process yielded the yeast cell biomass at a concentration of 39.30 g/L with a productivity of 3.28 g/L/h and a specific growth rate of 0.49 h^{-1}. However, the yeast cell density concentration was higher in the intensive multiple sequential batch SSC than in the single batch process. This process yielded yeast cell biomass at concentrations of 36.09–45.82 g/L with productivities of 3.01–3.82 g/L/h and specific growth rates of 0.29–0.44 h^{-1} in the first six batch cycle. The results suggested that the intensive multiple sequential batch simultaneous saccharification and cultivation of *K. marxianus* SS106 would be a promising process for high-cell-density yeast production for use as the inoculum in single-step ethanol fermentation. Furthermore, we also experimented with single-step ethanol production from raw cassava starch by *K. marxianus* SS106 in a 5-L stirred tank fermenter. This produced ethanol at a concentration of 61.72 g/L with a productivity of 0.86 g/L/h.

Keywords: simultaneous saccharification and cultivation (SSC); intensive multiple sequential batch cultivation; thermotolerant yeast; *Kluyveromyces marxianus*; ethanol production

1. Introduction

One of the problems associated with the conventional process for ethanol production based on cassava starch raw material is the different optimum temperatures for liquefaction, saccharification, and fermentation. This process requires high energy consumption because starch hydrolysis takes place at high temperatures that require enormous amounts of steam and an efficient water-based

cooling system to bring down the temperature to fermentation process [1,2]. To improve the ethanol production process from starchy materials, single-step ethanol production using a combination of raw starch hydrolysis and fermentation was developed here. This process used granular starch hydrolyzing enzyme and free cells of yeast at the same time for reducing the cost of energy input and fermentation time from multistage operation.

Kluyveromyces marxianus, a type of "non-conventional" yeast in the *Kluyveromyces* genus of the family Saccharomycetaceae, has recently been in the limelight for economic cellulosic ethanol production. Besides its ability of ethanol fermentation, *K. marxianus* possesses a number of advantages over *Saccharomyces cerevisiae*, which has been traditionally used in bioethanol production. *K. marxianus* is the fastest growing yeast, with a maximum growth rate of 0.80 h^{-1}, and *S. cerevisiae* is only 0.37 h^{-1}. *K. marxianus* can even grow at 52 °C due to its notable thermotolerance, while *S. cerevisiae* has optimum temperatures ranging from 30 to 37 °C. In addition, besides glucose, *K. marxianus* is able to utilize a variety of carbon sources, including inulin, xylose, and lactose, which cannot be used by *S. cerevisiae*. Furthermore, ethanol generation prefers an anaerobic environment; thus, the capability to grow under full anaerobiosis is also required for a yeast strain to be used in a fuel ethanol-producing process. *K. marxianus*, like *S. cerevisiae*, is a respiro-fermentative yeast, and the batch fermentation of *K. marxianus* in a strict anaerobic environment at 37 °C reached ethanol concentrations significantly higher than in aerobiosis. Based on the above, *K. marxianus* could be an ideal yeast for industrial bioethanol production. Currently, *K. marxianus* can only bear the maximum 6% (*v/v*) ethanol, which is measured by the growth ability in shake flask culture in YPD (yeast extract peptone dextrose) medium with 6% ethanol at 30 °C. The low ethanol tolerance leads to its low ethanol yield and is the major bottleneck to block its practical industry application so far [3].

In our previous studies, raw cassava starch hydrolysis was successfully done at a high temperature of 40 °C and low pH value of 3.0–4.0 [4]. Therefore, the selection and high cell inoculum production of yeast strain that could be tolerant to high temperatures, low pH values, and high ethanol concentrations are important and of interest in this study.

High temperature fermentation is a key requirement for effective ethanol production in tropical countries where average day-time temperatures are usually high throughout the year [5]. Therefore, several researchers studied the successful selections of thermotolerant yeast strains in ethanol fermentation. Most of the experiments have been focused on *S. cerevisiae* [6,7] and *K. marxianus* [8–10]. However, these strains were employed for ethanol production only by the simultaneous saccharification and fermentation process. Therefore, it is interesting to use the thermotolerant yeast strain for the single-step process in the ethanol production industry in Thailand.

Not only the selection of the thermotolerant yeast strain, but high-cell-density inoculum production is also very important for ethanol fermentation. The typical method employed for the increase in yeast cell number density is the fed-batch cultivation mode which has been proved to be one of the most successful processes for increasing cell concentration and volumetric productivity of standard batch cultivation [11]. Besides the fed-batch cultivation process, simultaneous saccharification and cultivation (SSC) could be focused in high-cell-density production. After starch liquefaction by alpha-amylase, nitrogen sources, mineral salts, and glucoamylase are added into liquefied slurry, concurrently with yeast inoculum, and SSC is conducted in a bioreactor. The presence of yeast with those enzymes reduces the sugar accumulation in a reactor. During cultivation, liquefied starch (oligomer called dextrin) is gradually hydrolyzed by glucoamylase to release glucose and is simultaneously utilized by yeast. This prevents the Crabtree effect that usually occurs in aerobic cultivation with high glucose concentration.

Here, the intensive multiple sequential batch cultivation method has been introduced to increase cell concentration, volumetric productivity and cost effectiveness. In intensive multiple sequential batch cultivation, a bioreactor is initially filled with a medium and yeast cells and then incubated under optimal conditions to achieve high-cell concentration. After the initial batch reaches the end of the exponential phase, a desired volume of culture is withdrawn as the product and then another equal volume of fresh medium is fed into the same bioreactor. The cultivation is again restarted under

the same conditions as the first batch, using the remaining culture in the bioreactor as the starting inoculum. Therefore, it is interesting to improve the efficiency of the SSC process for high-cell-density yeast inoculum production by intensive multiple sequential batch cultivation. Moreover, it also reduces the operation time for cleaning, sterilization, and inoculation [2,12]. In this study, we also looked for an appropriate yeast strain for the single-step ethanol production using a combination of raw starch hydrolysis and fermentation. The objective of this study is not only to select a thermotolerant yeast strain for single-step ethanol fermentation, but also to establish a practical approach to produce high-cell-density yeast biomass by intensive multiple sequential batch simultaneous saccharification and cultivation.

2. Materials and Methods

2.1. Materials

According to our studies [13], liquefied starch with a dextrose equivalent (DE) of 10–13 was prepared in a 10-L hydrolysis bioreactor. A 10% (*w/v*) suspension of cassava starch was added with 0.1% (*w/w*) of α-amylase (Spezyme Alpha, thermostable α-amylase; Dupont Industrial Biosciences, Shanghai, China). Then, the mixture was agitated at 100 rpm for 3 h at 85 °C. Glucose at a DE of 95 was prepared by hydrolysis of liquefied starch. After liquefaction, the slurry was cooled to 60 °C and subsequently added with 0.2% (*w/w*) of glucoamylase and bacteria pullulanase (Distillase ASP, a blend of enzymes; Dupont Industrial Biosciences, Shanghai, China). The mixture was agitated at 100 rpm for 20 h at 60 °C.

Raw cassava starch, used as the carbon source for single-step ethanol fermentation, was pretreated in the 10-L hydrolysis bioreactor. A 20% (*w/v*) of cassava starch slurry was pretreated with 0.1% (*w/w*) of Distillase ASP. The mixture was agitated at 100 rpm for 1 h at 60 °C [4]. After pretreatment, the starch slurry was cooled to 40 °C for the single-step ethanol fermentation. (The composition of cassava starch was analyzed by [14]. The moisture, protein, ash, fat, crude fiber, carbohydrate, and amylose contents ranged from 7.10 to 7.61%, 0.32 to 31.02%, 0.45 to 2.67%, 0.17 to 1.19%, 0.07 to 1.69%, 8.13 to 90.77%, and 23.04 to 29.45%, respectively.)

2.2. Media

The yeast malt (YM) medium was composed of 3 g of yeast extract, 5 g of malt extract, 5 g of peptone, 10 g of glucose, per liter. The fermentation medium utilized in the selection of thermotolerant yeasts for ethanol production at high temperatures was composed of 200 g of glucose from cassava starch hydrolysis, 10 g of sugarcane molasses, 3.8 g of $MgSO_4.7H_2O$, per liter. The yeast peptone dextrose (YPD) medium (used in study of growth kinetics) was composed of 10 g of yeast extract, 20 g of peptone, 50 g of glucose, per liter. The yeast production medium was composed of 100 g of liquefied starch, 20 g of yeast extract, 1.5 g of KH_2PO_4, 1.8 g of Na_2HPO_4, 0.2 g of $MgSO_4.7H_2O$, 1 mL of trace element solution, per liter [15]. The ethanol production medium (utilized in single-step ethanol fermentation) was composed of 200 g of pretreated raw cassava starch, 100 g of sugarcane molasses, 0.2 g of $(NH_4)_2HPO_4$, 1.5 g of KH_2PO_4, 1.8 g of Na_2HPO_4, 3.8 g of $MgSO_4.7H_2O$, per liter.

2.3. Screening and Isolating of Thermotolerant Yeast Strains

The yeast strains were isolated from dry cassava pulp and soil samples from a cassava starch factory, Chorchaiwat Industry Co., Ltd., Chonburi, Thailand. The first screening was done at 40 °C in YM medium at pH 5.5 with 1 *n* HCl. After inoculation, the cultures were incubated on a rotary incubator shaker (Lab Tech, Korea) at a shaking speed of 200 rpm for 48 h. The enriched cultures were spread on agar plates containing the same medium and incubated at the same temperature and time. The single colonies of the isolated strains were studied their morphology and picked. The purified strains were kept on a YM agar slant and incubated at the same temperature and time above, and after that were stored at 4 °C.

The thermotolerant strains were isolated based on their growth performances in YM medium by incubating them on a rotary incubator shaker at 35, 38, 40, 42, and 45 °C for 24 h at a shaking speed of 200 rpm. In addition, they were incubated at the designed temperature of 40 °C in the same medium with different initial pH of 3.0, 3.5, 4.0, 4.5, 5.0, and 5.5 for their growth study in acidic conditions. The successful cultured strains were selected and collected for further ethanol production at a high temperature.

2.4. Selection of Thermotolerant Yeast for Single-Step Ethanol Fermentation

Later, the selection of strains for ethanol production at the high temperature of 40 °C was conducted in 250 mL Erlenmeyer flasks each containing 50 mL of fermentation medium at pH 4.0. Inoculants were prepared by transferring one loop full of each isolate from the YM agar slant into the flask containing 50 mL of YM broth at the same temperature and then incubated on a rotary incubator shaker at 200 rpm for 24 h. After incubation, each culture was diluted with distilled water to adjust the optical density to 10.0 and transferred 10 mL of each isolate to the fermentation medium in the 250 mL flasks above, and then incubated at 40 °C on a rotary shaker at 100 rpm (anaerobic fermentation needs less air) for 48 h.

2.5. Growth Kinetics of the Selected Thermotolerant Yeast

Growth kinetics of the selected thermotolerant strain was studied by cultivation in a 250 mL Erlenmeyer flask containing YPD medium composed of 50 g/L of glucose, at 40 °C and pH 4.0. Five ml of inoculum (OD_{660} 10.0) was inoculated into the above flask. The culture was then incubated on a rotary shaker at 200 rpm for 48 h.

2.6. Optimization of StargenTM002 Concentration for Simultaneous Saccharification and Cultivation of the Selected Thermotolerant Yeast to Produce Cells at High-Density Concentration

Normally, yeast cannot directly utilize starch or oligosaccharide so that the StargenTM002 (a granular starch hydrolyzing enzyme, Dupont Industrial Biosciences, Shanghai, China) was essentially optimized before adding into liquefied starch with the SSC method. The optimization of StargenTM002 concentration was conducted in the 10-L lysis reactor containing 100 g/L of liquefied starch. Different StargenTM002 dosages of 0.025, 0.050, 0.075, and 0.100% (*w/w*) were employed to study their effects on liquefied starch hydrolysis. The hydrolyzation was carried out at 40 °C and a stirrer speed of 300 rpm for 24 h, as we have experimented that for this reactor a stirrer speed at 300 rpm (equivalent to the power inputs of 0.25 W/kg) gave the best results [13].

2.7. Single-Batch Simultaneous Saccharification and Cultivation of the Selected Thermotolerant Yeast to Produce Cells at High-Density Concentration

High-cell-density productions of the selected thermotolerant yeast strain were conducted in a 5-L stirred tank bioreactor (BIOSTAT B, Braun Biotech International, Germany). To evaluate the cell biomass production strategy, 50 g/L or a 100 g/L of liquefied starch was used as the carbon source for cultivation by the SSC method. The production medium composed of 3 L of liquefied starch mixed with nitrogen source and mineral salt solution was directly sterilized at 121 °C for 30 min. The medium was then inoculated with 10% (*v/v*) of inoculum from the shake flask and added with 0.1% (*w/w*) of StargenTM002 at the initial stage. The cultivations were conducted at 40 °C for 24 h. The aeration rates and agitation rates were set at 2 vvm and 636 rpm (for 50 g/L batch), and at 4 vvm and 802 rpm (for 100 g/L batch).

2.8. Intensive Multiple Sequential Batch Simultaneous Saccharification and Cultivation of the Selected Thermotolerant Yeast to Produce Cells at High-Density Concentration

The conditions for intensive multiple sequential batch cultivation were the same as those of single-batch cultivation with 0.1% (*w/w*) of StargenTM002. The appropriate broth replacement time point was at 12 h (the end of exponential growth phase) which was obtained from the results of

single-batch simultaneous saccharification and cultivation. At the end of each cycle (12 h), a 10% volume of culture remained in bioreactor to use as the starting inoculum for the next batch cycle, and another 90% volume was removed and collected for further analysis. Then, the equal volume of fresh production medium, with the addition of StargenTM002 as above, was added in order to initiate the next batch cycle. The SSC was intensively performed for multiple-batch cycles (8 cycles) until the yeast cell density concentration decreased.

2.9. Single-Step Ethanol Production to Form Simultaneous Raw Cassava Starch Hydrolysis and Fermentation

The single-step ethanol fermentation was conducted in a 5-L stirred tank fermenter containing 4 L of the ethanol production medium containing 200 g/L of pretreated raw cassava starch. Without sterilization, during medium mixing, 0.3% (*w/w*) of StargenTM002 and 2.0 g/L of thermotolerant yeast inoculum were added at the initial stage. The 0.3% (*w/w*) of StargenTM002 was used rather than the above dosages (Section 2.6) because: (i) The use of raw starch is more difficult to be hydrolyzed; (ii) the use of 2-time starch concentration at 200 g/L needs a higher amount of the enzyme; (iii) an overdose of enzymes helps complete hydrolysis. The ethanol fermentation condition was controlled at 40 °C, initial pH at 4, and an agitation rate at 300 rpm for 72 h without pH control throughout the fermentation. No medium sterilization and pH control were to mimic the industrial production operation.

The overall schematic scope of the studies can be summarized: (i) Screening and isolating of thermotolerant yeast strains; (ii) selection of thermotolerant yeasts for single-step ethanol fermentation; (iii) growth kinetics study of the selected strain; (ix) optimization of enzyme StargenTM002 concentration for simultaneous saccharification and cultivation (SSC) to produce cells at a high concentration; (x) study of single-batch SSC to produce cells at a high concentration; (xi) study of intensive multiple sequential batch SSC to produce cells at a high concentration; (xii) single-step ethanol production to form simultaneous raw cassava starch hydrolysis and fermentation.

2.10. Analytical Methods

The yeast cell growth was analyzed by measuring the optical density at 660 nm with a spectrophotometer and the dry cell weight concentration. A 1.5-mL sample was centrifuged at 10,000 rpm for 10 min. The cell was washed twice with distilled water, dried at 80 °C for 12 h, and weighed after cooling.

The concentrations of ethanol and glucose were determined using high-performance liquid chromatography (HPLC) (KNAUER Smartline, Berlin, Germany) with a refractive index (RI) detector (KNAUER Smartline 2300, Berlin, Germany) and a Eurokat H vertex column (KNAUER, Berlin, Germany). Eluent of 0.01 N sulfuric acid at a flow rate of 0.8 mL/min was used. The analyses were performed at 60 °C. The samples were 10-fold diluted, filtered through 0.45 μm filter, and injected into the column with an amount of 20 μl.

2.11. Statistical Analysis

The statistical analyses were done with a one-way analysis of variance (ANOVA) and the differences of the treatment mean values from 3 replications (each experiment was done in 3 replicates) were compared with the Tukey's range test method at a p-value of 0.05 using Minitab version 17.

2.12. Kinetic Parameters' Calculations

The six kinetic parameters were calculated using experimental data, i.e., cultivation time, t (h), cell biomass concentration, x (g/L), ethanol product concentration, p (g/L), and carbon (starch) substrate used, s (g/L). (i) The specific growth rate, μ (h^{-1}) is calculated from $\mu = \frac{dlnx}{dt}$ where the differential natural log of x is divided by the time change. (ii) The productivity or production rate of cell biomass, r_x (g/l/h), is from $r_x = \frac{dx}{dt}$. (iii) The productivity of ethanol product, r_p (g/L/h), is from $r_p = \frac{dp}{dt}$. (iv) The cell yield coefficient, $Y_{x/s}$ (g/g) is from $Y_{x/s} = \frac{\Delta x}{\Delta s}$, where Δs is starch substrate used (g/L) and Δx is cell

produced (g/L). (v) The ethanol product yield coefficient, $Y_{p/s}$ (g/g), is from $Y_{p/s} = \frac{\Delta p}{\Delta s}$, where Δs is the starch substrate used (g/L) and Δp is the ethanol produced (g/L). (xi) The production efficiency, Ef (%), is from $Ef = \frac{Y_{p/s}}{Y'_{p/s}} x100$, where $Y_{p/s}$ is from the experiment and $Y'_{p/s}$ is from the theoretical yield coefficient or stoichiometry.

3. Results and Discussion

3.1. Screening and Isolating of the Thermotolerant Yeast Strains

High temperature is a key physical parameter that limits the performance of the organism in terms of ethanol production [16]. The screening of thermotolerant yeast from industrial and natural resources in tropical regions is suitable for ethanol fermentation at high temperatures [17]. In this study thermotolerant yeasts were isolated from cassava pulp and soil samples from a cassava starch factory. Based on the colony characteristics, 15 potential isolates of yeast were obtained. The ability of the strains to grow at high temperature was tested at 35, 38, 40, 42, and 45 °C. The results showed that the 8 dominant isolates (strains) of CP202, CP203, SS101, SS103, SS106, SS108, SS111, and SS206 grew satisfactorily at 35–45 °C, but the remaining 7 isolates grew only at 35–40 °C.

In our study, the cultivation and fermentation were done at 35–40 °C, which were optimum temperatures of StargenTM002 for hydrolysis of raw cassava starch [4]. However, during ethanol fermentation, yeasts faced plenty of stresses simultaneously. The effects of combined stresses (high temperature, high ethanol concentration, and low pH value) on the fermentation performance of yeast strains has received attention [17]. In addition, a high temperature of 40 °C with low pH values of 3.0–4.0 gave high productivities of raw cassava starch hydrolysis in single-step ethanol fermentations. Therefore, we studied the combinations of a high temperature of 40 °C with different low pH values of 3.0, 3.5, 4.0, 4.5, 5.0, and 5.5 on the growth performance of all the natural isolates. The results showed that only 5 isolates grew at 40 °C under a wide range of pH values. At pH 4.5–5.5, the similar growth performance of all isolates was observed, whereas at pH 3.0–4.0, the satisfactory growth of only the strains SS101, SS106, SS108, SS111, and SS206 was achieved.

These results clearly indicate that the yeast strains SS101, SS106, SS108, SS111, and SS206 can be tolerant to high temperatures and grow under a wide range of pH values (Figure 1). Based on the results of their growth performances, these 5 dominant strains were selected as the candidates for ethanol production at a high temperature and used for further experiments.

3.2. Selection of Thermotolerant Yeasts for Ethanol Production at a High Temperature and a Low pH

There were no significant differences between the OD660 of 40 °C and 42 °C; thus, less temperature was chosen because of three reasons: (i) Energy saving for industry; (ii) milder biochemical reaction during cell growth and product formation; and (iii) in the industry, if the set point is 40 °C but the actual temperature is a bit higher due to the external environment and controlled system delay, yeast still grows. In addition, the values of pH 3 and 3.5 are normally too acidic for the systems: (i) A biological system uses more acid solution for control; (ii) strong acid condition operation is difficult and dangerous to both humans and all the processing equipment, e.g., corrosion. Therefore, the combination of a temperature of 40 °C and a pH value of 4.0 is the appropriate optimum condition. Thus, the five yeast strains from the previous screening were selected for their fermentative abilities at a high temperature in the fermentation medium containing 200 g/L of glucose. Fermentation was conducted at 40 °C with a low pH of 4.0.

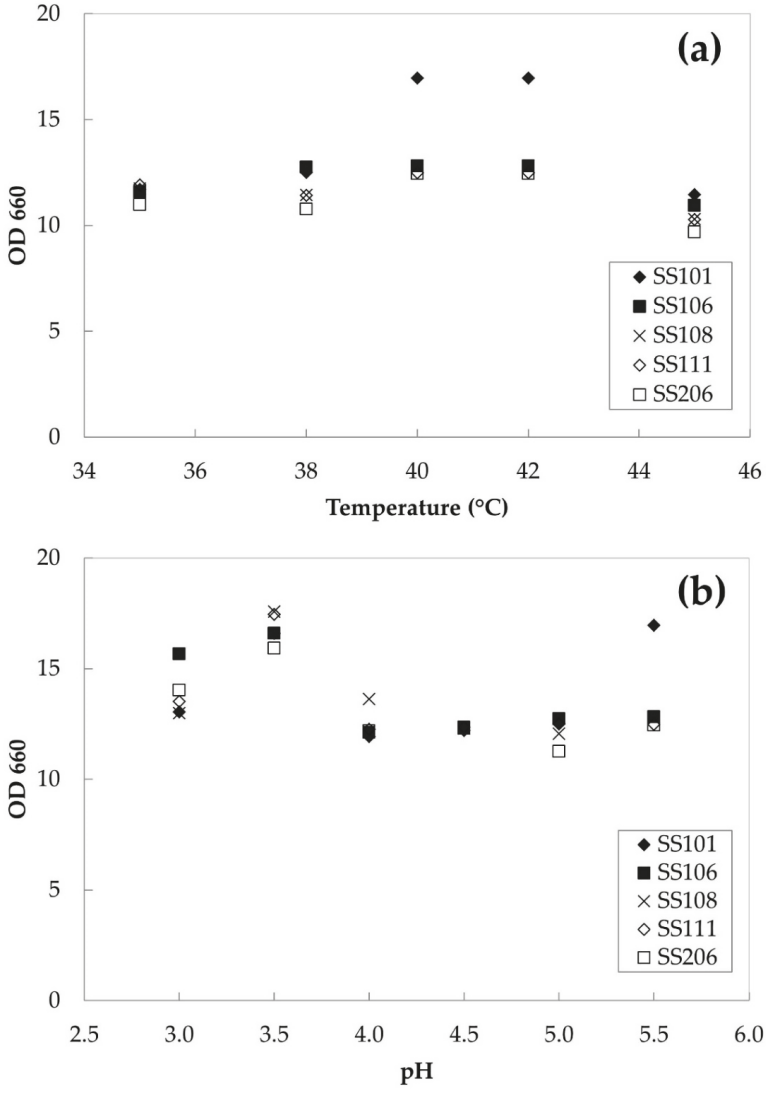

Figure 1. Effects of temperature (**a**) and pH (**b**) on cell growth (OD660) of SS101 (filled diamonds), SS106 (filled squares), SS108 (crosses), SS111 (open diamonds), and SS206 (open squares) cultivated in yeast malt (YM) medium composed of 10 g/L of glucose, shaken at 200 rpm for 24 h.

Table 1 summarizes the kinetic parameters of ethanol fermentation by the selected yeast strains under high temperature. The maximum ethanol concentration of 25.33 g/L and the yield coefficient of 0.40 g/g were obtained from strain SS106, which represented the highest production efficiency of 79.22% with the productivity of 0.53 g/L/h, while the remaining stains gave slightly lower ethanol concentrations and productivities. Based on the results of its growth performance at high temperatures and under a wide range of pH values producing the highest ethanol concentration and efficiency among the tested strains, strain SS106 showed the effectiveness of thermotolerant yeast for ethanol production at a high temperature, which can be utilized for single-step ethanol production using a combination of raw cassava starch hydrolysis and fermentation.

Table 1. Comparison of the kinetic parameters of selected yeast stains after 48 h of fermentation in fermentation medium composed of 200 g/L of glucose at 40 °C.

Strains	Ethanol Conc. (g/L)	Yield Coefficient (g/g)	Productivity (g/L/h)	Efficiency (%)
SS101	23.79 ± 0.21 ^{c}	0.35 ± 0.01 ^{c}	0.50 ± 0.00 ^{b}	69.44 ± 1.59 ^{c}
SS106	25.33 ± 0.27 ^{a}	0.40 ± 0.01 ^{a}	0.53 ± 0.01 ^{a}	79.22 ± 1.29 ^{a}
SS108	22.25 ± 0.34 ^{d}	0.38 ± 0.00 ^{b}	0.46 ± 0.01 ^{c}	73.45 ± 0.57 ^{b}
SS111	23.42 ± 0.32 ^{c}	0.37 ± 0.00 ^{b}	0.49 ± 0.01 ^{bc}	72.56 ± 0.63 ^{b}
SS206	24.77 ± 0.46 ^{b}	0.36 ± 0.00 ^{bc}	0.52 ± 0.01 ^{ab}	71.23 ± 0.57 ^{bc}

Statistic comparisons of those mean values within their own columns (among strains) at *p*-values of 0.05 show different characters, ^{a}, ^{b}, ^{c}, and ^{d}, which mean statically significant differences.

The strain SS106 was identified using the method of "26 rDNA sequencing and phylogenetic tree analysis" by the Thailand Institute of Scientific and Technological Research (TISTR). It was exposed to be *Kluyveromyces marxianus*. The molecular taxonomic study on the DNA sequence of the D1/D2 region in 26S rDNA proved that the sequences of strain SS106 are most similar to *K. marxianus* at level of 100%. Therefore, the strain SS106 was identified as *K. marxianus*.

Previous literature has described the ability of *K. marxianus* to grow and ferment at 40 °C or above [9,18], which is in good agreement with the results of our study. *K. marxianus* SS106 grows well at temperatures as high as 35–45 °C and it can efficiently produce ethanol at a high temperature. Furthermore, it would be advantageous to use a thermotolerant yeast strain *K. marxianus* for ethanol production by reducing the cooling cost and decreasing the risk of bacterial contamination [6,17]. Based on the results of this study and with the above advantages, it is indicated that the thermotolerant yeast *K. marxianus* SS106 shows high potential to be a candidate for feasible single-step ethanol production using a combination of raw cassava starch hydrolysis and fermentation.

3.3. Growth Kinetics of K. marxianus SS106 in Shake Flask Cultivation

Growth kinetics of *K. marxianus* SS106 in shake flask cultivation in YPD medium composed of 50 g/L of glucose, at 40 °C for 48 h was conducted. It was observed that the maximum cell biomass concentration produced was 15.91 g/L at a productivity of 0.66 g/L/h. The yield coefficient was 0.38 g/g with a specific growth rate of 0.07 h^{-1} (Table 2). However, this strain did not actually grow as well as expected in the shake flask cultivation due to insufficiently dissolved oxygen that resulted in the Crabtree effect. It produced ethanol rather than cell biomass at a high concentration of glucose at the first 12 h (data not shown). This phenomenon usually occurs in aerobic cultivation in most yeasts at high glucose concentration. For aerobic cultivation, it is necessary to control dissolved oxygen concentration in the further studies in order to maintain its enough saturation with air sparging during the cultivations. This is necessary to enhance the growth of *K. marxianus* SS106.

Table 2. Comparison of kinetic parameters of *K. marxianus* SS106 cell biomass productions in shake flask and in aerobic bioreactors at 40 °C with different substrate concentrations.

Cultivation Methods	Substrate (g/L)	Time (h)	Cell Mass conc. (g/L)	Specific Growth Rate (h^{-1})	Yield Coefficient (g/g)	Productivity (g/L/h)
Shake flask	50	24	15.91 ± 0.05 ^{b}	0.07 ± 0.00 ^{b}	0.38 ± 0.00 ^{c}	0.66 ± 0.00 ^{c}
Bioreactor I	50	12	17.36 ± 0.01 ^{b}	0.48 ± 0.00 ^{a}	0.41 ± 0.00 ^{b}	1.45 ± 0.00 ^{b}
Bioreactor II	100	12	39.30 ± 0.01 ^{a}	0.49 ± 0.00 ^{a}	0.50 ± 0.00 ^{a}	3.28 ± 0.00 ^{a}

Statistic comparisons of those values within their own columns (among culture methods) at *p*-values of 0.05 show different characters, ^{a}, ^{b}, and ^{c}, which mean statically significant differences.

3.4. Effect of Enzyme StargenTM002 Concentration on Liquefied Starch Hydrolysis for SSC of K. marxianus SS106

The liquefied starch at a concentration of 100 g/L was further saccharified (hydrolyzed) by different StargenTM002 dosages in a 10-L lysis reactor. The hydrolyzation was carried out at a stirring speed of 300 rpm and 40 °C for 24 h. Glucose concentrations were increased with increasing enzyme concentrations. The maximum glucose concentration was achieved with 0.10% (*w*/*w*) dosage (Figure 2). After 18 h of hydrolysis, 99.25 g/L of glucose was released from 100 g/L of liquefied starch when the highest StargenTM002 dosage of 0.10% (*w*/*w*) was employed. As it showed a complete hydrolysis, it also gave the highest productivity of 5.51 g/L/h. Therefore, this enzyme at the concentration of 0.1% (*w*/*w*) was used for further studies on batch and intensive multiple sequential batch SSC of *K. marxianus* SS106.

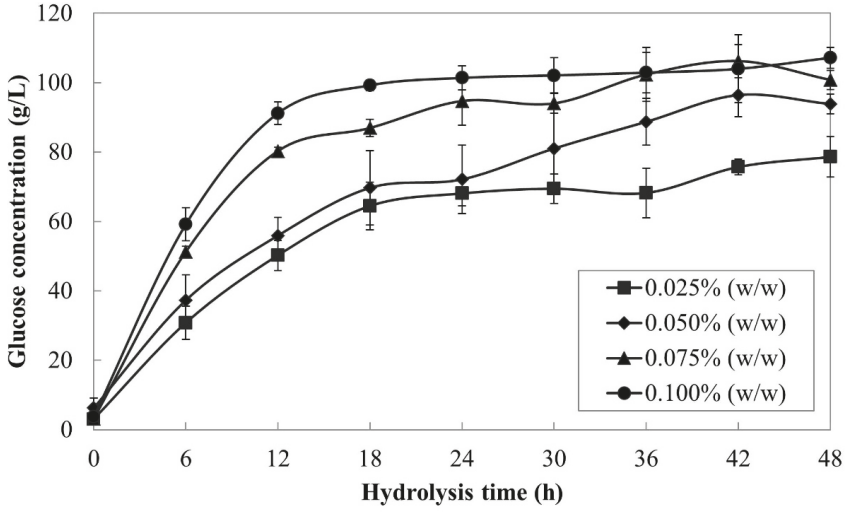

Figure 2. The effect of StargenTM002 at concentrations of 0.025% (squares), 0.050% (diamonds), 0.075% (triangles), and 0.100% (cycles) on liquefied starch hydrolysis at 40 °C with a stirring speed at 300 rpm for 24 h.

3.5. Batch Simultaneous Saccharification and Cultivation of K. marxianus SS106 in Stirred Tank Bioreactor to Produce Cells at High-Density Concentration

Many cultivation methods have been employed for an increase in yeast cell biomass. High-cell-density concentrations of yeast typically also used high concentrations of substrate aerobically, however, which can also be toxic growth inhibitors. To prevent the growth inhibition, liquefied starch (a glucose oligomer of DE 10–13) was used as a substrate for biomass production by the SSC method. Normally, glucose is the main substrate for yeast cells. It cannot directly be utilized by liquefied starch; therefore, an enzyme, StargenTM002, was supplementary and added into the medium with cultivation. During cultivation and yeast cell growth, liquefied starch was gradually hydrolyzed to release glucose by that enzyme and was gradually utilized by yeast cells.

The production of *K. marxianus* SS106 biomass was conducted in a 5-L stirred tank bioreactor containing the yeast production medium (composed of 50 g/L and 100 g/L of liquefied starch) and cultivated at 40 °C for 24 h. It can be observed that the quantities of biomass in the media using 50 g/L and 100 g/L of liquefied starch were changed in the same manner (Figure 3). The biomass concentrations were increased exponentially within the first 9 h. After that, the growths were limited and reached to the stationary phases. In contrast to the growths which were increasing from the start, glucose concentrations were slightly increased at the initial phases, after which they were rapidly

decreased. These results indicated that the rates of glucose uptake by *K. marxianus* SS106 were related to the cell growths. During SSC, glucose was continuously released by StargenTM002 activities. At the lag phases, the rates of liquefied starch hydrolyzation by the enzyme were higher than those of glucose utilizations by *K. marxianus* SS106 because of low cell concentrations at these phases resulting in slightly increased concentrations of glucose in the first 3 h of cultivations. On the other hand, after 3 h, the cultivations changed to log phases. In these times, exponential growth rates were observed. The rates of liquefied starch hydrolysis were lower than those of glucose utilizations. Therefore, glucose concentrations were steadily decreased with times in these phases.

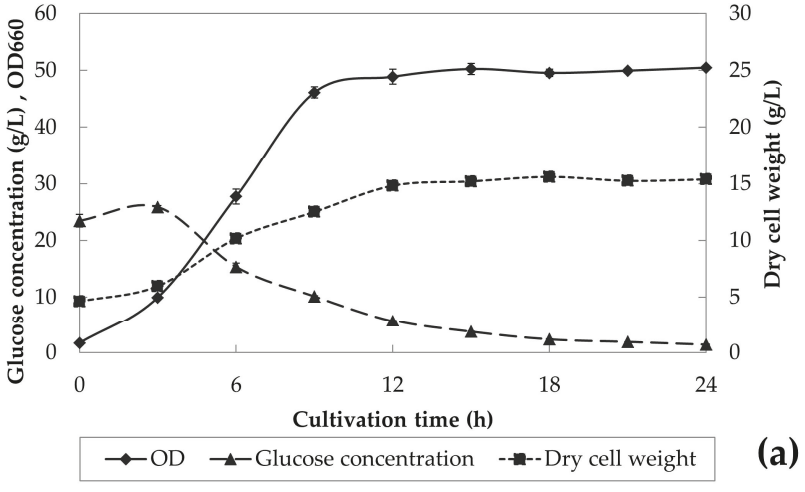

Figure 3. Changes in the optical density (diamonds), glucose (squares), and cell concentration (triangles) of *K. marxianus* SS106 in aerobic batch simultaneous saccharification and cultivation using (**a**) 50 g/L and (**b**) 100 g/L of liquefied starch as the substrate.

When compared with the previous experiments, it could be noticed that the growth rates of *K. marxianus* SS106 in the stirred tank bioreactor were much faster than that in the shake flask. Table 2 shows growth kinetic parameters of *K. marxianus* SS106 in the shake flask and in the bioreactors. It shows no significant difference between the cell biomass concentrations of the shake flask cultivation using glucose and the bioreactor using liquefied starch at the same concentration of 50 g/L as the carbon sources. However, the growth rates and the cell biomass production rates of *K. marxianus* SS106 in the bioreactors were greatly higher than those in shake flask cultivation. These results indicated that the use of liquefied starch as the carbon source for yeast cell cultivation in the bioreactor can achieve the effective growth.

The growth and productivity of *K. marxianus* SS106 increased due to the appropriate concentration of glucose in cultivation broth released from liquefied starch by StargenTM002 activities. This prevented the Crabtree effect that usually occurs in an aerobic cultivation at high glucose concentrations. Moreover, a sufficient oxygen concentration during cultivation also increased the growth. The bioreactor can control the dissolved oxygen concentration in cultivation broth, in order to keep enough saturation with the optimum aeration and agitation during the cultivation. Sufficient oxygen is important for cell growth. Oxygen is a primary electron acceptor in the electron transport chain and also effects yeast respiration. A high amount of dissolved oxygen from aeration results in an increase of cell biomass. In biomass production, the influence of oxygen supply on yeast growth at a steady state has been studied. Many research works have reported that the biomass concentration, yield coefficient, productivity, and substrate utilization rate were importantly increased by increasing the air supply [19,20].

Moreover, Table 2 also shows that there are increases of cell biomass and the production rate when increasing the liquefied starch at a concentration of 100 g/L. However, there is no significant difference between the specific growth rate of *K. marxianus* SS106 cultivated with 50 g/L of liquefied starch and that of 100 g/L. This result suggests that the increasing liquefied starch concentration improves the cell biomass, yield coefficient, and productivity of *K. marxianus* SS106. Therefore, the cell biomass of *K. marxianus* SS106 using 100 g/L of liquefied starch as the carbon source can be effectively produced by the SSC process.

3.6. Intensive Multiple Sequential Batch Simultaneous Saccharification and Cultivation of K. marxianus SS106 in Stirred Tank Bioreactor to Produce Cells at High-Density Concentration

High-cell-density cultivations are designed to achieve high product concentrations in broth by growing cells to high densities while maintaining high specific cell productivity. As a result, high-density cultivation has become an important tool in modern bioprocessing. It has been achieved with *Kluyveromyces marxianus*-improved ethanol accumulation using fed-batch technology [21].

Thus, to achieve high-cell density concentration, long-term stability and performance of simultaneous saccharification and cultivation of *K. marxianus* SS106 in the aerobic stirred tank bioreactor were carefully studied using the intensive multiple sequential batch technique. This method was performed by replacing the mature yeast culture broth with fresh medium. It can essentially promote cell biomass productivity and its growth rate as it reduces the time for growth of seed culture, inoculation, cleaning, sterilization, and other operations of the bioreactor, and avoids cessation of the process between each batch. The results obtained from eight continual cycles of intensive multiple sequential batches are presented in Figure 4 and Table 3. Each batch cycle employed in this experiment was completed after 12 h of cultivation, for a total of 96 h after eight batch cycles.

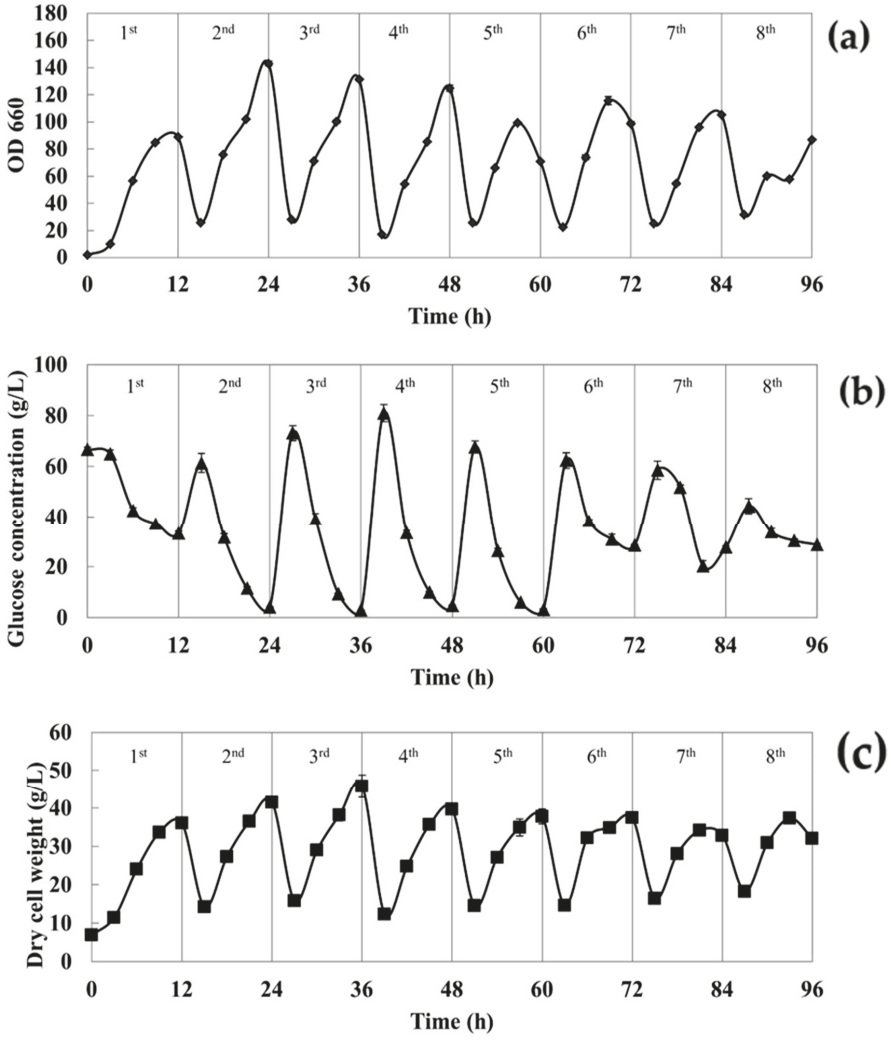

Figure 4. Changes in the optical density (**a**), glucose (**b**), and dry cell concentration (**c**) of *K. marxianus* SS106 in aerobically intensive multiple sequential batch simultaneous saccharification and cultivation using 100 g/L of liquefied starch as the substrate.

A similar trend of a decrease in the glucose concentration and subsequent increase in cell biomass production over the eight cycles of the intensive multiple sequential batch is shown in Figure 4. *K. marxianus* SS106 was, importantly, capable of continuously producing cell biomass for up to eight cycles through intensive multiple sequential batch cultivation. The adaptations of *K. marxianus* SS106 to their growth conditions were observed at the first cycle. It adapted to the new condition and medium. After that, the growth was able to stabilize, and the cell biomass kept producing until the finishing of every cycle.

Table 3. Kinetic parameters of *K. marxianus* SS106 cell biomass production undergoing intensive multiple sequential batch simultaneous saccharification and cultivation in an aerobic bioreactor.

Batch Cycles	Cell Mass Conc. (g/L)	Specific Growth Rate (h^{-1})	Yield Coefficient (g/g)	Productivity (g/L/h)
1	36.09 ± 0.38 ^{d}	0.44 ± 0.00 ^{a}	0.54 ± 0.00 ^{a}	3.01 ± 0.02 ^{c}
2	41.53 ± 1.07 ^{b}	0.35 ± 0.00 ^{c}	0.43 ± 0.00 ^{c}	3.46 ± 0.06 ^{b}
3	45.82 ± 4.27 ^{a}	0.35 ± 0.00 ^{c}	0.47 ± 0.03 ^{b}	3.82 ± 0.25 ^{a}
4	39.71 ± 0.37 ^{bc}	0.39 ± 0.00 ^{b}	0.42 ± 0.00 ^{c}	3.31 ± 0.02 ^{b}
5	37.80 ± 2.72 ^{c}	0.31 ± 0.00 ^{d}	0.39 ± 0.02 ^{d}	3.15 ± 0.16 ^{c}
6	37.42 ± 0.87 ^{c}	0.29 ± 0.00 ^{d}	0.52 ± 0.00 ^{a}	3.12 ± 0.05 ^{c}
7	32.87 ± 1.07 ^{e}	0.23 ± 0.00 ^{e}	0.45 ± 0.00 ^{b}	2.74 ± 0.06 ^{d}
8	32.07 ± 0.64 ^{e}	0.19 ± 0.00 ^{f}	0.45 ± 0.00 ^{b}	2.67 ± 0.04 ^{d}

Statistic comparisons of those values within their own columns (among batch cycles) at *p*-values of 0.05 show different characters, ^{a}, ^{b}, ^{c}, ^{d}, ^{e} and ^{f}, which mean statistically significant differences.

Table 3 shows the kinetic parameters of *K. marxianus* SS106 undergoing intensive multiple sequential batch SSC in an aerobic bioreactor. *K. marxianus* SS106 has shown its ability to undergo continual sequential batch run. The eight cycles could be operated by the intensive multiple sequential batch SSC method. During the intensive multiple sequential batch SSC, biomass production started to increase at the first cycle. Afterwards, growth was the highest at the end of third cycle and later the cell biomass slowly declined and subsequently remained nearly constant after the sixth cycle. The consistent cell biomass of 32.07–45.82 g/L with the specific growth rate of 0.19–0.44 h^{-1} and productivity of 2.67–3.82 g/L/h was obtained at the end of each cycle. During intensive multiple sequential batch SSC, cell biomass and productivity were continuously increased in the first three cycles. The highest cell biomass of 45.82 g/L and productivity of 3.82 g/L/h were clearly achieved at the end of the third cycle. No significant differences were observed ($p < 0.05$) in the values between the first and the sixth cycle, whereas low values occurred after the sixth cycle. Cell biomass and productivity after the sixth cycle were less than in the first cycle. The first and the second cycles were the climbing phases, the third was the peak, after that, they were slightly declining with more cycles and longer times. This is because the age (phase) of cells affects cell strength, growth, and yield. However, the results indicated that *K. marxianus* SS106 could tolerate the repeated use. Six cycles could be cultivated in the bioreactor from a total of eight cycles. For the averages of six cycles, a biomass of 39.73 g/L with a specific growth rate at 0.36 h^{-1} and a productivity of 3.31 g/L/h were achieved. This was essentially very high, and much higher when compared to those values of other research works, although some groups operated with fed-batch cultivation mode [22].

3.7. Single-Step Ethanol Production From Simultaneous Raw Cassava Starch Hydrolysis and Fermentation

Single-step ethanol production from especially simultaneous raw cassava starch hydrolysis and fermentation was demonstrated at 40 °C in a stirred tank fermenter containing ethanol production medium. After the additions of enzyme StargenTM002 and inoculum, the ethanol fermentation was performed at an agitation speed of 300 rpm for 72 h. It was observed that *K. marxianus* SS106 produced ethanol at a final concentration of 7.91% (*v/v*) with a productivity of 0.86 g/L/h (Figure 5). However, the fermentation completed by 48 h indicated that though it was using raw starch, the production time was still normal, as compared to general production in the industry using sugar as the raw material. The ethanol production result by this thermotolerant yeast strain was similar to that of Limtong et al. [5], who studied ethanol production at 37 °C in a 5-L jar fermenter at an agitation speed of 300 rpm and an aeration rate of 0.02 vvm. They found that *K. marxianus* DMKU 3–1042 yielded a final ethanol concentration of 8.15% (*v/v*) with a productivity of 1.3 g/L/h. In addition, here, it was interesting to

note that, except glycerol, the other by-products such as lactic acid and acetic acid were not produced when ethanol was produced at this high temperature by single-step fermentation of raw cassava starch with *K. marxianus* SS106 (data not shown). The SSF (simultaneous saccharification and fermentation) process using starch substrates is more promising, and commercial industrial production is also feasible in many countries. The advantages of the process are reduction in investment by having a single fermenter for both saccharification and fermentation. The feedback inhibition of sugars is greatly reduced. The fermentation time is very reduced in the SSF process [23].

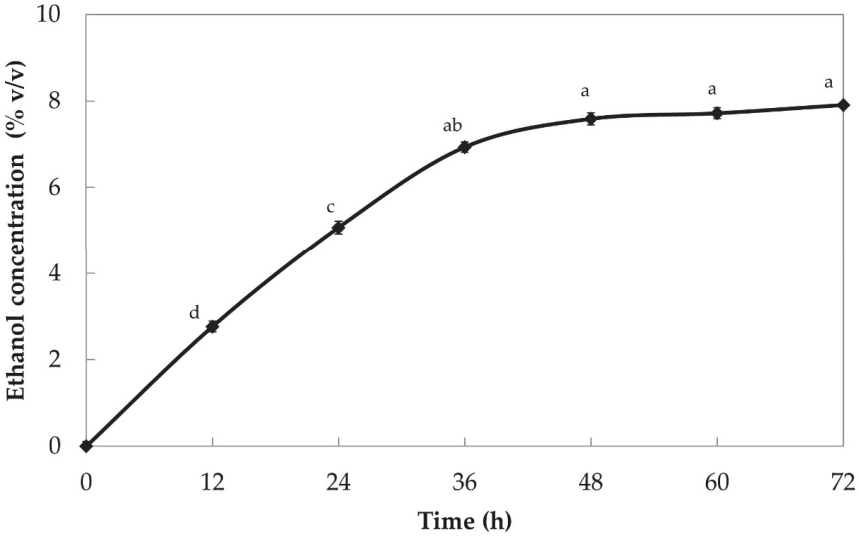

Figure 5. The yield of ethanol production by *K. marxianus* SS106 at 40 °C in 5-L fermenter using single-step ethanol fermentation. (Comparison of those values among fermentation times at *p*-value 0.05 shows different characters, a, b and c, which are statically significant difference.).

4. Conclusions

It is clear that the new isolated strain *K. marxianus* SS106 is a suitable potential strain that could be employed for single-step ethanol production using a combination of simultaneous raw cassava starch hydrolysis and fermentation. This new thermotolerant yeast strain can significantly tolerate high temperatures up to 42 °C and grows well under a wide range of pH values. For high-cell-density biomass production of *K. marxianus* SS106 in the stirred tank bioreactor, the simultaneous saccharification and aerobic cultivation using 100 g/L of liquefied starch as the substrate is an effective method. The yeast cell biomass could be produced at a concentration of 39.30 g/L with a productivity of 3.28 g/L/h and a specific growth rate of 0.49 h^{-1}. These values are very high and higher than those of other research works. Furthermore, intensive multiple sequential batch simultaneous saccharification and cultivation also shows excellent high-cell-density production. It produced the maximum yeast cell biomass at a concentration of 45.82 g/L with a productivity of 3.82 g/L/h and a specific growth rate of 0.44 h^{-1}. This method gave a high concentration of cell biomass and growth.

Again, we concluded that the advantages of this research work are as follows. (i) *K. marxianus* SS106 is the new potential industrial yeast strain. (ii) It is thermotolerant to high temperatures and low pH values. (iii) It can grow very well in both types of carbon source, i.e., liquefied starch (dextrin) and raw starch. (iv) It grows both aerobically to produce cell biomass used as an inoculum or other purposes, and anaerobically to produce ethanol, moreover, in single-step operation without acid by-products. (v) It can grow in several continual batch runs. (vi) It grows at a high rate, with high-cell

concentration, high productivity, and high efficiency, and (vii) this minimizes process steps of operation, cost, and time. (viii) It can be scaled-up to the industry.

Author Contributions: Conceptualization, K.M. and M.K.; methodology, investigation, analysis and writing—original draft preparation, R.R.; resources and data curation, S.C.; visualization and supervision S.C. All authors have read and agreed to the published version of the manuscript.

Funding: A research grant was from The Office of the Higher Education Commission. This work was also supported by the Biochemical Engineering Pilot Plant, Biological Science Graduate Program, and Department of Biology, Faculty of Science, Burapha University, Chonburi, Thailand.

Acknowledgments: The authors would like to sincerely thank Chorchiwat Industry Co., Ltd. who supported raw materials, some experiments, and analytical instruments for this study.

Conflicts of Interest: The authors declare no conflicts of interest. The funder had no role in the design of this study, analyses, or interpretation of data; in the writing of the manuscript; or in the decision to publish the experimental results.

References

1. Gohel, V.; Duan, G. No-cook process for ethanol production using Indian broken rice and pearl millet. *Int. J. Microbiol.* **2012**, *2012*, 680232. [CrossRef] [PubMed]
2. Navarrete, C.; Jacobsen, I.H.; Martínez, J.L.; Procentese, A. Cell factories for industrial production processes: current issues and emerging solutions. *Process* **2020**, *8*, 768. [CrossRef]
3. Mo, W.; Wang, M.; Zhan, R.; Yu, Y.; He, Y.; Lv, H. *Kluyveromyces marxianus* developing ethanol tolerance during adaptive evolution with significant improvements of multiple pathways. *Biotechnol. Biofuels* **2019**, *12*, 1–15. [CrossRef] [PubMed]
4. Krajang, M.; Chamsart, S. Raw cassava starch hydrolysis for single-step ethanol production using combination of raw starch hydrolysis and fermentation to pilot-scale. *Tawan-ok Res. J.* **2016**, *9*, 20–32.
5. Limtong, S.; Sringiew, C.; Yongmanitchai, W. Production of fuel ethanol at high temperature from sugar cane juice by a newly isolated *Kluyveromyces marxianus*. *Bioresour. Technol.* **2007**, *98*, 3367–3374. [CrossRef]
6. Watanabe, T.; Srichuwong, S.; Arakane, M.; Tamiya, S.; Yoshinaga, M.; Watanabe, I.; Yamamoto, M.; Ando, A.; Tokuyasu, K.; Nakamura, T. Selection of stress-tolerant yeasts for simultaneous saccharification and fermentation (SSF) of very high gravity (VHG) potato mash to ethanol. *Bioresour. Technol.* **2010**, *101*, 9710–9714. [CrossRef]
7. Cha, Y.L.; An, G.H.; Yang, J.; Moon, Y.H.; Yu, G.D.; Ahn, J.W. Bioethanol production from *Miscanthus* using thermotolerant *Saccharomyces cerevisiae* mbc 2 isolated from the respiration-deficient mutants. *Renew. Energy* **2015**, *80*, 259–265. [CrossRef]
8. Nachaiwieng, W.; Lumyong, S.; Yoshioka, K.; Watanabe, T.; Khanongnuch, C. Bioethanol production from rice husk under elevated temperature simultaneous saccharification and fermentation using *Kluyveromyces marxianus* CK8. *Biocatal. Agric. Biotechnol.* **2015**, *4*, 543–549. [CrossRef]
9. Yan, J.; Wei, Z.; Wang, Q.; He, M.; Li, S.; Irbis, C. Bioethanol production from sodium hydroxide/hydrogen peroxide-pretreated water hyacinth via simultaneous saccharification and fermentation with a newly isolated thermotolerant *Kluyveromyces marxianus* strain. *Bioresour. Technol.* **2015**, *193*, 103–109. [CrossRef]
10. Wu, W.; Hung, W.; Lo, K.; Chen, Y.; Wan, H.; Cheng, K. Bioethanol production from taro west using thermo-tolerant yeast *Kluyveromyces marxianus* K21. *Bioresour. Technol.* **2016**, *201*, 27–32. [CrossRef]
11. Alan, W.B. High-cell-density growth of microorganism. *Biotechnol. Genet. Eng.* **1994**, *12*, 535–561.
12. Bae, S.M.; Park, Y.C.; Lee, T.H.; Kweon, D.H.; Choi, J.H.; Kim, S.K.; Ryu, Y.W.; Seo, J.H. Production of xylitol by recombinant *Saccharomyces cerevisiae* containing xylose reductase gene in repeated fed-batch and cell-recycle fermentations. *Enzym. Microb. Technol.* **2004**, *35*, 545–549. [CrossRef]
13. Chamsart, S.; Sawangwon, C.; Thungkal, S.; Waiprib, Y. Enzymatic hydrolysis of cassava starch in a stirred tank lysis reactor using a high efficiency impeller. In Proceedings of the 15th Conference on Chemical Engineering and Applied Chemistry of Thailand, Pattaya Chonburi, Thailand, 27–28 October 2005.
14. Chinma, C.E.; Ariahu, C.C.; Abu, J.O. Chemical composition, functional and pasting properties of cassava starch and soy protein concentrate blends. *J. Food Sci. Technol.* **2011**, *50*, 1179–1185. [CrossRef] [PubMed]
15. Grothe, E.; Moo-Young, M.; Chisti, Y. Fermentation optimization for the production of poly (β-hydroxybutyric acid) microbial thermoplastic. *Enzym. Microb. Technol.* **1999**, *25*, 132–141. [CrossRef]

16. Choudhary, J.; Singh, S.; Nain, L. Thermotolerant fermenting yeasts for simultaneous saccharification fermentation of lignocellulosic biomass. *Electron. J. Biotechnol.* **2016**, *21*, 82–92. [CrossRef]
17. Dubey, R.; Jakeer, S.; Gaur, N.A. Screening of natural yeast isolates under the effects of stresses associated with second-generation biofuel production. *J. Biosci. Bioeng.* **2016**, *121*, 509–516. [CrossRef]
18. Moreno, A.D.; Ibarra, D.; Ballesteros, I.; Fernández, J.L.; Ballesteros, M. Ethanol from laccase-detoxified lignocellulose by the thermotolerant yeast *Kluyveromyces marxianus*—Effects of steam pretreatment conditions, process configurations and substrate loadings. *Biochem. Eng. J.* **2013**, *79*, 94–103. [CrossRef]
19. Pinheiro, R.; Belo, I.; Mota, M. Growth and β-galactosidase activity in culture of *Kluyveromyces marxianus* under increased air pressure. *Lett. Appl. Microbiol.* **2003**, *37*, 438–442. [CrossRef]
20. Blanco, C.A.; Rayo, J.; Giralda, J.M. Improving industrial full-scale production of baker's yeast by optimizing aeration control. *J. AOAC Int.* **2008**, *91*, 607–613. [CrossRef]
21. Subramaniam, R. High-density cultivation in the production of microbial products. *Chem. Biochem. Eng. Q.* **2019**, *32*, 451–464. [CrossRef]
22. Kanjanachumpol, P.; Kulpreecha, S.; Tolieng, V.; Thongchul, N. Enhancing polyhydroxybutyrate production from high cell density fed-batch fermentation of *Bacillus megaterium* BA-019. *Bioprocess Biosyst. Eng.* **2013**, *36*, 1463–1474. [CrossRef] [PubMed]
23. Kanagasabai, M.; Maruthai, K.; Thangavelu, V. Simultaneous saccharification and fermentation and factors influencing ethanol production in SSF process. In *Alcohol Fuels–Current Technologies and Future Prospect*; IntechOpen Limited: London, UK, 2020; Volume 15, pp. 1–13. [CrossRef]

processes

MDPI

Article

Microbial Communities, Metabolites, Fermentation Quality and Aerobic Stability of Whole-Plant Corn Silage Collected from Family Farms in Desert Steppe of North China

Chao Wang [1], Lin Sun [1], Haiwen Xu [2], Na Na [1], Guomei Yin [1], Sibo Liu [1], Yun Jiang [1,3] and Yanlin Xue [1,*]

[1] Inner Mongolia Engineering Research Center of Development and Utilization of Microbial Resources in Silage, Inner Mongolia Academy of Agriculture and Animal Husbandry Science, Hohhot 010031, China; wangchao200612@hotmail.co.jp (C.W.); linsun@cau.edu.cn (L.S.); nana13684752695@hotmail.com (N.N.); nmgvvip@hotmail.com (G.Y.); sbll2020@hotmail.com (S.L.); jiangyun0110@ufl.edu (Y.J.)

[2] College of Foreign Languages, Inner Mongolia University of Finance and Economics, Hohhot 010070, China; zguotong@hotmail.com

[3] Department of Animal Sciences, University of Florida, Gainesville, FL 32611, USA

* Correspondence: xueyanlin0925@Outlook.com; Tel.: +86-471-529-5628

Abstract: Whole-plant corn silages on family farms were sampled in Erdos (S1), Baotou (S2), Ulanqab (S3), and Hohhot (S4) in North China, after 300 d of ensiling. The microbial communities, metabolites, and aerobic stability were assessed. *Lactobacillus buchneri*, *Acinetobacter johnsonii*, and unclassified *Novosphingobium* were present at greater abundances than others in S2 with greater bacterial diversity and metabolites. *Lactobacillus buchneri*, *Lactobacillus parafarraginis*, *Lactobacillus kefiri*, and unclassified *Lactobacillus* accounted for 84.5%, and 88.2%, and 98.3% of bacteria in S1, S3, and S4, respectively. The aerobic stability and fungal diversity were greater in S1 and S4 with greater abundances of unclassified *Kazachstania*, *Kazachstania bulderi*, *Candida xylopsoci*, unclassified *Cladosporium*, *Rhizopus microspores*, and *Candida glabrata* than other fungi. The abundances of unclassified *Kazachstania* in S2 and *K. bulderi* in S3 were 96.2% and 93.6%, respectively. The main bacterial species in S2 were *L. buchneri*, *A. johnsonii*, and unclassified *Novosphingobium*; *Lactobacillus* sp. dominated bacterial communities in S1, S3, and S4. The main fungal species in S1 and S4 were unclassified *Kazachstania*, *K. bulderi*, *C. xylopsoci*, unclassified *Cladosporium*, *R. microspores*, and *C. glabrata*; *Kazachstania* sp. dominated fungal communities in S2 and S3. The high bacterial diversity aided the accumulation of metabolites, and the broad fungal diversity improved the aerobic stability.

Keywords: whole-plant corn silage; bacterial community; fungal community; metabolites; fermentation quality; aerobic stability

Citation: Wang, C.; Sun, L.; Xu, H.; Na, N.; Yin, G.; Liu, S.; Jiang, Y.; Xue, Y. Microbial Communities, Metabolites, Fermentation Quality and Aerobic Stability of Whole-Plant Corn Silage Collected from Family Farms in Desert Steppe of North China. *Processes* **2021**, *9*, 784. https://doi.org/10.3390/pr9050784

Academic Editor: Maria Tufariello

Received: 6 April 2021
Accepted: 27 April 2021
Published: 29 April 2021

1. Introduction

Family farms, as new agricultural business entities, partake in more commercially oriented agricultural production and management than their forerunners ("farming households") in China, even though their main labour force still consists of family members, and the major source of their income remains agricultural work [1]. Family farms are the main mode of management in the Inner Mongolian pastoral area of North China [2]. Whole-plant corn silage, alfalfa hay, grass hay, crop straw, and natural grass are the major forages of family farms in the desert steppe of Inner Mongolia. In general, these farmers ensile whole-plant corn without any additives to save processing costs [3]. Moreover, the microbial communities present in this form of whole-plant corn silage are still unclear, and understanding them is critical to explaining the fermentation quality and aerobic stability of such silage.

In the past decade, the development of next-generation sequencing technologies has helped to improve our understanding of the microbial communities present in silage [4]. *Lactobacillus* dominates the bacterial succession and determines the fermentation quality

of whole-plant corn silage during fermentation process [5,6]. The main bacterial species present in the silage at the end of the process are *Lactobacillus acetotolerans*, *Lactobacillus silagei*, *Lactobacillus parafarraginis*, *Lactobacillus buchneri*, and *Lactobacillus odoratitofui* [7]. The geographical location where at the corn was grown influences the bacterial succession process taking place in whole-plant corn silage and the bacterial community in the final silage [8,9]. Drouin et al. [10] reported that ensiling whole-plant corn with lactic acid bacteria (LAB) increases the Shannon indexes of bacterial and fungal communities and modifies the aerobic stability, and *Saccharomyces*, *Issatchenkia*, and *Kazachstania* cause aerobic deterioration during aerobic exposure. Nevertheless, the effect of the geographical location on the fungal community and the aerobic stability of whole-plant corn silage has not yet been reported on.

Recently, the silage metabolome has attracted new interest [11]. Some studies have reported the effect of inoculating on the metabolite contents of whole-plant corn silage, alfalfa silage, and sainfoin silage with LAB [6,9,12]; the dynamics of metabolites in whole-plant corn silages during fermentation process [6]; and the correlation of the main metabolites with the main bacterial species and fermentation quality in whole-plant corn silages [6]. Additionally, Wu et al. [13] analysed the metabolic profiles of high-moisture sweetcorn kernel silages. Biogenic amines—a class of metabolites in silage—affect the palatability of silages, and the feed intake and performance of ruminants [14]. However, the concentration and composition of the metabolites—especially the biogenic amines in silages on the desert steppe—remain unclear.

In the present study, whole-plant corn silages on family farms in the desert steppe of Inner Mongolia in North China were assessed after about 300 d of ensiling. The hypothesis of the present study was the differences in microbial communities, metabolites, and aerobic stability between whole-plant corn silages from different areas. The objective was to analyse the bacterial and fungal communities, the metabolites, the fermentation quality and the aerobic stability of whole-plant corn silages.

2. Materials and Methods

2.1. Sampling

The corn (*Zea mays* L.) used for ensiling came from replicates grown on 3 family farms of each sampling area (silage 1 (S1), Angsu Town, Erdos City, 108°4′29.093″ E, 38°14′24.212″ N, 1378 m; S2, Bayinhua Town, Baotou City, 109°54′15.260″ E, 42°16′34.133″ N, 1251 m; S3, Jiang'an Town, Ulanqab City, 110°51′14.249″ E, 43°10′06.845″ N, 1077 m; S4, Chengguan Town, Hohhot City, 111°39′31.784″ E, 39°55′19.160″ N, 1137 m) in Inner Mongolia (desert steppe), North China (Figure 1). The variety of corn used was 23 Yu (No, 2008022, corn hybrid, Henan Dajingjiu Seed Industry Co., Ltd., Shangqiu, China). The corn plants were harvested at the 2/3, 1/3, 1/3, and 1/2 milk-line stages in Erdos (on 15 September 2018), Baotou (on 1 September 2018), Ulanqab (on 4 September 2018), and Hohhot (on 8 September 2018), respectively according to local tradition, and chopped into 1–2 cm pieces by combine-harvester (John Deere (China) Investment Co., Ltd., Beijing, China). The chopped forages on each family farm were ensiled in a silo (length, 100 m; width, 10 m; height, 2 m) without any additives at a density of more than 700 kg/m^3. The samples of chopped forage were taken at filling to the 1/3, 1/2, and 2/3 of the length of the silo, respectively, and transported in ice boxes to the laboratory for analysis. After 30 d of ensiling, the silos were opened, and the silages were collected (around 30 cm thickness, from the front phase of the silo) for animal feeding on every morning. At about 300 d, the silages were sampled after the animals were fed. Subsamples were collected at 5 points along the face of a silo from each family farm: point 1, 1 m from the right wall, top film; point 2, 1 m from the left wall, top film; point 3, 1 m from the right wall, bottom; point 4, 1 m from the left wall, bottom; point 5, the centre of the silo's face. The subsamples (5 kg) were collected with a needle forage sampler about 30 cm long and uniformly mixed as a composite sample. The samples were transported in ice boxes to the laboratory for analysis.

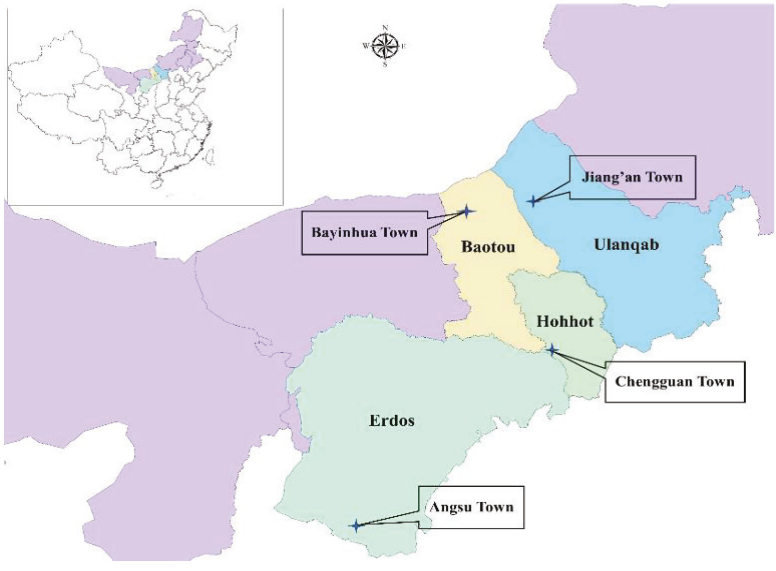

Figure 1. Map of sampling locations.

2.2. Analyses

The silage from each silo was randomly divided into 4 batches (4 kg each). Every batch from each silo was placed into a separate plastic drum (diameter, 40 cm; height, 50 cm), and the tops of the drums were covered with 2 layers of cheesecloth. One batch from each silo was used for assessing the aerobic stability, which was measured with a temperature recorder (SMOWO Multi-Channel Data Logger, MDL-1048A; Shanghai Tianhe Automation Instrument Co., Ltd., Shanghai, China) via the method of Wang et al. [15]. The recorder's temperature sensor probe was placed into the centre of the silage in the drum. The temperatures of room and silage were recorded every hour. One of the three batches from each silo was randomly selected at 0, 2, and 5 d for assessment of microbial counts and fermentation quality; the silages were assessed at 0 d for microbial communities and metabolites.

Extracts of forage or silage were prepared by homogenizing 20 g of chopped forage or silage with 180 mL of sterile water for 100 s using a flap-sterile homogenizer (LW-09, Shanghai Jingxin Industrial Development Co., Ltd., Shanghai, China) and then filtering through 2 layers of cheesecloth according to the methods of Owens et al. [16]. The pH of the extracts was detected with a pH meter (PB-10, Sartorius, Gottingen, Germany). Counts of LAB, *Escherichia coli*, bacteria, and yeast/moulds were taken by culturing on De Man Rogosa Sharpe agar, violet-red bile agar, nutrient agar, and potato dextrose agar, respectively, at 37 °C for 48 h in an incubator (LRH-70, Shanghai Yiheng Science Instruments Co., Ltd., Shanghai, China) [17]. Water-soluble carbohydrates (WSC) were measured via anthrone–sulfuric acid colorimetry using a spectrophotometer (Genesys 10; Thermo Fisher Scientific, Waltham, MA, USA) at 620 nm.

The organic acids (lactic acid, acetic acid, propionic acid, and butyric acid) in the silages were assessed using high-performance liquid chromatography (DAD, 210 nm, SPD-20A, Shimadzu Co., Ltd., Kyoto, Japan) (detector, SPD-20A diode array detector (210 nm); column, Shodex RS Pak KC-811 (50 °C, Showa Denko K.K., Kawasaki, Japan); mobile phase, 3 mM $HClO_4$ (1.0 mL/min)) [18]. The ammonia nitrogen content was determined via the Kjeldahl method using an autoanalyzer (Kjeltec 8400; FOSS Co., Ltd., Hillerød, Denmark).

The chopped forages or silages were dried using a forced-air oven (BPG-9240A, Shanghai Yiheng Scientific Instrument Co., Ltd., Shanghai, China) operated at 65 °C for

48 h, ground through a 1 mm screen with a mill (FS-6D; Fichi Machinery Equipment Co., Ltd., Jinan, Shandong, China), and then dried at 105 °C, until reaching a constant mass suitable for measuring dry matter (DM) content. The total nitrogen (TN) was assessed via the Kjeldahl method using an autoanalyzer with copper as the catalyst, and the crude protein (CP) concentration was calculated by multiplying the TN concentration by 6.25. The neutral detergent fibre (NDF) and acid detergent fibre (ADF) contents were determined via the method of Van Soest et al. [19] using an Ankom fiber analyzer (2000, Ankom, Macedon, NY, USA) without heat-stable amylase; acid detergent lignin (ADL) content was determined using a 72% H_2SO_4 solution [19].

The total bacterial DNA and fungal DNA were extracted using a DNA isolation kit (OMEGA-D4015-04) following the manufacturer's specifications. The DNA quality was evaluated via 1% (*w*/*v*) agarose gel electrophoresis. The full-length 16S rRNA gene was amplified via PCR using forward primer 5′-TAGRGTTYGATYMTGGCTCAG-3′ and reverse primer 5′-RGYTACCTTGTTACGACTT-3′; the full-length internal transcribed spacer (ITS) gene was amplified via PCR using forward primer 5′-TCCGTAGGTGAACCTGCGG-3′ and reverse primer 5′-TCCTCCGCTTATTGATATGC-3′. The amplification conditions were as follows: 95 °C for 3 min; 25 cycles of 98 °C for 20 s, 57 °C for 30 s and 72 °C for 90 s; a final extension of 72 °C for 2 min. The 16S rRNA and ITS libraries were built with a Pacific Biosciences Template Prep Kit (Pacific Biosciences, Menlo Park, CA, USA). Amplicon sequencing was performed with a PacBio Sequel instrument (Pacific Biosciences). Raw circular consensus sequencing (CCS) reads were obtain using PacBio SMRT Link CCS software. The sequence data reported in this study have been submitted to the NCBI Sequence Read Archive database under the accession number PRJNA650284.

The silage extracts were prepared as follows: 5 g silage and 10 mL extraction liquid (70% methanol) were vortexed for 30 s, oscillated for 1 h at 4 °C, filtered through a 0.22 μm membrane, and then dried to 1 mL with a vacuum concentrator in a glass vial [20]. The metabolites in the silage were analysed via liquid chromatography–electrospray ionization–tandem mass spectrometry (HPLC, Shim-pack UFLC Shimadzu CBM30A system; MS, Applied Biosystems 4500 QTRAP system) using measured silage extracts. The conditions of analysis were as follows: HPLC column, Waters ACQUITY UPLC HSS T3 C18 (1.8 μm, 2.1 mm × 100 mm); mobile phase, water (0.04% acetic acid)/acetonitrile (0.04% acetic acid); gradient program, 100:0 (*v*:*v*) at 0 min, 5:95 at 11.0 min, 5:95 at 12.0 min, 95:5 at 12.1 min, and 95:5 at 15.0 min; flow rate, 0.40 mL/min; temperature, 40 °C; injection volume, 5 μL [7]. The effluent was then connected to an ESI triple-quadrupole linear ion trap (QqQ-LIT) mass spectrometer [7]. The qualitative and quantitative analyses, the pre-processing and the determination of the relative concentrations of metabolites were all undertaken according to Yan et al. [20] and Xu et al. [6]. Biogenic amines (tyramine, putrescine, phenylethylamine, spermidine, and noradrenaline) were selected from the metabolites, and their relative concentrations were recorded.

2.3. Statistical Analyses

The data of fermentation quality and microbial count were analysed via a 4 × 3 factorial design. The model included 4 sampling areas and 3 aerobic exposure times, and their interaction. Using one-factor analysis of variance via the general linear model (GLM) of SAS (SAS System for Windows, version 9.1.3; SAS Institute Inc., Cary, NC, USA), we analysed the differences in the pH, microbial counts, and nutritional composition of fresh forage from 4 sampling areas, in the fermentation quality and microbial counts of silage among 4 sampling areas and 3 aerobic exposure times, and in the sequencing data, alpha diversity, nutritional composition, total metabolites, and biogenic amines of silage from 4 sampling areas. The interaction between the sampling area and aerobic exposure time was analysed using the PDIFF procedure of SAS. The differences were compared via least significant differences, and significance was declared at $p \leq 0.05$. The principal coordinates analysis (PCoA) of microbial beta diversity was performed using R 1.7.13 for Windows; the principal component analysis (PCA) of the metabolic profiles was performed using R 3.5.1.

3. Results

3.1. Characteristics of Whole-Plant Corns before Ensiling

The S1 and S4 had higher LAB counts than S2 and S3 ($p < 0.05$). The S2 and S3 displayed lower DM contents and greater WSC concentrations than S1 and S4 ($p < 0.05$), and S1 showed greater DM than S4 ($p < 0.05$). The S2 had the greatest level of CP, S4 contained the most NDF and ADF, and S3 had the lowest contents of ADF and ADL ($p < 0.05$) (Table 1).

Table 1. pH, microbial counts (log_{10} CFU/g fresh weight), dry matter content (DM, g/kg), and chemical component concentrations (g/kg DM) of whole-plant corn before ensiling (n = 3).

Items	S1	S2	S3	S4	SEM	*p*-Value
pH	6.05	5.99	6.03	6.08	0.027	0.160
Lactic acid bacteria	5.08b	5.78a	5.69a	5.10b	0.122	0.011
Escherichia coli	6.48	6.54	6.75	6.67	0.100	0.267
Bacteria	7.18	7.28	7.21	7.24	0.074	0.782
Yeast	6.42	6.38	6.41	6.21	0.086	0.346
DM	429a	300c	304c	318b	2.74	<0.001
Water-soluble carbohydrates	97.3b	123a	128a	106b	3.70	0.001
Crude protein	70.0b	77.8a	72.2b	67.3b	1.30	0.003
Neutral detergent fibre	483b	473b	467b	531a	4.15	<0.001
Acid detergent fibre	269b	270b	261c	281a	1.40	<0.001
Acid detergent lignin	37.8a	35.4a	28.1b	34.0a	1.18	0.002

S1, fresh corn collected from Erdos; S2, fresh corn collected from Baotou; S3, fresh corn collected from Ulanqab; S4, fresh corn collected from Hohhot. SEM, standard error of the mean. Values with different lowercase letters (a, b, and c) indicate there was a significant difference among silages.

3.2. Microbial Counts and Diversity

At 0 d of aerobic exposure, S1 and S4 showed greater LAB and yeast counts than S2 and S3 ($p < 0.05$), and S1 had a greater bacterial count than other silages ($p < 0.05$); additionally, S3 contained more LAB and yeast than S2, and fewer bacteria than S2 and S4 ($p < 0.05$) (Table 2). During aerobic exposure, the LAB counts in S2 and S3 increased ($p < 0.05$), and the bacteria and yeast counts in S1 dropped ($p < 0.05$). The bacteria count decreased at 2 d and increased at 5 d in S2 ($p < 0.05$), while it increased at 2 d and decreased at 5 d in S3 and S4 ($p < 0.05$). The aerobic exposure time affected the LAB and bacteria counts ($p < 0.05$). The sampling area influenced the counts of LAB, bacteria, and yeast ($p < 0.05$), on which the aerobic exposure time and the sampling area had a compound effect ($p < 0.05$). *Escherichia coli* and moulds were not detected in all the silages.

Totals of 166,552 and 141,221 clean reads of the full-length 16S rRNA and ITS genes, respectively, were obtained from 12 samples of whole-plant corn silage according to SMRT sequencing. The S4 had a greater number of 16S rRNA gene reads than S1 ($p < 0.05$), and these silages contained more than 10,000 clean reads. There were no differences in the numbers of clean reads of the ITS gene among the silages ($p > 0.05$), more than 10,000 clean reads were derived for each, except for S1 (9250). In terms of bacteria, S2 showed the highest Shannon and Simpson indexes among the silages, and it also had a higher Chao1 index and number of observed species than S4 ($p < 0.05$). As regards fungi, the numbers of observed species and the indexes of Shannon, Simpson and Chao1 indexes in S1 and S4 were higher than those in S2 and S3 ($p < 0.05$) (Table 3). According to PCoA, the bacterial communities in all the silages were clearly distinct from one another; however, the fungal communities in S1 and S4 were distinct from those in S2 and S3 (Figure 2).

Table 2. Microbial counts (log_{10} CFU/g fresh weight) of whole-plant corn silages during aerobic exposure (n = 3).

Items	Days	S1	S2	S3	S4	SEM	*p*-Value	*p*-Value		
								A	D	A*D
Lactic acid bacteria	0	7.95a	4.98Bc	7.03Bb	8.35a	0.273	<0.001	***	***	***
	2	8.13a	5.14Bc	7.53Bb	8.47a	0.159	<0.001			
	5	7.69b	7.03Ac	8.45Aa	8.27ab	0.185	0.002			
	SEM	0.214	0.281	0.214	0.091					
	p-value	0.389	0.004	0.009	0.373					
Bacteria	0	7.48Aa	5.92Ab	4.81Cc	6.20Cb	0.272	<0.001	***	***	***
	2	7.53Aa	4.91Bb	7.22Aa	7.92Aa	0.220	<0.001			
	5	4.81Bc	6.15Ab	6.29Bb	7.44Ba	0.119	<0.001			
	SEM	0.184	0.265	0.255	0.113					
	p-value	<0.001	0.035	0.002	<0.001					
Yeasts	0	7.73Aa	4.74c	6.57b	7.98a	0.281	0.001	***		***
	2	7.79Aa	5.36b	6.26b	7.68a	0.566	0.044			
	5	5.66Bd	6.31c	7.27b	7.84a	0.092	<0.001			
	SEM	0.103	0.633	0.353	0.085					
	p-value	<0.001	0.284	0.197	0.116					

S1, silage collected from Erdos; S2, silage collected from Baotou; S3, silage collected from Ulanqab; S4, silage collected from Hohhot. SEM, standard error of the mean. Values with different lowercase letters (a, b, c, and d) indicate there was a significant difference among silages on the same day. Values with different uppercase letters (A, B, and C) indicate there were significant differences between sampling times. A, sampling area; D, aerobic exposure time (d). ***, $p < 0.001$.

Table 3. Sequencing data and alpha diversity of bacteria and fungi in whole-plant corn silage (n = 3).

Items		S1	S2	S3	S4	SEM	*p*-Value
Bacteria	Raw reads	12,485b	14,773ab	15,728ab	17,517a	1060	0.055
	Clean reads	11,407b	12,746ab	14,549ab	16,815a	1084	0.036
	Observed species	247ab	347a	268ab	183b	25.6	0.013
	Shannon	2.71b	5.18a	2.17b	2.59b	0.180	<0.001
	Simpson	0.672c	0.911a	0.580d	0.754b	0.020	<0.001
	Chao1	398a	506a	426a	252b	41.2	0.014
Fungus	Raw reads	10,334	12,450	12,283	13,967	1203	0.279
	Clean reads	9250	12,354	12,205	13,264	1394	0.272
	Observed species	144a	73.3b	55.7b	164a	15.3	0.002
	Shannon	4.14a	0.779b	0.548b	3.67a	0.22	<0.001
	Simpson	0.874a	0.159b	0.129b	0.825a	0.020	<0.001
	Chao1	195a	112b	82.0b	193a	18.5	0.005

S1, silage collected from Erdos; S2, silage collected from Baotou; S3, silage collected from Ulanqab; S4, silage collected from Hohhot. SEM, standard error of the mean. Values with different lowercase letters (a, b, c, and d) indicate there was a significant difference among silages.

3.3. Bacterial Community

Lactobacillus dominated the bacterial communities in S1, S3, and S4 with abundances of 86.74%, 88.69%, and 98.49%, respectively. The main bacterial genera in S2 were *Lactobacillus* (28.70%), *Acinetobacter* (20.40%), *Novosphingobium* (7.80%), and *Afipia* (5.37%) (Figure 3a). The main bacterial species in S1, S3, and S4 were *L. buchneri* (52.74%, 65.79%, and 45.92%, respectively), *L. parafarraginis* (17.09%, 0.64%, and 40.06%, respectively), *Lactobacillus kefiri* (3.58%, 17.14%, and 0%, respectively) and unclassified *Lactobacillus* (11.05%, 4.68%, and 12.36%, respectively). The dominant bacterial species in S2 were *L. buchneri* (20.71%), *Acinetobacter johnsonii* (10.73%), unclassified *Novosphingobium* (7.64%), and *L. parafarraginis* (3.19%) (Figure 3b).

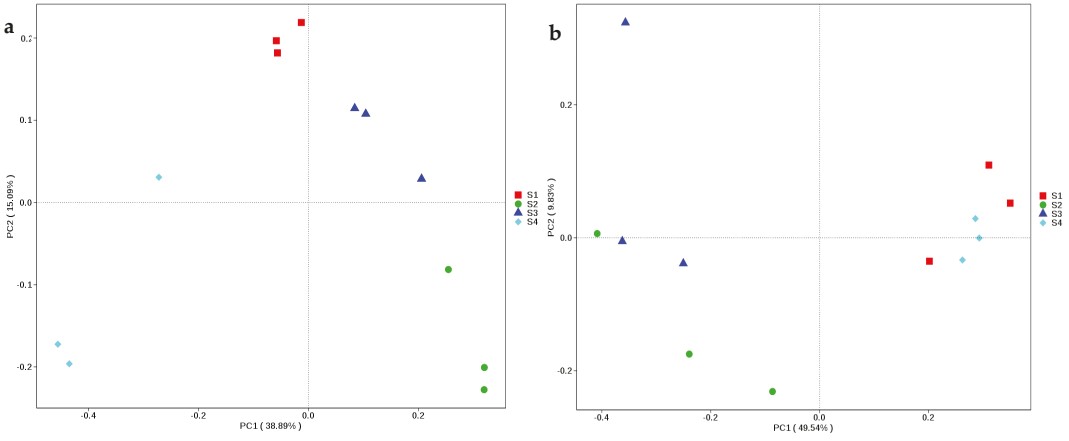

Figure 2. Non-metric multi-dimensional scaling based on Bray-Curtis assessment of bacterial (**a**) and fungal (**b**) diversities in whole-plant corn silages (n = 3). S1, silage collected from Erdos; S2, silage collected from Baotou; S3, silage collected from Ulanqab; S4, silage collected from Hohhot.

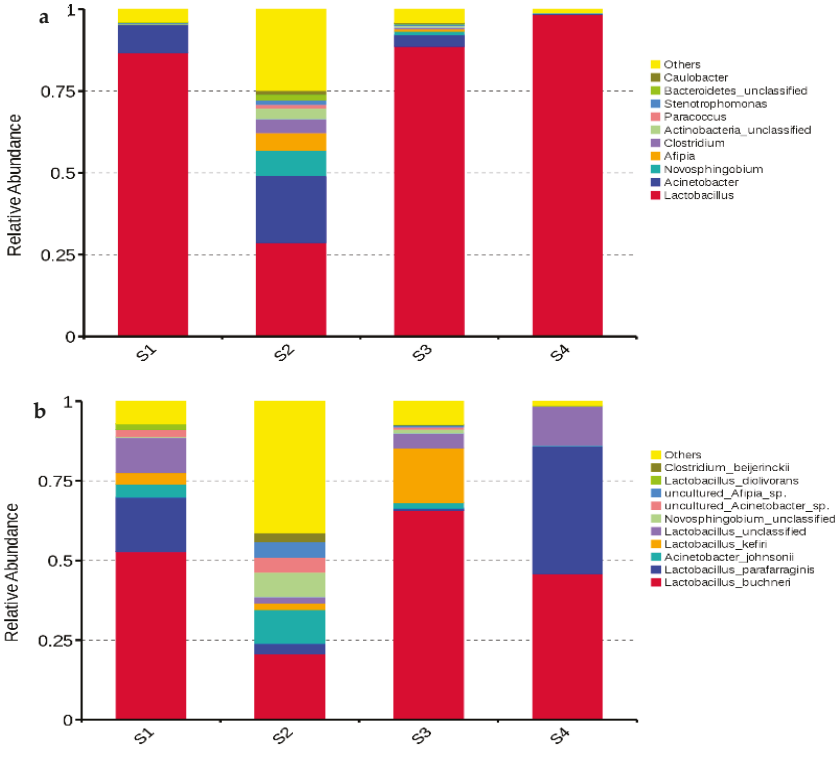

Figure 3. Relative abundances of bacterial genera (**a**) and species (**b**) in whole-plant corn silage (n = 3). S1, silage collected frm Erdos; S2, silage collected from Baotou; S3, silage collected from Ulanqab; S4, silage collected from Hohhot.

3.4. Fungal Community

The dominant fungal genus in S2 and S3 was *Kazachstania* with abundances of 97.32% and 98.24%, respectively; *Kazachstania* (54.86%) was also dominant in S4, followed by *Candida* (16.28%), *Rhizomucor* (10.56%), and *Cladosporium* (6.15%). The main fungal genera in S1 were *Candida* (42.73%), *Kazachstania* (19.34%), *Cladosporium* (13.90%), and *Rhizopus* (8.52%) (Figure 4a). The main fungal species in S1 and S4 were unclassified *Kazachstania* (15.84% and 18.72%, respectively), *Kazachstania bulderi* (3.13% and 35.53%, respectively), *Candida xylopsoci* (31.19% and 9.64%, respectively), unclassified *Cladosporium* (13.79% and 6.14%, respectively), *Rhizopus microsporus* (7.54% and 9.60%, respectively), and *Candida glabrata* (7.03% and 5.25%, respectively). The dominant fungal species in S2 was unclassified *Kazachstania* (96.21%), while *Kazachstania bulderi* (93.61%) dominated in S3 (Figure 4b).

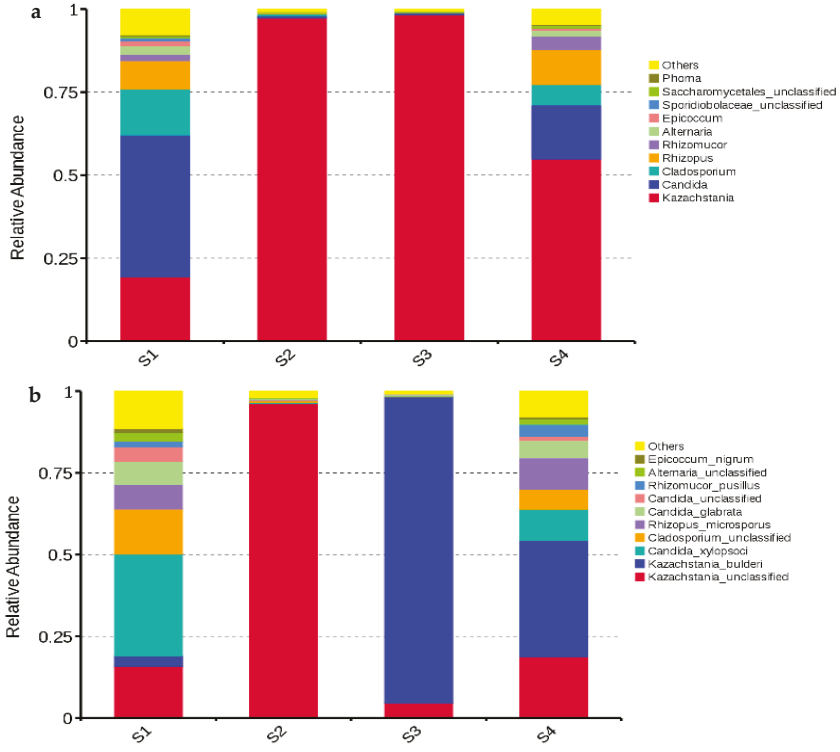

Figure 4. Relative abundances of fungal genera (**a**) and species (**b**) in whole-plant corn silage (n = 3). S1, silage collected from Erdos; S2, silage collected from Baotou; S3, silage collected from Ulanqab; S4, silage collected from Hohhot.

3.5. Metabolites

The silages collected from different sites (Erdos, Baotou, Ulanqab, and Hohhot) were clearly separated by PC1 and PC2 with 31% and 17% variation, respectively according to principal component analysis (Figure 5). A total of 668 substances were detected in 12 samples of whole-plant corn silages, which 292 substances were identified (Supplementary Table S1). The S2 had greater relative concentrations of total metabolites than other silages ($p < 0.05$) (Table 4). Five biogenic amines were detected in the whole-plant corn silages. The S2 showed the greatest abundances of phenylethylamine and spermidine among the silages ($p < 0.05$) (Table 4).

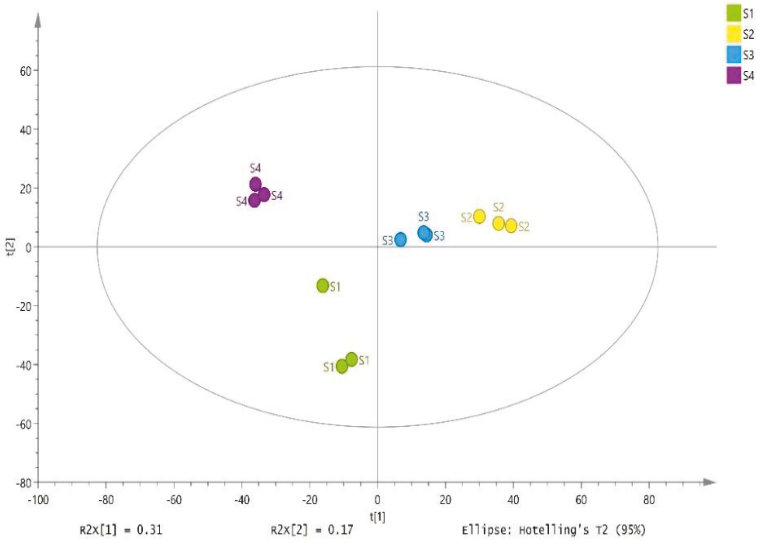

Figure 5. Principal component analysis of the metabolites in whole-plant corn silages (n = 3). S1, silage collected from Erdos; S2, silage collected from Baotou; S3, silage collected from Ulanqab; S4, silage collected from Hohhot.

Table 4. Relative concentrations of total metabolites and biogenic amines in whole-plant corn silage (n = 3).

Items		S1	S2	S3	S4	SEM	*p*-Value
Total metabolites		353b	4220a	399b	753b	571	0.004
Biogenic amines	Tyramine	10.5	107	1.30	>0	26.7	0.061
	Putrescine	3.08	34.1	2.06	>0	8.98	0.080
	Phenylethylamine	0.089b	0.804a	0.057b	0.198b	0.062	<0.001
	Spermidine	0.065b	0.518a	0.090b	>0 b	0.055	<0.001
	Noradrenaline	0.013	0.019	0.004	0.019	0.010	0.694

S1, silage collected from Erdos; S2, silage collected from Baotou; S3, silage collected from Ulanqab; S4, silage collected from Hohhot. SEM, standard error of the mean. The relative concentration of major metabolites was <0.001 and >0. Values with different lowercase letters (a and b) indicate there was a significant difference among silages.

3.6. Fermentation Quality and Chemistry Composition

At 0 d of aerobic exposure, S1 and S4 displayed higher pH and acetic acid, but lower lactic acid, than S2 and S3 ($p < 0.05$); S1 contained more lactic acid and less acetic acid than S4 ($p < 0.05$). The S3 contained less ammonia nitrogen than other silages ($p < 0.05$), and S1 and S2 contained less than S4 ($p < 0.05$). Propionic and butyric acids were not detected in the silages at 0 d of aerobic exposure (Table 5). The contents of lactic acid and ammonia nitrogen (except for in S4) decreased ($p < 0.05$) by aerobic exposure, but pH increased ($p < 0.05$) except for in S1. The acetic acid in S2 and S4 decreased ($p < 0.05$), while it decreased in S3 at 2 d and then increased at 5 d ($p < 0.05$). The aerobic exposure time and sampling area had single and interactive effects on the pH and the contents of lactic acid, acetic acid, propionic acid, and ammonia nitrogen in the silages ($p < 0.05$) (Table 5).

The DM content in S1 was higher than that in other silages ($p < 0.05$). S2 and S3 had greater CP than S1 and S4, with S1 showing higher than S4 ($p < 0.05$). The NDF concentration in S4 was greater than that in other silages ($p < 0.05$) (Table 6).

Table 5. pH, organic acid contents (g/kg dry matter) and ammonia nitrogen contents (g/kg total nitrogen) of whole-plant corn silages during aerobic exposure (n = 3).

Items	Days	S1	S2	S3	S4	SEM	*p*-Value	*p*-Value		
								A	D	A*D
pH	0	3.97a	3.61Bb	3.63Cb	3.97Ba	0.011	<0.001	***	***	***
	2	4.00a	3.69Bc	3.81Bb	4.02Ba	0.006	<0.001			
	5	4.01c	6.32Aa	4.04Ac	6.00Ab	0.051	<0.001			
	SEM	0.017	0.049	0.013	0.030					
	p-Value	0.307	<0.001	<0.001	<0.001					
Lactic acid	0	65.8Ac	124Aa	93.7Ab	53.5Ad	3.48	<0.001	***	***	***
	2	57.3ABc	121Aa	78.8Bb	49.6Ad	2.07	<0.001			
	5	46.4Ba	20.1Bbc	37.6Cab	9.70Bc	5.46	0.006			
	SEM	3.77	6.28	1.23	2.54					
	p-Value	0.029	<0.001	<0.001	<0.001					
Acetic acid	0	42.8b	28.1Ac	14.1Bd	54.6Aa	2.49	<0.001	***	***	***
	2	36.6b	23.7Bc	5.44Cd	53.1Aa	1.86	<0.001			
	5	33.1b	ND	44.1Aa	ND	0.896	<0.001			
	SEM	3.31	0.542	0.811	1.45					
	p-Value	0.118	<0.001	<0.001	<0.001					
Propionic acid	0	ND	ND	ND	ND	-	-	***	***	***
	2	ND	ND	ND	ND	-	-			
	5	1.95c	12.7Aa	ND	8.95Ab	0.726	<0.001			
	SEM	0.562	0.541	-	0.304					
	p-Valuee	0.078	<0.001	-	<0.001					
Ammonia nitrogen	0	48.1Ab	45.0Ab	39.5Ac	53.1a	1.33	<0.001	***	***	***
	2	47.4Ab	41.9Ac	40.2Ac	53.1a	0.689	<0.001			
	5	40.5Bb	28.6Bc	22.2Bd	55.2a	1.30	<0.001			
	SEM	0.841	1.38	1.10	1.20					
	p-Value	0.001	<0.001	<0.001	0.403					

S1, silage collected from Erdos; S2, silage collected from Baotou; S3, silage collected from Ulanqab; S4, silage collected from Hohhot. SEM, standard error of the mean. Values with different lowercase letters (a, b, c, and d) indicate there was a significant difference among silages on the same day. Values with different uppercase letters (A, B, and C) indicate there were significant differences among sampling times. A, sampling areas; D, aerobic exposure time (d). ***, $p < 0.001$. ND, no detected.

Table 6. Dry matter content (DM, g/kg) and chemical component concentrations (g/kg DM) of whole-plant corn silages (n = 3).

Items	S1	S2	S3	S4	SEM	*p*-Value
DM	435a	299b	305b	316b	4.20	<0.001
Water-soluble carbohydrates	12.1c	23.7b	27.2b	35.6a	1.15	<0.001
Crude protein	68.5b	72.4a	70.9a	66.7c	0.555	<0.001
Neutral detergent fibre	471b	465b	460b	526a	7.21	<0.001
Acid detergent fibre	265	267	255	266	9.87	0.832
Acid detergent lignin	35.5	31.7	21.3	33.9	4.37	0.173

S1, silage collected from Erdos; S2, silage collected from Baotou; S3, silage collected from Ulanqab; S4, silage collected from Hohhot. SEM, standard error of the mean. Values with different lowercase letters (a, b, and c) indicate there was a significant difference among silages.

3.7. Aerobic Stability

The temperatures of S1 and S4 did not exceed 2 °C above ambient temperature for 5 days after opening. The temperatures of S2 and S3 exceeded 2 °C above ambient temperature at 53 h and 39 h, respectively (Figure 6).

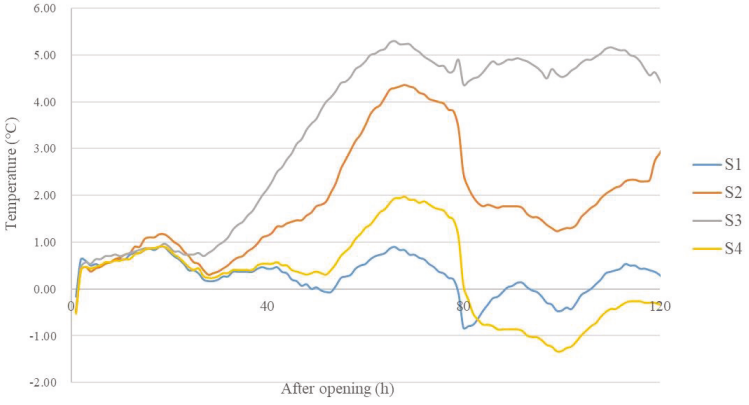

Figure 6. Temperature dynamics of silage reaching above-ambient temperature during aerobic exposure (n = 3). S1, silage collected from Erdos; S2, silage collected from Baotou; S3, silage collected from Ulanqab; S4, silage collected from Hohhot.

4. Discussion

In the present study, the materials displayed sufficient LAB counts (>5 $\log_{10}$ CFU/g FW) and WSC concentrations (>97 g/kg DM) (Table 1), resulting in a satisfactory fermentation quality for the whole-plant corn silages (Table 5). Before ensiling, S2 and S3 contained greater LAB and WSC contents and a lower DM content than S1 and S4 pre-ensiling (Table 1), indicating the conditions of the former two were more conducive to LAB fermentation during the ensiling process. This contributed to the lower pH and higher lactic acid contents in S2 and S3 (Table 5).

As the microbial community composition plays a crucial role in the fermentation quality and aerobic stability of silage, it is necessary to assess the bacterial and fungal communities in order to explain the different fermentation quality and aerobic stability among silages. In the present study, *Lactobacillus* was the most dominant bacterial genus in all silages, followed by *Acinetobacter* in S1 and S3, and by *Acinetobacter*, *Novosphingobium*, *Afipia*, *Clostridium*, and unclassified *Actinobacteria* in S2 (Figure 3a). This indicated that *Lactobacillus* is generally the dominant bacterial genus in whole-plant corn silages after ensiling for about 300 d. Moreover, previous studies also reported *Lactobacillus* at the greatest abundance in whole-plant corn silages collected from five regions in Southwest China [9] and three sites in Iran [8]. In silage with a good fermentation quality, the bacterial community is dominated by *Lactobacillus* [21], explaining the satisfactory fermentation quality of whole-plant corn silages in our study. *Acinetobacter* was found in sugarcane top silage [22], and *Novosphingobium* was detected in whole-plant corn silage [23] and red clover silage [24]. However, the effect of these genera to fermentation quality and aerobic stability are not clear and require further research.

In the present study, the main bacterial species in S2 were *L. buchneri*, *Acinetobacter johnsonii*, and unclassified *Novosphingobium* with abundances of 20.7%, 10.7% and 7.64%, respectively (Figure 3b). *Lactobacillus buchneri*, *L. parafarraginis*, *L. kefiri*, and unclassified *Lactobacillus* dominated the bacterial communities in S1, S3, and S4 with total abundances of 84.5%, 88.2%, and 98.3%, respectively (Figure 3b). The main LAB species in the silages after ensiling for about 300 d were *L. buchneri*, *L. parafarraginis*, *L. kefiri*, and *L. diolivorans* (Figure 3b), which belong to *L. buchneri* group as the sole heterofermentative LAB [25]. However, in previous studies, the main LAB species were *L. acetotolerans*, *L. silagei*, *L. buchneri*, *L. odoratitofui*, *L. farciminis*, and *L. parafarraginis* in whole-plant corn silages (90 d) with low pH (from 3.68 to 3.74) [7], *L. plantarum*, *L. buchneri*, and *L. brevisi* in alfalfa silage (90 d) with high pH (from 4.9 to 5.2) [26], *L. plantarum*, *L. hammesi*, *L. brevisi*, *L. coryniformis*, and *L. piscium* in Italian ryegrass silages (42 d) with pH ranging from 4.40 to 5.52 [10].

These studies suggested that homofermentative LAB co-existed with heterofermentative LAB in short silage (42–90 d). The differences in LAB population between our study and previous studies might result from the differences in silage age (300 d vs. 42–90 d), in the epiphytic population of bacteria on materials, and in the quality of the silages. The effects of short- and long-term storage on the microbial community and fermentation quality of silage requires further study. In the present study, the activities of heterofermentative LAB were weak in S2 and S3 under more acidic conditions (pH = 3.61 and 3.63, respectively) for a long period (about 300 d after ensiling), while they were stronger in S1 and S4 (pH 3.97). This is reflected in the higher acetic acid contents and LAB counts, and the lower lactic acid concentrations, in the latter at 0 and 2 d, along with greater aerobic stability (Table 5). The bacteria count decreased in S2 in the first 2 d, while it increased in S3 and S4 (Table 2). This might be because S2 still had a lower pH (3.69) and higher lactic acid content (121 g/kg DM) at 2 d than S1, S3, and S4 (Table 5). More acidic conditions might have reduced the bacterial activity in the silage, although the silage had been exposed to air for 2 d. *Acinetobacter johnsonii*, a known spoilage organism [27], was one of the more dominant bacterial species in S1 and S2, and it was present in S3 and S4 at low levels (Figure 3b). The effect of *A. johnsonii* on the fermentation quality and safety of silage requires further study.

The main fungal genera in S1 and S4 were *Kazachstania*, *Candida*, *Cladosporium*, *Rhizopus*, *Rhizomucor*, *Alternaria*, and *Epicoccum*, whereas *Kazachstania* dominated the fungal communities in S2 and S3 (Figure 4a). Other studies have reported dominant fungal genera of *Candida* and *Monascus* in whole-plant corn silage (90 d) [28], *Pichia*, *Sporisorium*, *Meyerozyma*, and *Hannaella* in sugarcane top silage (60 d) [22], *Issatchenki* in barley silage (60 d) [29], and *Candida*, *Kazachstania*, and *Pichia* in sugarcane top silage (90 d) [15]. These results suggest that, in contrast to the bacterial community, the dominant fungal community in the silage was different between the silages at the genera level. In the present study, *Kazachstania* dominated the fungal communities in S2 and S3 with poor aerobic stability (Figure 5). S2 and S3 had lower pH and acetic acid, and higher lactic acid than the other silages (Table 5). During aerobic exposure, the pH increased and the lactic acid decreased in S3, with acetic acid reducing at 2 d and increasing rapidly at 5 d. Between 2 and 5 d in S2, the pH increased quickly and the lactic acid decreased rapidly, with acetic acid disappearing at 5 d (Table 5). These results agree with the findings of Wang et al. for sugarcane top silage [15]. The results above indicate that *Kazachstania* might have a strong tolerance to lactic acid and be a yeast species that is crucially involved in initiating the aerobic deterioration of silage with a relatively low pH and acetic acid content. *Kazachstania* was also detected in barley silage [29] and sugarcane top silage [22] as minor taxa. *Candida* was the predominant fungal genus in S1 and S4 (Figure 4a), which had greater aerobic stability and higher acetic acid content (Table 5), and lower temperatures, than other silages (Figure 6) during aerobic exposure. However, Liu et al. [29] and Romero et al. [30] reported that a high abundance of *Candida* sp. was associated with a lower aerobic stability in silage, owing to *Candida* assimilating lactic acid after aerobic exposure [28]. The difference between our results and those of previous studies might be due to the higher acetic acid concentration in our study (42.8 g/kg) than in the studies of Romero et al. [4] and Liu et al. [29] (7.4 g/kg and 18.3 g/kg, respectively)—acetic acid inhibits fungus growth in silage and can enhance aerobic stability [4,28,30,31].

In the present study, the dominant fungal species in S1 and S4 were unclassified *Kazachstania*, *K. bulderi*, *C. xylopsoci*, unclassified *Cladosporium*, *Rhizopus microspores*, and *C. glabrata* with total abundances of 78.5% and 84.9% in fungal communities, respectively (Figure 4b). Unclassified *Kazachstania* and *K. bulderi* dominated the fungal communities in S2 and S3, respectively with abundances of 96.2% in S2 and 93.6% in S3 (Figure 4b). According to PCoA, the fungal species in S1 and S4 were connected, and were clearly separated from those of S2 and S3 (Figure 2). S1 and S4 thus had similar fungal species compositions, which were differentiated from those of S2 and S3. The differences in fungal species might be due to the differences in the fermentation processes of silage and in the epiphytic populations of fungi in the plant prior to ensiling [28]. Moreover, unclassified

Kazachstania, and *K. bulderi* belonging to *Kazachstania*, were the dominant fungi in S2 and S3, respectively (Figure 4b), and they had poor aerobic stability (Figure 6). This indicates that the aerobic deterioration taking place in the two silages might result from *Kazachstania* sp. growth after opening. Wang et al. [15] found *K. humilis* to be the key fungal yeast initiating aerobic deterioration in sugarcane top silage. *Kazachstania bulderi* was the predominant fungus in S3 and S4 in the present study. This strain was formerly named *Saccharomyces bulderi* [32] and was first isolated from maize silage as a novel species [33]. The present study first detected *C. xylopsoci*, *R. microspores*, and *Rhizomucor pusillus* in the silage in the form of fungal pathogens. *Candida xylopsoci* is usually isolated via fuel ethanol fermentation processes [34], *R. microsporus* has been detected in the traditional Chinese liquor *Daqu* using 18S rRNA gene sequencing [35], and *R. pusillus* has been identified in immunocompromised patients using real-time PCR [36]. The effects of these fungi on the fermentation quality and aerobic stability of silage should be investigated in future studies.

Moreover, Drouin et al. [10] revealed that ensiling whole-plant corn with LAB inoculant improved the aerobic stability of the silage, by maintaining a higher microbial diversity (Shannon index of bacteria and fungi), avoiding the dominance of a few bacteria, and preventing fungi from damaging silage quality. However, in the present study, the fungal communities in S1 and S4 had higher Shannon, Simpson, and Chao1 indexes, and greater aerobic stability, than S2 and S3, but the bacterial communities in S1, S3, and S4 had lower Shannon, Simpson, and Chao1 indexes than S2 (Table 3, Figure 6). This suggests that high fungal diversity, rather than bacterial diversity, contributes most significantly to aerobic stability in whole-plant corn silage.

S2 displayed the highest bacterial Shannon and Simpson indexes among the silages (Table 3), suggesting S2 had greater bacterial diversity in the present study. Additionally, the relative concentration of total metabolites in S2 was the highest among the silages (Table 4), and containing 93, 103, and 81 more metabolites identified than S1, S3, and S4, respectively (Supplementary Tables S2–S4). Previous studies showed that inoculating with LAB at ensiling increased the relative concentrations of some metabolites (e.g., organic acids, amino acids, and fatty acids) as well as the α-diversity (Shannon index) in whole-plant corn silages, sainfoin silages, and alfalfa silages [6,7,9,12]. This indicates that the high bacterial diversity might contribute to the accumulation of metabolites in whole-plant corn silages during fermentation process.

Biogenic amines in silages are produced by the decarboxylation of amino acids via the activities of plant enzymes and microbial enzymes, which accumulate during fermentation process and influence the palatability of silages, as well as the feed intake and performance of ruminants [14,37,38]. The intake of adequate amounts of biogenic amines can promote normal physiological activities in man and animals, but excessive amounts may result in food poisoning [38]. In the present study, tyramine, putrescine, phenylethylamine, spermidine, and noradrenaline were detected in whole-plant corn silages; the relative concentrations of tyramine and putrescine were considerable in S1, S2 and S3. Steidlová and Kalac also found that the concentrations of tyramine and putrescine were greater than those of histamine, cadaverine, tryptamine, spermidine and spermine in maize silages in 1999 (62 silages) and 2000 (51 silages) [14]. Nishino et al. [37] reported that inoculating with *Lactobacillus casei* reduced the concentrations of biogenic amines (histamine, tyramine, putrescine and cadaverine) in grass silage, maize silage, and total mixed ration silage, and that adding *L. buchneri* lowered the contents of biogenic amines in grass silages. Additionally, the activities of some undesirable bacterial genera (*Clostridia*, *Bacillus*, *Klebsiella*, *Escherichia*, *Pseudomonas*, *Citrobacter*, *Proteus*, *Salmonella*, *Shigella*, and *Photobacterium*) might result in the accumulation of biogenic amines in silages during ensiling [38,39]. In the present study, S2 contained higher *Bacillus*, *Pseudomonas*, and *Salmonella* contents than other silages, and greater *Escherichia* and *Klebsiella* than S3 and S4 (Supplementary Table S5), which might explain the higher relative concentrations of biogenic amines in S2 (Table 4).

5. Conclusions

Whole-plant corn silages showed a satisfactory fermentation quality after 300 d of ensiling. The main bacterial species in S2 were *L. buchneri*, *Acinetobacter johnsonii*, and unclassified *Novosphingobium*, while *L. buchneri*, *L. parafarraginis*, *L. kefiri*, and unclassified *Lactobacillus* dominated the bacterial communities in S1, S3, and S4. The main fungal species in S1 and S4 were unclassified *Kazachstania*, *K. bulderi*, *C. xylopsoci*, unclassified *Cladosporium*, *R. microspores*, and *C. glabrata*, while unclassified *Kazachstania* and *K. bulderi* dominated the fungal communities in S2 and S3, respectively, and were associated with these silages' poor aerobic stability. In whole-plant corn silage, high bacterial diversity helps the accumulation of metabolites, and high fungal diversity contributes to an improved aerobic stability.

Supplementary Materials: The following are available online at https://www.mdpi.com/article/10.3390/pr9050784/s1, Supplementary Table S1. Relative concentration of metabolites detected in whole-plant corn silages (n = 3). S1, silage collected from Erdos; S2, silage collected from Baotou; S3, silage collected from Ulanqab; S4, silage collected from Hohhot. (page: 1–16). Supplementary Table S2. Difference in metabolites identified between S1 and S2 (n = 3). S1, silage collected from Erdos; S2, silage collected from Baotou. (page: 17–19). Supplementary Table S3. Difference in metabolites identified between S2 and S3 (n = 3). S2, silage collected from Baotou; S3, silage collected from Ulanqab. (page: 20–22). Supplementary Table S4. Difference in metabolites identified between S2 and S4 (n = 3). S2, silage collected from Baotou; S4, silage collected from Hohhot. (page: 23–25). Supplementary Table S5. Relative abundance of *Bacillus*, *Pseudomonas*, *Escherichia*, *Klebsiella*, and *Salmonella* in whole-plant corn silages (n = 3). S1, silage collected from Erdos; S2, silage collected from Baotou; S3, silage collected from Ulanqab; S4, silage collected from Hohhot. (page: 26).

Author Contributions: Conceptualization, C.W. and Y.X.; methodology, C.W.; software, L.S.; validation, C.W. and L.S.; formal analysis, L.S., H.X., and N.N.; investigation, C.W. and L.S.; resources, G.Y. and S.L.; data curation, S.L., H.X., and N.N.; writing—original draft preparation, C.W.; writing—review and editing, H.X., Y.J., and Y.X.; visualization, G.Y.; supervision, Y.X.; project administration, Y.X.; funding acquisition, Y.X. All authors have read and agreed to the published version of the manuscript.

Funding: This study was funded by the National Key R&D Program of China (grant number, 2017YFE0104300) and the Science and Technology Project of Inner Mongolia (grant number, 2020GG0049).

Institutional Review Board Statement: Not applicable.

Informed Consent Statement: Informed consent was obtained from all subjects involved in the study.

Data Availability Statement: The data presented in this study are available on request from the corresponding author.

Conflicts of Interest: The authors declare no conflict of interest.

References

1. Gong, T.; Battese, G.E.; Villano, R.A. Family farms plus cooperatives in China: Technical efficiency in crop production. *J. Asian Econ.* **2019**, *64*, 101129. [CrossRef]
2. Sachurina. The change of the pastoral management mode in Inner Mongolia: Joint households, cooperatives, household pastures and corporations. *J. Arid Land Resour. Environ.* **2017**, *31*, 56–63. [CrossRef]
3. Wang, R.Z. Rational Forage and Livestock Allocation of Household Ranch in Inner Mongolia Pastoral Area. Master's Thesis, Inner Mongolia Agricultural University, Hohhot, China, 2017.
4. Romero, J.J.; Joo, Y.; Park, J.; Tiezzi, F.; Gutierrez-Rodriguez, E.; Castillo, M.S. Bacterial and fungal communities, fermentation, and aerobic stability of conventional hybrids and brown midrib hybrids ensiled at low moisture with or without a homo- and heterofermentative inoculant. *J. Dairy Sci.* **2018**, *101*, 3057–3076. [CrossRef]
5. Sun, L.; Bai, C.; Xu, H.; Na, N.; Jiang, Y.; Yin, G.; Liu, S.; Xue, Y. Succession of bacterial community during the initial aerobic, intense fermentation, and stable phases of whole-plant corn silages treated with lactic acid bacteria suspensions prepared from other silages. *Front. Microbiol.* **2021**, *12*, 655095. [CrossRef] [PubMed]
6. Xu, D.; Wang, N.; Rinne, M.; Ke, W.; Weinberg, Z.G.; Da, M.; Bai, J.; Zhang, Y.; Li, F.; Guo, X. The bacterial community and metabolome dynamics and their interactions modulate fermentation process of whole crop corn silage prepared with or without inoculants. *Microb. Biotechnol.* **2020**. [CrossRef]

7. Xu, D.; Ding, W.; Ke, W.; Li, F.; Zhang, P.; Guo, X. Modulation of metabolome and bacterial community in whole crop corn silage by inoculating homofermentative *Lactobacillus plantarum* and heterofermentative *Lactobacillus buchneri*. *Front. Microbiol.* **2019**. [CrossRef]
8. Gharechahi, J.; Kharazian, Z.A.; Sarikhan, S.; Jouzani, G.S.; Aghdasi, M.; Salekdeh, G.H. The dynamics of the bacterial communities developed in maize silage. *Microb. Biotechnol.* **2017**, *10*, 1663–1676. [CrossRef]
9. Guan, H.; Yan, Y.; Li, X.; Li, X.; Shuai, Y.; Feng, G.; Ran, Q.; Cai, Y.; Li, Y.; Zhang, X. Microbial communities and natural fermentation of corn silages prepared with farm bunker-silo in Southwest China. *Bioresour. Technol.* **2018**, *265*, 282–290. [CrossRef]
10. Drouin, P.; Tremblay, J.; Renaud, J.; Apper, E. Microbiota succession during aerobic stability of maize silage inoculated with *Lentilactobacillus buchneri* NCIMB 40788 and *Lentilactobacillus hilgardii* CNCM-I-4785. *MicrobiologyOpen* **2020**, *10*, e1153. [CrossRef]
11. Wilkinson, J.M.; Muck, R.E. Ensiling in 2050: Some challenges and opportunities. *Grass Forage sci.* **2019**, *74*, 178–187. [CrossRef]
12. Xu, D.; Ding, Z.; Wang, M.; Bai, J.; Ke, W.; Zhang, Y.; Guo, X. Characterization of the microbial community, metabolome and biotransformation of phenolic compounds of sainfoin (*Onobrychis viciifolia*) silage ensiled with or without inoculation of *Lactobacillus plantarum*. *Bioresour. Technol.* **2020**, *316*, 123910. [CrossRef]
13. Wu, Z.; Luo, Y.; Bao, J.; Luo, Y.; Yu, Z. Additives affect the distribution of metabolic profile, microbial communities and antibiotic resistance genes in high-moisture sweet corn kernel silage. *Bioresour. Technol.* **2020**, *315*, 123821. [CrossRef] [PubMed]
14. Steidlová, Š.; Kalac, P. Levels of biogenic amines in maize silages. *Anim. Feed Sci. Technol.* **2002**, *102*, 197–205. [CrossRef]
15. Wang, T.; Teng, K.; Cao, Y.; Shi, W.; Xuan, Z.; Zhou, J.; Zhang, J.; Zhong, J. Effects of *Lactobacillus hilgardii* 60TS-2, with or without homofermentative *Lactobacillus plantarum* B90, on the aerobic stability, fermentation quality and microbial community dynamics in sugarcane top silage. *Bioresour. Technol.* **2020**, *312*, 123600. [CrossRef]
16. Owens, V.N.; Albrecht, K.A.; Muck, R. EProtein degradation and ensiling characteristics of red clover and alfalfa wilted under varying levels of shade. *Can. J. Plant Sci.* **1999**, *79*, 209–222. [CrossRef]
17. Cai, Y. Identification and characterization of *Enterococcus* species isolated from forage crops and their influence on silage fermentation. *J. Dairy Sci.* **1999**, *82*, 2466–2471. [CrossRef]
18. Zhang, Q.; Li, X.J.; Zhao, M.M.; Yu, Z. Isolating and evaluating lactic acid bacteria strains for effectiveness of *Leymus chinensis* silage fermentation. *Lett. Appl. Microbiol.* **2014**, *59*, 391–397. [CrossRef]
19. Van Soest, P.J.; Robertson, J.B.; Lewis, B.A. Methods for dietary fiber neutral detergent fiber and nonstarch polysaccharides in relation to animal nutrition. *J. Dairy Sci.* **1991**, *74*, 3583–3594. [CrossRef]
20. Yan, N.; Du, Y.; Liu, X.; Chu, M.; Shi, J.; Zhang, H.; Liu, Y. A comparative UHPLCQqQ-MS-based metabolomics approach for evaluating Chinese and North American wild rice. *Food Chem.* **2019**, *275*, 618–627. [CrossRef] [PubMed]
21. McEniry, J.; O'Kiely, P.; Clipson, N.; Forristal, P.; Doyle, E. Bacterial community dynamics during the ensilage of wilted grass. *J. Appl. Microbiol.* **2008**, *105*, 359–371. [CrossRef] [PubMed]
22. Zhang, L.; Zhou, X.; Gu, Q.; Liang, M.; Mu, S.; Zhou, B.; Huang, F.; Lin, B.; Zou, C. Analysis of the correlation between bacteria and fungi in sugarcane tops silage prior to and after aerobic exposure. *Bioresour. Technol.* **2019**, *291*, 121835. [CrossRef] [PubMed]
23. Zhang, Y.; Liu, Y.; Meng, Q.; Zhou, Z.; Wu, H. A mixture of potassium sorbate and sodium benzoate improved fermentation quality of whole-plant corn silage by shifting bacterial communities. *J. Appl. Microbiol.* **2020**, *128*, 1312–1323. [CrossRef] [PubMed]
24. Ali, N.; Wang, S.; Zhao, J.; Dong, Z.; Li, J.; Nazar, M.; Shao, T. Microbial diversity and fermentation profile of red clover silage inoculated with reconstituted indigenous and exogenous epiphytic microbiota. *Bioresour. Technol.* **2020**, 123606. [CrossRef] [PubMed]
25. Muck, R.E.; Nadeau, E.M.G.; McAllister, T.A.; Contreras-Govea, F.E.; Santos, M.C.; Kung, L. Silage review: Recent advances and future uses of silage additives. *J. Dairy Sci.* **2018**, *101*, 3980–4000. [CrossRef]
26. Guo, X.S.; Ke, W.C.; Ding, W.R.; Ding, L.M.; Xu, D.M.; Wang, W.W.; Zhang, P.; Yang, F.Y. Profiling of metabolome and bacterial community dynamics in ensiled *Medicago sativa* inoculated without or with *Lactobacillus plantarum* or *Lactobacillus buchneri*. *Sci. Rep.* **2018**, *8*, 357. [CrossRef]
27. Wang, X.Y.; Xie, J. Assessment of metabolic changes in *Acinetobacter johnsonii* and *Pseudomonas fluorescens* co-culture from bigeye tuna (*Thunnus obesus*) spoilage by ultrahigh-performance liquid chromatography-tandem mass spectrometry. *LWT Food Sci. Technol.* **2020**, *123*, 109073. [CrossRef]
28. Keshri, J.; Chen, Y.; Pinto, R.; Kroupitski, Y.; Weinberg, Z.G.; Sela, S. Microbiome dynamics during ensiling of corn with and without *Lactobacillus plantarum* inoculant. *Appl. Microbiol. Biot.* **2018**, *102*, 4025–4037. [CrossRef] [PubMed]
29. Liu, B.; Huan, H.; Gu, H.; Xu, N.; Shen, Q.; Ding, C. Dynamics of a microbial community during ensiling and upon aerobic exposure in lactic acid bacteria inoculation-treated and untreated barley silages. *Bioresour. Technol.* **2019**, *273*, 212–219. [CrossRef] [PubMed]
30. Romero, J.J.; Zhao, Y.; Balseca-Paredes, M.A.; Tiezzi, F.; Gutierrez-Rodriguez, E.; Castillo, M.S. Laboratory silo type and inoculation effects on nutritional composition, fermentation, and bacterial and fungal communities of oat silage. *J. Dairy Sci.* **2017**, *100*, 1812–1828. [CrossRef]
31. Li, Y.; Nishino, N. Effects of inoculation of *Lactobacillus rhamnosus* and *Lactobacillus buchneri* on fermentation, aerobic stability and microbial communities in whole crop corn silage. *Grassl. Sci.* **2011**, *57*, 184–191. [CrossRef]
32. Boyaci-Gunduz, C.P.; Erten, H. Predominant yeasts in the sourdoughs collected from some parts of Turkey. *Yeast* **2020**, *37*. [CrossRef] [PubMed]

33. Middelhoven, W.J.; Kurtzman, C.P.; Vaughan-Martini, A. *Saccharomyces bulderi* sp. nov., a yeast that ferments gluconolactone. *Antonie Van Leeuwenhoek* **2000**, *77*, 223–228. [CrossRef] [PubMed]
34. Basilio, A.C.M.; de Araujo, P.R.L.; de Morais, J.O.F.; da Silva Filho, E.A.; de Morais, M.A.; Simoes, D.A. Detection and identification of wild yeast contaminants of the industrial fuel ethanol fermentation process. *Curr. Microbiol.* **2008**, *56*, 322–326. [CrossRef] [PubMed]
35. Yan, S.; Chen, X.; Guang, J. Bacterial and fungal diversity in the traditional Chinese strong flavour liquor *Daqu*. *J. Inst. Brew.* **2019**, *125*, 443–452. [CrossRef]
36. Hadaschik, E.; Koschny, R.; Willinger, B.; Hallscheidt, P.; Enk, A.; Hartschuh, W. Pulmonary, rhino-orbital and cutaneous mucormycosis caused by *Rhizomucor pusillus* in an immunocompromised patient. *Clin. Exp. Dermatol.* **2012**, *37*, 355–357. [CrossRef]
37. Nishino, N.; Hattori, H.; Wada, H.; Touno, E. Biogenic amine production in grass, maize and total mixed ration silages inoculated with *Lactobacillus casei* or *Lactobacillus buchneri*. *J. Appl. Microbiol.* **2007**, *103*, 325–332. [CrossRef] [PubMed]
38. Scherer, R.; Gerlach, K.; Südekum, K.H. Biogenic amines and gamma-amino butyric acid in silages: Formation, occurrence and influence on dry matter intake and ruminant production. *Anim. Feed Sci. Technol.* **2015**, *210*, 1–16. [CrossRef]
39. Santos, M.H.S. Biogenic amines: Their importance in foods. *Int. J. Food Microbiol.* **1996**, *29*, 213–231. [CrossRef]

processes

MDPI

Article

Bacterial Succession Pattern during the Fermentation Process in Whole-Plant Corn Silage Processed in Different Geographical Areas of Northern China

Chao Wang [1,†], Hongyan Han [2,†], Lin Sun [1], Na Na [1], Haiwen Xu [3], Shujuan Chang [4], Yun Jiang [5] and Yanlin Xue [1,*]

1 Inner Mongolia Engineering Research Center of Development and Utilisation of Microbial Resources in Silage, Inner Mongolia Academy of Agriculture and Animal Husbandry Science, Hohhot 010031, China; wangchao200612@hotmail.co.jp (C.W.); linsun@cau.edu.cn (L.S.); nana13684752695@hotmail.com (N.N.)
2 State Key Laboratory of Reproductive Regulation and Breeding of Grassland Livestock, School of Life Sciences, Inner Mongolia University, Hohhot 010070, China; hanhongyan1018@Outlook.com
3 College of Foreign Languages, Inner Mongolia University of Finance and Economics, Hohhot 010070, China; xhw@imufe.edu.cn
4 Inner Mongolia Key Laboratory of Remote Sensing of Grassland and Emergency Response Technic, Inner Mongolia Forestry and Grassland Monitoring and Planning Institute, Hohhot 010020, China; schang9@emich.edu
5 Department of Animal Sciences, University of Florida, Gainesville, FL 32611, USA; jiangyun0110@ufl.edu
* Correspondence: xueyanlin0925@Outlook.com; Tel.: +86-471-5295628
† These authors have contributed equally to this study and share first authorship.

Abstract: Whole-plant corn silage is a predominant forage for livestock that is processed in Heilongjiang province (Daqing city and Longjiang county), Inner Mongolia Autonomous Region (Helin county and Tumet Left Banner) and Shanxi province (Taigu and Shanyin counties) of North China; it was sampled at 0, 5, 14, 45 and 90 days after ensiling. Bacterial community and fermentation quality were analysed. During fermentation, the pH was reduced to below 4.0, lactic acid increased to above 73 g/kg DM ($p < 0.05$) and *Lactobacillus* dominated the bacterial community and had a reducing abundance after 14 days. In the final silages, butyric acid was not detected, and the contents of acetic acid and ammonia nitrogen were below 35 g/kg DM and 100 g/kg total nitrogen, respectively. Compared with silages from Heilongjiang and Inner Mongolia, silages from Shanxi contained less *Lactobacillus* and more *Leuconostoc* ($p < 0.05$), and had a separating bacterial community from 14 to 90 days. *Lactobacillus* was negatively correlated with pH in all the silages ($p < 0.05$), and positively correlated with lactic and acetic acid in silages from Heilongjiang and Inner Mongolia ($p < 0.05$). The results show that the final silages had satisfactory fermentation quality. During the ensilage process, silages from Heilongjiang and Inner Mongolia had similar bacterial-succession patterns; the activity of *Lactobacillus* formed and maintained good fermentation quality in whole-plant corn silage.

Keywords: whole-plant corn silage; bacterial community; succession pattern; fermentation quality; fermentation process

Citation: Wang, C.; Han, H.; Sun, L.; Na, N.; Xu, H.; Chang, S.; Jiang, Y.; Xue, Y. Bacterial Succession Pattern during the Fermentation Process in Whole-Plant Corn Silage Processed in Different Geographical Areas of Northern China. *Processes* **2021**, *9*, 900. https://doi.org/10.3390/pr9050900

Academic Editors: Maria Tufariello and Francesco Grieco

Received: 28 April 2021
Accepted: 19 May 2021
Published: 20 May 2021

1. Introduction

Ensiling fresh crops is an advanced technology for storing forage and supplying higher-quality forage to livestock throughout the year [1–4]. Compared with hay, silage exhibits greater dry-matter digestibility, metabolizable energy and crude-protein content, which contribute to improved liveweight gain [5].

In recent decades, whole-plant corn silage has become the predominant forage for the global dairy industry [6]. The characteristics of whole-plant corn silage are good fermentation quality and high energy, along with physically effective fibre, lower harvesting costs, minimised risks of production, elevated yield per area and flexibility to harvest corn for forage or grain [6–9]. In addition, more than 133 million dairy cattle globally consume

about 665 million tons of silage each year, and whole-plant corn silage accounts for more than 40% of forage in dairy cattle farms [10,11].

Previous studies focused on the effects of the growing location and storing temperature on microbial communities and/or succession in whole-plant corn silage [2,12,13]. Gharechahi et al. [12] studied the dynamics of bacterial communities during the ensilage process in whole-plant corn silages obtained from Gorgan (temperate), Isfahan (warm and dry) and Qazvin (cold and dry) in Iran. Guan et al. [2] found different microbial communities in whole-plant corn that originated from five major ecological areas of the provinces of Sichuan, Chongqing and Guizhou in Southwest China. Additionally, high temperature affected the dynamics of the bacterial community in whole-plant corn silage, and resulted in a shift from a homofermentative to a heterofermentative lactic acid bacteria (LAB) population [13]. Moreover, most researchers are interested in the dynamics of microbial communities during the fermentation process in whole-plant corn silage with or without inoculants. Sun et al. [9] reported on bacterial succession in whole-plant corn silage during the initial aerobic, intense fermentation and stable phases. The study also found the LAB fermentation relay during the fermentation process, which was reflected by *Weissella*, *Lactococcus* and *Leuconostoc* in the first 5 h; *Weissella*, *Lactococcus*, *Leuconostoc*, *Lactobacillus* and *Pediococcus* between 5 and 24 h; *Lactobacillus* from 24 h to 60 days [9]. In addition, other studies revealed that adding LAB inoculants could promote bacterial-community succession, improve fermentation quality, and contribute to the accumulation of metabolites in whole-plant corn silage [11,14–17].

Heilongjiang, Inner Mongolia and Shanxi were among the top five provinces regarding whole-plant corn silage production in China in 2016 [18]. In addition, Heilongjiang has a temperate monsoon climate, and Inner Mongolia and Shanxi have a temperate continental climate. We hypothesised that there were differences in bacterial-succession patterns in whole-plant corn silage from different geographical locations. Thus, the objectives of this study were to determine changes in bacterial communities during the fermentation process in whole-plant corn silages processed in Heilongjiang, Inner Mongolia and Shanxi of North China.

2. Materials and Methods

2.1. Materials and Silage Preparation

The corn (*Zea mays* L.) plants used for ensiling were raised in experimental farms at 6 locations in 3 areas of North China: Heilongjiang province (Daqing city (H_D; 124°43′42.074″ E, 46°18′32.083″ N) and Longjiang county (H_L; 123°7′32.120″ E, 47°21′23.396″ N), cold and wet agricultural area), Inner Mongolia Autonomous Region (Helin county (I_H; 111°36′21.625″ E, 40°28′47.672″ N) and Tumet Left Banner (I_T; 111°9′31.399″ E, 40°41′29.832″ N), temperate and dry pastoral area) and Shanxi province (Taigu (S_T; 112°37′53.792″ E, 37°25′57.230″ N) and Shanyin (S_S; 112°52′06.676″ E, 39°32′54.503″ N) counties, temperate and dry agricultural area) (Figure 1). The variety of corn was 23 Yu for ensiling (no. 2008022, Henan Dajingjiu Seed Industry Co., Ltd., Shangqiu, China). Corn was harvested from 3 fields as replicates in each location; the harvesting stage according to local tradition was 1/3, 1/2 and 1/2 milk-line stage in Heilongjiang, Inner Mongolia and Shanxi, respectively. After harvesting, fresh forage from each field was chopped into 1 to 2 cm pieces using a chaff cutter (Hongguang Industry &Trade Co. Ltd., Ningbo Zhejiang, China), uniformly mixed and randomly divided into 5 batches (500 g per batch) that were ensiled in 5 plastic bags sealed with a vacuum sealer. Silage bags (500 g per bag) were stored at ambient temperature (22 °C to 25 °C) and sampled at 0, 5, 14, 45 and 90 days after ensiling.

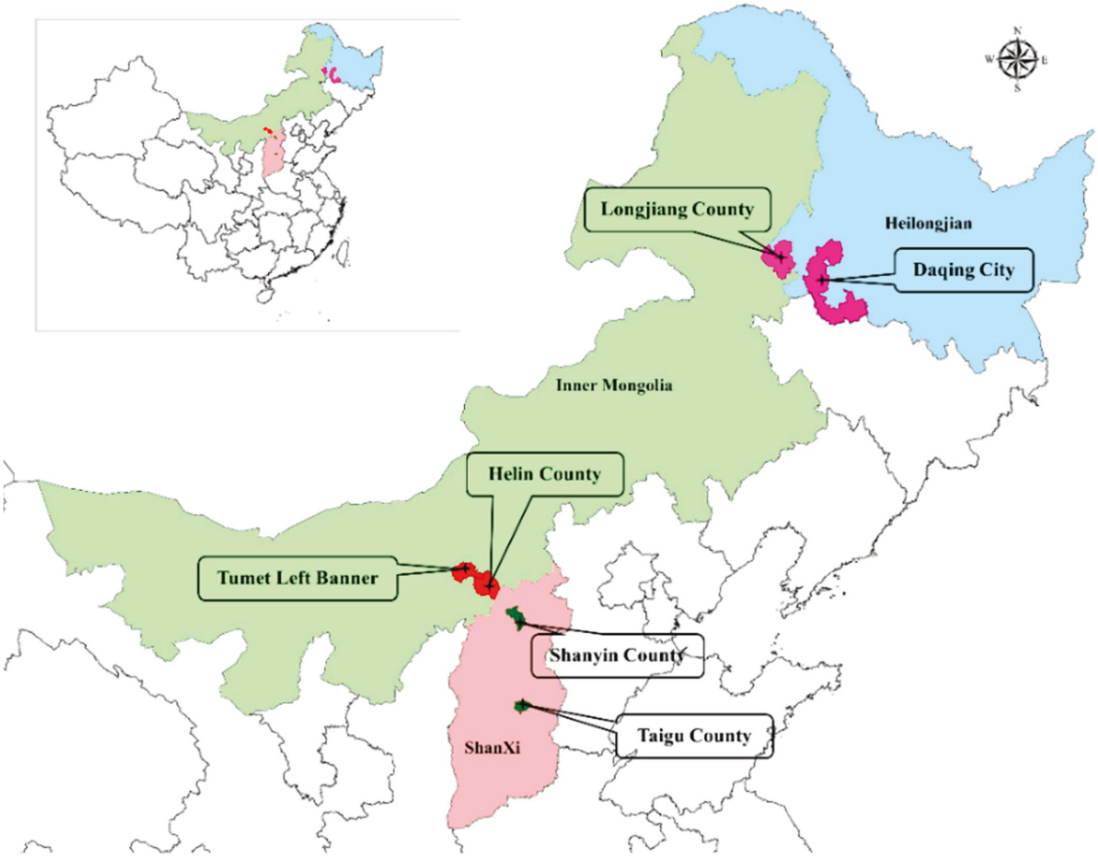

Figure 1. Sampling locations of whole-plant corn. Heilongjiang province (Daqing city (124°43′42.074″ E, 46°18′32.083″ N) and Longjiang county (123°7′32.120″ E, 47°21′23.396″ N), cold and wet agricultural area), Inner Mongolia Autonomous Region (Helin county (111°36′21.625″ E, 40°28′47.672″ N) and Tumet Left Banner (111°9′31.399″ E, 40°41′29.832″ N), temperate and dry pastoral area) and Shanxi province (Taigu (112°37′53.792″ E, 37°25′57.230″ N) and Shanyin (112°52′06.676″ E, 39°32′54.503″ N) counties, temperate and dry agricultural area).

2.2. Analyses

2.2.1. Physicochemical Analysis

The dry-matter content was measured as follows: drying in a forced-air oven (BPG-9240A, Shanghai Yiheng Scientific Instrument Co., Ltd., Shanghai, China) at 65 °C for 48 h, grinding through a 1 mm screen using a mill (FS-6D; Fichi Machinery Equipment Co., Ltd., Jinan Shandong, China) and drying at 105 °C until a constant mass was reached. The silage extract was prepared as follows: a mixture of 20 g fresh silage and 180 mL sterile water was homogenised for 100 s in a flap-type sterile homogeniser (JX-05, Shanghai Jingxin Industrial Development Co., Ltd., Shanghai, China) and filtered through 4 layers of cheesecloth. The pH of silage was established using a pH meter (PB-10, Sartorius, Gottingen, Germany) to measure the silage extract. Concentrations of lactic acid (LA), acetic acid (AA), propionic acid (PA) and butyric acid in the silages were determined by high-performance liquid chromatography (HPLC; 20A; Shimadzu Co., Ltd., Kyoto, Japan; (detector, SPD-20A diode array detector (210 nm); column, Shodex RS Pak KC-811 (50 °C, Showa Denko K.K., Kawasaki, Japan); mobile phase, 3 mM $HClO_4$ (1.0 mL/min)) [19]. Ammonia nitrogen

(AN) and total nitrogen (TN) contents were measured with a Kjeltec autoanalyser (8400; Foss Co., Ltd., Hillerød, Denmark) according to the Kjeldahl method [20].

2.2.2. Microbial Analysis

The counts of LAB, enterobacteria, total aerobic bacteria and yeast in silage were determined by culturing on MRS agar, violet red bile agar, nutrient agar and potato dextrose agar, respectively, at 37 °C for 48 h in an incubator (LRH-70, Shanghai Yiheng Science Instruments Co., Ltd., Shanghai, China) [21].

Then, 20 g of silage from each bag was placed into a self-styled bag at each sampling time and stored at −80 °C to analyse the bacterial communities. Bacterial DNA in silage was extracted by the E.Z.N.A. ®®Stool DNA Kit (D4015, Omega Bio-Tek, Inc., Doraville, GA, USA) according to the manufacturer's instructions. Amplification of the V3–V4 region of the bacterial rRNA gene was operated by polymerase chain reaction (PCR) with primers 341F (5′-CCTACGGGNGGCWGCAG-3′) and 805R (5′-GACTACHVGGGTATCTAATCC-3′) as follows: 98 °C for 30 s, followed by 32 cycles of denaturation at 98 °C for 10 s, annealing at 54 °C for 30 s, an extension at 72 °C for 45 s, and a final extension at 72 °C for 10 min [22]. PCR products were purified by AMPure XT beads (Beckman Coulter Genomics, Danvers, MA, USA), quantified by Qubit (Invitrogen, Carlsbad, CA, USA) and sequenced on an Illumina NovaSeq PE250 platform. High-quality clean tags were obtained from raw reads under specific filtering conditions according to fqtrim (version 0.94). Alpha diversity and beta diversity were calculated by QIIME2, the sequence alignment of species annotation was performed by BLAST, and the alignment databases were SILVA and NT-16S. The stacked bars of bacterial genera were made by Excel (Microsoft 365, Microsoft Corporation, Seattle, DC, USA) according to the relative abundance of the bacterial community. Differences in bacterial communities among sampling areas at each sampling time were analysed using the Mann–Whitney U and Kruskal–Wallis tests by R version 3.6.1. Principal-component analysis (PCA) of the bacterial communities among sampling areas at each sampling time was performed with R version 3.5.0 using OmicStudio tools at https://www.omicstudio.cn/tool (accessed on 10 February 2021).

2.3. Statistical Analyses

Data on the dry matter, fermentation quality, microbial counts, bacterial sequencing, and alpha diversity of whole-plant corn silage were analysed as a 3 × 5 factorial design. The model included the effects of the sampling area, sampling time, and their interaction. Differences among sampling locations and sampling times were analysed by one-factor analysis of variance using the general linear model (GLM) procedure of SAS (version 9.1.3; SAS Inst. Inc., Cary, NC, USA). The interaction of sampling area and sampling time was analysed using the PDIFF procedure of SAS. Differences were compared with the least significant difference, and significance was declared at $p \leq 0.05$. Correlation between bacterial community (top 10 genera) and fermentation quality (pH, LA, AA and PA) was established with R 3.6.1.

3. Results

3.1. Fermentation Quality and Microbial Counts

Sampling area influenced pH and contents of AA, PA and AN ($p < 0.05$); sampling time affected pH, LA, AA, PA and AN ($p < 0.05$). Moreover, pH, AA and AN were interactively influenced by sampling area and sampling time ($p < 0.05$; Table 1). The counts of LAB, enterobacteria and total aerobic bacteria were affected by the sampling area ($p < 0.05$), and the sampling time influenced LAB, enterobacteria, total aerobic bacteria and yeast ($p < 0.05$), which were also interactively impacted by the sampling area and sampling time ($p < 0.05$; Table 2). No butyric acid or mould were detected in the silages.

Table 1. Dry matter (g/kg), pH, organic acid contents (g/kg dry matter) and ammonia nitrogen (g/kg total nitrogen) of whole-plant corn silages during fermentation (n = 3).

Items	Day	H_D	H_L	I_H	I_T	S_T	S_S	SEM	*p*-Value	*p*-Value		
										A	T	A × T
Dry matter	0	254 ^{c}	245 ^{c}	285 ^{b}	288 ^{b}	303 ^{a}	302 ^{ABa}	4.14	<0.001	<0.001	0.007	0.0694
	5	256 ^{b}	254 ^{b}	312 ^{a}	301 ^{a}	307 ^{a}	303 ^{ABa}	8.53	<0.001			
	14	248 ^{c}	253 ^{c}	289 ^{b}	298 ^{ab}	304 ^{ab}	317 ^{ABa}	6.58	<0.001			
	45	256 ^{b}	240 ^{b}	280 ^{a}	302 ^{a}	302 ^{a}	287 ^{Ba}	5.72	<0.001			
	90	257 ^{d}	250 ^{d}	291 ^{c}	294 ^{c}	309 ^{b}	331 ^{Aa}	4.02	<0.001			
	SEM	4.56	5.67	6.93	5.62	6.04	7.02					
	p-value	0.645	0.407	0.068	0.385	0.893	0.012					
pH	0	6.03 ^{A}	5.96 ^{A}	6.06 ^{A}	6.07 ^{A}	5.98 ^{A}	5.99 ^{A}	0.029	0.106	<0.001	<0.001	<0.001
	5	3.91 ^{Ba}	3.87 ^{Ba}	3.74 ^{Bb}	3.72 ^{Bb}	3.75 ^{Bb}	3.85 ^{Ba}	0.020	<0.001			
	14	3.87 ^{BCa}	3.86 ^{Ba}	3.58 ^{Cc}	3.62 ^{Cc}	3.75 ^{Bb}	3.83 ^{Ba}	0.018	<0.001			
	45	3.81 ^{Ca}	3.78 ^{Cab}	3.74 ^{Bbc}	3.67 ^{BCd}	3.69 ^{Ccd}	3.76 ^{Cab}	0.016	<0.001			
	90	3.80 ^{Ca}	3.62 ^{Db}	3.52 ^{Cc}	3.53 ^{Dc}	3.58 ^{Db}	3.60 ^{Db}	0.012	<0.001			
	SEM	0.019	0.018	0.023	0.025	0.013	0.019					
	p-value	<0.001	<0.001	<0.001	<0.001	<0.001	<0.001					
Lactic acid	0	ND	ND	ND	ND	ND	ND	-	-	0.148	<0.001	0.092
	5	111 ^{BCa}	72.6 ^{Bb}	72.9 ^{Cb}	93.6 ^{Bb}	76.5 ^{Cb}	80.8 ^{Cb}	4.81	<0.001			
	14	99.6 ^{Cbc}	72.8 ^{Bc}	92.5 ^{Bbc}	174 ^{Aa}	100 ^{Bbc}	117 ^{Ab}	6.48	<0.001			
	45	123 ^{ABb}	128 ^{Ab}	152 ^{Aa}	94.3 ^{Bc}	119 ^{Ab}	100 ^{Bc}	4.67	<0.001			
	90	139 ^{Aa}	73.0 ^{Bc}	138 ^{Aa}	96.0 ^{Bb}	122 ^{Aa}	100 ^{Bb}	4.87	<0.001			
	SEM	5.35	4.46	5.07	5.06	4.03	4.13					
	p-value	<0.001	<0.001	<0.001	<0.001	<0.001	<0.001					
Acetic acid	0	ND	ND	ND	ND	ND	ND	-	-	<0.001	<0.001	0.038
	5	23.9 ^{BCa}	14.2 ^{Bb}	12.0 ^{Bb}	6.11 ^{Ac}	13.4 ^{Bb}	12.9 ^{Bb}	1.09	<0.001			
	14	19.8 ^{Ca}	10.8 ^{Bbc}	10.5 ^{Bbc}	8.70 ^{Ac}	14.7 ^{Babc}	16.8 ^{ABab}	1.71	0.006			
	45	27.2 ^{Ba}	32.3 ^{Aa}	20.0 ^{Aab}	7.54 ^{Ac}	23.4 ^{Aab}	20.4 ^{Aab}	3.80	0.012			
	90	33.5 ^{Aa}	17.5 ^{Bc}	21.2 ^{Abc}	9.57 ^{Ad}	24.0 ^{Ab}	18.6 ^{ABc}	1.41	<0.001			
	SEM	1.57	4.12	0.934	1.30	0.630	1.52					
	p-value	<0.001	0.004	<0.001	0.003	<0.001	<0.001					

Table 1. *Cont.*

Items	Day	H_D	H_L	I_H	I_T	S_T	S_S	SEM	*p*-Value	*p*-Value		
										A	T	A × T
Propionic acid	0	ND	ND	ND	ND	ND	ND	-	-	<0.001	<0.001	0.076
	5	N^{D}	3.39 ^{Ba}	2.93 ^{Da}	2.24 ^{Ca}	3.08 ^{Ca}	N^{D}	0.2880	<0.001			
	14	6.39 ^{Cb}	3.99 ^{Bbc}	N^{D}	1.22 ^{Cc}	14.6 ^{Ba}	N^{D}	1.1440	<0.001			
	45	10.9 ^{Bb}	13.9 ^{Ab}	6.17 ^{Bc}	6.86 ^{Bc}	17.3 ^{Ba}	6.41 ^{Bc}	0.9800	<0.001			
	90	16.3 ^{Ab}	11.2 ^{Ac}	9.61 ^{Ac}	10.6 ^{Ac}	20.5 ^{Aa}	10.3 ^{Ac}	0.9965	<0.001			
	SEM	0.947	1.10	0.565	0.717	0.891	0.521					
	p-value	<0.001	<0.001	<0.001	<0.001	<0.001	<0.001					
Ammonia nitrogen	0	8.47 ^{Da}	9.70 ^{Ca}	7.67 ^{Ca}	2.59 ^{Db}	5.98 ^{Dab}	10.1 ^{Ca}	1.2479	0.010	<0.001	<0.001	<0.001
	5	39.4 ^{Ca}	33.8 ^{Bb}	33.1 ^{Bb}	23.1 ^{Cc}	33.9 ^{Cb}	25.8 ^{Bc}	1.2595	<0.001			
	14	61.4 ^{Ba}	35.2 ^{Bc}	51.0 ^{Ab}	26.4 ^{Bc}	29.0 ^{Bc}	31.5 ^{Bc}	2.5968	<0.001			
	45	99.7 ^{Aa}	62.8 ^{Ab}	50.3 ^{Ac}	36.1 ^{Ad}	59.3 ^{Ab}	46.9 ^{Ac}	1.9001	<0.001			
	90	91.4 ^{Aa}	66.2 ^{Ab}	50.8 ^{Acd}	36.3 ^{Ae}	61.0 ^{Abc}	44.9 ^{Ade}	3.4829	<0.001			
	SEM	2.65	1.61	2.02	0.995	1.45	3.72					
	p-value	<0.001	<0.001	<0.001	<0.001	<0.001	<0.001					

Whole-plant corn silages were processed at 6 locations in 3 areas of North China: Heilongjiang province (Daqing city (H_D; 124°43′42.074″ E, 46°18′32.083″ N) and Longjiang county (H_L; 123°7′32.120″ E, 47°21′23.396″ N), cold and wet agricultural area), Inner Mongolia Autonomous Region (Helin county (I_H; 111°36′21.625″ E, 40°28′47.672″ N) and Tumet Left Banner (I_T; 111°9′31.399″ E, 40°41′29.832″ N), temperate and dry pastoral area) and Shanxi province (Taigu (S_T; 112°37′53.792″ E, 37°25′57.230″ N) and Shanyin (S_S; 112°52′06.676″ E, 39°32′54.503″ N) counties, temperate and dry agricultural area). Sampling times were at 0, 5, 14, 45 and 90 days after ensiling. Note: SEM, standard error of the mean; A, sampling area; T, sampling time. Values with different uppercase ($^{A–D}$) and lowercase ($^{a–e}$) letters indicate significant differences among sampling times of each lactation and sampling locations at the same time, respectively. ND, not detected.

Table 2. Microbial counts (log colony-forming units/g fresh weight) of whole-plant corn silages during fermentation (n = 3).

Items	Day	H_D	H_L	I_H	I_T	S_T	S_S	SEM	*p*-Value	*p*-Value		
										A	T	A × T
Lactic acid bacteria	0	8.36 ^{Bb}	8.50 ^{Bb}	6.80 ^{Cd}	9.21 ^{Aa}	7.41 ^{Cc}	6.33 ^{Be}	0.076	<0.001	0.047	<0.001	0.012
	5	8.97 ^{Ab}	8.88 ^{Ab}	8.31 ^{Bc}	8.95 ^{Bb}	9.35 ^{Aa}	9.43 ^{Aa}	0.085	<0.001			
	14	8.77 ^{Ab}	8.71 ^{Ab}	8.65 ^{Ab}	7.86 ^{Cc}	8.55 ^{Bb}	9.31 ^{Aa}	0.075	<0.001			
	45	6.49 ^{Cb}	7.45 ^{Ca}	6.65 ^{Cb}	6.59 ^{Db}	6.10 ^{Db}	6.61 ^{Bb}	0.146	<0.001			
	90	5.35 ^{Db}	6.49 ^{Da}	4.75 ^{Dc}	5.16 E^{b}	4.05 ^{Ed}	4.13 ^{Cd}	0.071	<0.001			
	SEM	0.087	0.061	0.072	0.063	0.125	0.133					
	p-value	<0.001	<0.001	<0.001	<0.001	<0.001	<0.001					

Table 2. *Cont.*

Items	Day	H_D	H_L	I_H	I_T	S_T	S_S	SEM	*p*-Value	*p*-Value		
										A	T	A × T
Enterobacteria	0	6.53 ^{Ad}	8.44 ^{Aa}	7.48 ^{Ac}	7.99 ^{Ab}	7.30 ^{Ac}	6.06 ^{Ae}	0.096	<0.001	0.048	<0.001	0.004
	5	ND	ND	ND	ND	ND	ND	-	-			
	14	ND	ND	ND	ND	ND	ND	-	-			
	45	ND	ND	ND	ND	ND	ND	-	-			
	90	ND	ND	ND	ND	ND	ND	-	-			
	SEM	0.035	0.036	0.063	0.026	0.004	0.062					
	p-value	<0.001	<0.001	<0.001	<0.001	<0.001	<0.001					
Total aerobic bacteria	0	7.81 ^{Bc}	9.12 ^{Ab}	9.13 ^{Ab}	9.50 ^{Aa}	7.64 ^{Cc}	6.91 ^{Cd}	0.091	<0.001	0.009	<0.001	<0.001
	5	8.73 ^{Aa}	8.79 ^{Ba}	8.29 ^{Bb}	8.99 ^{Ba}	9.08 ^{Aa}	9.12 ^{Ba}	0.120	0.004			
	14	8.75 ^{Ab}	8.54 ^{Cc}	8.50 ^{Bc}	7.83 ^{Cd}	8.49 ^{Bc}	9.44 ^{Aa}	0.060	<0.001			
	45	6.19 ^{Cc}	8.53 ^{Ca}	4.68 ^{Ce}	6.67 ^{Db}	6.20 ^{Dc}	5.65 ^{Ed}	0.043	<0.001			
	90	6.22 ^{Cb}	5.61 ^{Dc}	4.78 ^{Cd}	5.42 ^{Ec}	4.39 ^{Ee}	6.69 ^{Da}	0.070	<0.001			
	SEM	0.054	0.655	0.081	0.092	0.115	0.066					
	p-value	<0.001	<0.001	<0.001	<0.001	<0.001	<0.001					
Yeasts	0	5.59 ^{Cd}	5.26 ^{Dd}	7.72 ^{Bb}	8.19 ^{Aa}	6.19 ^{Cc}	6.60 ^{Cc}	0.134	<0.001	0.648	<0.001	<0.001
	5	8.09 ^{Ac}	7.25 ^{Bd}	9.22 ^{Aa}	8.19 ^{Ac}	8.73 ^{Ab}	8.46 ^{Bbc}	0.132	<0.001			
	14	7.74 ^{Aa}	7.54 ^{Ab}	7.72 ^{Ba}	7.59 ^{Bab}	7.50 ^{Bb}	7.43 ^{Ab}	0.044	0.002			
	45	6.15 ^{Bab}	6.55 ^{Ca}	3.77 ^{Ce}	5.46 ^{Cc}	5.97 ^{Cb}	4.77 ^{Dd}	0.133	<0.001			
	90	6.65 ^{Ba}	4.83 ^{Eb}	3.64 ^{Cc}	5.23 ^{Db}	4.73 ^{Db}	5.11 ^{Db}	0.203	<0.001			
	SEM	0.170	0.071	0.083	0.070	0.113	0.239					
	p-value	<0.001	<0.001	<0.001	<0.001	<0.001	<0.001					

Whole-plant corn silages were processed at 6 locations in 3 areas of North China: Heilongjiang province (Daqing city (H_D; 124°43′42.074″ E, 46°18′32.083″ N) and Longjiang county (H_L; 123°7′32.120″ E, 47°21′23.396″ N), cold and wet agricultural area), Inner Mongolia Autonomous Region (Helin county (I_H; 111°36′21.625″ E, 40°28′47.672″ N) and Tumet Left Banner (I_T; 111°9′31.399″ E, 40°41′29.832″ N), temperate and dry pastoral area) and Shanxi province (Taigu (S_T; 112°37′53.792″ E, 37°25′57.230″ N) and Shanyin (S_S; 112°52′06.676″ E, 39°32′54.503″ N) counties, temperate and dry agricultural area). Sampling times were at 0, 5, 14, 45 and 90 days after ensiling. Note: SEM, standard error of the mean; A, sampling area; T, sampling time. Values with different uppercase ($^{A–E}$) and lowercase ($^{a–e}$) letters indicate significant differences among sampling times of each lactation and sampling locations at the same time, respectively. ND, not detected.

3.2. Bacterial Communities

A total of 5,669,279 clean reads were obtained from 90 samples of whole-plant corn silage according to 16S rRNA. Sampling area and sampling time affected the observed species diversity, Shannon, Simpson and CHAO1 indices ($p < 0.05$), and had an interactive effect on observed species and CHAO1 ($p < 0.05$) (Table 3). According to PCA, bacterial communities in I5_H_1, I5_H_2, I5_H_3 and S5_S_1 were separated from other silages at 5 days after ensiling (Figure 2A). Silages from Shanxi (S14_S and S14_T) and I14_H had separation from other silages at 14 days (Figure 2B); additionally, silages from Shanxi (S_S and S_T) were clearly separated from other silages at 45 and 90 days (Figure 2C,D).

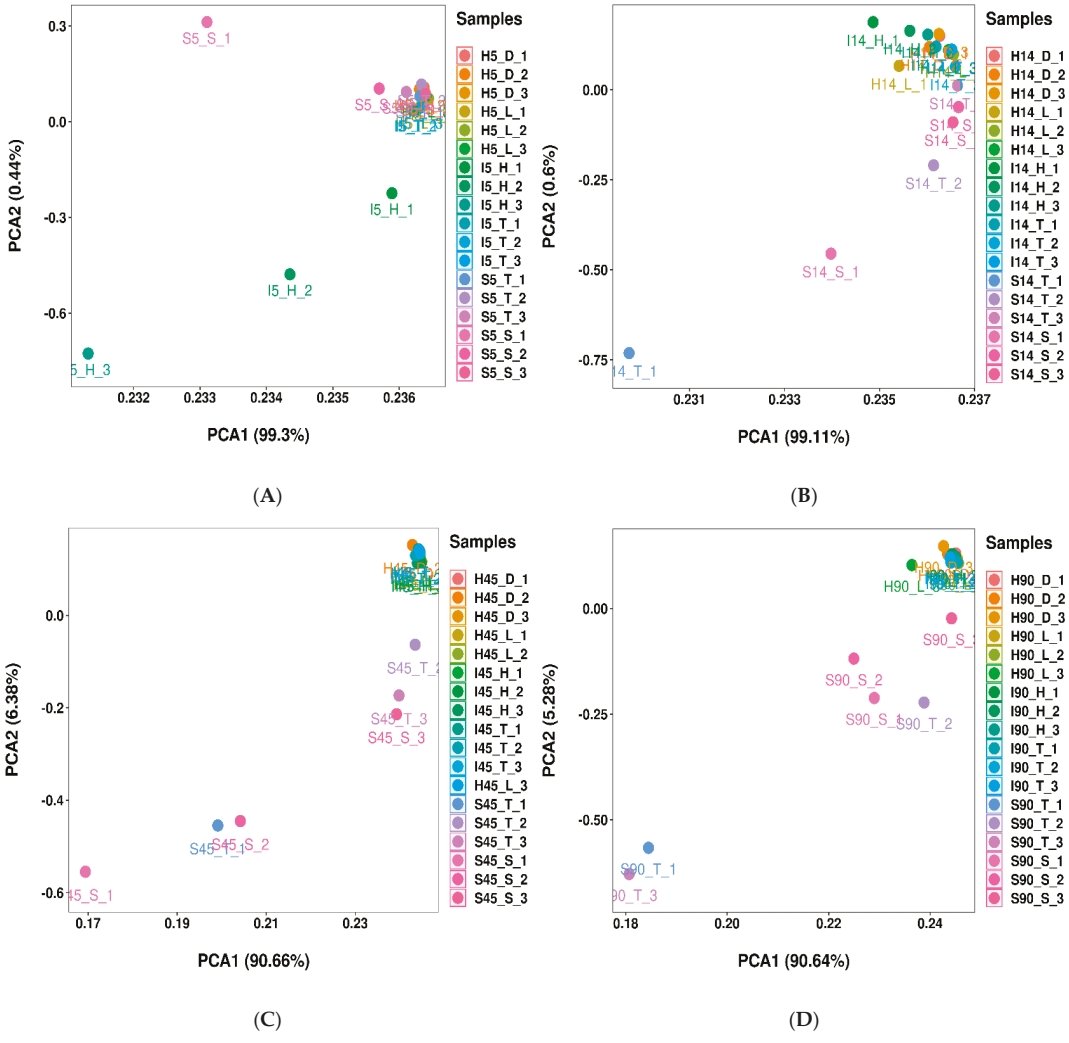

Figure 2. Principal-component analysis of bacterial communities at (**A**) 5, (**B**) 14, (**C**) 45 and (**D**) 90 days after ensiling (n = 3). Whole-plant corn silages were processed at 6 locations in 3 areas of North China: Heilongjiang province (Daqing city (H_D; 124°43′42.074″ E, 46°18′32.083″ N) and Longjiang county (H_L; 123°7′32.120″ E, 47°21′23.396″ N), cold and wet agricultural area), Inner Mongolia Autonomous Region (Helin county (I_H; 111°36′21.625″ E, 40°28′47.672″ N) and Tumet Left Banner (I_T; 111°9′31.399″ E, 40°41′29.832″ N), temperate and dry pastoral area) and Shanxi province (Taigu (S_T; 112°37′53.792″ E, 37°25′57.230″ N) and Shanyin (S_S; 112°52′06.676″ E, 39°32′54.503″ N) counties, temperate and dry agricultural area).

In silages from Heilongjiang, *Sphingobacterium*, *Stenotrophomonas*, *Sphingomonas* and *Allorhizobium–Neorhizobium–Pararhizobium–Rhizobium* in H_D were the dominant bacterial genera at 0 days (17.4%, 14.8% and 7.61%, respectively), decreased rapidly in the first 5 days, and then stayed at a low level. *Leuconostoc*, *Weissella* and *Sphingobacterium* in H0_L dominated the bacterial community. *Leuconostoc* and *Weissella* in H_L quickly reduced in the first 5 days and then stayed at a low level. The abundance of *Sphingobacterium* in H_L was reduced to 0.319% at 5 days, and then increased to 7.98% at 90 days. Moreover, the abundance of *Lactobacillus* in H_D and H_L was 1.72% and 0.32% at 0 days, increased rapidly to 84.1% and 92.3% at 5 days and was then reduced to 71.23% and 70.4% at 90 days, respectively (Figure 3A).

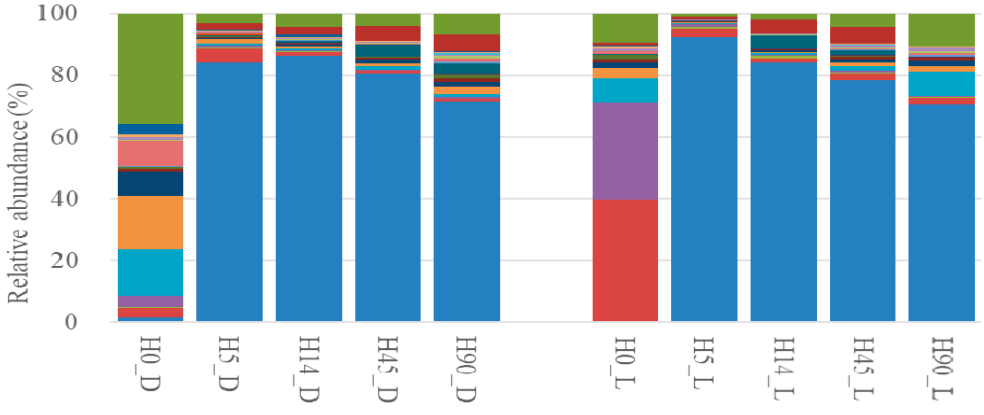

(**A**)

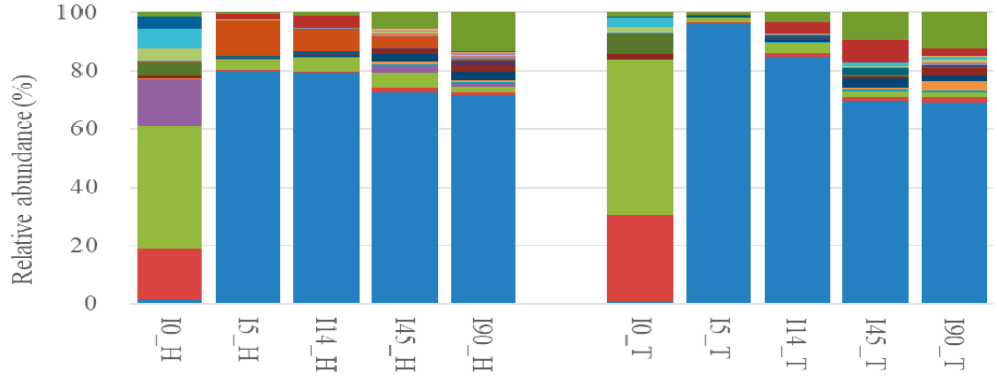

(**B**)

Figure 3. *Cont.*

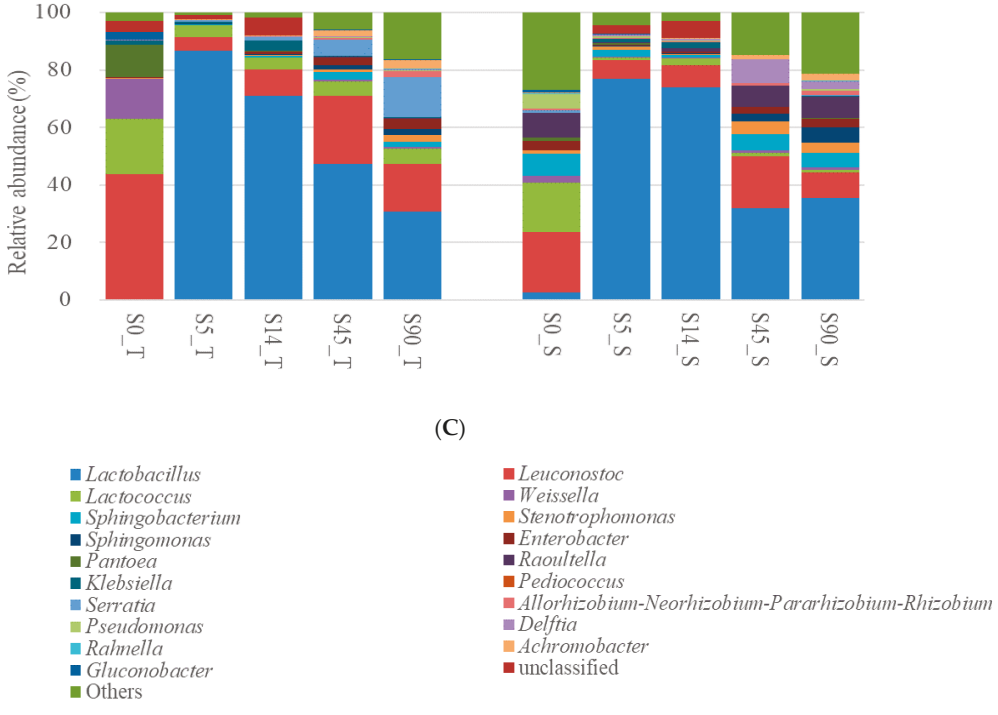

Figure 3. Relative abundance of bacterial communities (genus level) in whole-plant corn silage from (**A**) Heilongjiang, (**B**) Inner Mongolia and (**C**) Shanxi at 0, 5, 14, 45 and 90 days after ensiling (n = 3). Whole-plant corn silages were processed at 6 locations in 3 areas of North China: Heilongjiang province (Daqing city (H_D; 124°43′42.074″ E, 46°18′32.083″ N) and Longjiang county (H_L; 123°7′32.120″ E, 47°21′23.396″ N), cold and wet agricultural area), Inner Mongolia Autonomous Region (Helin county (I_H; 111°36′21.625″ E, 40°28′47.672″ N) and Tumet Left Banner (I_T; 111°9′31.399″ E, 40°41′29.832″ N), temperate and dry pastoral area) and Shanxi province (Taigu (S_T; 112°37′53.792″ E, 37°25′57.230″ N) and Shanyin (S_S; 112°52′06.676″ E, 39°32′54.503″ N) counties, temperate and dry agricultural area).

In silages from Inner Mongolia, *Lactobacillus* in I_H and I_T had a rapidly rising abundance in the first 5 days (80.2% and 95.8%, respectively), and it decreased to 71.6% and 69.0% at 90 days, respectively. Abundances of *Leuconostoc* and *Lactococcus* rapidly decreased in the first 5 days, and then maintained low levels in silages. *Weissella* in I_H was quickly reduced from 15.9% at 0 days to 0.20% at 5 days, and then stayed at a low level. *Pediococcus* in I_H increased from 0.32% at 0 days to 12.5% at 5 days, and then reduced to 0.76% at 90 days. No *Weissella* and *Pediococcus* were detected in I_T (Figure 3B).

In silages from Shanxi, the main bacterial genera at 0 days were *Leuconostoc*, *Lactococcus*, *Weissella* and *Pantoea* in S_T, and *Leuconostoc*, *Lactococcus* and *Sphingobacterium* in S_S. The abundance of *Lactobacillus* in S_T and S_S rapidly increased in the first 5 days (86.6% and 77.0%, respectively), and then reduced to 30.8% and 35.6% at 90 days, respectively. *Leuconostoc* in S_T and S_S reduced to 4.90% and 6.32 % at 5 days, increased to 23.68% and 17.85% at 45 days and then decreased to 16.53% and 8.73% at 90 days, respectively. *Lactococcus* in S_T was reduced to 3.95% at 5 days, and then increased to 5.37% at 90 days; in S_S, it was decreased in the first 5 days and then stayed at a low level. *Weissella* was a minor taxon after 5 days in the silages (Figure 3C). H5 and S5 contained more *Leuconostoc* and less *Pediococcus* than those in I5 ($p < 0.05$); additionally, I5 and S5 had higher levels of *Lactococcus* than those in H5 ($p < 0.05$) (Figure 4A). At 14, 45 and 90 days, silages from Heilongjiang and Inner Mongolia contained greater amounts of *Lactobacillus* and less *Leuconostoc* than

those from Shanxi ($p < 0.05$). Moreover, silages from Heilongjiang had lower *Lactococcus* than that of other silages from 14 to 90 days ($p < 0.05$) (Figure 4B–D).

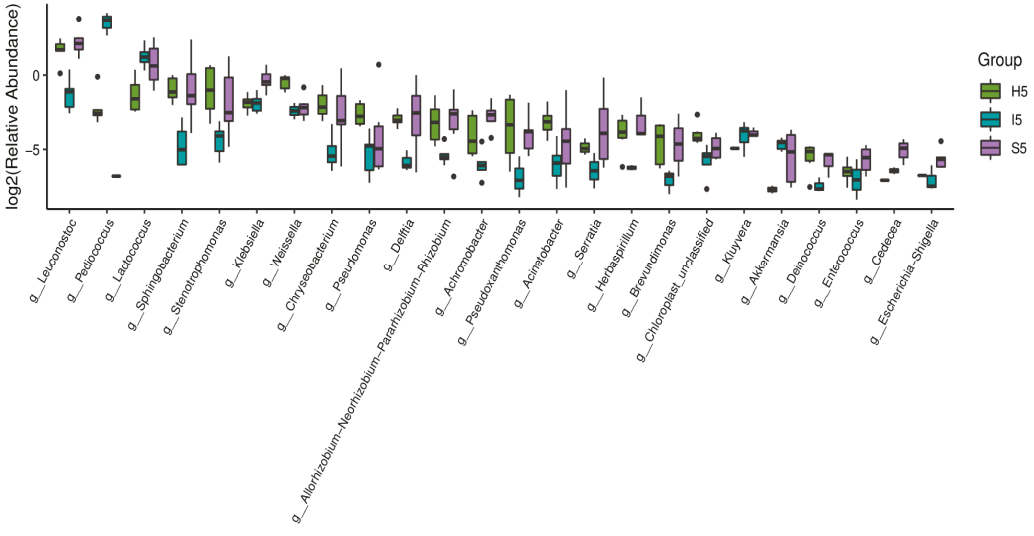

(**A**)

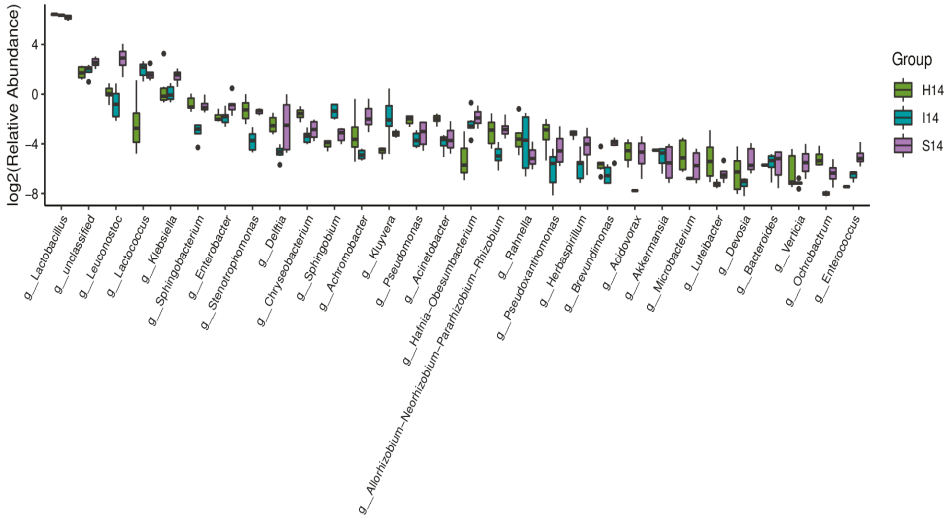

(**B**)

Figure 4. *Cont.*

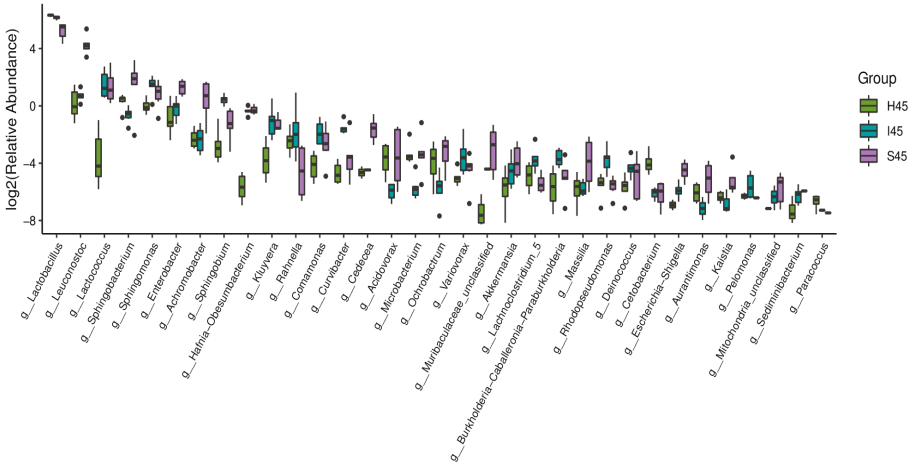

(**C**)

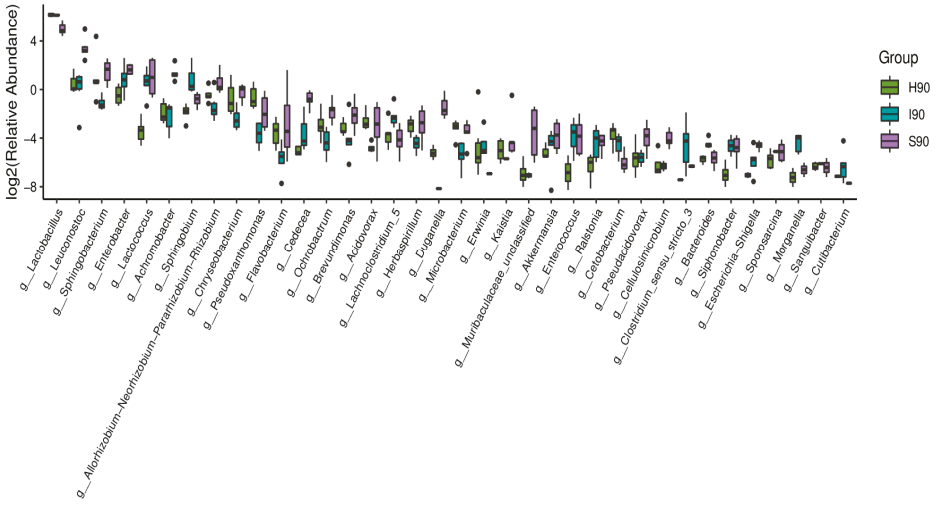

(**D**)

Figure 4. Difference in bacterial communities (genus level) among silages from Heilongjiang (H; cold and wet agricultural area), Inner Mongolia (I; temperate and dry pastoral area), and Shanxi (S; temperate and dry agricultural area) at (**A**) 5 and (**B**) 14 days after ensiling (n = 6), and (**C**) 45 and (**D**) 90 days after ensiling (n = 6).

Table 3. Sequencing data and alpha diversity of bacteria and fungi in whole-plant corn silage during fermentation (n = 3).

Items	Day	H_D	H_L	I_H	I_T	S_T	S_S	SEM	*p*-Value	*p*-Value		
										A	T	A × T
Raw reads	0	72672B5	77394	57874 ^{C}	61165	76717 ^{A}	46439 ^{C}	6798	0.048	<0.001	<0.001	0.002
	5	82678 ^{A}	84881	82158 ^{AB}	82724	82624 ^{A}	84795 ^{A}	1217	0.420			
	14	83060 ^{A}	85767	86449 ^{A}	85417	84053 ^{A}	83291 ^{A}	1454	0.656			
	45	83672 ^{Aa}6	80723 ^{a}	68678 ^{BCb}	82555 ^{a}	64388 ^{Bbc}	59492 ^{Bc}	1995	<0.001			
	90	80527 ^{Aa}	69953 ^{ab}	63394 ^{Cbc}	74775 ^{ab}	56173 ^{Bc}	53520 ^{BCc}	3522	0.001			
	SEM	1768	3461	4412	6015	3256	2531					
	p-value	0.007	0.051	0.004	0.074	<0.001	<0.001					
Clean reads	0	59974 ^{B}	70842	43763 ^{B}	48132 ^{B}	62964 ^{AB}	40468 ^{B}	6401	0.040	<0.001	<0.001	<0.001
	5	67089 ^{ABab}	71377 ^{ab}	63326 ^{Ab}	75744 ^{Aa}	69921 ^{Aab}	75001 ^{Aa}	1968	0.009			
	14	67377 ^{AB}	69169	69527 ^{A}	75848 ^{A}	68202 ^{A}	72667 ^{A}	2016	0.146			
	45	73966 ^{Aa}	68423 ^{a}	60153 ^{Ab}	73618 ^{Aa}	53947 ^{ABbc}	48486 ^{Bc}	2315	<0.001			
	90	71015 ^{Aa}	62192 ^{abc}	57832 ^{Aabc}	66824 ^{Aab}	50882 ^{Bbc}	47072 ^{Bc}	3807	0.006			
	SEM	2024	4567	4166	4066	3753	2236					
	p-value	0.006	0.641	0.015	0.011	0.017	<0.001					
Observed species	0	632 ^{Aa}	236 ^{b}	121 ^{Bb}	102 ^{Cb}	135 ^{Cb}	232 ^{b}	40.4	<0.001	<0.001	<0.001	0.003
	5	307 ^{C}	184	143 ^{B}	89.3 ^{C}	138 ^{C}	255	36.8	0.054			
	14	300 ^{C}	253	176 ^{B}	189 ^{B}	212 ^{BC}	257	22.1	0.077			
	45	326 ^{C}	321	244 ^{A}	315 ^{A}	252 ^{AB}	310	25.8	0.151			
	90	411 ^{B}	292	291 ^{A}	251 ^{AB}	309 ^{A}	340	34.8	0.244			
	SEM	22.2	40.8	1544	23.3	21.2	28.5					
	p-value	<0.0001	0.2324	<0.0001	<0.0001	0.0007	0.1154					
Shannon	0	6.99 ^{Aa}	2.72 ^{b}	3.27 ^{Bb}	2.62 ^{Bb}	3.07 ^{Bb}	4.46 ^{ABb}	0.767	0.017	<0.001	<0.001	0.839
	5	4.74 ^{Ba}	3.19 ^{ab}	3.60 ^{ABab}	1.36 ^{Cb}	2.85 ^{Bab}	3.56 ^{Bab}	0.521	0.096			
	14	4.97 ^{B}	4.31	3.70 ^{AB}	2.68 ^{B}	3.83 ^{AB}	3.81 ^{B}	0.334	0.057			
	45	4.90 ^{B}	4.78	4.35 ^{A}	3.76 ^{A}	3.90 ^{AB}	5.16 ^{AB}	0.352	0.197			
	90	5.39 ^{B}	4.52	4.52 ^{A}	3.56 ^{A}	4.82 ^{A}	5.69 ^{A}	0.384	0.076			
	SEM	0.199	0.724	0.217	0.271	0.268	0.405					
	p-value	<0.001	0.263	0.011	<0.001	0.003	0.019					

Table 3. *Cont.*

Items	Day	H_D	H_L	I_H	I_T	S_T	S_S	SEM	*p*-Value	*p*-Value		
										A	T	A × T
Simpson	0	0.976 ^{A}	0.483	0.718	0.655 ^{A}	0.750 ^{BC}	0.871 ^{AB}	0.116	0.140	0.009	0.005	0.956
	5	0.897 ^{Ba}	0.665 ^{ab}	0.841 ^{a}	0.407 ^{Bb}	0.691 ^{Cab}	0.748 ^{Ba}	0.075	0.051			
	14	0.920 ^{Ba}	0.829 ^{a}	0.842 ^{a}	0.630 ^{Ab}	0.814 ^{ABa}	0.805 ^{ABa}	0.037	0.013			
	45	0.893 ^{B}	0.881	0.864	0.715 ^{A}	0.835 ^{AB}	0.916 ^{A}	0.042	0.268			
	90	0.920 ^{B}	0.856	0.860	0.725 ^{A}	0.901 ^{A}	0.933 ^{A}	36.9	0.228			
	SEM	0.012	0.110	0.045	0.055	0.030	0.031					
	p-value	0.005	0.125	0.205	0.005	0.005	0.011					
Chao1	0	648 ^{Aa}	250 ^{b}	124 ^{Bb}	107 ^{Cb}	139 ^{Cb}	234 ^{b}	40.6	<0.001	<0.001	<0.001	0.002
	5	319 ^{C}	193	149 ^{B}	98.0 ^{C}	145 ^{C}	271	38.1	0.050			
	14	313 ^{C}	262	186 ^{B}	208 ^{B}	219 ^{BC}	271	23.6	0.117			
	45	340 ^{C}	337	250 ^{A}	336 ^{A}	261 ^{AB}	317	25.6	0.086			
	90	433 ^{B}	301	297 ^{A}	260 ^{B}	316 ^{A}	349		0.221			
	SEM	23.4	40.6	17.1	26.2	22.0	29.5					
	p-value	<0.001	0.205	<0.001	<0.001	<0.001	0.128					

Whole-plant corn silages were processed at 6 locations in 3 areas of North China: Heilongjiang province (Daqing city (H_D; 124°43′42.074″ E, 46°18′32.083″ N) and Longjiang county (H_L; 123°7′32.120″ E, 47°21′23.396″ N), cold and wet agricultural area), Inner Mongolia Autonomous Region (Helin county (I_H; 111°36′21.625″ E, 40°28′47.672″ N) and Tumet Left Banner (I_T; 111°9′31.399″ E, 40°41′29.832″ N), temperate and dry pastoral area) and Shanxi province (Taigu (S_T; 112°37′53.792″ E, 37°25′57.230″ N) and Shanyin (S_S; 112°52′06.676″ E, 39°32′54.503″ N) counties, temperate and dry agricultural area). Sampling times were at 0, 5, 14, 45 and 90 days after ensiling. Note: SEM, standard error of the mean; A, sampling area; T, sampling time. Values with different uppercase ($^{A–C}$) and lowercase ($^{a–c}$) letters indicate significant differences among 6 sampling locations at the same time.

3.3. Correlation between Fermentation Quality and Bacterial Genera

pH had a negative correlation with *Lactobacillus* in all silages ($p < 0.05$). It correlated positively with *Weissella* in silages from Heilongjiang ($p < 0.05$), and with *Lactococcus*, *Leuconostoc* and *Weissella* in silages from Inner Mongolia and Shanxi ($p < 0.05$). *Lactobacillus* had a positive correlation with LA and AA contents in silages from Heilongjiang and Inner Mongolia ($p < 0.05$). LA concentration was negatively correlated with *Weissella* in silages from Heilongjiang ($p < 0.05$), with *Lactococcus* and *Leuconostoc* in silages from Inner Mongolia ($p < 0.05$), and with *Lactococcus*, *Leuconostoc* and *Weissella* in silages from Shanxi ($p < 0.05$). The AA content had a negative correlation with *Lactococcus* and *Leuconostoc* in silages from Inner Mongolia ($p < 0.05$), and with *Lactococcus* and *Weissella* in silages from Shanxi ($p < 0.05$) (Figure 5).

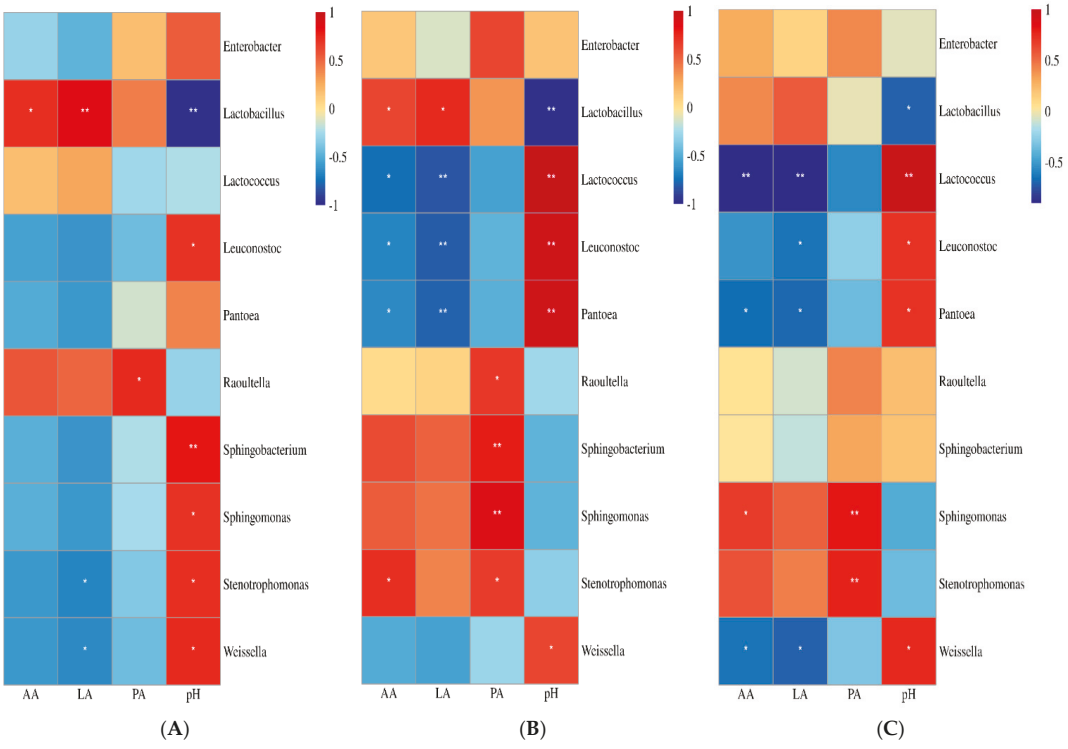

Figure 5. Correlation between the main bacterial genera (top 10) and fermentation quality (pH, lactic acid (LA), acetic acid (AA) and propionic acid (PA)) in silages from Heilongjiang (**A**; cold and wet agricultural area), Inner Mongolia (**B**; temperate and dry pastoral area), and Shanxi (**C**; temperate and dry agricultural area) during fermentation ($n = 30$).

4. Discussion

In the present study, whole-plant corn from Heilongjiang contained lower DM content (254 and 245 g/kg; Table 1), which might have been due to earlier harvesting (1/3 milk-line stage), and the cooler and wetter environment. This is similar to previous studies [2,12] that reported that the growing environment and harvesting stage influence the DM content of whole-plant corn. Earlier-harvesting corn contained lower DM content and greater amounts of water-soluble sugars, and its final silage had lower pH and greater lactic acid [23]. However, in the present study, silages from Inner Mongolia, with 285 and 288 g/kg of DM content, had a lower pH than that of other silages at 14 and 90 days, and less AN than that of silages from Heilongjiang at 45 and 90 days. In addition, the sampling

area did not affect LA concentration in the final silages (Table 1). This indicated that silages from Inner Mongolia had better satisfactory fermentation quality than that of other silages. Moreover, silages from Heilongjiang had higher AN than that of other silages (except for I_T) at 45 and 90 days, and contained the lowest DM content (Table 1). This indicated that the high moisture content in whole-plant corn before ensiling was not conducive to reducing AN content during fermentation. Whole-plant corn silage after 5 days of ensiling is in a stable fermentation phase according to Sun et al. [9]. The pH was less than 4.0 at 5 days and reached the lowest point at 60 days in all the silages except for H_D, which agreed with a previous study [9]; moreover, lactic acid reached a high level (>76 g/kg DM) at 5 days and increased to its peak point at 14 or 45 days; AN content increased to its highest point at 45 days (Table 1). Ferrero et al. [24] also reported reduced pH and increased contents of lactic acid and AN in whole-plant corn silage after 15 days of ensiling. Those mentioned-above indicated that, during the stable fermentation phase, fermentation did not stop, and fermentation parameters changed to some extent in whole-plant corn silage.

The main bacterial genera were *Leuconostoc*, *Weissella*, *Sphingobacterium* and *Stenotrophomonas* in H0, and *Leuconostoc*, *Lactococcus*, *Weissella* and *Pantoea* in I0 and S0 (Figure 3 and Supplementary Figure S1). H0 contained less *Lactococcus* and more *Sphingobacterium*, *Stenotrophomonas* and *Sphingomonas* than I0 and S0 (Supplementary Figure S2). Additionally, the bacterial community in I0 and S0 flocked together (except for S0_S_1) and separated from H0_D, H0_L_2 and H0_L_3 according to PCA (Supplementary Figure S3). This suggested that whole-plant corn from Inner Mongolia and Shanxi had a similar epiphytic bacterial community and differed from those from Heilongjiang. The different epiphytic bacterial community in raw materials might have resulted from the different geographical location [2,12,25]. Sampling locations in Inner Mongolia and Shanxi belong to a temperate continental climate and are close to each other; sampling locations in Heilongjiang, on the other hand, locate in temperate monsoon climates and are far from the other sampling locations (Figure 1). Guan et al. [2] and Gharechahi et al. [12] also reported the unique bacterial community in whole-plant corn from different sampling sites. The abundance of *Lactobacillus* was 1.02%, 1.08% and 1.51% in H0, I0 and S0, respectively (Figure 3 and Supplementary Figure S1); the same results were reported by previous studies [2,11–15,24,26]. This generally indicated that *Lactobacillus* is a minor taxon in whole-plant corn before ensiling. Additionally, the main LAB genera in fresh forages were *Leuconostoc*, *Weissella* and/or *Lactococcus* in the present study (Figure 3 and Supplementary Figure S1). This indicated that *Leuconostoc*, *Weissella* and *Lactococcus* might play a major role during the early stage (the first 24 h) of fermentation [9]. LAB counts in the raw materials were more than 10^6 colony-forming units/g fresh weight in the present study, and similar results were reported by a previous study [9,24]. This suggests that LAB count in whole-plant corn before ensiling is sufficient for satisfactory fermentation quality in the final silage.

According to Sun et al. [9], after 3 days of ensiling, whole-plant corn silage is in a stable fermentation phase, during which *Lactobacillus* plays a key role among bacterial genera in silage. In the present study, *Lactobacillus* had greater abundance than that of other bacterial genera in silages with low pH (<4.0) from 5 to 90 days (Figure 3 and Supplementary Figure S1). Results were consistent with those of previous studies [9,11,12,14,27]. Moreover, Xu et al. [26], Drouin et al. [28] and Wang et al. [29] revealed that *Lactobacillus* was the dominant bacterial genus in the final whole-plant corn silage. This showed that *Lactobacillus* usually dominates bacterial community succession in whole-plant corn silage during fermentation. However, after 5 days of ensiling, the abundance of *Lactobacillus* was reduced (Figure 3 and Supplementary Figure S1), and LAB count began to decrease in all silages (Table 2). Sun et al. [9] also observed the reduced abundance of *Lactobacillus* and decreased LAB count during the stable phase in whole-plant corn silage without any inoculant. This suggested that the epiphytic *Lactobacillus* on whole-plant corn might have weak acid resistance. *Weissella* is the most important LAB genus in whole-plant corn silage from 5 to 24 h after ensiling [9,14]. It is an obligatory heterofermentative LAB species that converts water-soluble sugars into LA and AA during the early stage of fermentation

in silage [30]. In the present study, no *Weissella* was detected in I_T during the ensiling process (Figure 3), which might have resulted in the lower AA concentration in I_T than that in other silages at 5, 45 and 90 days (Table 1). *Sphingobacterium*, *Stenotrophomonas*, *Sphingomonas*, *Enterobacter*, *Pantoea*, *Raoultella*, *Klebsiella*, *Serratia* and *Rahnella* are enterobacteria as facultatively anaerobic Gram-negative bacteria [31], some of which are undesirable in silage [23]. In the present study, the total abundances of those genera rapidly decreased in the first 5 days, and then increased to 12.9%, 9.33% and 24.9% in H90, I90 and S90, respectively (Supplementary Figure S1). Those above-mentioned suggested that it is necessary to add inoculants with greater capacity for acid production and resistance during the ensiling of whole-plant corn, especially *Lactobacillus* inhibiting enterobacteria.

In the present study, *Pediococcus* had considerable abundance in I5_H (12.5%), while it was a minor taxon in other silages (<0.5%), which might have been the cause of the bacterial community in I5_H being separated from other silages at 5 days (Figure 2A). According to PCA, the bacterial community in silages from Shanxi began to separate at 14 days, and separated clearly from other silages at 45 and 90 days (Figure 2). Moreover, the bacterial community in silages from Heilongjiang and Inner Mongolia clustered together as the ensiling process (Figure 2). The above-mentioned results indicated that silages from Heilongjiang and Inner Mongolia had a similar bacterial succession pattern during the fermentation process and differed from the silages from Shanxi. Additionally, compared with silages from Heilongjiang and Inner Mongolia, silages from Shanxi had a higher reducing rate of *Lactobacillus* from 14 to 90 days (Figure 3 and Supplementary Figure S1), and contained less *Lactobacillus* as the dominant bacterial genus (Figure 4). This suggested that *Lactobacillus* in silages from Shanxi had weaker acid resistance than that in other silages, which might have contributed to the different bacterial succession pattern in whole-plant corn silages among sampling areas. Silva et al. [32] also reported a tendency of bacterial communities to cluster together in whole-plant corn silage during the ensiling process. However, Xu et al. [11] and Keshri et al. [14] reported that the bacterial community in final silages clearly separated from silages at other sampling times.

Sun et al. [9] reported that *Lactobacillus* in whole-plant corn silage dominates the bacterial community during the stable phase and correlates negatively with pH from 1 to 60 days after ensiling. In the present study, *Lactobacillus* dominated the bacterial community during fermentation and had a negative correlation with pH in all silages and a positive correlation with LA and AA concentrations in the silages from Heilongjiang and Inner Mongolia (Figure 5). In addition, *Lactobacillus* also correlated positively with LA and AA without reaching the significance level in the silages from Shanxi (Figure 5C). The final silages had lower pH (from 3.52 to 3.80) and AN content (from 36.6 to 91.4 g/kg TN), and higher LA content (from 73.0 to 139 g/kg DM) (Table 1). Guan et al. [2] also found a positive correlation between LA content and *Lactobacillus* in whole-plant corn silages collected from five sampling sites in Southwest China. Previous studies reported that *Lactobacillus* dominated the bacterial community during fermentation in silages with good fermentation quality [11–14,17,33]. This indicated that the activity of *Lactobacillus* in silage mainly contributes to forming and maintaining satisfactory fermentation quality in silage during the ensilage process. In the present study, *Leuconostoc*, *Lactococcus* and *Weissella* had a positive correlation with pH, and were negatively correlated with LA and AA in silages (except for *Lactococcus* as a minor taxon in silages from Heilongjiang). Sun et al. [9] reported that *Leuconostoc*, *Lactococcus* and *Weissella* in whole-plant corn silage had an important effect on bacterial succession and the reduced pH in the first 24 h of ensiling, but positively correlated with pH from 1 to 60 days as minor taxa. This suggested that *Leuconostoc*, *Lactococcus* and *Weissella* might be inhibited under anaerobic and acidic environments, and played a limited role in whole-plant corn silage after 5 days of fermentation. Correlations of *Stenotrophomonas*, *Sphingomonas*, *Enterobacter* and *Pantoea* with fermentation quality were similar in silages from Inner Mongolia and Shanxi, which differed from the silages from Heilongjiang (Figure 5). The reason for the different correlations might be that the final silages from Inner Mongolia and Shanxi contained a lower abundance of LAB genera

than that of their materials and had similar changes in abundance of those genera during fermentation (Supplementary Figure S1). Ogunade et al. [34] found a negative correlation of *Pantoea*, *Pseudomonas*, *Sphingomonas* and *Stenotrophomonas* with pH in alfalfa silage. The effect of those bacterial genera on fermentation quality of silage needs to be further studied.

5. Conclusions

The geographic growth location mainly impacted the epiphytic bacterial community on whole-plant corn. Whole-plant corn silages had satisfactory fermentation quality. *Lactobacillus* was a minor taxon in fresh forage and dominated the bacterial community in whole-plant corn silages during the fermentation process. The acid resistance of *Lactobacillus* in whole-plant corn silage determined the bacterial succession pattern during fermentation, and silages from Heilongjiang and Inner Mongolia had similar bacterial succession pattern. The activity of *Lactobacillus* during the ensilage process contributed to forming and maintaining a satisfactory fermentation quality in whole-plant corn silage.

Supplementary Materials: The following are available online at https://www.mdpi.com/article/10.3390/pr9050900/s1, Figure S1: Relative abundance of bacterial communities (genus level) in whole-plant corn silage from Heilongjiang (H; cold and wet agricultural area), Inner Mongolia (I; temperate and dry pastoral area) and Shanxi (S; temperate and dry agricultural area) at 0, 5, 14, 45 and 90 days after ensiling, Figure S2: Difference in bacterial communities (genus level) among whole-plant corn from Heilongjiang (H; cold and wet agricultural area), Inner Mongolia (I; temperate and dry pastoral area) and Shanxi (S; temperate and dry agricultural area), Figure S3: Principal component analysis of a bacterial community in whole-plant corn. Corn grown at six locations in three areas of Northern China: Heilongjiang province (Daqing city (H_D; 124°43′42.074″ E, 46°18′32.083″ N) and Longjiang county (H_L; 123°7′32.120″ E, 47°21′23.396″ N), cold and wet agricultural area), Inner Mongolia Autonomous Region (Helin county (I_H; 111°36′21.625″ E, 40°28′47.672″ N) and Tumet Left Banner (I_T; 111°9′31.399″ E, 40°41′29.832″ N), temperate and dry pastoral area) and Shanxi province (Taigu (S_T; 112°37′53.792″ E, 37°25′57.230″ N) and Shanyin (S_S; 112°52′06.676″ E, 39°32′54.503″ N) counties, temperate and dry agricultural area), Figure S4: Principal component analysis of a bacterial community in whole-plant corn silages from Heilongjiang province (Daqing city (H_D; 124°43′42.074″ E, 46°18′32.083″ N) and Longjiang county (H_L; 123°7′32.120″ E, 47°21′23.396″ N), cold and wet agricultural area), Inner Mongolia Autonomous Region (Helin county (I_H; 111°36′21.625″ E, 40°28′47.672″ N) and Tumet Left Banner (I_T; 111°9′31.399″ E, 40°41′29.832″ N), temperate and dry pastoral area) and Shanxi province (Taigu (S_T; 112°37′53.792″ E, 37°25′57.230″ N) and Shanyin (S_S; 112°52′06.676″ E, 39°32′54.503″ N) counties, temperate and dry agricultural area) at 0, 5, 14, 45 and 90 days after ensiling.

Author Contributions: Conceptualisation, C.W., H.H. and Y.X.; methodology, C.W., H.H. and L.S.; software, L.S., N.N. and S.C.; validation, C.W., H.H. and Y.X.; visualisation, S.C.; formal analysis, L.S. and N.N.; investigation, C.W., H.H., L.S. and N.N.; resources, C.W. and H.H.; data curation, C.W., H.H. and H.X.; writing—original draft, C.W. and H.H.; writing—review and editing, C.W., H.H., H.X., Y.J. and Y.X.; supervision, Y.X.; project administration, Y.X.; funding acquisition, Y.X. All authors have read and agreed to the published version of the manuscript.

Funding: This study was funded by the National Key R&D Program of China (grant number 2017YFE0104300) and the Science and Technology Project of Inner Mongolia (grant number 2020GG0049).

Institutional Review Board Statement: Not applicable.

Informed Consent Statement: Informed consent was obtained from all subjects involved in the study.

Data Availability Statement: The data presented in this study are available on request from the corresponding author.

Conflicts of Interest: The authors declare no conflict of interest.

References

1. Grant, R.; Ferraretto, L. Silage review: Silage feeding management: Silage characteristics and dairy cow feeding behavior. *J. Dairy Sci.* **2018**, *101*, 4111–4121. [CrossRef] [PubMed]

2. Guan, H.; Yan, Y.; Li, X.; Li, X.; Shuai, Y.; Feng, G.; Ran, Q.; Cai, Y.; Li, Y.; Zhang, X. Microbial communities and natural fermentation of corn silages prepared with farm bunker-silo in Southwest China. *Bioresour. Technol.* **2018**, *265*, 282–290. [CrossRef] [PubMed]
3. Wilkinson, J.M.; Rinne, M. Highlights of progress in silage conservation and future perspectives. *Grass Forage Sci.* **2017**, *73*, 40–52. [CrossRef]
4. Zhang, L.; Zhou, X.; Gu, Q.; Liang, M.; Mu, S.; Zhou, B.; Huang, F.; Lin, B.; Zou, C. Analysis of the correlation between bacteria and fungi in sugarcane tops silage prior to and after aerobic exposure. *Bioresour. Technol.* **2019**, *291*, 121835. [CrossRef]
5. Kaiser, A.G.; Piltz, J.W.; Burns, H.M.; Griffiths, N.W. *TOPFODDER Sucessful Silage*, 2nd ed.; Dairt Australia and New South Wales Department of Primary Industries: Orange, NSW, Australia, 2004.
6. Ferraretto, L.; Shaver, R.; Luck, B. Silage review: Recent advances and future technologies for whole-plant and fractionated corn silage harvesting. *J. Dairy Sci.* **2018**, *101*, 3937–3951. [CrossRef]
7. Buxton, D.R.; Muck, R.E.; Harrison, J.H. *Silage Science and Technology*; American Society of Agronomy: Madison, WI, USA, 2003.
8. Khan, N.A.; Yu, P.; Ali, M.; Cone, J.W.; Hendriks, W.H. Nutritive value of maize silage in relation to dairy cow performance and milk quality. *J. Sci. Food Agric.* **2015**, *95*, 238–252. [CrossRef]
9. Sun, L.; Bai, C.; Xu, H.; Na, N.; Jiang, Y.; Yin, G.; Liu, S.; Xue, Y. Succession of Bacterial Community During the Initial Aerobic, Intense Fermentation, and Stable Phases of Whole-Plant Corn Silages Treated with Lactic Acid Bacteria Suspensions Prepared From Other Silages. *Front. Microbiol.* **2021**, *12*, 591. [CrossRef]
10. Jin, L.; Dunière, L.; Lynch, J.P.; Zaheer, R.; Turkington, K.; Blackshaw, R.E.; Lupwayi, N.Z.; O'Donovan, J.T.; Harker, K.N.; McAllister, T.; et al. Impact of ferulic acid esterase-producing lactobacilli and fibrolytic enzymes on ensiling and digestion kinetics of mixed small-grain silage. *Grass Forage Sci.* **2016**, *72*, 80–92. [CrossRef]
11. Xu, D.; Wang, N.; Rinne, M.; Ke, W.; Weinberg, Z.G.; Da, M.; Bai, J.; Zhang, Y.; Li, F.; Guo, X. The bacterial community and metabolome dynamics and their interactions modulate fermentation process of whole crop corn silage prepared with or without inoculants. *Microb. Biotechnol.* **2021**, *14*, 561–576. [CrossRef]
12. Gharechahi, J.; Kharazian, Z.A.; Sarikhan, S.; Jouzani, G.S.; Aghdasi, M.; Salekdeh, G.H. The dynamics of the bacterial communities developed in maize silage. *Microb. Biotechnol.* **2017**, *10*, 1663–1676. [CrossRef]
13. Guan, H.; Shuai, Y.; Yan, Y.; Ran, Q.; Wang, X.; Li, D.; Cai, Y.; Zhang, X. Microbial Community and Fermentation Dynamics of Corn Silage Prepared with Heat-Resistant Lactic Acid Bacteria in a Hot Environment. *Microorganisms* **2020**, *8*, 719. [CrossRef]
14. Keshri, J.; Chen, Y.; Pinto, R.; Kroupitski, Y.; Weinberg, Z.G.; Sela, S. Microbiome dynamics during ensiling of corn with and without Lactobacillus plantarum inoculant. *Appl. Microbiol. Biotechnol.* **2018**, *102*, 4025–4037. [CrossRef]
15. Jiang, F.-G.; Cheng, H.-J.; Liu, D.; Wei, C.; An, W.-J.; Wang, Y.-F.; Sun, H.-T.; Song, E.-L. Treatment of Whole-Plant Corn Silage with Lactic Acid Bacteria and Organic Acid Enhances Quality by Elevating Acid Content, Reducing pH, and Inhibiting Undesirable Microorganisms. *Front. Microbiol.* **2020**, *11*, 593088. [CrossRef]
16. Wang, M.; Franco, M.; Cai, Y.; Yu, Z. Dynamics of fermentation profile and bacterial community of silage prepared with alfalfa, whole-plant corn and their mixture. *Anim. Feed. Sci. Technol.* **2020**, *270*, 114702. [CrossRef]
17. Zhang, Y.; Liu, Y.; Meng, Q.; Zhou, Z.; Wu, H. A mixture of potassium sorbate and sodium benzoate improved fermentation quality of whole-plant corn silage by shifting bacterial communities. *J. Appl. Microbiol.* **2020**, *128*, 1312–1323. [CrossRef]
18. Ni, Y.; Wang, M. Spatiotemporal evolution of China's silage corn industry and the factors driving its develop-ment. *Pratacult. Sci.* **2019**, *7*, 1915–1924. [CrossRef]
19. Zhang, Q.; Li, X.; Zhao, M.; Yu, Z. Isolating and evaluating lactic acid bacteria strains for effectiveness of Leymus chinensis silage fermentation. *Lett. Appl. Microbiol.* **2014**, *59*, 391–397. [CrossRef]
20. AOAC International. *Official Methods of Analysis*, 18th ed.; AOAC International: Gaithersburg, MD, USA, 2005.
21. Cai, Y. Identification and Characterization of Enterococcus Species Isolated from Forage Crops and Their Influence on Silage Fermentation. *J. Dairy Sci.* **1999**, *82*, 2466–2471. [CrossRef]
22. Logue, J.B.; Stedmon, C.A.; Kellerman, A.M.; Nielsen, N.J.; Andersson, A.F.; Laudon, H.; Lindström, E.; Kritzberg, E.S. Experimental insights into the importance of aquatic bacterial community composition to the degradation of dissolved organic matter. *ISME J.* **2016**, *10*, 533–545. [CrossRef]
23. McDonald, P.; Henderson, A.R.; Heron, S.J.E. *The Biochemistry of Silage*, 2nd ed.; Cambrian Printers, Ltd.: Merlow, UK; Bucks, UK; Aberystwyth, UK; Wales, UK, 1991.
24. Ferrero, F.; Tabacco, E.; Piano, S.; Casale, M.; Borreani, G. Temperature during conservation in laboratory silos affects fermentation profile and aerobic stability of corn silage treated with Lactobacillus buchneri, Lactobacillus hilgardii, and their combination. *J. Dairy Sci.* **2021**, *104*, 1696–1713. [CrossRef]
25. McGarvey, J.; Franco, R.; Palumbo, J.; Hnasko, R.; Stanker, L.; Mitloehner, F. Bacterial population dynamics during the ensiling of Medicago sativa (alfalfa) and subsequent exposure to air. *J. Appl. Microbiol.* **2013**, *114*, 1661–1670. [CrossRef]
26. Xu, D.; Ding, W.; Ke, W.; Li, F.; Zhang, P.; Guo, X. Modulation of Metabolome and Bacterial Community in Whole Crop Corn Silage by Inoculating Homofermentative Lactobacillus plantarum and Heterofermentative Lactobacillus buchneri. *Front. Microbiol.* **2019**, *9*, 3299. [CrossRef]
27. Drouin, P.; Tremblay, J.; Chaucheyras-Durand, F. Dynamic Succession of Microbiota during Ensiling of Whole Plant Corn Following Inoculation with Lactobacillus buchneri and Lactobacillus hilgardii Alone or in Combination. *Microorganisms* **2019**, *7*, 595. [CrossRef]

28. Drouin, P.; Tremblay, J.; Renaud, J.; Apper, E. Microbiota succession during aerobic stability of maize silage inoculated with Lentilactobacillus buchneri NCIMB 40788 and Lentilactobacillus hilgardii CNCM-I. *MicrobiologyOpen* **2021**, *10*, e1153. [CrossRef]
29. Wang, C.; Sun, L.; Xu, H.; Na, N.; Yin, G.; Liu, S.; Jiang, Y.; Xue, Y. Microbial Communities, Metabolites, Fermentation Quality and Aerobic Stability of Whole-Plant Corn Silage Collected from Family Farms in Desert Steppe of North China. *Processes* **2021**, *9*, 784. [CrossRef]
30. Cai, Y.; Benno, Y.; Ogawa, M.; Ohmomo, S.; Kumai, S.; Nakase, T. Influence of Lactobacillus spp. from an Inoculant and of Weissella and Leuconostoc spp. from Forage Crops on Silage Fermentation. *Appl. Environ. Microbiol.* **1998**, *64*, 2982–2987. [CrossRef] [PubMed]
31. Ávila, C.; Carvalho, B. Silage fermentation—Updates focusing on the performance of micro-organisms. *J. Appl. Microbiol.* **2019**, *128*, 966–984. [CrossRef]
32. da Silva, E.; Smith, M.; Savage, R.; Polukis, S.; Drouin, P.; Kung, L. Effects of Lactobacillus hilgardii 4785 and Lactobacillus buchneri 40788 on the bacterial community, fermentation and aerobic stability of high-moisture corn silage. *J. Appl. Microbiol.* **2021**, *130*, 1481–1493. [CrossRef]
33. Liu, B.; Huan, H.; Gu, H.; Xu, N.; Shen, Q.; Ding, C. Dynamics of a microbial community during ensiling and upon aerobic exposure in lactic acid bacteria inoculation-treated and untreated barley silages. *Bioresour. Technol.* **2019**, *273*, 212–219. [CrossRef]
34. Ogunade, I.; Jiang, Y.; Cervantes, A.P.; Kim, D.; Oliveira, A.; Vyas, D.; Weinberg, Z.; Jeong, K.; Adesogan, A. Bacterial diversity and composition of alfalfa silage as analyzed by Illumina MiSeq sequencing: Effects of Escherichia coli O157:H7 and silage additives. *J. Dairy Sci.* **2018**, *101*, 2048–2059. [CrossRef]

processes

MDPI

Review

Fermentation of Organic Residues to Beneficial Chemicals: A Review of Medium-Chain Fatty Acid Production

Panagiota Stamatopoulou, Juliet Malkowski, Leandro Conrado, Kennedy Brown and Matthew Scarborough *

Department of Civil and Environmental Engineering, University of Vermont, Burlington, VT 05405, USA; Panagiota.Stamatopoulou@uvm.edu (P.S.); Juliet.Malkowski@uvm.edu (J.M.); Leandro.Fernandes@uvm.edu (L.C.); Kennedy.Brown@uvm.edu (K.B.)
* Correspondence: Matthew.Scarborough@uvm.edu and mscarbor@uvm.edu

Received: 14 October 2020; Accepted: 23 November 2020; Published: 28 November 2020

Abstract: Medium-chain fatty acids (MCFAs) have a variety of uses in the production of industrial chemicals, food, and personal care products. These compounds are often produced through palm refining, but recent work has demonstrated that MCFAs can also be produced through the fermentation of complex organic substrates, including organic waste streams. While "chain elongation" offers a renewable platform for producing MCFAs, there are several limitations that need to be addressed before full-scale implementation becomes widespread. Here, we review the history of work on MCFA production by both pure and mixed cultures of fermenting organisms, and the unique metabolic features that lead to MCFA production. We also offer approaches to address the remaining challenges and increase MCFA production from renewable feedstocks.

Keywords: chain elongation; carboxylate platform; medium-chain fatty acids; carboxylic acids; mixed culture fermentation

1. Introduction

Microbial fermentation processes play an important role in food production, nutrient cycling, and pollution remediation. For more than 9000 years, humans have relied on microbial fermentation to produce and protect food [1], and fermentation processes have been used to convert wastes into valuable products since at least the 13th century [2]. One wide-spread application of fermentation processes to recover valuable products from wastes is anaerobic digestion. Anaerobic digestion is used to produce biogas (a mixture of carbon dioxide, methane, moisture, and other trace gasses) from organic wastes, including sewage sludge, agricultural and food production residues, and high-strength industrial wastes. There are estimated to be more than 20,000 large-scale anaerobic digestion facilities across the globe [3]. These facilities largely combust biogas to generate heat and electrical power, but biogas can also be converted to renewable natural gas to augment fossil-fuel derived natural gas. Anaerobic digestion to produce biogas is a well-studied process and has been widely implemented, but there is interest in producing valuable chemicals other than biogas from these renewable feedstocks.

Medium-chain fatty acids (MCFAs) are monocarboxylic acids containing 6 to 12 carbon atoms (Table 1). Currently, MCFAs are largely produced as a byproduct of palm refining. Palm kernels contain a relatively high content of octanoic acid (aka, caprylic acid, C8), decanoic acid (aka, capric acid, C10) and dodecanoic acid (aka, lauric acid, C12) [4]. MCFAs have also gained attention as dietary supplements, especially as medium-chain triglycerides (MCTs; three MCFAs attached to a glycerol backbone) [5]. MCTs are typically produced from the hydrolysis and separation of fatty acids from kernel or palm oil and re-esterification to a glycerol backbone, and contain 50–80% C8 [6].

MCTs are used as a supplement in livestock feed [7–9] and are marketed under many tradenames for human consumption (e.g., MCT Oil, Brain Octane Oil). In addition to their role as a nutritional supplement, MCFAs are also used for the production of personal care products, pharmaceuticals, dyes, and antimicrobials [10]. MCFAs have also been proposed as a precursor for liquid transportation fuels [11,12].

Table 1. Properties of short- and medium-chain fatty acids.

Compound Name	Common Synonyms	Solubility [1] (mg L^{-1})	Electron Density [2] (g COD g^{-1})	pK_a
Acetic acid	Ethanoic acid, C2	Miscible	1.07	4.76
Propionic acid	Propanoic acid, C3	Miscible	1.51	4.88
Butyric acid	Butanoic acid, C4	60,000	1.82	4.82
Pentanoic acid	Valeric acid, C5	24,000	2.04	4.84
Hexanoic acid	Caproic acid, C6	10,300	2.20	4.80
Heptanoic acid	Enanthic acid, C7	2820	2.34	4.80
Octanoic acid	Caprylic acid, C8	735 [3]	2.44	4.89
Nonanoic acid	Pelargonic acid, C9	284 [4]	2.53	4.95
Decanoic acid	Capric acid, C10	62	2.60	4.90
Undecanoic acid	Undecylic acid, C11	52	2.66	4.95
Dodecanoic acid	Lauric acid, C12	4.8	2.72	5.30

[1] Solubility in water obtained from PubChem [13] at 25 °C unless otherwise noted. [2] Electron density is presented as the chemical oxygen demand (COD). This value is the theoretical mass of O_2 required to completely oxidize a compound. [3] Solubility for octanoic acid was obtained by averaging the solubilities at 20 and 30 °C. [4] Solubility for nonanoic acid is reported for 20 °C.

MCFA production has been demonstrated by pure-cultures and mixed microbial communities (microbiomes) sourced from a variety of inocula. In bioreactor experiments, with either pure cultures or mixed communities, a variety of end products are typically formed, including short-chain fatty acids (SCFAs) and MCFAs. Studies of pure cultures provide valuable insights into MCFA production, and many novel MCFA-producing organisms have been described in recent years. Microbial communities are believed to be advantageous for MCFA production from complex feedstocks due to their ability to consume a wide range of substrates and to respond to perturbations due to changes in feedstock characteristics. Since the mid 2010's, the targeted production of MCFAs over short-chain fatty acids (SCFAs) has been termed "chain elongation," and the technology has previously been reviewed by Angenent et al. [10] and others [14,15]. However, there have been many recent developments in MCFA production that warrant further review. Therefore, this review summarizes the current body of knowledge using both pure cultures and mixed microbial communities. Metabolic features, energetics, and thermodynamics that may drive MCFA production are then considered. Lastly, future work is proposed to improve our understanding of MCFA production and to elucidate tools to improve MCFA production from complex feedstocks.

2. Medium-Chain Fatty Acid Production by Bacterial Isolates

MCFAs have been known as a potential fermentation product for over 100 years. Work with bacterial isolates producing MCFAs has provided insights into the metabolism of MCFA production and the phylogenetic diversity of MCFA-producing organisms. Here, we summarize the chronological body of work on MCFA production leading to the 13 isolated bacterial strains currently known to produce MCFAs. We also discuss the variety of substrates that can be used and the natural environments from which these bacteria were isolated. Characteristics of the known MCFA-producing bacterial isolates are summarized in Table 2.

Rhodospirillum rubrum [16] was the first MCFA-producing bacterium to be isolated (originally named *Spirillum rubrum* in 1887 [17,18]). During dark fermentation, *R. rubrum* consumes glucose, fructose, sucrose and carbon monoxide, and produces C6 [10,19]. In the 1940s, *Clostridium kluyveri* was isolated from canal mud. *C. kluyveri* is an anaerobic, non-saccharolytic bacterium that produces C6 and C8, using ethanol, n-propanol and pyruvate as electron donors, and C2, C3 and C4 as electron

acceptors [14,20–22]. *C. kluyveri* is one of the most well-studied MCFA-producing species and a complete genome for this organism became available in 2008 [23]. The proposed metabolism of MCFA production is largely based on experiments performed with *C. kluveryi*, and supporting genomic evidence [22–26] and is discussed later in this review. Shortly after the isolation of *C. kluyveri* in 1938, *Eubacterium limosum* was isolated from pea-blanching wastes, and converted methanol and C2 to C4 and C6 [27,28].

Shortly after the isolation of *C. kluveryi* and *E. limosum*, Prevot and Taffanel isolated *Ramibacteriurn alactolyticum* [29]. In 1967, this organism was shown to produce carboxylic acid products, including C6 and C8, from sugars and lactate [30]. In 1973, the name was changed to *Eubacterium alactolyticum* [31], and 26 years later, the organism was renamed again as *Pseudoramibacter alactolyticus* [29]. The complete genome of *P. alactolyticus* was sequenced in 2011 as part of the Human Microbiome Project [32]. In 1951, a third MCFA-producing microbe was isolated from the rumen of a sheep [33]. *Rumen organism LC*, as it was initially named, used sugars and lactate to produce even- and odd-chain carboxylic acids. In 1958, the organism was renamed *Peptostreptococcus elsdenii* [34], and in 1971 Rogosa reclassified the isolate as the genus *Megasphaera* [35] and named the type species *Megasphaera elsdenii*. *M. elsdenii* is a well-studied organism that has been used for the production of MCFAs from a variety of complex and simple substrates [36–43]. The complete genome of the *M. elsdenii* type strain was made available in 2011 [44], and three additional strain genomes have been sequenced since then [45,46]. In 2020, a metabolic reconstruction and model of *M. elsdenii* was published [47].

Several additional MCFA-producing strains have been described since the early 2000s. In 2003, *Eubacterium pyruvativorans* was isolated from a sheep rumen [48]. *E. pyruvativorans* converts C3 and C4 to C5 and C6, using methanol and pyruvate as electron donors [48]. *Ruminococcaceae* bacterium CPB6, isolated from a fermentation pit in 2015, produces C6 from lactate and has been used to convert wastes from liquor-making to MCFAs [49,50]. The genome of the *Ruminococcaceae* bacterium CPB6 was published in 2017 [51]. *Caproiciproducens galactitolivorans* (originally *Clostridium* sp. BS-1 [52,53]) was isolated from an anaerobic digester and described in 2015. *C. galactitolvorans* produces C6 from galactitol and its genome was sequenced in 2019 [54,55]. In 2017 a new species of *Megasphaera* was described. *Megasphaera hexanoica* converts sugars, including fructose and mannose, to even- and odd-chain fatty acids, including C6. *M. hexanoica* was isolated from a cow rumen, and follow-up work has investigated conditions to increase MCFA production [56,57].

In the first nine months of 2020, five additional MCFA-producing bacteria have been isolated. *Caproicibacter fermentans* is a C6-producing bacterium isolated from a methanogenic bioreactor [58]. *Clostridium* sp. BL-3, BL-4 and BL-6 convert lactate to C6. One of the isolates, BL-4, also produces iso-butyrate. [59,60]. *Caproiciproducens* sp. 7D4C2 was recently isolated from an MCFA-producing bioreactor and produces C6 from sugars [61]. Further, though not isolated, two *Candidatus* species of bacteria, *Candidatus Weimeria bifida* and *Candidatus Pseudoramibacter fermentans*, were described in 2020 and metabolic reconstructions were proposed based on metagenomic and metatranscriptomic analyses [62].

MCFA-producing isolates have been derived from a variety of natural sources, from canal mud to rumens to the human body. This wide range of isolation sources suggests that MCFA production may have yet undiscovered roles within natural ecosystems. With the exception of *R. rubrum*, all of the MCFA-producing isolates belong to the Firmicutes phylum, and there are currently six genera of MCFA-producing bacteria within the Firmicutes: *Clostridium*, *Pseudoramibacter*, *Megasphaera*, *Eubacterium*, *Caproicproducens*, and *Caproicbacter.* It is expected that many more MCFA-producing bacteria will be isolated in coming years, and studies with these organisms and their genomes are expected to provide new insights into MCFA production.

Table 2. Isolated bacterial strains known to produce MCFAs.

Name	Isolation Source	Substrates	Products	Reference
Clostridium kluyveri	Canal mud	Glucose, Fructose, Sorbitol, Mannitol, Lactate, Pyruvate, Serine, Formate	C4, C5, Ethyl crotonate, C6, C7, C8, CO_2 and H_2	[14,20–23]
Megasphaera elsdenii	Sheep rumen	Glucose, Fructose, Maltose, Mannitol, Sorbitol, Lactate	C2, C3, C4, C5, C6, CO_2 and H_2	[14,33–35]
Ruminococcaceae bacterium CPB6	Fermentation pit	Lactate, Ethanol, Glucose	C4, C6	[14,49,50]
Caproiciproducens galactitolivorans BS-1	Wastewater treatment plant	Galactitol, C2	Ethanol, Butanol, C2, C4, C6, H_2	[52,53]
Eubacterium limosum	Pea-blanching wastes	H_2 and CO_2	C2, C4, C5, C6	[14,27,28]
Eubacterium pyruvativorans	Sheep rumen	Formate, Acetate, Propionate, iso-butyrate, C4, Lactate	C4, C5, C6	[48]
Rhodospirillum rubrum	Dead mouse	Glucose, Fructose, Sucrose, CO	C6	[10,16–19]
Pseudoramibacter alactolyticus	Lung abscess	Glucose	Formate, C2, C4, C5, C6, C8	[29–31,63]
Megasphaera hexanoica	Cow rumen	Fructose, Mannose	C2, iso-butyrate, iso-valerate, C6, H_2, CO_2, H_2S	[56,57]
Clostridium sp. BL-3	Anaerobic bioreactor	Lactate, Ethanol, Xylose, Fructose	C2, C4, iso-butyrate, C6	[59,60]
Clostridium sp. BL-4	Anaerobic bioreactor	Lactate, Ethanol, Xylose, Fructose	C2, C4, iso-butyrate, C6	[59,60]
Clostridium sp. BL-6	Anaerobic bioreactor	Lactate, Ethanol, Xylose, Fructose	C2, C4, iso-butyrate, C6	[59,60]
Caproiciproducens sp. 7D4C2	Open-culture, chain-elongating bioreactor	Glucose, Fructose	Lactate, C2, C4, C6, H_2, CO_2	[61]

3. MCFA Production form Complex Feedstocks with Microbial Communities

While microbial isolates are important for understanding MCFA production, the application of large-scale MCFA production is expected to rely on microbial communities using "open culture" processes [10]. Several renewable substrates have been tested for MCFA production, including the organic fraction of municipal solid waste (OFMSW), food waste (FW), lignocellulosic biomass and residues of lignocellulosic biomass refining (LCB), waste from grain ethanol production, brewing distilling, and wine making (EBDWW), dairy processing wastes (DPW) and manure. In some processes, pretreatments have been used to condition the feedstock, including homogenization and microbial pre-treatment (Figure 1). Homogenization typically includes the addition of water to convert high-solid feedstocks into pumpable liquids. Microbial hydrolysis and fermentation (a.k.a, acid digestion) rely on anaerobic microbes to break down complex organic matter and to ferment a portion of the resulting hydrolysis products to acids and alcohols. Both liquid- and solid-state processes (generating an acid-rich leachate) have been used. Alternatively, feedstocks can be fed directly to a single reactor that performs hydrolysis, fermentation, and MCFA production. Sometimes, a supplemental electron donor (such as ethanol) is added. The MCFA-production step has been tested using both suspended-growth and attached-growth processes. Further, up-flow granular sludge processes have been used. The advantage of attached growth and granular processes is that they decouple the solids retention time from the hydraulic retention time, allowing the growth of slow-growing microbes without the need for high hydraulic retention times. If included, the extraction of MCFAs takes place either subsequent to MCFA production or as part of the same reactor system. When implemented on a reactor recirculation

stream this process is referred to as pertraction. An advantage of pertraction is that it prevents the accumulation of MCFAs within the fermentation broth. While most tested extraction processes rely on liquid–liquid separation with organic solvents, electrolytic extraction has also been proposed [64]. Typical processes for MCFA production are depicted in Figure 1. The selected processes largely depend on the complexity of the feedstock and the availability of electron donors to drive MCFA production. Here, we provide a review of past research on converting complex organic substrates to MCFAs based on the type of feedstock (Table 3). Past studies have investigated different feedstocks, reactor configurations, hydraulic retention times (HRTs), and inoculum sources. We summarize these studies based on net conversion of chemical oxygen demand (COD) provided to the reactor, including both COD in the feedstock and COD added as a supplemental electron donor.

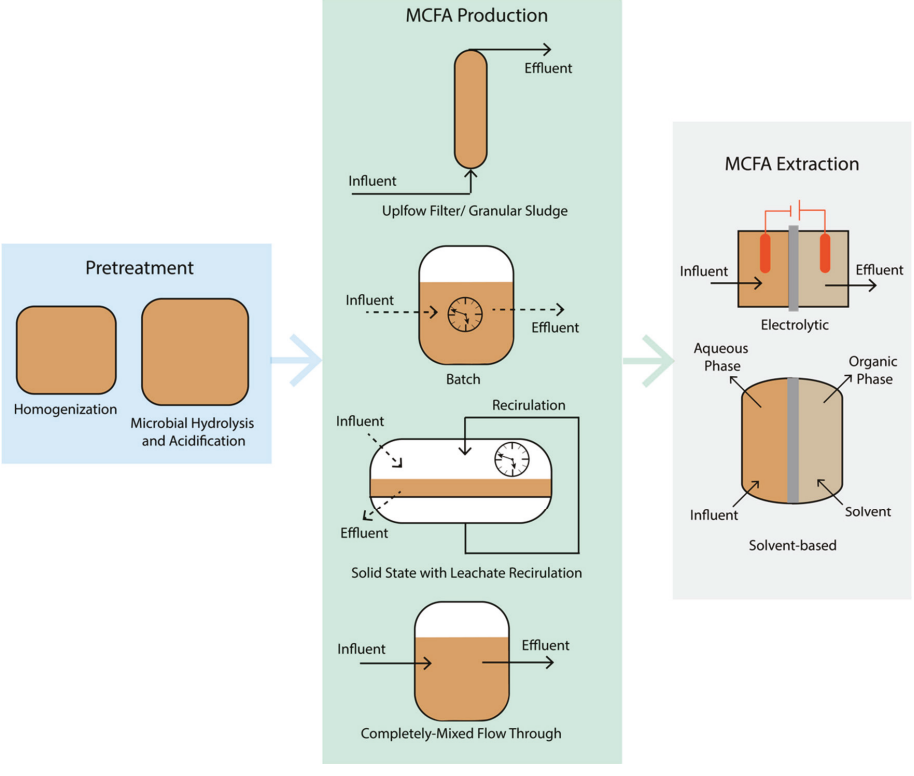

Figure 1. Processes for converting organic wastes to MCFAs. Several processes have been implemented for converting organic waste streams to MCFAs.

Table 3. A summary of studies investigating MCFA production from high-strength organic feedstocks.

Substrate Type	Specific Substrates	Supplemental Electron Donor	Reactor Type	HRT (d)	Pre-Treatment	Inoculum	COD Conversion	Productivity (g COD L^{-1} d^{-1})			Other Products	Ref.
								C6	C7	C8		
OFMSW	Influent waste from a full-scale organic waste treatment facility	Ethanol	Up-flow fixed bed	0.46	Microbial hydrolysis and acidification	Acetate and ethanol consuming consortium	19%	61	4.6	2.1	C2, C3, C4, C5	[65]
OFMSW	Approximately 90% yard waste and 10% food waste	None	Batch leach bed with leachate recirculation	35	Homogenization	OFMSW	5.6%	0.17	0.10	0.035	C2, C3, C4, C5	[66]
OFMSW	Approximately 90% yard waste and 10% food waste	Ethanol	Batch leach bed with leachate recirculation	28	Homogenization	OFMSW	2.3%	0.13	0.033	0	C2, C3, C4, C5	[66]
FW	Restaurant wastes	None	Leach bed with leachate recirculation	7	Homogenization	Full-scale granular anaerobic digester sludge	19%	7.3	NR	NR	C2, C3, C4	[67]
FW	Outdated food scraps	Ethanol	Continuously stirred flow-through	4	Microbial hydrolysis and acidification	Lab-scale bioreactor	28%	13	0.35	0.37	C2, C4	[68]
FW	Outdated food scraps	Ethanol	Continuously stirred flow-through	1	Microbial hydrolysis and acidification	Lab-scale bioreactor	8.2%	16	0.058	0.061	C2, C4	[68]
FW	Food waste from homes	Ethanol	Continuously mixed batch	51	Microbial hydrolysis and acidification	Undescribed anaerobic bacteria	4.1%	0.12	0.0043	0.0048	C2, C3, C4, C5, C10	[69]
FW	Food waste from homes	Ethanol	Continuously mixed batch	28	Microbial hydrolysis and acidification	Undescribed anaerobic bacteria, *C. kluyveri*	12%	0.64	0.01	0.01	C2, C3, C4, C5, C10	[69]

Table 3. *Cont.*

Substrate Type	Specific Substrates	Supplemental Electron Donor	Reactor Type	HRT (d)	Pre-Treatment	Inoculum	COD Conversion	Productivity (g COD L^{-1} d^{-1})			Other Products	Ref.
								C6	C7	C8		
FW	Outdated food scraps	None	Fed-batch	45	None	Lab-scale bioreactor	14%	4.20	NR	trace	C2, C3, C4, C5	[70]
LCB	Shredded paper and chicken manure	Ethanol	Continuously mixed batch	27	None	Marine bacteria	14%	0.81	NR	NR	C2, C4	[71]
LCB	Switchgrass ethanol production residues	None	Continuously stirred flow-through	6	None	Municipal wastewater acid digester sludge	22%	3.1	trace	0.40	C2,C4,C5	[72]
LCB	Milled switchgrass	None	Unmixed batch	3	None	Rumen fluid	0.33%	0.034	NR	NR	C2, C3, C4, C5	[73]
LCB	Milled switchgrass	Ethanol	Unmixed batch	3	None	Rumen fluid	0.17%	0.017	NR	NR	C2, C3, C4, C5	[73]
LCB	Milled switchgrass	Ethanol	Unmixed batch	3	None	Rumen fluid, *C. kluyveri*	35%	3.6	NR	NR	C2, C3, C4, C5	[73]
LCB	Farmland grass	None	Continuously stirred flow-through	2	Microbial hydrolysis and acidification	Lab-scale bioreactor	5.4%	5.7	NR	NR	C2, C3, C4, C5	[74]
LCB	Corn silage	None	Batch	13	None	Digestate from full-scale silage digester	3.8%	0.10	NR	0.0077	C2, C3, C4, C5	[75]
LCB	Corn stover hydrolysate	None	Fed-batch	9.6	Dilution	*Megasphaera elsdenii*	23%	0.29	NR	NR	C2, C4	[37]
EBDWW	Stillage and beer from a wheat bioethanol facility	None	Continuously stirred flow-through	7.5	None	Lab-scale bioreactor	18%	3.0	NR	trace	C2, C3, C4, C5, C10	[53]
EBDWW	Corn beer	None	Sequencing batch reactor	15	None	Digestate from first phase of full-scale silage digester	58%	1.7	0.056	2.70	C2, C3, C4, C6	[75]

Table 3. *Cont.*

Substrate Type	Specific Substrates	Supplemental Electron Donor	Reactor Type	HRT (d)	Pre-Treatment	Inoculum	COD Conversion	Productivity (g COD L^{-1} d^{-1})			Other Products	Ref.
								C6	C7	C8		
EBDWW	Solids-free thin stillage	None	Up-flow reactor, granular sludge	0.5	None	Reactor fermenting solid-free thin stillage	29%	1.5	0.046	0.037	C2, C3, C4, C5	[76]
EBDWW	Thin stillage from bioethanol production	None	Continuously stirred flow-through	6	None	Thin stillage	0.11%	0.060	NR	NR	C2, C3, C4, C5	[64]
EBDWW	Chinese liquor-making wastewater	None	Expanded granular sludge bed	8	Dilution	Pit mud and activated sludge	77%	0.55	0.057	0.081	C2, C3, C4, C5	[77]
EBDWW	Lactate-rich liquor-brewing wastewater	None	Fed-batch	3	Dilution	*Ruminococcaceae* bacterium strain CPB6, Municipal wastewater sludge	51%	11.6	NR	NR	C2, C4	[50]
EBDWW	Wine lees with 11% ethanol by volume	None	Continuously stirred flow-through	9.5	Dilution	Lab-scale bioreactor	67%	2.0	NR	2.0	C2, C3, C4, C5	[78]
DPW	Yogurt acid whey	None	Up-flow anaerobic filter	2.1	Microbial hydrolysis and acidification (thermophilic)	Lab-scale food waste fermentation	61%	21	4.3	4.9	C2, C3, C4, C5, C9	[79]
DPW	Quark acid whey	None	Up-flow anaerobic sludge blanket	2.5	None	Full-scale anaerobic digester sludge	32%	0.24	NR	trace	C2, C3, C4, C5	[80]
DPW	Cheese whey	None	Up-flow packed-bed reactor	6	None	Lab-scale acidogenic reactor	22%	1.5	NR	NR	C2, C3, C4, C5	[81]
Manure	Swine manure	Ethanol	Batch	76	Microbial hydrolysis and acidification	Full-scale anaerobic digester sludge	28%	0.11	0.084	0.034	C2, C3, C4, C5	[82]

3.1. Organic Fraction of Municipal Solid Waste (OFMSW)

Organic fraction of municipal solid waste (OFMSW) consists of yard waste, food waste, and other organic waste materials. As such, it can contain a mixture of plant- and animal-based products that vary widely in composition. High fractions of yard waste can increase the cellulose, hemicellulose, and lignin content, while high amounts of meat wastes can increase the protein content. OFMSW is collected as a solid material and may require dilution and homogenization prior to processing, especially if the food waste is treated in liquid-based reactors. An alternative leach bed-based approach has also been proposed. In these configurations, leachate is circulated through the solid waste to stimulate fermentation and capture fermentation products [66]. The highest productivities and COD conversion were obtained in work using an up-flow fixed-bed reactor supplemented with ethanol, relying on a two-stage process in which OFMSW was pre-fermented prior to MCFA-production [65]. The lower productivity of MCFAs in other OFMSW experiments [66] may be partly contributed to by a high fraction of yard waste in the feedstock. Cellulose, hemicellulose, and lignin polymers in yard waste are particularly recalcitrant [83]. While OFMSW is an abundant feedstock, it contains recalcitrant materials that may necessitate pre-treatment (e.g., hydrolysis) to achieve high conversion efficiencies of COD to MCFAs.

3.2. Food Waste (FW)

Food waste (FW) (a component of OFMSW) is another abundant organic waste that has been tested as a feedstock for MCFA production. As with OFMSW, FW characteristics can also vary significantly, with vegetables and starch-based products providing carbohydrates of various monomeric and polymeric compositions and meats providing high quantities of protein and fat. The pre-processing of food waste can include homogenization and pre-fermentation. De-packaging of food waste is an additional concern [84]. Work published in 2018 by Nzeteu et al. [67] demonstrated the use of a leach bed reactor with liquid recirculation, and achieved a maximum conversion of 19% of the influent COD in food waste to C6. Base on the characterization of reactor influent and effluent, they showed that 90% of hemicellulose, 60% of proteins, 50% of cellulose, and 20% of fats were degraded. In addition to the sustained demonstration with the leachate reactor, Nzeteu and colleagues tested the ability to produce additional MCFAs from the leachate bed effluent through the addition of either ethanol, H_2, or both ethanol and H_2 as supplemental electron donors in batch experiments. They found that lactate in the leachate reactor effluent was converted to C6 when H_2 or a combination of H_2 and ethanol was added. Another process for processing food waste is a two-stage configuration in which food waste is first pre-treated in a hydrolysis and fermentation bioreactor. Roghair and colleagues [68] used a batch hydrolysis and fermentation reactor operated at a pH of 5.5 and retention time of 18 days to acidify food waste prior to feeding to an MCFA-producing bioreactor. In total, 28% of the COD was converted to MCFAs with a 4 day retention time, but decreasing the retention time to 1 day reduced MCFA production [68]. Reddy et al. performed batch tests with and without bioaugmentation with *C. kluyveri* and found that the augmentation of *C. kluyveri* improved MCFA production [69]. Contreras-Davila et al. enriched a bioreactor that produced lactate as an intermediate to MCFAs, and the microbial community was dominated by species related to the genera *Lactobacillus* and *Caproicproducens* [70]. While lacking the high lignocellulosic content of OFMSW, the production of MCFAs from food waste still has challenges, including the de-packaging of abundant food wastes (such as those obtained from a grocery store). High protein content is also a concern due to potential ammonia toxicity as amino acids are degraded.

3.3. Lignocellulosic Biomass (LCB)

LCB feedstocks include the non-grain parts of crops (such as corn-stover), non-food plants (such as switchgrass), and paper. Lomkar, Fu and Holtzapple showed the production of C6 from a mixture of chicken manure and shredded paper by adding supplemental ethanol in batch experiments [71]. Scarborough, et al. demonstrated the production of C6 and C8 from the stillage (the material remaining

after distillation) of a switchgrass biorefining process [72]. The lignocellulosic stillage was rich in xylose and complex carbohydrates, and lactate accumulated as an intermediate upon spike-feeding the reactor with stillage. Subsequent multi-omic studies suggested that two organisms, Ca. *Weimeria bifida* and Ca. *Pseudoramibacter fermentans*, expressed genes for producing MCFAs [62,85]. Metabolic modeling, however, suggested that all of the MCFAs were produced by Ca. *Weimeria bifida* from xylose, while Ca. *Pseudoramibacter bifida* was predicted to produce C4 [86]. Other studies have explored the use of grass directly [73,74]. Weimer, Nerdahl and Brandl achieved a high conversion of COD (35%) with milled grass and ethanol using a microbiome from cow rumen fluid augmented with *C, kluyveri* [73]. Khor et al. used a two-stage process in which grass was first fermented to lactate using a leach bed reactor [74]. Leach bed fermenter effluent was converted to C6 in a microbial community enriched in *Clostridium-related* organisms. MCFAs were extracted via electrolytic extraction and Kolbe electrolysis was used to convert the enriched caproate stream into dodecane, which can be used as a liquid transportation fuel [74]. MCFA production from corn silage (partly fermented corn stover commonly used as animal feed) has also been demonstrated [75]. Corn stover hydrolysate (produced from the chemical depolymerization and enzymatic hydrolysis of corn stover) has also been converted to MCFAs using a pure culture of *M. elsdenii* [37]. The high COD and carbon content of LCB feedstocks make them attractive for MCFA production. Further, integrating MCFA production into next generation biorefineries may provide additional sources of revenue.

3.4. Ethanol, Brewery, Distillery, and Winery Waste (EBDWW)

EBDWW includes high-strength organic streams containing stillage (material remaining after distillation), yeast biomass (trub, dregs, or lees), and spent grains. EBDWW can contain high amounts of ethanol, which is a well-studied electron donor for MCFA production [10]. Multiple studies have investigated MCFA production from beer and/or stillage from grain-based ethanol biorefineries [53,64,75,76]. Andersen et al. produced C6 and C8 from beer and stillage derived from wheat-based ethanol production. The production of C10 was also reported, and the microbial community was enriched in *Lactobacillus* and *Clostridium*-related organisms [53]. While ethanol was provided in the feedstock (targeting an influent concentration of 6 g/L under steady-state conditions), lactate was also predicted to be an important electron donor produced as an intermediate from carbohydrates [56]. Urban et al. converted 58% of the COD in corn beer to MCFAs, extracted the MCFAs with pertraction, and converted MCFAs to alkanes using Kolbe electrolysis [75]. Similar to work by Khor et al. [74], Urban et al. demonstrated the complete conversion of a complex organic material to alkanes with MCFAs as an intermediate. Carvajal-Arroyo et al. implemented a granular sludge process to convert 29% of COD in stillage to MCFAs [76]. The resulting granules were enriched in *Ruminococcaceae*-related organisms. Andersen et al. converted stillage to a mixture of VFAs—including a minor amount of C6—in a bioreactor integrated with electrolytic extraction. Electrolytic extraction has the advantage of removing the MCFA products while also supplying H_2 as an electron donor and consuming H+ to reduce or eliminate the need for the addition of pH control chemicals [64]. Wu et al. used an up-flow granular sludge reactor to convert 77% of the COD in liquor-making wastewater to MCFAs (77%). Zhu et al. used a recently isolated MCFA-producing strain (*Ruminococcaceae* CPB6) and converted 51% of COD in lactate-rich liquor-making wastewater to MCFAs [50]. Kucek et al. also achieved high conversion efficiencies from wine lees (a waste stream from wine production containing yeast biomass) using a bioreactor equipped with a pertraction system. In summary, EBDWW feedstocks are attractive due to their high organic content and availability of electron donors, including ethanol and lactate, which can drive MCFA production from the carbohydrates remaining in the waste stream.

3.5. Dairy Processing Wastewater (DPW)

Cheese, milk and yogurt processing produce low-value streams that are rich in organic materials. DPW can be rich in simple substrates, such as lactose, that have the potential for many biorefining applications. Whey, a dairy-derived protein, is also abundant. Three known studies have investigated

the use of DPW for MCFA production. Using acid whey from yogurt production, Xu et al. used a two-stage, temperature-phased process to produce MCFAs from acid whey. The MCFA production reactor was coupled to a pertraction system, and a sample from the first stage fermentation was diluted to maintain target organic loading rates. This system achieved a 61% conversion of COD and the highest production rates of MCFAs reported in the literature thus far [79]. The high production rates are likely due to an easily-degradable substrate, pre-fermentation to produce lactic acid, the use of an up-flow filtration reactor to decouple solids retention time from the hydraulic retention time, and the removal of MCFAs with pertraction to prevent product inhibition. In another study, acid whey from the production of quark (a curd cheese product) was used as a feedstock to produce C6 with an up-flow sludge-blanket reactor [80]. As with other studies, the microbial community was enriched in *Ruminococcaceae*-related organisms [80]. In a third study, the feedstock was created by mixing cheese whey with water [81]. This study provided a robust analysis of different operational parameters, including the HRT and the organic loading rate. The biofilm generated in the up-flow reactor was enriched in microbial communities, including organisms related to *Lactobacillus*, *Clostridium*, and *Ruminococcaceae* [81]. DPW are an attractive substrate due to their high content of simple substrates, including sugars (such as lactose) and lactate.

3.6. Manure

To our knowledge, there has been only one published study investigating manure as a substrate for MCFA production. Zhang et al. used a two-stage batch system to convert swine manure to MCFAs [82]. The swine manure contained 37% solids, and the solids were comprised of 25% hemicellulose, 20% protein, 18% cellulose, and 6.5% fat. Diluted manure was used as the feedstock, and ethanol was added as a supplemental electron donor. A COD conversion of 28% was achieved, but this required a long duration of 76 days. Still, this study demonstrates that manure may be a suitable substrate for MCFA production.

3.7. Ideal Feedstocks and Processes for MCFA Production

Past work shows that MCFAs can be produced from a wide variety of feedstocks (Table 3). Supplemental electron donors, such as ethanol, can be added to potentially increase MCFA yield, but the addition of ethanol results in significant economic and environmental costs [87]. Feedstocks containing easily degradable materials—such as DPW, containing high amounts of sugar—may not require supplementation with an electron donor. Further, some feedstocks—such as EBDWW—may be rich in electron donor materials, such as lactate or ethanol. A variety of reactor configurations have also been tested. Pretreatment with microbial hydrolysis and acidification may improve MCFA yields for some substrates, and the real-time removal of products via pertraction can greatly increase production rates. However, there is still much work required to optimize reactor systems, based on cost and productivity, for MCFA production.

4. Metabolic Features of Medium-Chain Fatty Acid Production

The primary route for MCFA production is believed to be reverse β-oxidation. β-oxidation is a route of fatty acid catabolism, and metabolic engineering to reverse this pathway in model organisms has been suggested [88]. Certain fermenting organisms, however, have long been known to use reverse β-oxidation as a strategy for redox balancing. Here, we focus on the natural metabolism of MCFA-producing bacteria described through various phenotypic and genomic studies.

4.1. Reverse β-Oxidation

MCFAs are proposed to be produced by reverse β-oxidation (Figure 2) [10,89]. The cycle is initiated by an acyl-CoA C-acyl transferase (E.C. 2.3.1.16, E.C. 2.3.1.9) that combines acetyl-CoA with an acyl-CoA (e.g., acetyl-CoA, propionyl-CoA, butyryl-CoA, valeryl-CoA, hexanoyl-CoA). In the second step, the 3-hydroxyacl-CoA is reduced via 3-hydroxyacyl-CoA dehydrogenase (E.C. 1.1.1.157, E.C. 1.1.1.35) with electrons from NADH. In the third step, enoyl-CoA hydratase (aka, crotonase; E.C. 4.2.1.55, E.C. 4.2.1.17) creates a double bond between the second and third carbons creating

an enoyl-CoA. In the fourth step, an electron-bifurcating acyl-CoA dehydrogenase (E.C. 1.3.1.109) oxidizes two molecules of NADH, with one electron pair being transferred to the enoyl-CoA and one being transferred to ferredoxin, producing reduced ferredoxin (Fd_{RED}) and an acyl-CoA [90]. The electron-bifurcating acyl-CoA dehydrogenase complex relies on two electron transfer flavoproteins (EtfA and EtfB) to mediate the transfer of electrons [91]. In total, reverse β-oxidation increases the length of an acyl-CoA by two carbons, while oxidizing three molecules of NADH to NAD^+ and reducing one molecule of oxidized ferredoxin (Fd_{OX}) to Fd_{RED}.

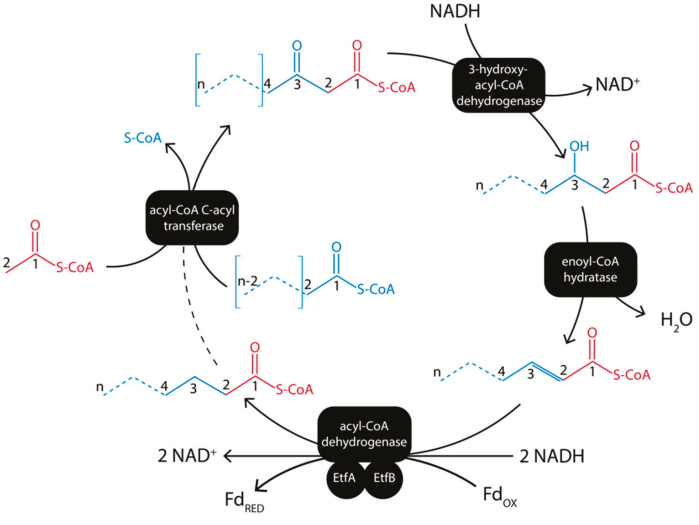

Figure 2. Reverse β-oxidation with an electron-bifurcating acyl-CoA dehydrogenase.

4.2. Terminating Reverse β-Oxidation

Reverse β-oxidation produces a CoA-ligated carboxylate (Figure 2). The terminal step of reverse β-oxidation is the cleaving of the carboxylate from CoA. Acyl-CoA hydrolases (E.C. 3.1.2.20) use water to cleave the CoA from the acid (Figure 3). A CoA transferase (E.C. 2.8.3.8) transfers a CoA from one acid to another. The replacement of the CoA with phosphate acyl transferases (e.g., phosphate butyryl transferase, E.C. 2.3.1.19) and subsequent ADP phosphorylation via a kinase (e.g., butyrate kinase, E.C. 2.7.2.7) have also been proposed [92].

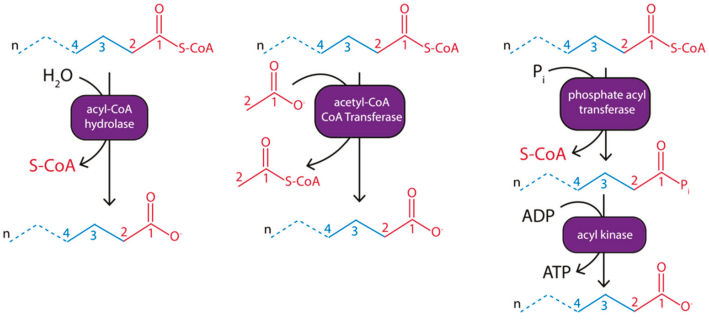

Figure 3. Terminal enzymes for hydrolyzing the CoA-ligated products of reverse β-oxidation to release a carboxylate and CoA.

4.3. Energy-Conservation Coupled with Reverse β-Oxidation

Reverse β-oxidation does not directly produce ATP. Instead, organisms are predicted to use one or more enzymes to couple highly exergonic redox reactions to the generation of an ion motive force (IMF). The IMF can be used to generate ATP via a membrane-bound ATP synthase. One example is the *Rhodobacter* nitrogen fixation (RNF) complex (aka, ion-translocating ferredoxin NAD^+ oxidoreductase, E.C. 7.2.1.2) (Figure 4). The RNF complex couples the reduction of NAD^+ by Fd_{RED} with the translocation of proton or sodium ions across the cell membrane to generate IMF. This enzyme complex has been found in many fermenting bacteria, as well as methanogenic archaea [93–96]. The catalyzed reaction is reversible and the RNF complex plays a role in maintaining ratios of intracellular NADH and Fd_{RED} [97]. Another example is a membrane-bound energy-conserving hydrogenase (ECH) that couples the reduction of protons by Fd_{RED} with IMF generation. Regardless of the route of IMF generation, Fd_{RED} (a highly electronegative electron carrier) is needed to generate IMF. Therefore, the electron-bifurcating acyl-CoA dehydrogenase (Figure 2) is key to producing energy from reverse β-oxidation.

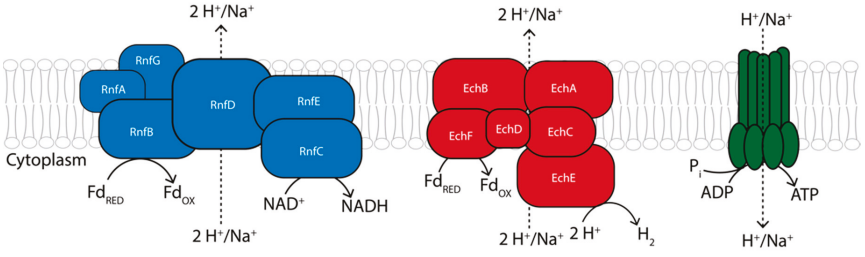

Figure 4. Membrane-bound enzymes for energy conservation in MCFA-producing bacteria. The RNF complex couples the reduction of NAD+ with Fd_{RED} with ion translocation to generate an ion motive force. Similarly, energy-conserving hydrogenase couples the reduction of protons with Fd_{RED} to ion translocation. The ion motive force is consumed by ATP synthase to produce ATP.

4.4. Additional Electron Bifurcating Enzymes for Energy Conservation and Redox Management

Other enzymes are proposed to conserve energy by producing or conserving Fd_{RED} to use for IMF generation [98]. One example is NAD(P)+ transhydrogenase (Nfn) (Figure 5), which transfers electrons from NADH and Fd_{RED} to NADPH and can be used in reverse to produce Fd_{RED} and NADH from NADPH [26]. Another example is HydABC (Figure 5), which produces H_2 through the bifurcation of electrons from Fd_{RED} and NADH [99]. While Nfn produces Fd_{RED} directly, HydABC decreases the amount of Fd_{RED} needed for H^+ reduction compared to ferredoxin hydrogenase (Hyd1, E.C. 1.12.7.2) (Figure 5). Alternatively, HydABC may be used in reverse for the production of Fd_{RED} and NADH from H_2.

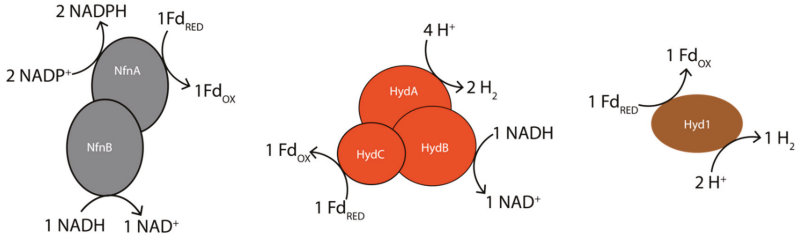

Figure 5. Additional enzymes for redox balancing in MCFA-producing bacteria. NfnAB couples NADH and Fd_{RED} oxidation with $NADP^+$ reduction. HydABC relies on electrons from both NADH and Fd_{RED} to reduce protons. A ferredoxin hydrogenase uses only Fd_{RED} for hydrogen production.

4.5. Hypothesized Routes for MCFA Production from Ethanol with and without Acetate as an Electron Acceptor

To illustrate how bacteria tie MCFA production to energy conservation, we considered the well-studied example of ethanol and C2 conversion to MCFAs [23,89,98]. Ethanol conversion with reverse β-oxidation is well described in *C. Kluyveri*, and the metabolism has been reconstructed for C4 and C6 production from the co-utilization of ethanol and acetate [10,23]. One example of this overall transformation is the conversion of 1 mol C2 and 2 mols ethanol to C6 (Figure 6). In our example, we assumed C2 is incorporated via acetyl-CoA CoA transferase (Figure 3). Under this condition, C6 production results in the production of 1 mol of ATP (0.5 mol ATP per mol ethanol). Under this condition, no H_2 is predicted to be produced. The ratio of ethanol-to-C2, however, is not fixed and H_2 is predicted as a product when the molar ratio of ethanol-to-C2 is greater than 2:1 (Figures S1–S13).

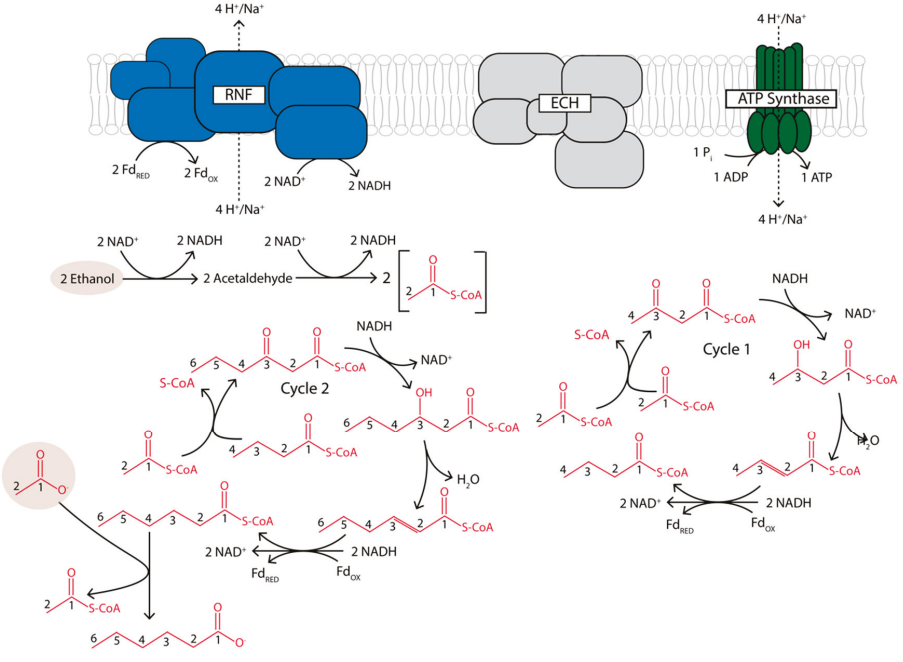

Figure 6. An example model of C6 production from ethanol (2 mols) and acetate (1 mol) without production of H_2.

While ethanol and acetate can be used as co-substrates, acetate is not required as an electron acceptor for converting ethanol to MCFAs [100]. When 2 mols of ethanol are converted to acetyl-CoA, a total of 4 mols NADH are predicted to be produced (Figure 7). One cycle of reverse β-oxidation consumes 3 mols NADH, leaving 1 mol NADH and 1 mol Fd_{RED}. There are multiple potential ways to maintain redox balance, depending on the hydrogenase present. With ECH, Fd_{RED} could reduce H^+ to H_2 while producing IMF (Figure 7). IMF can then be consumed by the RNF complex to transfer electrons from the remaining NADH to Fd_{RED}, in order to recycle NAD^+. Fd_{RED} can also be used via ECH to generate IMF that drives ATP synthase. In this model (Figure 7A), 0.5 mol ATP are predicted (0.25 mol ATP per mol of ethanol). If 3 moles of ethanol are consumed, then six NADH are produced (Figure 7B). Two cycles of reverse β-oxidation would consume all six NADH and produce 2 mols Fd_{RED}. Then, the 2 mols Fd_{RED} could be used to generate IMF with ECH, resulting in the net production of 1 mol ATP (0.333 mol ATP per mol of ethanol consumed). Thus, the production of C6 is predicted to increase the ATP yield by 33% per mol ethanol compared to C4 production. These two scenarios

illustrate how MCFA production can increase ATP production compared to the production of C4, but the overall ATP production is lower than when acetate is used as an electron acceptor (Figure 6).

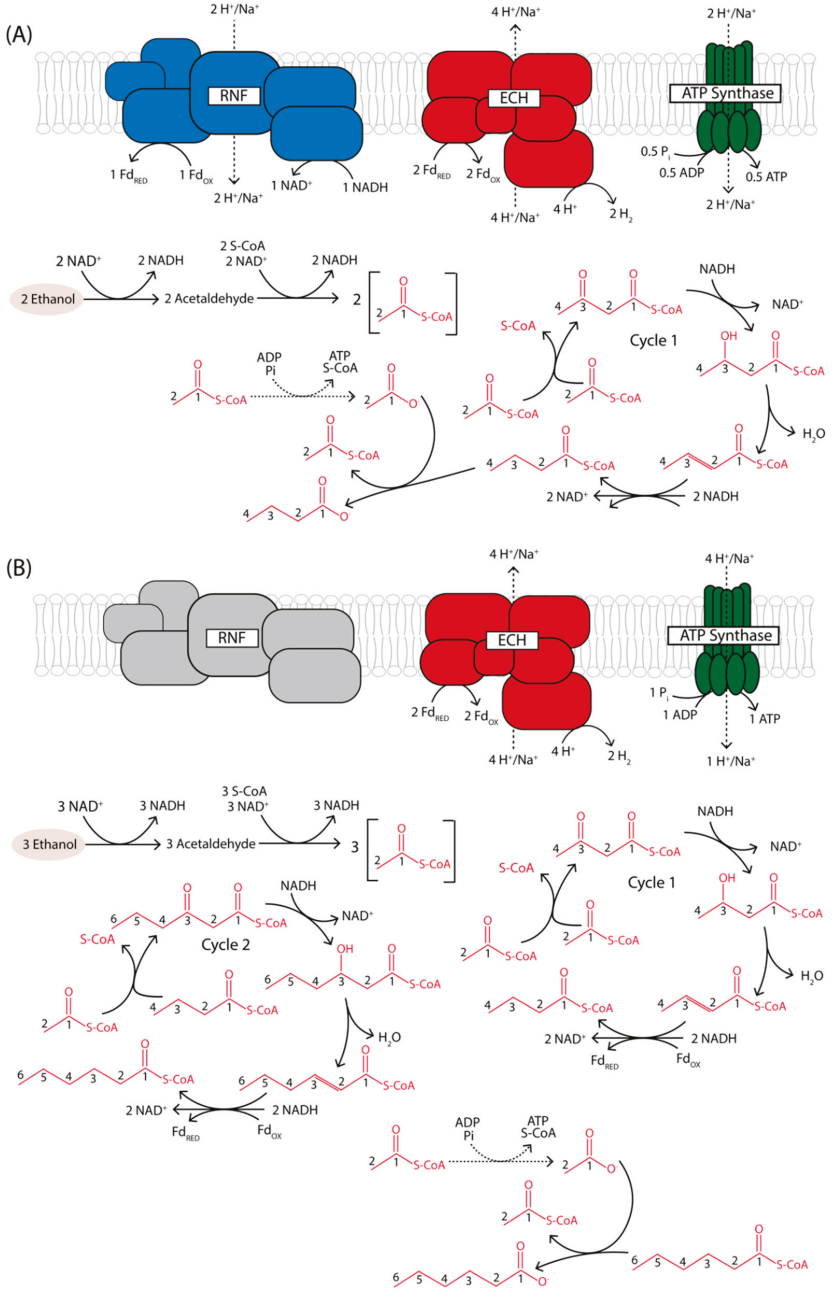

Figure 7. Example models of C4 production (**A**) and C6 production (**B**) when ethanol is used as a sole substrate without acetate as an electron acceptor. The conversion of C6 is predicted to increase the ATP yield per mol of ethanol by 33%.

4.6. Thermodynamic and Energetic Drivers of MCFA Production

The energetic drivers of MCFA production have been explored [101], but recent discoveries of novel energy-conserving mechanisms in anaerobic bacteria suggest that energetic drivers are not fully elucidated [90]. To illustrate the potential energetic drivers of MCFA-production, we considered the conversion of ethanol to MCFAs. All free energies of formation were assumed based on previously described methods [85]. When consuming ethanol as a sole substrate, H_2 is predicted to be produced for all scenarios, and it is shown that the amount of H_2 produced decreases with the length of the product (Equations (1)–(4)). The reaction depicted in Equation (3) was also described in Angenent et al. [10].

$$1\,C_2H_6O\ +\ 1\,H_2O\ \rightarrow 1\,C_2H_3O_2^{-} + 2\,H_2 + 1\,H^{+} \quad \Delta G0' = +9.65\ \text{kJ mol}^{-1}\ \text{ethanol} \tag{1}$$

$$1\,C_2H_6O \rightarrow \frac{1}{2}\,C_4H_7O_2^{-} + 1\,H_2 + \frac{1}{2}\,H^{+} \quad \Delta G0' = -14.5\ \text{kJ mol}^{-1}\ \text{ethanol} \tag{2}$$

$$1\,C_2H_6O_2 \rightarrow \frac{1}{3}\,C_6H_{11}O_2^{-} + \frac{1}{3}\,H_2O + \frac{2}{3}\,H_2\ + \frac{1}{3}H^{+} \quad \Delta G0' = -22.6\ \text{kJ mol}^{-1}\ \text{ethanol} \tag{3}$$

$$1\,C_2H_6O_2\ \rightarrow \frac{1}{4}\,C_8H_{15}O_2^{-} + \frac{1}{2}\,H_2O + \frac{1}{2}\,H_2 + \frac{1}{4}\,H^{+} \quad \Delta G0' = -27.4\ \text{kJ mol}^{-1}\ \text{ethanol} \tag{4}$$

The co-consumption of ethanol and acetate reduces the need for H_2 production (Equations (5)–(8)) as acetate can accept electrons that would otherwise be used to produce H_2. When consuming 1 mol C2 per mol of product (Equations (5)–(8)), no H_2 is predicted. The ratios of ethanol-to-C2, however, are not fixed and the utilization of 3 mols ethanol to 2 mols acetate has been described previously for *C. kluyveri* [10]. Many ethanol-to-C2 ratios have been tested, and high ratios of ethanol to acetate have been shown to favor MCFA production [100].

$$1\,C_2H_6O\ +\ 1\,C_2H_3O_2^{-} \rightarrow 1\,C_4H_7O_2^{-} + 1\,H_2O \quad \Delta G0' = -38.6\ \text{kJ mol}^{-1}\ \text{ethanol} \tag{5}$$

$$1\,C_2H_6O\ +\frac{1}{2}C_2H_3O_2^{-} \rightarrow \frac{1}{2}\,C_6H_{11}O_2^{-} + 1\,H_2O \quad \Delta G0' = -38.7\ \text{kJ mol}^{-1}\ \text{ethanol} \tag{6}$$

$$1\,C_2H_6O + \frac{1}{3}C_2H_3O_2^{-} \rightarrow \frac{1}{3}C_8H_{15}O_2^{-} + 1\,H_2O \quad \Delta G0' = -39.7\ \text{kJ mol}^{-1}\ \text{ethanol} \tag{7}$$

$$1\,C_2H_6O\ + \tfrac{2}{3}\,C_2H_3O_2^{-} \rightarrow \tfrac{5}{6}\,C_4H_7O_2^{-} + \tfrac{2}{3}\,H_2O\ + \tfrac{1}{3}\,H_2\ + \tfrac{1}{6}H^{+} \quad \Delta G0' = -30.6\ \text{kJ mol}^{-1}\ \text{ethanol} \tag{8}$$

Metabolic reconstructions of ethanol consumption predict that hydrogen-producing enzymes play a role in determining the most energetically favorable products (Table 4). If C2 is produced from ethanol, no net ATP production is predicted with Hyd1. With ECH, up to 1.0 mol ATP per mol ethanol is predicted, but the amount of free energy needed to generate this much ATP is only feasible at H_2 partial pressures below 10^{-5} atm, assuming a minimum quantum of –50 kJ per mol ATP [102] (Figure 7). With Hyd1, longer products are predicted to increase the ATP yield. With ECH, shorter products increase the ATP yield, but these scenarios all rely on low H_2 partial pressures for the predicted ATP production to be feasible (Figure 7). The co-utilization of C2 can obviate the need for H_2 production, and the predicted ATP yield (0.5 mol ATP per mol ethanol) when no H_2 is produced is higher than all scenarios using ethanol as a sole substrate and Hyd1 as the hydrogenase. If Hyd1 is the only hydrogenase available, co-utilization of C2 with ethanol is always predicted to produce more ATP per mol ethanol than consumption of ethanol as a sole substrate, and all products result in the same ATP yield (0.5 mol ATP per mol ethanol). However, if ECH is available, the ATP yield is higher if ethanol is the sole substrate, but the overall free energy release is lower per mol ATP produced. This suggests that ethanol consumers with ECH may only co-utilize acetate under high H_2 partial pressures.

Table 4. Predicted ATP production and free energy release for the conversion of ethanol to acetate, butyrate, hexanoate, and octanoate with either a ferredoxin hydrogenase (Hyd1) or energy-conserving hydrogenase (ECH).

Ethanol: Acetate	Product	Hydrogenase	ATP/mol Ethanol			$\Delta G^{0'}$/mol ATP	Model
			SLP [1]	ATPS [2]	Total		
1:0	C2	Hyd1	1.00	−1.00	0	-	Figure S1
1:0	C4	Hyd1	0.500	−0.250	0.250	−58.0	Figure S2
1:0	C6	Hyd1	0.333	0	0.330	−68.5	Figure S3
1:0	C8	Hyd1	0.250	0.125	0.375	−73.1	Figure S4
1:0	C2	ECH	1.00	0	1.00	+9.65	Figure S5
1:0	C4	ECH	0.500	0.250	0.750	−19.3	Figure S6
1:0	C6	ECH	0.333	0.333	0.678	−33.7	Figure S7
1:0	C8	ECH	0.250	0.375	0.625	−43.8	Figure S8
1:1	C4	None	0	0.500	0.500	−65.4	Figure S9
2:1	C6	None	0	0.500	0.500	−77.4	Figure S10
3:1	C8	None	0	0.500	0.500	−79.4	Figure S11
3:2	C4	Hyd1	0.167	0.250	0.417	−73.4	Figure S12
3:2	C4	ECH	0.167	0.417	0.584	−52.4	Figure S13

[1] The ATP predicted to be produced from substrate-level phosphorylation (SLP). [2] The ATP predicted to be produced via ATP synthase (ATPS).

To further illustrate the potential importance of H_2 and hydrogenase enzymes, we performed a thermodynamic analysis to assess the feasibility of a subset of predictions (Table 4) with varying conditions of H_2 partial pressure. We considered either Hyd1 or ECH as the sole enzyme for hydrogen production. All products are predicted to result in thermodynamically favorable reactions up to a partial pressure of 10^{-1} atm (Figure 8A). At H_2 partial pressures greater than 10^{-1} atm, the production of acetate as the sole product is predicted to be infeasible ($\Delta G^{0'} > 0$). Because the overall reaction is the same regardless of the type of hydrogenase assumed, there is only one line per product shown in Figure 8A. We then incorporated the predicted ATP yields from our metabolic reconstructions (Figure 8B). With ECH, the predicted free energy release per mol ATP is greater than −50 kJ at increasing H_2 partial pressures for each potential product (C2 = 10^{-5} atm; C4 = 10^{-4} atm; C6 = 10^{-3} atm; C8 = 10^{-1} atm). This suggests that H_2 partial pressure may be a control to drive the production of MCFAs if ECH is used as a hydrogenase. With Hyd1, the production of acetate from ethanol is predicted to produce a net of 0 ATP in order to maintain redox balance (Figure S1). ATP predictions from all other products are feasible up to a H_2 partial pressure of 3 atm, indicating that H_2 partial pressure may not be an appropriate control to drive MCFA production if Hyd1 is the hydrogenase.

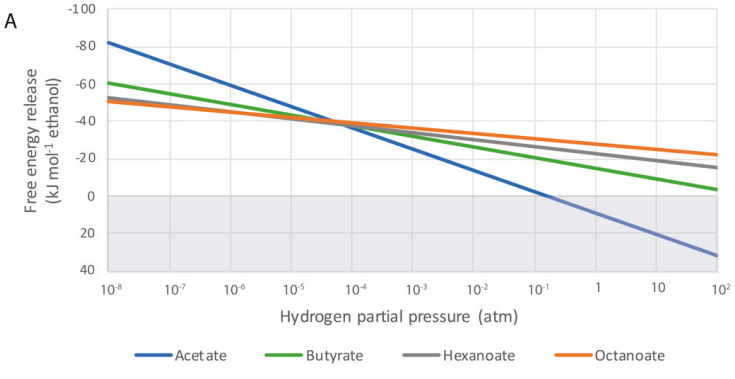

Figure 8. *Cont.*

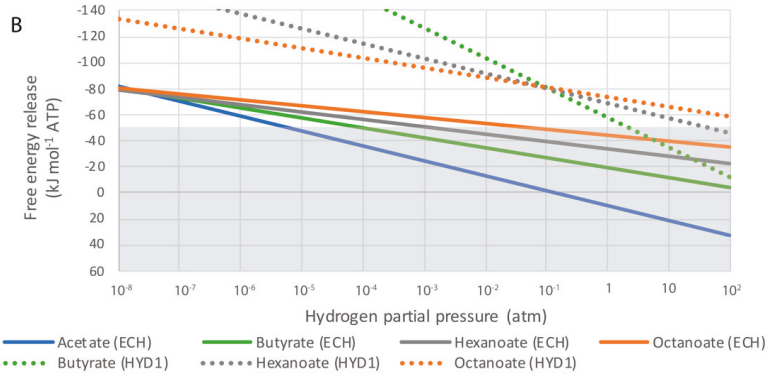

Figure 8. Free energy release for different products from ethanol under a range of H_2 partial pressures. Plots show the overall free energy release (**A**) and the free energy release per mol of ATP (**B**). Areas shaded in gray are considered infeasible and the dashed lines represent scenarios with Hyd1 as a hydrogenase instead of ECH.

5. Path Forward

Taken together, the metabolic reconstructions and thermodynamic analysis suggests that (1) the most energetically advantageous products depend on enzymes other than those directly performing reverse β-oxidation, and (2) the infinite number of combinations of substrate ratios and product formation make simulating MCFA production a challenge. Still, as we learn more about the behavior of microbes producing MCFAs and how these microbes interact with complex microbial communities, we should improve our ability to design, diagnose, and control MCFA-producing bioreactors. We have identified specific knowledge gaps below.

5.1. Controlling Product Length

Controlling the terminal product length remains a challenge. While we have illustrated that some conditions should favor the production of MCFAs over C2 and C4, almost all studies to date create mixtures of end products, varying in length from C2 to C6 or C8 (Table 3). The highest specificities of C6 and C8 production have resulted from the incorporation of pertraction systems [103]. This real-time removal of C6 and C8 is thought to increase their production in part because the protonated forms of MCFAs are toxic [104–106]. Thus, their production may be limited by their toxic effects. While there has been recent work on the toxic effects of these compounds in MCFA-producing bioreactors [107], an improved understanding of the toxicity of these products is needed. Quantifying these effects, for instance via Monod-based inhibition terms, would be particularly valuable for modeling the impacts of MCFA toxicity and the favorable production of specific carbon chain lengths across various systems.

Enzyme specificity is also expected to control the length of the terminal product. The enzymes directly involved in reverse β-oxidation (Figure 2) and the termination of reverse β-oxidation (Figure 3) are all likely to play a role in dictating the predominant product length. Individual enzymes of the fatty acid biosynthesis (Fab) pathway are well characterized, and metabolic engineering approaches have been used to produce specific chain lengths [108,109]. Additional kinetic studies of reverse β-oxidation enzymes can inform modeling approaches, and structural studies could enable metabolic engineering to improve enzyme specificity towards target products. Genetically tractable MCFA-producers, however, are only beginning to emerge [36]. As metabolic engineering tools continue to improve and additional MCFA-producing isolates become available, isolate-based studies should elucidate strategies to improve the control of target chain lengths.

5.2. Microbial Community Assembly, Function, and Resiliency

The many microbial community-based studies for MCFA production have elucidated common functional guilds that become enriched in these communities, while phylogenetically distinct, functional roles tend to be conserved. As an example, several reactors fed carbohydrates have been enriched in *Lactobacillus* species and lactate-consuming MCFA producers. A framework for these functional guilds was recently proposed [86].

Further, these microbial communities have demonstrated resilience (sustained production of MCFAs) when operated as open cultures, often fed with non-sterile feedstocks. This resilience may be due to the presence of MCFAs, which select for only organisms with some tolerance to these products. In addition, although these communities contain organisms that rely on oxygen-sensitive ferredoxin [110], they survive in conditions with feedstocks that likely contain small amounts of oxygen. Thus, we predict that facultative anaerobes (such as *Lactobacillus*-related organisms) may play a role in quenching oxygen. When separating stages of fermentation (e.g., two-stage processes, Figure 1) or implementing pertraction, it is important to consider the traits that may make these microbial communities resilient.

5.3. Product Uses

MCFA production from renewable feedstocks may allow for reduced dependence on palm refining and fossil fuels. While MCFAs currently have high market prices, it is expected that the widespread production of MCFAs would reduce their value. Thus, more work on refining MCFAs to other products is needed. Kolbe electrolysis has already been demonstrated as a potential option to convert MCFAs to alkanes for use as a liquid transportation fuel. Another option may be to purify MCFAs and use them as a feed supplement. MCFAs are expected to have many of the same potential benefits as MCTs and may have potential as a dietary supplement for both humans and animals. More work on the role of MCFAs as a platform chemical is needed, and this work should consider the potential societal and environmental benefits along with the economic benefits. Thus, emphasis on life cycle assessment of MCFA-production is needed, and the study performed by Chen et al. provides a good example [87]. If implemented with sustainable approaches, MCFA production from organic wastes will be a step towards local circular bioeconomies which are critical for addressing persistent environmental and social challenges [111].

Supplementary Materials: The following are available online at http://www.mdpi.com/2227-9717/8/12/1571/s1, Figure S1: Proposed model for conversion of ethanol to acetate with Hyd1, Figure S2: Proposed model for conversion of ethanol to butyrate with Hyd1, Figure S3: Proposed model for conversion of ethanol to hexanoate with Hyd1, Figure S4: Proposed model for conversion of ethanol to octanoate with Hyd1, Figure S5: Proposed model for conversion of ethanol to acetate with ECH, Figure S6: Proposed model for conversion of ethanol to butyrate with ECH, Figure S7: Proposed model for conversion of ethanol to hexanoate with ECH, Figure S8: Proposed model for conversion of ethanol to octanoate with ECH, Figure S9: Proposed model for conversion of ethanol and acetate to butyrate, Figure S10: Proposed model for conversion of ethanol and acetate to hexanoate, Figure S11: Proposed model for conversion of ethanol and acetate to octanoate, Figure S12: Proposed model for conversion of ethanol and acetate to butyrate with an ethanol-to-acetate ratio of 3:2 and Hyd1, Figure S13: Proposed model for conversion of ethanol and acetate to butyrate with an ethanol-to-acetate ratio of 3:2 and ECH.

Author Contributions: Conceptualization, M.S. and P.S.; review of literature—P.S., J.M., and L.C.; writing—original draft preparation, M.S. and P.S.; writing—review and editing, P.S., J.M., L.C., K.B. and M.S.; supervision, M.S. All authors have read and agreed to the published version of the manuscript.

Funding: This research received no external funding.

Acknowledgments: We thank the College of Engineering and Mathematical Sciences at the University of Vermont for supporting M.S. with start-up funding and J.M. and K.B. with a summer research experience for undergraduates.

Conflicts of Interest: The authors declare no conflict of interest.

References

1. McGovern, P.E.; Zhang, J.; Tang, J.; Zhang, Z.; Hall, G.R.; Moreau, R.A.; Nunez, A.; Butrym, E.D.; Richards, M.P.; Wang, C.S.; et al. Fermented beverages of pre- and proto-historic China. *Proc. Natl. Acad. Sci. USA* **2004**, *101*, 17593–17598. [CrossRef]
2. He, P.J. Anaerobic digestion: An intriguing long history in China. *Waste Manag.* **2010**, *30*, 549–550. [CrossRef] [PubMed]
3. World Biogas Association. *Global Potential of Biogas*; World Biogas Association: London, UK, 2019.
4. Mancini, A.; Imperlini, E.; Nigro, E.; Montagnese, C.; Daniele, A.; Orru, S.; Buono, P. Biological and Nutritional Properties of Palm Oil and Palmitic Acid: Effects on Health. *Molecules* **2015**, *20*, 17339–17361. [CrossRef] [PubMed]
5. Marten, B.; Pfeuffer, M.; Schrezenmeir, J. Medium-chain triglycerides. *Int. Dairy J.* **2006**, *16*, 1374–1382. [CrossRef]
6. Bach, A.C.; Babayan, V.K. Medium-chain triglycerides: An update. *Am. J. Clin. Nutr.* **1982**, *36*, 950–962. [CrossRef]
7. Sun, Y.; Bu, D.P.; Wang, J.Q.; Cui, H.; Zhao, X.W.; Xu, X.Y.; Sun, P.; Zhou, L.Y. Supplementing different ratios of short- and medium-chain fatty acids to long-chain fatty acids in dairy cows: Changes of milk fat production and milk fatty acids composition. *J. Dairy Sci.* **2013**, *96*, 2366–2373. [CrossRef]
8. Vyas, D.; Teter, B.B.; Erdman, R.A. Milk fat responses to dietary supplementation of short- and medium-chain fatty acids in lactating dairy cows. *J. Dairy Sci.* **2012**, *95*, 5194–5202. [CrossRef]
9. Zentek, J.; Buchheit-Renko, S.; Ferrara, F.; Vahjen, W.; Van Kessel, A.G.; Pieper, R. Nutritional and physiological role of medium-chain triglycerides and medium-chain fatty acids in piglets. *Anim. Health Res. Rev.* **2011**, *12*, 83–93. [CrossRef]
10. Angenent, L.T.; Richter, H.; Buckel, W.; Spirito, C.M.; Steinbusch, K.J.J.; Plugge, C.M.; Strik, D.; Grootscholten, T.I.M.; Buisman, C.J.N.; Hamelers, H.V.M. Chain Elongation with Reactor Microbiomes: Open-Culture Biotechnology To Produce Biochemicals. *Environ. Sci. Technol.* **2016**, *50*, 2796–2810. [CrossRef]
11. Sarria, S.; Kruyer, N.S.; Peralta-Yahya, P. Microbial synthesis of medium-chain chemicals from renewables. *Nat. Biotechnol.* **2017**, *35*, 1158–1166. [CrossRef]
12. Harvey, B.G.; Meylemans, H.A. 1-Hexene: A renewable C6 platform for full-performance jet and diesel fuels. *Green Chem.* **2014**, *16*, 770–776. [CrossRef]
13. Kim, S.; Chen, J.; Cheng, T.; Gindulyte, A.; He, J.; He, S.; Li, Q.; Shoemaker, B.A.; Thiessen, P.A.; Yu, B.; et al. PubChem 2019 update: Improved access to chemical data. *Nucleic Acids Res.* **2019**, *47*, D1102–D1109. [CrossRef] [PubMed]
14. Han, W.H.; He, P.J.; Shao, L.M.; Lu, F. Road to full bioconversion of biowaste to biochemicals centering on chain elongation: A mini review. *J. Environ. Sci.* **2019**, *86*, 50–64. [CrossRef] [PubMed]
15. Venkateswar Reddy, M.; Kumar, G.; Mohanakrishna, G.; Shobana, S.; Al-Raoush, R.I. Review on the production of medium and small chain fatty acids through waste valorization and CO2 fixation. *Bioresour. Technol.* **2020**, *309*, 123400. [CrossRef] [PubMed]
16. Molisch, H. *Die Purpurbakterien Nach Neuen Untersuchungen: Eine Mikrobiologische Studie*; Verlag von Gustav Fischer: Jena, German, 1907.
17. Esmarch, E. Über die Reinkultur eines Spirillum. Zentralblatt fur Bakteriologie, Parasitenkunde, Infektionskrankheiten und Hygiene. *Abteilung I* **1887**, *1*, 225–230.
18. Munk, A.C.; Copeland, A.; Lucas, S.; Lapidus, A.; Del Rio, T.G.; Barry, K.; Detter, J.C.; Hammon, N.; Israni, S.; Pitluck, S.; et al. Complete genome sequence of Rhodospirillum rubrum type strain (S1). *Stand. Genomic Sci.* **2011**, *4*, 293–302. [CrossRef]
19. Gest, H. A serendipic legacy: Erwin Esmarch's isolation of the first photosynthetic bacterium in pure culture. *Photosynt. Res.* **1995**, *46*, 473–478. [CrossRef]
20. Barker, H.A. The production of caproic and butyric acids by the methane fermentation of ethyl alcohol. *Arch. Mikrobiol.* **1937**, *8*, 415–421. [CrossRef]
21. Barker, H.A.; Taha, S.M. Clostridium kluyverii, an Organism Concerned in the Formation of Caproic Acid from Ethyl Alcohol. *J. Bacteriol.* **1942**, *43*, 347–363. [CrossRef]
22. Gildemyn, S.; Molitor, B.; Usack, J.G.; Nguyen, M.; Rabaey, K.; Angenent, L.T. Upgrading syngas fermentation effluent using Clostridium kluyveri in a continuous fermentation. *Biotechnol. Biofuels* **2017**, *10*, 83. [CrossRef]

23. Seedorf, H.; Fricke, W.F.; Veith, B.; Bruggemann, H.; Liesegang, H.; Strittmatter, A.; Miethke, M.; Buckel, W.; Hinderberger, J.; Li, F.; et al. The genome of Clostridium kluyveri, a strict anaerobe with unique metabolic features. *Proc. Natl. Acad. Sci. USA* **2008**, *105*, 2128–2133. [CrossRef] [PubMed]
24. Richter, H.; Molitor, B.; Diender, M.; Sousa, D.Z.; Angenent, L.T. A Narrow pH Range Supports Butanol, Hexanol, and Octanol Production from Syngas in a Continuous Co-culture of Clostridium ljungdahlii and Clostridium kluyveri with In-Line Product Extraction. *Front. Microbiol.* **2016**, *7*, 1773. [CrossRef] [PubMed]
25. Li, F.; Hinderberger, J.; Seedorf, H.; Zhang, J.; Buckel, W.; Thauer, R.K. Coupled ferredoxin and crotonyl coenzyme A (CoA) reduction with NADH catalyzed by the butyryl-CoA dehydrogenase/Etf complex from Clostridium kluyveri. *J. Bacteriol.* **2008**, *190*, 843–850. [CrossRef] [PubMed]
26. Wang, S.; Huang, H.; Moll, J.; Thauer, R.K. NADP+ reduction with reduced ferredoxin and NADP+ reduction with NADH are coupled via an electron-bifurcating enzyme complex in Clostridium kluyveri. *J. Bacteriol.* **2010**, *192*, 5115–5123. [CrossRef]
27. Genthner, B.R.; Davis, C.L.; Bryant, M.P. Features of rumen and sewage sludge strains of Eubacterium limosum, a methanol- and H2-CO2-utilizing species. *Appl. Environ. Microbiol.* **1981**, *42*, 12–19. [CrossRef]
28. Chen, W.S.; Ye, Y.; Steinbusch, K.J.J.; Strik, D.P.B.T.B.; Buisman, C.J.N. Methanol as an alternative electron donor in chain elongation for butyrate and caproate formation. *Biomass Bioenergy* **2016**, *93*, 201–208. [CrossRef]
29. Prevot, A.; Taffanel, J. Action of water soluble vitamins on the fermentation of glucose by Plectridium tetani. *Compte Rendu des Seances de la Societe de Biologie* **1942**, *136*, 384–385.
30. Holdeman, V.L.; Cato, E.P.; Moore, W.E.C. Amended Description of Ramibacterium Alactolyticum Prevot and Taffanel With Proposal of a Neotype Strain. *Int. J. Syst. Bacteriol.* **1967**, *17*, 323–341. [CrossRef]
31. Moore, W.E.C.; Holdeman, L.V. New Names and Combinations in the Genera Bacteroides Castellani and Chalmers, Fusobacterium Knorr, Eubacterium Prevot, Propionbacterium Delwich, and Lactobacillus Orla-Jensen. *Int. J. Syst. Bacteriol.* **1973**, *23*, 69–74. [CrossRef]
32. Integrative Human Microbiome Project Research Network Consortium. The Integrative Human Microbiome Project. *Nature* **2019**, *569*, 641–648. [CrossRef]
33. Elsden, S.R.; Lewis, D. The production of fatty acids by a gram-negative coccus. *Biochem. J.* **1953**, *55*, 183–189. [CrossRef] [PubMed]
34. Gutierrez, J.; Davis, R.E.; Lindahl, I.L.; Warwick, E.J. Bacterial Changes in the Rumen During the Onset of Feed-lot Bloat of Cattle and Characteristics of Peptostreptococcus elsdenii n. sp. *Appl. Microbiol.* **1959**, *7*, 16–22. [CrossRef] [PubMed]
35. Rogosa, M. Transfer of Peptostreptococcus elsdenii Gutierrez et al. to a New Genus, Megasphaera [M. elsdenii (Gutierrez et al.) comb. nov.]. *Int. J. Syst. Bacteriol.* **1971**, *21*, 187–189. [CrossRef]
36. Riley, L.A.; Hatmaker, E.A.; Guss, A.M.; Westpheling, J. Development of emerging model microorganisms: Megasphaera elsdenii for biomass and organic acid upgrading to fuels and chemicals. In Proceedings of the 2019 Genomic Sciences Program Annual Principal Investigator (PI) Meeting, Tysons, VA, USA, 25 February 2019.
37. Nelson, R.; Peterson, D.; Karp, E.; Beckham, G.; Salvachúa, D. Mixed Carboxylic Acid Production by Megasphaera elsdenii from Glucose and Lignocellulosic Hydrolysate. *Fermentation* **2017**, *3*, 10. [CrossRef]
38. Weimer, P.J.; Moen, G.N. Quantitative analysis of growth and volatile fatty acid production by the anaerobic ruminal bacterium Megasphaera elsdenii T81. *Appl. Microbiol. Biotechnol.* **2013**, *97*, 4075–4081. [CrossRef]
39. Prabhu, R.; Altman, E.; Eiteman, M.A. Lactate and Acrylate Metabolism by Megasphaera elsdenii under Batch and Steady-State Conditions. *Appl. Environ. Microb.* **2012**, *78*, 8564–8570. [CrossRef]
40. Henning, P.H.; Horn, C.H.; Leeuw, K.J.; Meissner, H.H.; Hagg, F.M. Effect of ruminal administration of the lactate-utilizing strain Megasphaera elsdenii (Me) NCIMB 41125 on abrupt or gradual transition from forage to concentrate diets. *Anim. Feed Sci. Tech.* **2010**, *157*, 20–29. [CrossRef]
41. Soto-Cruz, O.; Favela-Torres, E.; Saucedo-Castaneda, G. Modeling of growth, lactate consumption, and volatile fatty acid production by Megasphaera elsdenii cultivated in minimal and complex media. *Biotechnol. Progr.* **2002**, *18*, 193–200. [CrossRef]
42. Soto-Cruz, O.; Chavez-Rivera, R.; Saucedo-Castaneda, G. Stimulation of the Megasphaera elsdenii's butyrate production in continuous culture by a yeast additive. *Braz. Arch. Biol. Technol.* **2001**, *44*, 179–184. [CrossRef]
43. Hino, T.; Kuroda, S. Presence of lactate dehydrogenase and lactate racemase in Megasphaera elsdenii grown on glucose or lactate. *Appl. Environ. Microbiol.* **1993**, *59*, 255–259. [CrossRef]

44. Marx, H.; Graf, A.B.; Tatto, N.E.; Thallinger, G.G.; Mattanovich, D.; Sauer, M. Genome sequence of the ruminal bacterium Megasphaera elsdenii. *J. Bacteriol.* **2011**, *193*, 5578–5579. [CrossRef] [PubMed]
45. Hatmaker, E.A.; Klingeman, D.M.; O'Dell, K.B.; Riley, L.A.; Papanek, B.; Guss, A.M. Complete Genome Sequences of Two Megasphaera elsdenii Strains, NCIMB 702410 and ATCC 25940. *Microbiol. Resour. Announc.* **2019**, *8*. [CrossRef] [PubMed]
46. Bag, S.; Ghosh, T.S.; Das, B. Whole-Genome Sequence of a Megasphaera elsdenii Strain Isolated from the Gut of a Healthy Indian Adult Subject. *Genome Announc.* **2017**, *5*. [CrossRef] [PubMed]
47. Lee, N.R.; Lee, C.H.; Lee, D.Y.; Park, J.B. Genome-Scale Metabolic Network Reconstruction and In Silico Analysis of Hexanoic acid Producing Megasphaera elsdenii. *Microorganisms* **2020**, *8*, 539. [CrossRef] [PubMed]
48. Wallace, R.J.; McKain, N.; McEwan, N.R.; Miyagawa, E.; Chaudhary, L.C.; King, T.P.; Walker, N.D.; Apajalahti, J.H.A.; Newbold, C.J. Eubacterium pyruvativorans sp. nov., a novel non-saccharolytic anaerobe from the rumen that ferments pyruvate and amino acids, forms caproate and utilizes acetate and propionate. *Int. J. Syst. Evol. Microbiol.* **2003**, *53*, 965–970. [CrossRef]
49. Zhu, X.; Tao, Y.; Liang, C.; Li, X.; Wei, N.; Zhang, W.; Zhou, Y.; Yang, Y.; Bo, T. The synthesis of n-caproate from lactate: A new efficient process for medium-chain carboxylates production. *Sci. Rep.* **2015**, *5*, 14360. [CrossRef] [PubMed]
50. Zhu, X.; Zhou, Y.; Wang, Y.; Wu, T.; Li, X.; Li, D.; Tao, Y. Production of high-concentration n-caproic acid from lactate through fermentation using a newly isolated Ruminococcaceae bacterium CPB6. *Biotechnol. Biofuels* **2017**, *10*, 102. [CrossRef]
51. Tao, Y.; Zhu, X.; Wang, H.; Wang, Y.; Li, X.; Jin, H.; Rui, J. Complete genome sequence of Ruminococcaceae bacterium CPB6: A newly isolated culture for efficient n-caproic acid production from lactate. *J. Biotechnol.* **2017**, *259*, 91–94. [CrossRef]
52. Jeon, B.S.; Kim, B.C.; Um, Y.; Sang, B.I. Production of hexanoic acid from D-galactitol by a newly isolated Clostridium sp. BS-1. *Appl. Microbiol. Biotechnol.* **2010**, *88*, 1161–1167. [CrossRef]
53. Andersen, S.J.; De Groof, V.; Khor, W.C.; Roume, H.; Props, R.; Coma, M.; Rabaey, K. A Clostridium Group IV Species Dominates and Suppresses a Mixed Culture Fermentation by Tolerance to Medium Chain Fatty Acids Products. *Front. Bioeng. Biotechnol.* **2017**, *5*, 8. [CrossRef]
54. Bengelsdorf, F.R.; Poehlein, A.; Daniel, R.; Durre, P. Genome Sequence of the Caproic Acid-Producing Bacterium Caproiciproducens galactitolivorans BS-1(T) (JCM 30532). *Microbiol. Resour. Announc.* **2019**, *8*. [CrossRef] [PubMed]
55. Kim, B.C.; Seung Jeon, B.; Kim, S.; Kim, H.; Um, Y.; Sang, B.I. Caproiciproducens galactitolivorans gen. nov., sp. nov., a bacterium capable of producing caproic acid from galactitol, isolated from a wastewater treatment plant. *Int. J. Syst. Evol. Microbiol.* **2015**, *65*, 4902–4908. [CrossRef] [PubMed]
56. Jeon, B.S.; Kim, S.; Sang, B.I. Megasphaera hexanoica sp. nov., a medium-chain carboxylic acid-producing bacterium isolated from a cow rumen. *Int. J. Syst. Evol. Microbiol.* **2017**, *67*, 2114–2120. [CrossRef] [PubMed]
57. Kim, H.; Jeon, B.S.; Sang, B.I. An Efficient New Process for the Selective Production of Odd-Chain Carboxylic Acids by Simple Carbon Elongation Using Megasphaera hexanoica. *Sci. Rep.* **2019**, *9*, 11999. [CrossRef] [PubMed]
58. Flaiz, M.; Baur, T.; Brahner, S.; Poehlein, A.; Daniel, R.; Bengelsdorf, F.R. Caproicibacter fermentans gen. nov., sp. nov., a new caproate-producing bacterium and emended description of the genus Caproiciproducens. *Int. J. Syst. Evol. Microbiol.* **2020**, *70*, 4269–4279. [CrossRef] [PubMed]
59. Liu, B.; Popp, D.; Strauber, H.; Harms, H.; Kleinsteuber, S. Draft Genome Sequences of Three Clostridia Isolates Involved in Lactate-Based Chain Elongation. *Microbiol. Resour. Announc.* **2020**, *9*. [CrossRef]
60. Liu, B.; Popp, D.; Sträuber, H.; Harms, H.; Kleinsteuber, S. Lactate-based microbial chain elongation for n-caproate and iso-butyrate production: Genomic and metabolic features of three novel Clostridia isolates. *Res. Sq.* in press. **2020**. [CrossRef]
61. Esquivel-Elizondo, S.; Bağcı, C.; Temovska, M.; Jeon, B.S.; Bessarab, I.; Williams, R.B.H.; Huson, D.H.; Angenent, L.T. The isolate Caproiciproducens sp. 7D4C2 produces n -caproate at mildly acidic conditions from hexoses: Genome and rBOX comparison with related strains and chain-elongating bacteria. *BioRxiv* **2020**. [CrossRef]

62. Scarborough, M.J.; Myers, K.S.; Donohue, T.J.; Noguera, D.R. Medium-Chain Fatty Acid Synthesis by "Candidatus Weimeria bifida" gen. nov., sp. nov., and "Candidatus Pseudoramibacter fermentans" sp. nov. *Appl. Environ. Microbiol.* **2020**, *86*. [CrossRef]
63. Willems, A.; Collins, M.D. Phylogenetic relationships of the genera Acetobacterium and Eubacterium sensu stricto and reclassification of Eubacterium alactolyticum as Pseudoramibacter alactolyticus gen. nov., comb. nov. *Int. J. Syst. Bacteriol.* **1996**, *46*, 1083–1087. [CrossRef]
64. Andersen, S.J.; Candry, P.; Basadre, T.; Khor, W.C.; Roume, H.; Hernandez-Sanabria, E.; Coma, M.; Rabaey, K. Electrolytic extraction drives volatile fatty acid chain elongation through lactic acid and replaces chemical pH control in thin stillage fermentation. *Biotechnol. Biofuels* **2015**, *8*, 1–14. [CrossRef] [PubMed]
65. Grootscholten, T.I.M.; Strik, D.P.B.T.B.; Steinbusch, K.J.J.; Buisman, C.J.N.; Hamelers, H.V.M. Two-stage medium chain fatty acid (MCFA) production from municipal solid waste and ethanol. *Appl. Energy* **2014**, *116*, 223–229. [CrossRef]
66. Grootscholten, T.I.M.; dal Borgo, F.K.; Hamelers, H.V.M.; Buisman, C.J.N. Promoting chain elongation in mixed culture acidification reactors by addition of ethanol. *Biomass Bioenergy* **2013**, *48*, 10–16. [CrossRef]
67. Nzeteu, C.O.; Trego, A.C.; Abram, F.; O'Flaherty, V. Reproducible, high-yielding, biological caproate production from food waste using a single-phase anaerobic reactor system. *Biotechnol Biofuels* **2018**, *11*, 108. [CrossRef]
68. Roghair, M.; Liu, Y.C.; Strik, D.P.B.T.B.; Weusthuis, R.A.; Bruins, M.E.; Buisman, C.J.N. Development of an Effective Chain Elongation Process From Acidified Food Waste and Ethanol Into n-Caproate. *Front. Bioeng. Biotech.* **2018**, *6*. [CrossRef]
69. Reddy, M.V.; Hayashi, S.; Choi, D.; Cho, H.; Chang, Y.C. Short chain and medium chain fatty acids production using food waste under non-augmented and bio-augmented conditions. *J. Clean. Prod.* **2018**, *176*, 645–653. [CrossRef]
70. Contreras-Davila, C.A.; Carrion, V.J.; Vonk, V.R.; Buisman, C.N.J.; Strik, D.P.B.T.B. Consecutive lactate formation and chain elongation to reduce exogenous chemicals input in repeated-batch food waste fermentation. *Water Res.* **2020**, *169*, 115215. [CrossRef]
71. Lonkar, S.; Fu, Z.; Holtzapple, M. Optimum alcohol concentration for chain elongation in mixed-culture fermentation of cellulosic substrate. *Biotechnol. Bioeng.* **2016**, *113*, 2597–2604. [CrossRef]
72. Scarborough, M.J.; Lynch, G.; Dickson, M.; McGee, M.; Donohue, T.J.; Noguera, D.R. Increasing the economic value of lignocellulosic stillage through medium-chain fatty acid production. *Biotechnol. Biofuels* **2018**, *11*, 200. [CrossRef]
73. Weimer, P.J.; Nerdahl, M.; Brandl, D.J. Production of medium-chain volatile fatty acids by mixed ruminal microorganisms is enhanced by ethanol in co-culture with Clostridium kluyveri. *Bioresour. Technol.* **2015**, *175*, 97–101. [CrossRef]
74. Khor, W.C.; Andersen, S.; Vervaeren, H.; Rabaey, K. Electricity-assisted production of caproic acid from grass. *Biotechnol. Biofuels* **2017**, *10*, 180. [CrossRef] [PubMed]
75. Urban, C.; Xu, J.; Sträuber, H.; dos Santos Dantas, T.R.; Mühlenberg, J.; Härtig, C.; Angenent, L.T.; Harnisch, F. Production of drop-in fuels from biomass at high selectivity by combined microbial and electrochemical conversion. *Energy Environ. Sci.* **2017**, *10*, 2231–2244. [CrossRef]
76. Carvajal-Arroyo, J.M.; Candry, P.; Andersen, S.J.; Props, R.; Seviour, T.; Ganigué, R.; Rabaey, K. Granular fermentation enables high rate caproic acid production from solid-free thin stillage. *Green Chem.* **2019**, *21*, 1330–1339. [CrossRef]
77. Wu, Q.; Feng, X.; Guo, W.; Bao, X.; Ren, N. Long-term medium chain carboxylic acids production from liquor-making wastewater: Parameters optimization and toxicity mitigation. *Chem. Eng. J.* **2020**, *388*. [CrossRef]
78. Kucek, L.A.; Xu, J.J.; Nguyen, M.; Angenent, L.T. Waste Conversion into n-Caprylate and n-Caproate: Resource Recovery from Wine Lees Using Anaerobic Reactor Microbiomes and In-line Extraction. *Front. Microbiol.* **2016**, *7*. [CrossRef]
79. Xu, J.; Hao, J.; Guzman, J.J.L.; Spirito, C.M.; Harroff, L.A.; Angenent, L.T. Temperature-Phased Conversion of Acid Whey Waste Into Medium-Chain Carboxylic Acids via Lactic Acid: No External e-Donor. *Joule* **2018**, *2*, 280–295. [CrossRef]

80. Duber, A.; Jaroszynski, L.; Zagrodnik, R.; Chwialkowska, J.; Juzwa, W.; Ciesielski, S.; Oleskowicz-Popiel, P. Exploiting the real wastewater potential for resource recovery—n-caproate production from acid whey. *Green Chem.* **2018**, *20*, 3790–3803. [CrossRef]
81. Domingos, J.M.B.; Martinez, G.A.; Scoma, A.; Fraraccio, S.; Kerckhof, F.-M.; Boon, N.; Reis, M.A.M.; Fava, F.; Bertin, L. Effect of Operational Parameters in the Continuous Anaerobic Fermentation of Cheese Whey on Titers, Yields, Productivities, and Microbial Community Structures. *ACS Sustain. Chem. Eng.* **2017**, *5*, 1400–1407. [CrossRef]
82. Zhang, W.; Yin, F.; Dong, H.; Cao, Q.; Wang, S.; Xu, J.; Zhu, Z. Bioconversion of swine manure into high-value products of medium chain fatty acids. *Waste Manag.* **2020**, *113*, 478–487. [CrossRef]
83. Zoghlami, A.; Paes, G. Lignocellulosic Biomass: Understanding Recalcitrance and Predicting Hydrolysis. *Front. Chem.* **2019**, *7*, 874. [CrossRef]
84. Badgett, A.; Newes, E.; Milbrandt, A. Economic analysis of wet waste-to-energy resources in the United States. *Energy* **2019**, *176*, 224–234. [CrossRef]
85. Scarborough, M.J.; Lawson, C.E.; Hamilton, J.J.; Donohue, T.J.; Noguera, D.R. Metatranscriptomic and Thermodynamic Insights into Medium-Chain Fatty Acid Production Using an Anaerobic Microbiome. *mSystems* **2018**, *3*. [CrossRef] [PubMed]
86. Scarborough, M.J.; Hamilton, J.J.; Erb, E.A.; Donohue, T.J.; Noguera, D.R. Diagnosing and Predicting Mixed-Culture Fermentations with Unicellular and Guild-Based Metabolic Models. *mSystems* **2020**, *5*. [CrossRef] [PubMed]
87. Chen, W.S.; Strik, D.; Buisman, C.J.N.; Kroeze, C. Production of Caproic Acid from Mixed Organic Waste: An Environmental Life Cycle Perspective. *Environ. Sci. Technol.* **2017**, *51*, 7159–7168. [CrossRef] [PubMed]
88. Dellomonaco, C.; Clomburg, J.M.; Miller, E.N.; Gonzalez, R. Engineered reversal of the beta-oxidation cycle for the synthesis of fuels and chemicals. *Nature* **2011**, *476*, 355–359. [CrossRef]
89. Thauer, R.K.; Jungermann, K.; Henninger, H.; Wenning, J.; Decker, K. The energy metabolism of Clostridium kluyveri. *Eur. J. Biochem.* **1968**, *4*, 173–180. [CrossRef]
90. Buckel, W.; Thauer, R.K. Flavin-Based Electron Bifurcation, Ferredoxin, Flavodoxin, and Anaerobic Respiration With Protons (Ech) or NAD(+) (Rnf) as Electron Acceptors: A Historical Review. *Front. Microbiol.* **2018**, *9*, 401. [CrossRef]
91. Buckel, W.; Thauer, R.K. Flavin-Based Electron Bifurcation, A New Mechanism of Biological Energy Coupling. *Chem. Rev.* **2018**, *118*, 3862–3886. [CrossRef]
92. Hartmanis, M.G.; Gatenbeck, S. Intermediary Metabolism in Clostridium acetobutylicum: Levels of Enzymes Involved in the Formation of Acetate and Butyrate. *Appl. Environ. Microbiol.* **1984**, *47*, 1277–1283. [CrossRef]
93. Kuhns, M.; Trifunovic, D.; Huber, H.; Muller, V. The Rnf complex is a Na(+) coupled respiratory enzyme in a fermenting bacterium, Thermotoga maritima. *Commun. Biol.* **2020**, *3*, 431. [CrossRef]
94. Tremblay, P.L.; Zhang, T.; Dar, S.A.; Leang, C.; Lovley, D.R. The Rnf complex of Clostridium ljungdahlii is a proton-translocating ferredoxin:NAD+ oxidoreductase essential for autotrophic growth. *mBio* **2012**, *4*, e00406–e00412. [CrossRef] [PubMed]
95. Biegel, E.; Schmidt, S.; Gonzalez, J.M.; Muller, V. Biochemistry, evolution and physiological function of the Rnf complex, a novel ion-motive electron transport complex in prokaryotes. *Cell. Mol. Life Sci.* **2011**, *68*, 613–634. [CrossRef] [PubMed]
96. Biegel, E.; Schmidt, S.; Muller, V. Genetic, immunological and biochemical evidence for a Rnf complex in the acetogen Acetobacterium woodii. *Environ. Microbiol.* **2009**, *11*, 1438–1443. [CrossRef] [PubMed]
97. Westphal, L.; Wiechmann, A.; Baker, J.; Minton, N.P.; Muller, V. The Rnf Complex Is an Energy-Coupled Transhydrogenase Essential To Reversibly Link Cellular NADH and Ferredoxin Pools in the Acetogen Acetobacterium woodii. *J. Bacteriol.* **2018**, *200*. [CrossRef]
98. Buckel, W.; Thauer, R.K. Energy conservation via electron bifurcating ferredoxin reduction and proton/Na(+) translocating ferredoxin oxidation. *Biochim. Biophys. Acta* **2013**, *1827*, 94–113. [CrossRef] [PubMed]
99. Schut, G.J.; Adams, M.W. The iron-hydrogenase of Thermotoga maritima utilizes ferredoxin and NADH synergistically: A new perspective on anaerobic hydrogen production. *J. Bacteriol.* **2009**, *191*, 4451–4457. [CrossRef]
100. Spirito, C.M.; Marzilli, A.M.; Angenent, L.T. Higher Substrate Ratios of Ethanol to Acetate Steered Chain Elongation toward n-Caprylate in a Bioreactor with Product Extraction. *Environ. Sci. Technol.* **2018**, *52*, 13438–13447. [CrossRef]

101. Spirito, C.M.; Richter, H.; Rabaey, K.; Stams, A.J.; Angenent, L.T. Chain elongation in anaerobic reactor microbiomes to recover resources from waste. *Curr. Opin. Biotechnol.* **2014**, *27*, 115–122. [CrossRef]
102. Thauer, R.K.; Jungermann, K.; Decker, K. Energy conservation in chemotrophic anaerobic bacteria. *Bacteriol. Rev.* **1977**, *41*, 100–180. [CrossRef]
103. Kucek, L.A.; Spirito, C.M.; Angenent, L.T. High n-caprylate productivities and specificities from dilute ethanol and acetate: Chain elongation with microbiomes to upgrade products from syngas fermentation. *Energy Environ. Sci.* **2016**, *9*, 3482–3494. [CrossRef]
104. Royce, L.A.; Yoon, J.M.; Chen, Y.X.; Rickenbach, E.; Shanks, J.V.; Jarboe, L.R. Evolution for exogenous octanoic acid tolerance improves carboxylic acid production and membrane integrity. *Metab. Eng.* **2015**, *29*, 180–188. [CrossRef] [PubMed]
105. Fu, Y.; Yoon, J.M.; Jarboe, L.; Shanks, J.V. Metabolic flux analysis of Escherichia coli MG1655 under octanoic acid (C8) stress. *Appl. Microbiol. Biotechnol.* **2015**, *99*, 4397–4408. [CrossRef] [PubMed]
106. Borrull, A.; Lopez-Martinez, G.; Poblet, M.; Cordero-Otero, R.; Rozes, N. New insights into the toxicity mechanism of octanoic and decanoic acids on Saccharomyces cerevisiae. *Yeast* **2015**, *32*, 451–460. [CrossRef] [PubMed]
107. Roghair, M.; Liu, Y.; Adiatma, J.C.; Weusthuis, R.A.; Bruins, M.E.; Buisman, C.J.N.; Strik, D.P.B.T.B. Effect of n-Caproate Concentration on Chain Elongation and Competing Processes. *ACS Sustain. Chem. Eng.* **2018**, *6*, 7499–7506. [CrossRef]
108. Deng, X.; Chen, L.; Hei, M.; Liu, T.; Feng, Y.; Yang, G.Y. Structure-guided reshaping of the acyl binding pocket of 'TesA thioesterase enhances octanoic acid production in E. coli. *Metab. Eng.* **2020**, *61*, 24–32. [CrossRef]
109. Tan, Z.; Yoon, J.M.; Chowdhury, A.; Burdick, K.; Jarboe, L.R.; Maranas, C.D.; Shanks, J.V. Engineering of E. coli inherent fatty acid biosynthesis capacity to increase octanoic acid production. *Biotechnol. Biofuels* **2018**, *11*, 87. [CrossRef]
110. Petering, D.; Fee, J.A.; Palmer, G. The oxygen sensitivity of spinach ferredoxin and other iron-sulfur proteins. The formation of protein-bound sulfur-zero. *J. Biol. Chem.* **1971**, *246*, 643–653.
111. D'Amato, D.; Droste, N.; Allen, B.; Kettunen, M.; Lähtinen, K.; Korhonen, J.; Leskinen, P.; Matthies, B.D.; Toppinen, A. Green, circular, bio economy: A comparative analysis of sustainability avenues. *J. Clean. Prod.* **2017**, *168*, 716–734. [CrossRef]

processes

MDPI

Review

Quantification of Volatile Compounds in Wines by HS-SPME-GC/MS: Critical Issues and Use of Multivariate Statistics in Method Optimization

Sandra Pati [1], Maria Tufariello [2,*], Pasquale Crupi [3,4], Antonio Coletta [3], Francesco Grieco [2,*] and Ilario Losito [5]

[1] Department of Agricultural, Food and Environmental Sciences (SAFE), University of Foggia, Via Napoli 25, 71100 Foggia, Italy; s.pati@unifg.it
[2] CNR–Institute of Sciences of Food Production (ISPA), Via Prov. le, Lecce-Monteroni, 73100 Lecce, Italy
[3] CREA-VE, Council for Agricultural Research and Economics, Research Centre for Viticulture and Enology, Via Casamassima 148, 70010 Turi (BA), Italy; pasquale.crupi@crea.gov.it (P.C.); antonio.coletta@crea.gov.it (A.C.)
[4] Interdisciplinary Department of Medicine, University of Bari "Aldo Moro", P.zza Giulio Cesare 11, 70124 Bari, Italy
[5] Department of Chemistry and SMART Inter-Department Research Center, University of Bari "Aldo Moro", Via E. Orabona 4, 70126 Bari, Italy; ilario.losito@uniba.it
* Correspondence: maria.tufariello@ispa.cnr.it (M.T.); francesco.grieco@ispa.cnr.it (F.G.); Tel.: +39-08-3242-2600 (M.T.); +39-08-3242-2612 (F.G.); Fax: +39-08-3242-2620 (M.T. & F.G.)

Abstract: The aim of this review is to explore and discuss the two main aspects related to a HeadSpace Solid Phase Micro-Extraction Gas-Chromatography/Mass-Spectrometry (HS-SPME-GC/MS) quantitative analysis of volatile compounds in wines, both being fundamental to obtain reliable data. In the first section, recent advances in the use of multivariate optimization approaches during the method development step are described with a special focus on factorial designs and response surface methodologies. In the second section, critical aspects related to quantification methods are discussed. Indeed, matrix effects induced by the complexity of the volatile profile and of the non-volatile matrix of wines, potentially differing between diverse wines in a remarkable extent, often require severe assumptions if a reliable quantification is desired. Several approaches offering different levels of data reliability including internal standards, model wine calibration, a stable isotope dilution analysis, matrix-matched calibration and standard addition methods are reported in the literature and are discussed in depth here.

Keywords: wine; HS-SPME-GC/MS; multivariate statistical analysis; calibration

Citation: Pati, S.; Tufariello, M.; Crupi, P.; Coletta, A.; Grieco, F.; Losito, I. Quantification of Volatile Compounds in Wines by HS-SPME-GC/MS: Critical Issues and Use of Multivariate Statistics in Method Optimization. *Processes* **2021**, *9*, 662. https://doi.org/10.3390/pr9040662

Academic Editor: José Manuel Moreno-Rojas

Received: 18 March 2021
Accepted: 9 April 2021
Published: 9 April 2021

1. Introduction

A wine aroma profile (and thereby a volatile profile) is one of the most important quality criteria affecting wine acceptability by consumers [1]. Its characterization is very complex because volatile molecules usually belong to different classes such as alcohols, esters, aldehydes, acids, terpenes, phenols and lactones [2] with a wide range of polarity and concentrations. Furthermore, the non-volatile wine matrix affects the partitioning of aroma compounds between the matrix and the gas phase depending on their specific chemical properties and their interactions with aroma compounds [3].

An effective extraction from the aqueous wine matrix is essential for the accurate qualitative and quantitative analysis of wine volatiles. Therefore, various extraction and preconcentration approaches have been developed followed by separation and identification usually by mono-dimensional or bi-dimensional gas chromatography coupled to mass spectrometry (GC/MS, GC X GC/MS). Liquid-liquid [4], simultaneous distillation [5], solid phase [6], solid phase micro- [7], supercritical fluid [8] and stir bar sorptive extraction [9], among others, have been largely described for the analysis of wine volatile compounds [10].

On the other hand, headspace solid phase microextraction (HS-SPME), firstly described by Arthur and Pawliszyn [11], is considered to be one of the most effective techniques employed [10]. As HS-SPME is based on the partitioning of the analyte between the extracting phase immobilized on a fused silica fiber (as in all SPME approaches) and the headspace of the wine, it exploits a favorable transfer of volatile compounds into the latter. As with all SPME approaches, it combines sampling, analyte isolation and enrichment into one step and is suitable for full automation; moreover, as heat can be exploited for the desorption of the volatile analytes from the extracting phase, it does not require solvents either for the extraction or for the analyte desorption stage.

As with other SPME approaches, HS-SPME is usually a non-exhaustive extraction technique in which only a small percentage of the analyte is removed from the sample matrix. Both equilibrium and pre-equilibrium approaches can be employed. In the first case, enough time is available during the extraction step to reach the partitioning equilibrium between the sample matrix and the extraction phase and convection conditions do not affect the amount of analyte extracted. Under these conditions, if the sample volume (V_s) is much larger than the product between the volume of the extracting phase on the fiber (V_f) and the partition coefficient of the analyte between the fiber coating and the sample headspace (K_{fs}) it can be easily demonstrated that the amount of analyte extracted is proportional to the sample concentration but it does not depend on the sample volume. Indeed, the following equation is valid:

$$n = K_{fs} V_f C_0$$

where n is the mass of an analyte absorbed on or partitioned into the coating and C_0 is the initial concentration of the analyte in the sample [12].

In the second case, a short pre-equilibrium extraction is carried out and, if the convection is constant, the amount of extracted analyte is proportional to the extraction time. Even though the sensitivity is usually lower than that achievable with equilibrium extraction, the extraction time is shorter, thus reducing the overall analysis time. On the other hand, a non-equilibrium extraction requires a strict control of extraction conditions (e.g., convection, if present, time and temperature) in order to guarantee an acceptable reproducibility for quantitative analysis.

In all cases, the development of a quantitative SPME method requires a careful optimization of parameters affecting the extraction efficiency such as the type and volume of the extracting phase, the agitation method, the extraction time and sample modification (pH, ionic strength, organic solvent content) and, especially when volatile analytes are involved, temperature. Moreover, as volatile compounds absorbed on/partitioned into the fiber coating are usually thermally desorbed by exposing the fiber to the heated space inside a GC injector before being separated into a GC column and detected, the desorption conditions of analytes (temperature, transport gas flow, eventual presence and characteristics of a liner into the GC injector) need to be optimized too.

The use of multivariate statistics approaches, in particular those pertaining to the design of experiments (DoE) instead of the classical univariate (one-at-a-time, OVAT) approach, has become increasingly relevant in recent years [13–15]. The increasing relevance of HS-SPME in wine analysis applications is illustrated by the linear increase in the number of publications on the topic occurred since the introduction of SPME (Figure 1).

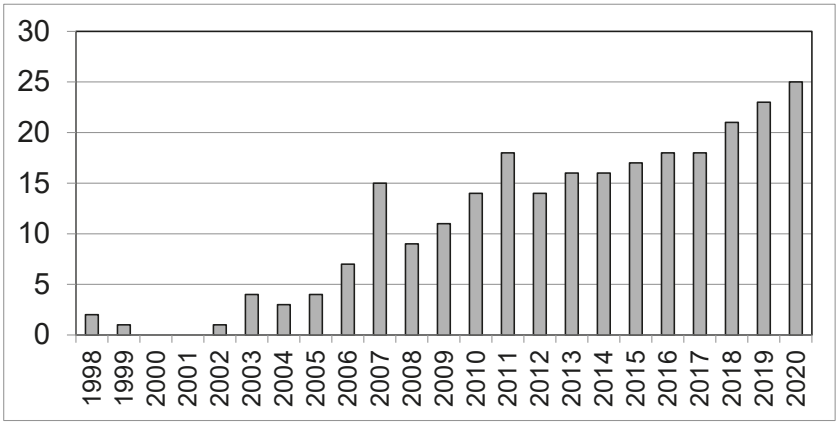

Figure 1. The number of papers related to Solid Phase Micro-Extraction (SPME) applications to wine.

In particular, the histogram in Figure 1 shows the number of papers related to SPME applications to wine based on a search on the Scopus database between 1998 and 2020 using the keywords "HS-SPME/wine/volatile" and excluding reviews, conference and data papers and book chapters. Despite the numerous reports describing SPME applications [2,16,17], papers concerning the critical issues of SPME-GC/MS quantification methods for wine volatiles are still limited and the number of rigorous quantitative applications reported in the literature is still low. This evidence can be considered a remarkable lack as divergent results concerning matrix effects [18,19] and standardization methods [20,21] have been reported in the literature for the quantification of wine volatiles.

Starting from the considerations made so far, this paper aims to review two relevant aspects related to the application of HS-SPME-GC/MS to the quantitative analysis of volatile compounds in wines: 1) recent advances in the use of optimization approaches in the method development stage; 2) critical aspects related to quantification methods so far reported. Indeed, both of these aspects are expected to contribute significantly to a successful application of HS-SPME-GC/MS methods pursuing the assessment of the safety, quality, authenticity and/or traceability of wines through the profile of their volatile compounds.

2. Optimization of HS-SPME Parameters with Multivariate Statistical Analysis

The success of HS-SPME depends on the analyte distribution between the matrix and the headspace, which is influenced in turn by a few parameters including the vapor pressure of volatiles, matrix ionic strength, stirring and equilibration time and temperature. The extraction time and temperature, the fiber sample distance and the nature and thickness of the fiber coating also play important roles in terms of extraction yield [15,22,23]. In light of this, statistical approaches able to optimize many factors simultaneously should be adopted to select the best conditions for the achievement of reliable and reproducible results. Multivariate statistics techniques can be successfully exploited for this purpose [24–27] (Figure 2).

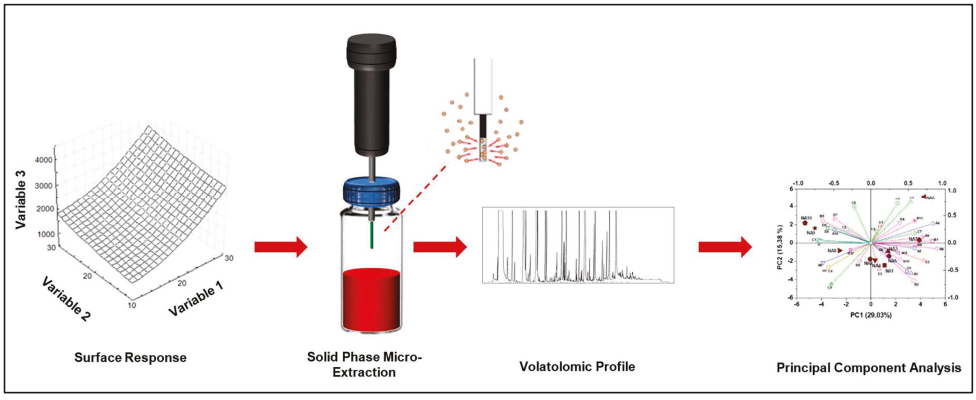

Figure 2. Optimization of Headspace Solid Phase Microxtraction (HS-SPME) parameters with a multivariate statistical analysis.

As a general approach, optimization procedures start with the definition of a measurable quantity, Y, as a reference parameter for the goodness/quality of the experiment itself. In most cases, the goodness of the experiment and the value of the Y parameter are positively correlated. Once Y is identified, factors X_i (experimental parameters) with i ranging from 1 to k that are expected to affect the results of the experiment must be selected. In determining the best procedure for optimizing the factors, however, it must be taken into account that: (1) a range of admissible values has to be determined for each factor; (2) it is usually not possible to experimentally test all of the possible values of a single factor in its range nor all of the possible combinations of different factors.

Once the variability ranges have been established for the factors, optimization based on multivariate statistics can be achieved through two fundamental approaches related to the DoE: two-level factorial designs and response surface methodologies (RSM) [28–30] with the latter including, among others, central composite (CCD) [25,31], Doehlert matrix (DM) [32,33], three-level factorial (3K) and Box Behnken (BBD) designs [27].

Factorial designs are a class of experimental designs offering a relatively large amount of useful information from a small number of experiments; for this reason, they are often exploited for a screening of factors. When the number of experiments that can be carried out is limited, factorial designs offer an efficient way of obtaining the maximum information from these experiments. In this type of approach, a number of levels (different values of each factor within its variability range) is established. A measurement is made for each possible combination of the levels of each of the k factors. The results are compared and the combination that maximizes the Y parameter is determined by developing a relatively simple model based on the responses. In the two-level full factorial design, two levels per factor are established; the number of combinations and therefore the number of measurements to be made is thus 2^k. In a more generic case, if a number N of levels per factor is set, the number of measurements to be taken is N^k [34–37].

This approach is quite different from the classical univariate approach (OVAT), which is based on the evaluation of the effect of one variable at a time with all other variables kept constant; thus, it is unable to provide information on the interactions among factors. It is worth noting that several univariate optimization studies have been conducted to determine the optimal conditions for the volatile extraction of wine by HS-SPME [15]. However, factorial designs may lead to similar accomplishments with a reduced number of experiments. Carrillo et al. [38] employed a full factorial design (2^4) to establish the relative influence of four factors (type of fiber, temperature, pre-incubation time and sodium chloride addition) and their interactions on the chromatographic responses of extracted compounds in order to develop a method for the determination of oak-derived volatile compounds in wine. Robotti et al. [39] used an experimental design for the optimization of

the SPME procedure according to both the maximum signal intensity and repeatability. In a study on Maresco sparkling wine volatiles, Tufariello et al. [21] focused on the equilibration of parameters and extraction times through a full two-factor three-level design with the purpose of optimizing the overall time of analysis and eventually finding an interaction factor between the two parameters affecting the analytical response.

A more complex approach to the DoE sometimes following the application of a factorial design is represented by the response surface methodology (RSM) [29,40,41]. In this case, the experiment is designed to provide a more refined model of the response surface, estimating interactions and even quadratic effects related to factors. RSM designs are used to find optimal process settings (in many cases as an improvement of those found using the factorial design), to troubleshoot process problems and weak points and make a product or process more robust against external and non-controllable influences. In this case, given k factors, a quadratic model of response Y is commonly adopted including N terms: a constant term, k independent linear terms and k independent quadratic terms (i.e., one for each factor in both cases) and $k(k\text{-}1)/2$ mixed quadratic terms that take into account the interactions between all possible couples of different factors. A minimum of N measurements based on different combinations of experimental factor values is thus required to obtain the parameters of the model through the resolution of a linear system of N equations in N unknowns. Under these conditions, however, no estimate of the parameter variability (and then of its significance) can be obtained in this case unless a number of experiments greater than that of the parameters is performed, e.g., by replicating experiments for specific combinations of factors. A multivariate linear regression can be adopted to find the values of parameters (and obtain estimates of their variability) in this case.

A fundamental aspect to guarantee a good robustness of the results especially when the number of measurements has to be minimized is the choice of the combinations of the k factor values. This is the aspect that most differentiates RSM approaches actually reported in the literature for the optimization of the extraction conditions for wine volatile compounds. Arcanjo et al. [31] reported the application of RSM based on a rotatable central composite design (RCCD) to improve the conditions for extracting volatiles from Isabel wine. In this work, the RCCD was used to evaluate the effects of three independent parameters: temperature, equilibration and extraction time on three different responses, namely, the total number of peaks detected upon a chromatographic separation, the total area under the detected peaks and the area of the peak of isoamyl acetate, a typical volatile compound present in wine headspace, to define the best conditions for a high extractability of volatiles. A central composite design (CCD) based on a factorial design plus eight axial points plus five replicates in the center of the design was chosen by Barros et al. [42] to develop a new automatic HS-SPME method for the determination of volatiles in white wines produced from several grape cultivars. The Box Behnken design (BBD) was applied in research for characterizing aroma-active monoterpenes in berries to determine optimum levels of three variables influencing the terpene recovery on SPME fiber: extraction temperature, extraction time and equilibrium time and consequently to display their linear and quadratic effects [29]. Recently, the DoE approach consisting of a definitive screening design (DSD) and latent variable modelling has been reported for the optimization of a method based on the HS-SPME-GC/MS analysis of volatile fatty acids in wine [14]. A DSD is a particular class of three levels of screening designs and is capable of providing estimates of the main effects that are unbiased or unconfounded regarding all second-order interactions and among themselves. The original version of the DSD was restricted to quantitative factors [43] but a more recent evolution extended the application to incorporate two-level categorical factors [44]. These designs require a low number of runs, one more than twice the number of factors. For more than six factors, they also have the potential capability to estimate the full quadratic model.

3. Matrix Effects and Calibration Approaches

Wine volatile composition (influencing the headspace-extracting phase partition coefficient), the non-volatile wine matrix (influencing the liquid-headspace partition coefficient) along with ethanol levels (influencing both coefficients) were assessed as the factors mainly responsible for matrix effects [3,19,45]. Indeed, SPME is extremely sensitive to any experimental parameter that may affect the liquid-headspace and the headspace-extracting phase distribution coefficients.

Rocha et al. [45] investigated the effect of variations in the concentration of each analyzed standard on the other components of a model wine in order to clarify the extent of the changes in the concentration of one matrix component on the headspace equilibrium and, consequently, in the SPME absorption of the other liquid matrix components. The authors showed that the increase of the concentration of one compound results in a decrease of the absorption of all of the others and, as a consequence, of their relative response factors. Compounds with higher relative response factors were less influenced by the matrix composition. Thus, quantification by SPME was shown to be highly dependent on the matrix composition.

Rodríguez-Bencomo et al. [3] investigated the effects of five representative matrices, namely, a young white wine, a young red wine, an oak-aged red wine, a sparkling wine and a sweet, aged wine after deodorization, compared with a control model wine with no matrix effect. The authors found that the wine non-volatile fraction (composed of monosaccharides and disaccharides, amino acids, polyphenols and proteins and other high molecular weight compounds) strongly affected the volatility of odorous molecules through two different effects: retention and salting-out effects. In the first case, the volatile compound was retained by the non-volatile matrix (particularly by mannoproteins); thus, a decrease in the amount of aroma in the headspace was observed; in the second case there was the opposite situation, i.e., a few soluble non-volatile compounds (monosaccharides, disaccharides and amino acids) could bind water molecules thus decreasing the amount of free water in the matrix and increasing the concentration of the target compound, which in turn favored its volatilization. The behavior of the investigated matrices was quite different. Indeed, the non-volatile matrix composition is not the same in all wines; as an example, a red wine is significantly richer than a white wine in terms of polyphenols and tannins with effects on analyte solubility and on the interactions of the analyte matrix components.

Ferreira et al. [19] adopted three non-volatile matrices obtained from a white wine, a young red wine and an aged red wine, respectively, after complete dealcoholization and de-aromatization to investigate matrix effects in an SPME wine analysis. The authors revealed strong effects due to ethanol to the content of other major volatiles and to the composition of the non-volatile matrix depending on both the wine matrix composition and the compound nature. In particular, the authors showed that the effect of ethanol, which has potential effects on analyte solubility and on fiber extraction, due to potential competition, was higher than 20% of the total variability in 20 out of 61 investigated compounds. In general, the higher the ethanol level, the smaller the peak area. The effect of the levels of major volatile compounds accounted for more than 20% of the total variability in 19 cases and in a few, the effect of this factor became dominant. In most cases, the higher the level of major volatile compounds, the lower the signal. The authors attributed this behavior likely to competitive effects in the fiber exerted by some major compounds. The non-volatile matrix exerted an effect higher than 20% in 21 cases and in 11 cases became the dominant factor. In this case, the effects did not follow a well-defined trend, suggesting that intermolecular interactions occurred between a few analytes and matrix components.

In order to quantify volatile compounds in wine while keeping matrix effects into account, several approaches have been proposed including internal standards, model wine calibration, a stable isotope dilution analysis (SIDA), matrix-matched calibrations and standard addition methods (Table 1).

Table 1. Advantages and disadvantages of SPME calibration methods.

Calibration Methods	Advantages	Disadvantages
Internal standard (IS)	Simple, versatile, not time-consuming	Analytes and an IS are assumed to have the same instrumental response and to be influenced equivalently by matrix effects. Semi-quantitative analysis.
Model wine calibration with an IS	Simple	Analytes and an IS are assumed to be influenced equivalently by matrix effects. Quantification errors may occur. Loss of complete sets of the standards required for the calibration.
Stable isotope dilution analysis (SIDA)	Accurate results	Isotope labelled standards to be used as an IS are not available for all analytes of interest.
Matrix-matched calibration	Matrix effects can be evaluated. Accurate results	Requires different blank matrices according to the complexity of the matrix.
Standard addition method	Matrix effects can be evaluated. Accurate results	Time-consuming.

The use of an internal standard (IS) added to the matrix to be analyzed before extraction can compensate for matrix effects, losses of analytes during extraction and irreproducibility in instrumental responses but cannot fully avoid them; thus, quantification mistakes may occur. The IS must not be present (at least at detectable levels) in the samples, it should be similar in analytical behavior to the target analytes and it should be well-resolved from the latter. The compounds 4-methyl-2-pentanol and 2-octanol are the most used internal standards for volatile wine analysis [46,47]. An internal standard can also be employed for the equilibrium in fiber standardization. In this case, it is loaded on to the fiber coating prior to the extraction step instead of being spiked into the sample. The technique was developed for automated sampling from milliliter quantities of liquids in vials and used for the analysis of benzene, toluene, ethylbenzene, xylenes [48] and two carbamate pesticides [49] in a wine sample. However, no application has been yet reported in the literature for the determination of a wide range of volatile compounds in wine.

In general, quantitation with an IS is based on the calculation of the ratio between analytical responses (usually chromatographic peak areas) obtained for the analyte and the IS that is subsequently multiplied by the IS concentration. The analyte concentration is thus expressed as IS equivalents. By using this equation, the response factor (i.e., the ratio between a signal produced by an analyte and the quantity of the analyte producing the signal) of all analytes is supposed to be equal to the one of the IS. This is a quite drastic assumption when HS-SPME is adopted because it implies not only that analytes and the IS have the same instrumental response but also that they exhibit a similar behavior in terms of transfer into the headspace and of yield of extraction and then of desorption from the SPME coating. In other terms, they are expected to be influenced equivalently by matrix effects.

As it cannot be usually expected that the IS behaves the same as all of the analytes and, indeed, this requisite is generally not verified, quantification based on an IS is considered a semi-quantitative method. However, this approach is simple, versatile and can be successfully used when just a comparison of the number of individual compounds among samples is desired [50,51]. As the conversion of the analyte/IS response ratio into the analyte concentration can be misleading, many authors have expressed their results as a chromatographic peak area percentage for each volatile in order to compare it among the studied treatments [52,53]. In this case, an equal matrix effect on all analytes is also supposed to occur and the single peak area/total peak area ratio allows just a rough correction.

In model wine calibration, commercial standards are dissolved in ethanol and successively diluted in a wine model solution (e.g., 12% ethanol and 5 g/L of tartaric acid at pH 3.2 or more complex ethanolic solutions) to prepare the different levels of a calibration

curve for each compound. Volatile compounds are analyzed at each calibration level using the same method as that adopted for real wine samples and linear regression is applied to calculate the respective concentration [54]. In this case, a different response of analytes due to their different nature can be inferred; however, no matrix effect can be considered. The internal standard can be added to the model wine calibration solutions and real samples to compensate for the losses of analytes during extraction, irreproducibility in the instrumental response and matrix effects. However, this approach is reliable only if the matrix effect is assumed to be equal for the IS and for all of the analytes. In this case, a calibration plot is developed by calculating the ratio of the peak area of the analyte to the IS one for calibration solutions containing different analyte concentrations with a fixed IS concentration. This ratio is subsequently used to calibrate the sample [55,56]. In order to improve the accuracy of results, the use of multiple standards has been also proposed [57].

When the approach of model wine calibration is used, the accuracy of the data can be established by the calculation of recovery R, which is obtained by comparing a wine sample spiked with known concentrations of the analytes (C_{added}, generally one or two levels) and an unspiked wine extracted and analyzed by the same procedure. Concentrations of the spiked (C_{spiked}) and unspiked ($C_{unspiked}$) samples are then calculated using the calibration line equation and R is finally evaluated as: $(C_{spiked}–C_{unspiked})/C_{added})$. However, percent recoveries exceeding 100 are often found for several analytes thus suggesting the presence of enhancive matrix effects, which are not easily confirmable if the recovery is calculated at a single or at two concentration levels [21].

Furthermore, a complete set of the standards required for the calibration is generally not commercially available. Therefore, the concentrations of volatile compounds for which it is not possible to establish calibration curves were estimated by several authors on the basis of the equations of compounds with the same functional groups and/or similar numbers of C atoms [55]. However, the ideal internal standard is an isotopically labeled analogue (usually its polydeuterated analogue) of the analyte of interest. Indeed, calibration with isotope labelled standards can produce satisfactory results though the compounds are not available for all analytes of interest and thus should be synthesized. In this case, each analyte is assumed to experience the same matrix effects as its isotopically labelled homologue.

Sejer Pedersen et al. [58] described a new method for the analysis of geraniol, nerol, linalool and α-terpineol in wine based on the preparation of [$2H_7$]-geraniol, [$2H_7$]-nerol, [$2H_7$]-linalool and [$2H_7$]-α-terpineol for the use of internal standards followed by liquid-liquid extraction and a GC/MS analysis. Standard solutions with unlabeled compounds and internal standards were prepared for calibration purposes. For comparison, they also used an HS-SPME-GC/MS method finding an adequate sensitivity and limits of quantitation down to 1 μg L^{-1} or below with, however, a worse signal-to-noise ratio especially at lower concentrations.

Siebert et al. [59] first proposed the use of polydeuterated internal standards for stable isotope dilution analyses of 31 wine fermentation products by HS-SPME-GC/MS. Nine of the labelled standards were commercially available while 22 were synthesized. Capone et al. [60] developed a SIDA method for the quantitative analysis of seven C6 compounds. The two methods above [58,59] were successfully used by Ugliano et al. [61] and Bindon et al. [62]. Furthermore, Bindon et al. quantified isobutyl methoxypyrazine (IBMP), isopropyl methoxypyrazine (IPMP) and sec-butyl methoxypyrazine (SBMP) using IBMP-d3 as an internal standard. More recently, Tomasino et al. [63] used the SIDA approach to quantify monoterpene isomers in forty-six Pinot Gris wines by HS-SPME multidimensional gas chromatography mass spectrometry. Dang et al. [64] quantified volatile phenols using relative peak areas, i.e., the ratio between the peak area of the analyte and the one of the normalizing standard (d3-4-methylguaiacol). Bee-DiGregorio et al. [65] used deuterated internal standards for the linalool and 3-isobutyl-2-methoxypyrazine determinations. The authors prepared calibration solutions by spiking unlabeled and deuterated internal standards into Chardonnay juice or Pinot Noir homogenate containing no detectable linalool

or 3-isobutyl-2-methoxypyrazine, respectively. However, although the SIDA has been shown to offer an effective strategy when a narrow range of analytes is investigated, this approach remains little used (just three out of twenty-five wine publications in 2020 used this method).

Among the further quantification methods cited before, matrix-matched calibration involves the preparation of several standard solutions in a sample matrix and then the extraction, desorption and analysis of volatile analytes under the same conditions are adopted for real samples so that a calibration line can be obtained in the presence of matrix effects. As usual, the calibration line equation can be subsequently used to estimate the concentrations of analytes in real samples once these are subjected to extraction and analysis and the corresponding analyte responses are obtained. Provided that standards are available for the analytes of interest, multi-analyte stock solutions can be prepared and then easily used for the preparation of matrix-matched multiple standards. Unfortunately, the matrix-matched calibration has a significant limitation as it requires a blank matrix, i.e., a matrix totally free from target analytes, to be available, which is a quite difficult requirement in the case of wine.

Liu et al. [66] firstly proposed the use of a volatile-free wine obtained by distillation for calibration purposes. The authors compared the chromatographic peak areas of 19 compounds, which were obtained using several model wine matrices including water, an 11.5% ethanol/water (*v*/*v*) solution, a concentrated synthetic wine, a 'volatile-free' wine and a real wine spiked with the same number of analytes. The peak areas of the analytes decreased significantly with the increase in the complexity of the matrix composition suggesting the presence of interactions between the interfering substances and the analytes. The slopes of the calibration lines (taking into account the peak area relative to an internal standard) obtained using the model wine matrices were completely out of the confidence interval of the slope values related to the volatile-free wine and the real wine for most of the volatile compounds. Conversely, the slopes of the linear models obtained with the volatile-free wine were within the confidence interval of the slopes obtained with the real wine for 16 out of the 19. A few other authors have used different deodorized and representative wines [3,19] according to the complexity of the matrix (e.g., young white wine, young red wine, oak-aged red wine), confirming the occurrence of interactions between the matrix and the analytes and the need to use a de-aromatized matrix for accurate calibrations. Furthermore, beside using a de-aromatized matrix, Ferreira et al. [19] proposed the employment of a large pool of internal standards and a calibration strategy based on the calculation of multivariate internal standards (MIS) as linear combinations of the normalized signals of multi-internal standards. However, in order to verify the occurrence of matrix effects when proposing other matrices for calibration, all of the authors cited so far [3,19,66] compared the results with a calibration in real wine. In other words, they used the technique of standard addition as a control because this calibration technique is considered the most reliable.

The technique of standard addition [67] is based on the addition of known concentrations of the analyte of interest to multiple aliquots of the sample, leaving the sample volume (and the proportion ethanol/water) virtually unchanged. Thus, no effect of ethanol can be observed as no variation of its concentration occurs. The sample as such and the spiked samples are subsequently analyzed and a plot of the analytical response versus the added concentration is constructed for each analyte. In this case, the intercept of the regression line on the axis reporting added concentrations provides an estimate of the concentration in the original sample. In the context of the HS-SPME-GC/MS analysis of wine volatiles, the standard addition method was adopted by Carrillo et al. [38] for the quantification of volatile oak compounds in aged red wines. In this case, a significant difference with the results provided by the internal standard method was found for most of the compounds [38]. The standard addition method was also used by Pizarro et al. [68] to quantify haloanisoles and volatile phenols in both white and red wines. The method was also adopted in conjunction with vacuum-assisted HS-SPME-GC/MS for the determination

of haloanisoles in red wines [69]. Recently, Tufariello et al. [21] compared a model wine calibration and the standard addition method for the quantification of volatiles in a white sparkling wine. As a result, they found that the quantification based on the model wine was not accurate for several analytes (with concentrations differing even by one order of magnitude) due to both suppressive and enhancive effects, depending on the analyte, on the final response exerted by the wine matrix. Therefore, although time-consuming, especially if a large number of samples has to be analyzed, the standard addition method should be the eligible method when accurate quantitative results for wine volatiles are highly desirable.

4. Conclusions

HS-SPME-GC/MS is a well-established technique for the analysis of volatile compounds in wine, offering undeniable and well-known advantages such as easiness of use, solventless analyte extraction and potentially high sensitivity. Unfortunately, the presence of many variables to optimize in the method development step may become a difficult challenge. However, the use of multivariate optimization approaches can be very useful to reduce the complexity of method optimization due to their capability to provide a lot of information when many factors are involved without requiring a high number of experiments. The quantification step of analytes is another critical point that needs to be carefully considered when performing an HS-SPME-GC/MS analysis of wine volatile compounds due to the potentially high relevance of matrix effects. Indeed, different quantification methods are usually adopted but none of them appear to be free from drawbacks such as failures in matrix effect reproduction (e.g., using model wines that cannot be considered reliable surrogates of real wines) or the need for time-consuming measurements (such as the standard addition method) or expensive compounds (such as isotopically labelled standards). The choice of the most appropriate quantification method should thus depend on a careful balance between the actual goal of the analysis (sometimes absolute concentrations of specific analytes implying more complex approaches are not strictly required) and practical aspects.

Author Contributions: Conceptualization, S.P. and I.L. review of literature—S.P., M.T., F.G., P.C., A.C.; writing—original draft preparation, M.T., S.P. and I.L.; writing—review and editing, S.P., M.T., F.G., P.C.; supervision, I.L. All authors have read and agreed to the published version of the manuscript.

Funding: This research received no external funding.

Institutional Review Board Statement: Not applicable.

Informed Consent Statement: Not applicable.

Data Availability Statement: Data sharing not applicable.

Acknowledgments: This work was partially supported by the Apulia Region projects: "Innovazione nella tradizione: tecnologie innovative per esaltare le qualità dei vini autoctoni spumante della murgia barese-INVISPUBA" (P.S.R. Puglia 2014/2020 Misura 16.2); "Birra: dal campo al boccale - BE^2R" (P.S.R. Puglia 2014/2020 Misura 16.2). We would like to thank Domenico Genchi, Leone D'Amico, Vittorio Falco and Giovanni Colella of the Institute of Sciences of Food Production—CNR for their skilled technical support provided during the realization of this work.

Conflicts of Interest: The authors declare no conflict of interest.

References

1. Charters, S.; Pettigrew, S. The dimensions of wine quality. *Food Qual. Prefer.* **2007**, *18*, 997–1007. [CrossRef]
2. Panighel, A.; Flamini, R. Applications of Solid-Phase Microextraction and Gas Chromatography/Mass Spectrometry (SPME-GC/MS) in the Study of Grape and Wine Volatile Compounds. *Molecules* **2014**, *19*, 21291–21309. [CrossRef] [PubMed]
3. Rodriguez-Bencomo, J.J.; Munoz-Gonzalez, C.; Andujar-Ortiz, I.; Jose Martin-Alvarez, P.; Victoria Moreno-Arribas, M.; Angeles Pozo-Bayon, M. Assessment of the effect of the nonvolatile wine matrix on the volatility of typical wine aroma compounds by headspace solid phase microextraction/gas chromatography analysis. *J. Sci. Food Agric.* **2011**, *91*, 2484–2494. [CrossRef] [PubMed]

4. Ferreira, V.; Rapp, A.; Cacho, J.; Hastrich, H.; Yavas, I.J. Fast and quantitative determination of wine flavor compounds using microextraction with Freon 113. *J. Agric. Food Chem.* **1993**, *41*, 1413–1420. [CrossRef]
5. Bosch-Fusté, J.; Riu-Aumatell, M.; Guadayol, J.M.; Caixach, J.; Lopez-Tamames, E.; Buxaderas, S. Volatile profiles of sparkling wines obtained by three extraction methods and gas chromatography–mass spectrometry (GC–MS) analysis. *Food Chem.* **2007**, *105*, 428–435. [CrossRef]
6. Ugliano, M.; Moio, L. Changes in the Concentration of Yeast-Derived Volatile Compounds of Red Wine during Malolactic Fermentation with Four Commercial Starter Cultures of Oenococcus oeni. *J. Agric. Food Chem.* **2005**, *53*, 10134–10139. [CrossRef]
7. Pozo-Bayón, M.A.; Pueyo, E.; Martín-Álvarez, P.J.; Polo, M.C. Polidimethylsiloxane solid-phase microextraction-gas chromatography method for the analysis of volatile compounds in wines. Its application to the characterization of varietal wines. *J. Chromatogr. A* **2001**, *922*, 267–275. [CrossRef]
8. Geffroy, O.; Morère, M.; Lopez, R.; Pasquier, G.; Condoret, J.S. Investigating the Aroma of Syrah Wines from the Northern Rhone Valley Using Supercritical CO_2-Dearomatized Wine as a Matrix for Reconstitution Studies. *J. Agric. Food Chem.* **2020**, *68*, 11512–11523. [CrossRef]
9. Teodosiu, C.; Gabur, I.; Cotea, V.V.; Peinado, R.A.; López de Lerma, N. Alternative Winemaking Techniques to Improve the Content of Phenolic and Aromatic Compounds in Wines. *Agriculture* **2021**, *11*, 233.
10. Román, S.M.; Rubio-Bretón, P.; Pérez-Álvarez, E.P.; Garde-Cerdán, T. Advancement in analytical techniques for the extraction of grape and wine volatile compounds. *Int. Food Res. J.* **2020**, *137*, 109712. [CrossRef]
11. Arthur, C.L.; Pawliszyn, J. Solid-phase microextraction with thermal desorption using silica optical fibers. *Anal. Chem.* **1990**, *62*, 2145–2148. [CrossRef]
12. Zhang, Z.; Yang, M.J.; Pawliszyn, J. Solid-Phase Microextraction. *Anal. Chem.* **1994**, *66*, 844A–853A. [CrossRef]
13. Risticevic, S.; Niri, V.H.; Vuckovic, D.; Pawliszyn, J. Recent developments in solid-phase microextraction. *Anal. Bioanal. Chem.* **2009**, *393*, 781–795. [CrossRef]
14. Pereira, A.C.; Reis, M.S.; Leça, J.M.; Rodrigues, P.M.; Marques, J.C. Definitive Screening Designs and latent variable modelling for the optimization of solid phase microextraction (SPME): Case study—Quantification of volatile fatty acids in wines. *Chemom. Intell. Lab. Syst.* **2018**, *179*, 73–81. [CrossRef]
15. Azzi-Achkouty, S.; Estephan, N.; Ouaini, N.; Rutledge, D.N. Headspace solid-phase microextraction for wine volatile analysis. *Crit. Rev. Food Sci. Nutr.* **2017**, *57*, 2009–2020. [CrossRef]
16. Ouyang, G.; Pawliszyn, J. A critical review in calibration methods for solid-phase microextraction. *Anal. Chim. Acta* **2008**, *627*, 184–197. [CrossRef] [PubMed]
17. Risticevic, S.; Pawliszyn, J. Solid-Phase Microextraction in Targeted and Nontargeted Analysis: Displacement and Desorption Effects. *Anal. Chem.* **2013**, *85*, 8987–8995. [CrossRef]
18. Williams, C.; Buica, A. Comparison of an Offline SPE–GC–MS and Online HS–SPME–GC–MS Method for the Analysis of Volatile Terpenoids in Wine. *Molecules* **2020**, *25*, 657. [CrossRef] [PubMed]
19. Ferreira, V.; Herrero, P.; Zapata, J.; Escudero, A. Coping with matrix effects in headspace solid phase microextraction gas chromatography using multivariate calibration strategies. *J. Chromatogr. A* **2015**, *1407*, 30–41. [CrossRef] [PubMed]
20. Vaz Freire, L.M.T.; Costa Freitas, A.M.; Relva, A.M. Optimization of solid phase microextraction analysis of aroma compounds in a Portuguese Muscatel wine must. *J. Microcolumn Sep.* **2001**, *13*, 236–242. [CrossRef]
21. Tufariello, M.; Pati, S.; D'Amico, L.; Bleve, G.; Losito, I.; Grieco, F. Quantitative issues related to the headspace-SPME-GC/MS analysis of volatile compounds in wines: The case of Maresco sparkling wine. *LWT—Food Sci. Technol.* **2019**, *108*, 268–276. [CrossRef]
22. Câmara, J.S.; Arminda Alves, M.; Marques, J.C. Development of headspace solid-phase microextraction-gas chromatography–mass spectrometry methodology for analysis of terpenoids in Madeira wines. *Anal. Chim. Acta* **2006**, *555*, 191–200. [CrossRef]
23. Kamgang Nzekoue, F.; Angeloni, S.; Caprioli, G.; Cortese, M.; Maggi, F.; Marini, U.; Marconi, B.; Perali, A.; Ricciutelli, M.; Sagratini, G.; et al. Fiber−sample distance, an important parameter to be considered in headspace solid-phase microextraction applications. *Anal. Chem.* **2020**, *92*, 7478–7484. [CrossRef] [PubMed]
24. Ferreira, D.C.; Hernandes, K.C.; Nicolli, K.P.; Souza-Silva, É.A.; Manfroi, V.; Zini, C.A.; Welke, J.E. Development of a method for determination of target toxic carbonyl compounds in must and wine using HS-SPME-GC/MS-SIM after preliminary GC×GC/TOFMS analyses. *Food Anal. Methods* **2019**, *12*, 108–120. [CrossRef]
25. Pellati, F.; Benvenuti, S.; Yoshizaki, F.; Bertelli, D.; Rossi, M.C. Headspace solid-phase microextraction-gas chromatography–mass spectrometry analysis of the volatile compounds of Evodia species fruits. *J. Chromatogr. A* **2005**, *1087*, 265–273. [CrossRef] [PubMed]
26. de Bona Sartor, S.; Sganzerla, M.; Teixeira Filho, J.; Teixeira Godoy, H. Multivariate optimization of volatile compounds extraction in Chardonnay wine by headspace-solid phase micro extraction and gas chromatography coupled with tandem mass spectrometry. *Am. J. Anal. Chem.* **2016**, *7*, 712–723. [CrossRef]
27. Muñoz-Redondo, J.M.; Ruiz-Moreno, J.M.; Puertas, B.; Cantos-Villar, E.; Moreno-Rojas, J.M. Multivariate optimization of headspace solid-phase microextraction coupled to gas chromatography-mass spectrometry for the analysis of terpenoids in sparkling wines. *Talanta* **2020**, *208*, 120483. [CrossRef]
28. Hanrahan, G.; Lu, K. Application of factorial and response surface methodology in modern experimental design and optimization. *Crit. Rev. Anal. Chem.* **2006**, *36*, 141–151. [CrossRef]

29. Chmiel, T.; Kupska, M.; Wardencki, W.; Namieśnik, J. Application of response surface methodology to optimize solid-phase microextraction procedure for chromatographic determination of aroma-active monoterpenes in berries. *Food Chem.* **2017**, *221*, 1041–1056. [CrossRef]
30. Borges, T.H.; Ramalhosa, E.; Seiquer, I.; Pereira, J.A. Use of response surface methodology (RSM) for the identification of the best extraction conditions for Headspace Solid-Phase Micro Extraction (HS-SPME) of the volatile profile of cv. arbequina extra-virgin olive oil. *Eur. J. Lipid Sci. Technol.* **2018**, *120*, 1700356. [CrossRef]
31. Arcanjo, N.M.D.O.; Bezerra, T.K.A.; Da Silva, F.L.H.; Madruga, M.S. Optimization of the HS-SPME-GC/MS technique for determining volatile compounds in red wines made from Isabel grapes (Vitis labrusca). *Food Sci. Technol. Camp.* **2015**, *35*, 676–682. [CrossRef]
32. Martinez-Urunuela, A.; Gonzalez-Sáiz, J.M.; Pizarro, C. Optimisation of a headspace solid-phase microextraction method for the direct determination of chloroanisoles related to cork taint in red wine. *J. Chromatogr. A* **2004**, *1056*, 49–56. [CrossRef]
33. Kowalski, C.H.; Silva, G.A.D.; Poppi, R.J.; Godoy, H.T.; Augusto, F. Neuro-genetic multi-optimization of the determination of polychlorinated biphenyl congeners in human milk by headspace solid phase microextraction coupled to gas chromatography with electron capture detection. *Anal. Chim. Acta* **2007**, *585*, 66–75. [CrossRef]
34. Deming, S.N.; Morgan, S.L. *Experimental Design: A Chemometric Approach*; Elsevier: Amsterdam, The Netherlands, 1993.
35. Lundstedt, T.; Seifert, E.; Abramo, L.; Thelin, B.; Nyström, A.; Pettersen, J.; Bergman, R. Experimental design and optimization. *Chemom. Intell. Lab. Syst.* **1998**, *42*, 3–40. [CrossRef]
36. Otto, M. *Chemometrics: Statistics and Computer Application in Analytical Chemistry*; Wiley-VCH: Hoboken, NJ, USA, 1999.
37. Hanrahan, G.; Zhu, J.; Gibani, S.; Patil, D.G. Chemometrics: Experimental design. In *Encyclopedia of Analytical Science*; Worsfold, P.J., Townshend, A., Poole, C.F., Eds.; Elsevier: Oxford, UK, 2005; Volume 2, pp. 8–13.
38. Carrillo, J.D.; Garrido-López, A.; Tena, M.T. Determination of volatile oak compounds in wine by headspace solid-phase microextraction and gas chromatography–mass spectrometry. *J. Chromatogr. A* **2006**, *1102*, 25–36. [CrossRef]
39. Robotti, E.; Campo, F.; Riviello, M.; Bobba, M.; Manfredi, M.; Mazzucco, E.; Gosetti, F.; Calabrese, G.; Sangiorgi, E.; Marengo, E. Optimization of the Extraction of the Volatile Fraction from Honey Samples by SPME-GC-MS, Experimental Design, and Multivariate Target Functions. *J. Chem.* **2017**, *2017*, 6437857. [CrossRef]
40. Burin, V.M.; March, S.; de Revel, G.; Bordignon-Luiz, M.T. Development and validation of method for heterocyclic compounds in wine: Optimization of HS-SPME conditions applying a response surface methodology. *Talanta* **2013**, *117*, 87–93. [CrossRef]
41. Torchio, F.; Giacosa, S.; Vilanova, M.; Segade, S.R.; Gerbi, V.; Giordano, M.; Rolle, L. Use of response surface methodology for the assessment of changes in the volatile composition of Moscato bianco (*Vitis vinifera* L.) grape berries during ripening. *Food Chem.* **2016**, *212*, 576–584. [CrossRef]
42. Barros, E.P.; Moreira, N.; Pereira, G.E.; Ferreira Leite, S.G.; Rezende, C.M.; Guedes de Pinho, P. Development and validation of automatic HS-SPME with a gas chromatography-ion trap/mass spectrometry method for analysis of volatiles in wines. *Talanta* **2012**, *101*, 177–186. [CrossRef]
43. Jones, B.; Nachtsheim, C.J. A class of three-level designs for definitive screening in the presence of second-order effects. *J. Qual. Technol.* **2011**, *43*, 1–15. [CrossRef]
44. Jones, B.; Nachtsheim, C.J. Definitive Screening Designs with Added Two-Level Categorical Factors. *J. Qual. Technol.* **2013**, *45*, 121–129. [CrossRef]
45. Rocha, S.; Ramalheira, V.; Barros, A.; Delgadillo, I.; Coimbra, M.A. Headspace Solid Phase Microextraction (SPME) Analysis of Flavor Compounds in Wines. Effect of the Matrix Volatile Composition in the Relative Response Factors in a Wine Model. *J. Agric. Food Chem.* **2001**, *49*, 5142–5151. [CrossRef] [PubMed]
46. Terpou, A.; Ganatsios, V.; Kanellaki, M.; Koutinas, A.A. Entrapped Psychrotolerant Yeast Cells within Pine Sawdust for Low TemperatureWine Making: Impact on Wine Quality. *Microorganisms* **2020**, *8*, 764. [CrossRef] [PubMed]
47. Moreno-Olivares, J.D.; Paladines-Quezada, D.; Fernández-Fernández, J.I.; Bleda-Sánchez, J.A.; Martínez-Moreno, A.; Gil-Muñoz, R. Study of aromatic profile of different crosses of Monastrell white wines. *J. Sci. Food Agric.* **2020**, *100*, 38–49. [CrossRef] [PubMed]
48. Wang, Y.; O'Reilly, J.; Chen, Y.; Pawliszyn, J. Equilibrium in-fibre standardisation technique for solid-phase microextraction. *J. Chromatogr. A* **2005**, *1072*, 13–17. [CrossRef] [PubMed]
49. Zhou, S.N.; Zhang, X.; Ouyang, G.; Es-haghi, A.; Pawliszyn, J. On-Fiber Standardization Technique for Solid-Coated Solid-Phase Microextraction. *Anal. Chem.* **2007**, *79*, 1221–1230. [CrossRef]
50. Furdíková, K.; Machýnáková, A.; Drtilová, T.; Špánik, I. Comparison of different categories of slovak tokaj wines in terms of profiles of volatile organic compounds. *Molecules* **2020**, *25*, 669. [CrossRef] [PubMed]
51. Karimali, D.; Kosma, I.; · Badeka, A. Varietal classification of red wine samples from four native Greek grape varieties based on volatile compound analysis, color parameters and phenolic composition. *Eur. Food Res. Tech.* **2020**, *246*, 41–53. [CrossRef]
52. Almeida Santos, C.V.; Gomes da Silva, M.; Cabrita, M.J. Impact of SO_2 and bentonite addition during fermentation on volatile profile of two varietal white wines. *LWT Food Sci. Technol.* **2020**, *133*, 109893. [CrossRef]
53. Castillo, M.; da Silva, E.; Câmara, J.S.; Khadem, M. Molecular identification and VOMs characterization of Saccharomyces cerevisiae strains isolated from Madeira region winery environments. *Processes* **2020**, *8*, 1058. [CrossRef]
54. Oliveira, A.S.; Furtado, I.; Bastos, M.D.L.; de Pinho, P.G.; Pinto, J. The influence of different closures on volatile composition of a white wine. *Food Packag. Shelf Life* **2020**, *23*, 100465. [CrossRef]

55. Kong, C.-L.; Li, A.-H.; Suc, J.; Wang, X.-C.; Chen, C.-Q.; Tao, Y.-S. Flavor modification of dry red wine from Chinese spine grape by mixed fermentation with Pichia fermentans and S. cerevisiae. *LWT Food Sci. Technol.* **2019**, *109*, 83–92. [CrossRef]
56. Hu, K.; Jin, G.J.; Xu, Y.H.; Tao, Y.S. Wine aroma response to different participation of selected Hanseniaspora uvarum in mixed fermentation with Saccharomyces cerevisiae. *Int. Food Res. J.* **2018**, *108*, 119–127. [CrossRef] [PubMed]
57. Rebière, L.; Clark, A.C.; Schmidtke, L.M.; Prenzler, P.D.; Scollary, G.R. A robust method for quantification of volatile compounds within and between vintages using headspace-solid-phase micro-extraction coupled with GC–MS—application on Semillon wines. *Anal. Chim. Acta* **2010**, *660*, 149–157. [CrossRef]
58. Sejer Pedersen, D.; Capone, D.L.; Skouroumounis, G.K.; Pollnitz, A.P.; Sefton, M.A. Quantitative analysis of geraniol, nerol, linalool, and α-terpineol in wine. *Anal. Bioanal. Chem.* **2003**, *375*, 517–522. [CrossRef]
59. Siebert, T.E.; Smyth, H.E.; Capone, D.L.; Neuwöhner, C.; Pardon, K.H.; Skouroumounis, G.K.; Herderich, M.J.; Sefton, M.A.; Pollnitz, A.P. Stable isotope dilution analysis of wine fermentation products by HS-SPME-GC–MS. *Anal. Bioanal. Chem.* **2005**, *381*, 937–947. [CrossRef]
60. Capone, D.L.; Black, C.A.; Jeffery, D.W. Effects of 3-mercaptohexan-1-ol precursor concentrations from prolonged storage of Sauvignon blanc grapes prior to crushing and pressing. *J. Agric. Food Chem.* **2012**, *60*, 3515–3523. [CrossRef]
61. Ugliano, M.; Siebert, T.; Mercurio, M.; Capone, D.L.; Henschke, P.A. Volatile and color composition of young and model-aged Shiraz wines as affected by diammonium phosphate supplementation before alcoholic fermentation. *J. Agric. Food Chem.* **2008**, *56*, 9175–9182. [CrossRef]
62. Bindon, K.; Varela, C.; Kennedy, J.; Holt, H.; Herderich, M. Relationships between harvest time and wine composition in *Vitis vinifera* L. cv. Cabernet Sauvignon 1. Grape and wine chemistry. *Food Chem.* **2013**, *138*, 1696–1705. [CrossRef]
63. Tomasino, E.; Song, M.; Fuentes, C. Odor Perception Interactions between Free Monoterpene Isomers and Wine Composition of Pinot Gris Wines. *J. Agric. Food Chem.* **2020**, *68*, 3220–3227. [CrossRef]
64. Dang, C.; Jiranek, V.; Taylor, D.K.; Wilkinson, K.L. Removal of Volatile Phenols From Wine Using Crosslinked Cyclodextrin Polymers. *Molecules* **2020**, *25*, 910. [CrossRef]
65. Bee-DiGregorio, M.Y.; Feng, H.; Pan, B.S.; Dokoozlian, N.K.; Sacks, G.L. Polymeric Sorbent Sheets Coupled to Direct Analysis in Real Time Mass Spectrometry for Trace-Level Volatile Analysis—A Multi-Vineyard Evaluation Study. *Foods* **2020**, *9*, 409. [CrossRef]
66. Liu, M.; Zeng, Z.; Tian, Y. Elimination of matrix effects for headspace solid phase microextraction of important volatile compounds in red wine using a novel coating. *Anal. Chim. Acta* **2005**, *540*, 341–353. [CrossRef]
67. Bader, M. A systematic approach to standard addition methods in instrumental analysis. *J. Chem. Educ.* **1980**, *57*, 703–706. [CrossRef]
68. Pizarro, C.; Peres-del-Notario, N.; Gonzalez-Saiz, J.M. Multiple headspace solid-phase microextraction for eliminating matrix effect in the simultaneous determination of haloanisoles and volatile phenols in wines. *J. Chromatogr. A* **2007**, *1166*, 1–8. [CrossRef]
69. Vakinti, M.; Mela, S.M.; Fernandez, E.; Psillakis, E. Room temperature and sensitive determination of haloanisoles in wine using vacuum-assisted headspace solid-phase microextraction. *J. Chromatogr. A* **2019**, *1602*, 142–149. [CrossRef]

MDPI
St. Alban-Anlage 66
4052 Basel
Switzerland
Tel. +41 61 683 77 34
Fax +41 61 302 89 18
www.mdpi.com

Processes Editorial Office
E-mail: processes@mdpi.com
www.mdpi.com/journal/processes

MDPI
St. Alban-Anlage 66
4052 Basel
Switzerland

Tel: +41 61 683 77 34
Fax: +41 61 302 89 18

www.mdpi.com

ISBN 978-3-0365-4010-8